FUNCTIONAL CORRELATIONS OF C-TAIL CONFORMATION IN A SKELETAL MUSCLE CHLORIDE CHANNEL

A thesis submitted to the University of South Australia in fulfilment of the requirements for the award of the degree of

Doctor of Philosophy

(Pharmacy and Biomedical Sciences)

by

Linlin Ma, M.D., M.Sc. (Medical Genetics)

School of Pharmacy and Medical Sciences

Division of Health Sciences

University of South Australia

AUGUST 2009

TABLE OF CONTENTS

LIST OF FIGURES iv

LIST OF TABLES vi

LIST OF ABBREVIATIONS vii

SUMMARY xi

DECLARATION xiii

ACKNOWLEDGEMENTS xiv

DEDICATION xvii

CHAPTER 1: LITERATURE REVIEW 1

1.1 General introduction of CLC chloride channel/transporter family 2
1.2 Structural characters of the proteins 7
1.2.1 The general structure of the transmembrane domain, the pore region and the selectivity filter 8
1.2.2 The pore region and the selectivity filter 11
1.3 Physiological properties of CLC channels/transporters 15
1.3.1 Ion selectivity and permeation 15
1.3.2 Gating 15
1.4 Channels vs transporters 21
1.5 Cytoplasmic tails 22
1.6 Project aims 27

CHAPTER 2: GENERAL METHODS 31

2.1 Chemicals and water 31
2.2 Materials and methods for molecular biology study 31
2.2.1 Polymerase chain reactions (PCR) to get DNA sequence 31
2.2.2 DNA purification by gel extraction 33
2.2.3 Restriction digestion 34
2.2.4 DNA ligation 34
2.2.5 Bacteria strains 34
2.2.6 Bacterial cultivation 35
2.2.7 Preparation of competent cells 36
2.2.8 Transformation of competent cells with plasmid DNA 36
2.2.9 Purification of plasmid DNA from bacterial cultures 37
2.2.10 Qualification and quantification of plasmid DNA 38
2.3 Protein expression in HEK293T cells 38

2.4 Protein detection and protein-protein interaction test 40
2.4.1 Total protein extraction 40
2.4.2 Membrane protein extraction 40
2.4.3 Protein quantification 41
2.4.4 GST-pulldown assay 41
2.4.5 SDS-PAGE 41
2.4.6 Western blot 42
2.5 Electrophysiological study of hClC-1 channel 42
2.6 Fluorescence resonance energy transfer (FRET) study 44

CHAPTER 3: ANALYSIS OF CARBOXYL TAIL FUNCTION IN THE SKELETAL MUSCLE Cl^- CHANNEL hClC-1 47

3.1 Introduction 47
3.2 Materials and methods 50
3.2.1 Plasmid constructs of hClC-1 50
3.2.2 Deletion-scanning and alanine-scanning mutagenesis 50
3.2.3 Cell culture and transfection 51
3.2.4 GST-Pulldown Assay and Western Blotting 52
3.2.5 Electrophysiology 52
3.2.6 Data analysis 53
3.3 Results 53
3.3.1 Investigation of the effects of tags on split channel studies 53
3.3.2 Identification of interacting regions in split channel G-f-*N*720 + 721*C*-m 54
3.3.3 Interaction between the whole C-tail and the membrane-resident domain 59
3.4 Discussion 64

CHAPTER 4: FUNCTIONAL STUDY OF CYTOPLASMIC LOOPS OF HUMAN SKELETAL MUSCLE CHLORIDE CHANNEL hCLC-1 68

4.1 Introduction 68
4.2 Materials and methods 69
4.2.1 Basic constructs of hClC-1 69
4.2.2 Deletion and alanine-exchange mutagenesis 69
4.2.3 Cell culture and transfection 71
4.2.4 GST-pull-down Assay and Western Blot 71
4.2.5 Purification of membrane proteins 72
4.2.6 Electrophysiology 72
4.2.7 Data analysis 73
4.3 Results 73
4.3.1 Roles of cytoplasmic loops in the interaction between the membrane-resident domain and the cytoplasmic tail 73
4.3.2 Physiological significance of the cytoplasmic loops for the channel function 76
4.4 Discussion 83

CHAPTER 5: LATERAL DISPLACEMENT OF hClC-1 CARBOXYL TERMINALS DURING COMMON GATING AND LIMITS ON THEIR CYTOPLASMIC LOCATION **87**

5.1 Introduction 87
5.2 Materials and methods 89
5.2.1 Constructs of hClC-1 89
5.2.2 Cell culture and transfection 91
5.2.3 Electrophysiology 91
5.2.4 Spectra FRET and FRET efficiency quantification 91
5.3 Results 94
5.3.1 Validation of function and FRET in C-terminal tagged hClC-1 channels 94
5.3.2 FRET in truncated hClC-1, *N*887, resembles that in ClC-0 97
5.3.3 FRET study of mutants indicates a strong link between fast gating and common gating in hClC-1 100
5.3.4 FRET study of split hClC-1 channel N451-Cerulean + 380C-eYFP places constraints on the position of the C-terminal perpendicular to the plane of the membrane 103
5.4 Discussion 106

CHAPTER 6: GENERAL DISCUSSION, CONCLUSIONS AND FUTURE DIRECTIONS **111**

6.1 General discussion 111
6.1.1 Split channel strategy and trafficking signal 111
6.1.2 CBS domains and their physiological functions 113
6.1.3 Loops in CLC proteins 116
6.1.4 The common gating 117
6.2 Conclusions 120
6.3 Future directions 123
6.3.1 Further dissect the physical and physiological roles of cytoplasmic loops in hClC-1 123
6.3.2 Further study on the short peptide L863 to R888 123
6.3.3 Locate the interacting sites in the membrane-resident pore region for the C-tail of hClC-1 by FRET studies 124
6.3.4 Further study of common gating mechanism by chimera using FRET 124
6.3.5 Find the interacting proteins of hClC-1 125
6.3.6 Study of myotonic mtations in hClC-1 126

BIBLIOGRAPHY **128**

APPENDIX A: SEQUENCES OF PRIMERS **144**

APPENDIX B: cDNA SEQUENCE OF HUMAN ClC-1 **148**

APPENDIX C: PUBLISHED PAPERS **152**

LIST OF FIGURES

Figure	Title	Page
1	Structural views of bacterial CLC protein	10
2	Structure of the ion conducting pore and the selectivity filter in StCLC and EcCLC	13
3	A comparison of the dimeric organization of cytoplasmic domains of ClC-Ka, ClC-5 and ClC-0	26
4	Schematic diagram of hClC-1	49
5	Electrophysiological analyses of split channels	55
6	Interaction between various 721*C*-m mutants and G-f-*N*720	57
7	Effects of CBS domains and related regions on the interaction between complemented channel fragments G-f-*N*720 and 721*C*-m	61
8	Interaction between 598*C*-m and G-f-*N*720ΔCBS1	63
9	Roles of the cytoplasmic loops in the binding between G-f-*N*720Δ and 598*C*-m.	74
10	Expression and trafficking study of the loop alanine-exchange mutants of hClC-1.	79
11	Electrophysiological analyses of WT hClC-1 and alanine-exchange mutations of loops.	80
12	A comparison of gating characteristics in cytoplasmic loop alanine-exchange mutants of hClC-1	81
13	Schematic diagram of an hClC-1 monomer	90
14	Spectra FRET	93
15	Electrophysiological comparison of YFP tagged hClC-1 channel and WT hClC-1	95
16	FRET efficiency measurement from C-termini tagged hClC-1 channels	96
17	Electrophysiological features of truncated hClC-1 channel *N*887-Cerulean	98
18	FRET efficiency measurements from truncated hClC-1 channel *N*887	99
19	FRET study of hClC-1 mutants C277S, E232Q and the double mutant E232QC277S	101
20	Electrophysiological analysis and FRET efficiency measurements from split hClC-1 channel *N*451- Cerulean + 380*C*-eYFP	104

21 Diagrammatic representation of coupling between fast and common gating in hClC-1 110

LIST OF TABLES

Table	Title	Page
1	Properties of Vertebrate CLC proteins	6
2	Constructs used in the present study (Chapter 3)	51
3	$V_{1/2}$ of overall channel open probability (P_o) , fast gating (P_o^f) and common gating (P_o^c) for WT hClC-1 and split hClC-1 channels	56
4	Constructs of hClC-1 used in the present study (Chapter 4)	70
5	$V_{1/2}$ of channel open probability (P_o), fast gating (P_o^f) and common gating (P_o^c) for WT hClC-1 and loop alanine-exchange mutants	78
6	Constructs of hClC-1 used and discussed in the present study (Chapter 5)	89
A-1	Primers for amplifying full-length hClC-1 or hClC-1 fragments	144
A-2	Sequencing primers	145
A-3	Primers for deletion mutagenesis	145
A-4	Primers for alanine-exchange mutagenesis	146

LIST OF ABBREVIATIONS

Abbreviation	Meaning
A	Ampere (s)
Å	Angstrom (s)
aa	Amino acid (s)
ATP	Adenosine triphosphate
bp	Base pairs
Br^-	Bromide ion (s)
BSA	Bovine serum albumin
Ca^{2+}	Calcium ion (s)
cAMP	Adenosine 3', 5' -cyclic monophosphate
CBS	Cystathionine beta-synthase
cDNA	Complementary DNA
CFTR	cystic fibrosis transmembrane conductance regulator
cGMP	Guanosine 3', 5' -cyclic monophosphate
CPA	Clofibric acid–derivative p-chlorophenoxy-acetic acid
Cl^-	Chloride ion (s)
CLC	Voltage-gated Cl^- channel / transporter family
CLCN1	ClC-1 chloride channel gene
CLIC	Chloride intracellular channels
$[Cl^-]_i$	Intracellular chloride concentration
$[Cl^-]_o$	Extracellular chloride concentration
CNS	Central nervous system
CPA	p-chlorophenoxy-acetic acid
C-tail	Carboxyl tail
COOH	Carboxyl
Δ	Delta (deletion)
Da	Dalton (s)
DIDS	Stilbenedisulfonate 4,4-diisothiocyanatostilbene-2,2′-disulfonic acid
DMEM	Dulbecco's Modified Eagle's Medium

DMSO	Dimethyl sulfoxide
DNA	Deoxyribonucleic acid
DNAse	deoxyribonuclease
dNTP	Deoxynucleotide 5’ triphosphate (mixed dATP, dCTP, dGTP and dTTP)
DTT	Dithiothreitol
DXE	Di-acidic ER-exit signal
EcClC	*Escherichia coli* ClC
E.coli	*Escherichia coli*
EDTA	Ethylenediaminetetra-acetic acid
endA1	nonspecific endonuclease1
F^-	Fluoride ion (s)
f-	N-terminal FLAG tag
FCS	Fetal calf serum
G-	GST-fusion
GABA	γ-aminobutyric acid
GFP	Green fluorescent protein
GST	Glutathione S-transferase
h	Hour (s)
H^+	Hydrogen ion (s)
hClC-1	Human skeletal muscle Cl^- channel
HEK293T cells	Human embryonic kidney cells type 293T
HEPES	N-2-Hydroxyethylpiperazine-N’-2-ethanesulphonic acid
HRP	Horseradish peroxidase
I^-	Iodide ion (s)
K^+	Potassium ion (s)
kb	Kilo base
kDa	Kilo Daltons
kHz	Kilo Hertz
K_{off}	Dissociation constant
LB	Luria-Bertani media
Mg^{2+}	Magnesium ion (s)

MΩ	Mega Ohm (s)
MOPS	3-[N-morpholino] propane-sulfonic acid
-m	C-terminal c-myc tag
mV	Milli Volt (s)
Na^+	Sodium ion (s)
nA	Nano Ampere (s)
ng	Nano gram (s) (10^{-9} gram)
NCS	Newborn Calf Serum
NO_3^-	Nitrate ion (s)
N-region	N-terminal region
OH^-	Hydroxide ion (s)
PAGE	Polyacrylamide gel electrophoresis
PBS	Phosphate buffered saline
PCR	Polymerase chain reaction
pH_i	Internal pH
pH_o	External pH
pmol	Picomol (10^{-12})
P_o	Open probability
P_o^c	Open probability of the common gate
P_o^f	Open probability of the fast gate
pS	Pico-Siemens
rClC-1	Rat ClC-1
recA	Homologous recombination deficient
RNase	Ribonuclease
S_{cen}	Central ion binding site
SCN^-	Thiocyanate ion (s)
SDS	Sodium dodecyl sulphate
SEM	Standard error
S_{ext}	External ion binding site
S_{int}	Internal ion binding site
SPR	Surface plasmon resonance
StClC	*Salmonella enterica* serovar *typhimurium* ClC

τ_1	Fast time constant
τ_2	Slow time constant
TAE	Tris acetate EDTA
TBST	Tris-buffered saline with Tween-20
Tm	Melting temperature
TM	Transmembrane
TRP channel	Transient receptor potential channel
Tris	Tris (hydroxymethyl) aminomethane
Tween 20	Polyoxyethylene sorbitan monolaurate
μ	Micro (10^{-6})
μl	Microlitre
μM	Micromolar
μg	Microgram
U	Unit (s)
UV	Ultra-violet
$V_{1/2}$	Voltage at which open probability = 0.5 ($1+P_{min}$)
v/v	Volume by volume
WT	Wild-type
w/v	Weight by volume
Zn^{2+}	Zinc ion (s)

SUMMARY

Like other CLC channel and transporter proteins, hClC-1 is homodimeric with a separate chloride permeation pore in each subunit. It has two distinct gating processes, fast gating which regulates each pore independently and common gating which closes both pores simultaneously. Fast gating is associated with a glutamate side-chain carboxyl group that swings into and out of each permeation pathway, although some evidence suggests that changes in pore conformation might also be involved. Common gating, however, is much more complicated and remains poorly understood.

My objectives, therefore, were to investigate the common gating of hClC-1, especially unknown aspects of the conformation of its long cytoplasmic carboxyl-tail (C-tail) and interactions between its C-tail and membrane-resident regions. Anticipating the C-tail's two cystathionine beta-synthase (CBS) domains might be functionally important, I used mutagenesis, split channel methods, GST-pulldown and patch-clamping to assess suspected contact between them. I found strong binding of a membrane-resident channel fragment, *N*720 (M1 to S720) containing CBS1, to its complement, 721*C* (G721 to L988) containing CBS2. This binding is, however, unaffected by deletion of CBS1 from *N*720 when it interacts with the full C-tail (598*C*). Channel function is preserved when these two fragments are co-expressed, showing that a CBS1-CBS2 interaction is not essential for reconstitution of these fragments and, so, is probably not required for channel assembly, either. Rather, the interaction might normally assist in bringing some part of the CBS2/C-tail region into appropriate proximity with the membrane-resident portion of the protein. Conversely, functionally important sequences between amino acids 800 and 888 could be deleted from 721*C* without affecting its binding to *N*720.

Since the C-tail of hClC-1 might modulate common gating of the channel through binding to the cytoplasmic loops linking the transmembrane helices, I examined the roles of loops DE, FG, HI and JK in binding to the C-tail and their involvement in channel function. No significant binding between the C-tail and any of these individual cytoplasmic loops was found, although other interactions are conceivable. Nevertheless, alanine-exchange mutation of specific loops either eliminated Cl^- currents or had pronounced effects on gating which might, therefore, depend not only on the transmembrane helices and C-tail of the channel but also on some of its cytoplasmic loops.

Prior research on a related channel showed that large conformational changes, notably at the C-termini, occurred during common gating. Using fluorescence resonance energy transfer (FRET), I confirmed this finding for hClC-1 by showing significant movements of the C-termini that paralleled common gating (separation during closure and approach on opening).
A comparison of FRET in single mutants E232Q and C277S and double mutant E232QC277S, strongly suggests that fast and common gating are closely coupled in hClC-1. Similarly, using fluorophore-labelled split channel constructs, I estimated the previously unknown cytoplasmic depth of the C-termini as less than 4 nm.

In conclusion, these results aid our understanding of the muscle disease, dominant myotonia congenita, which is associated with aberrant common gating in hClC-1, and they significantly advance our knowledge of the biophysics of ion channels in general.

DECLARATION

I declare that this thesis presents work carried out by myself and does not incorporate without acknowledgment any material previously submitted for a degree or diploma in any university. To the best of my knowledge it does not contain any materials previously published or written by another person except where due reference is made in the text; and all substantive contributions by others to the work presented, including jointly authored publications, is clearly acknowledged.

Linlin Ma

ACKNOWLEDGEMENTS

Being lucky enough to have such a fantastic PhD journey in Australia, first of all, I would like to thank University of South Australia for opening the magic door for me and thank the Department of Education, Science and Training (DEST) of Australian Government for providing me with the "International Postgraduate Research Scholarships (IPRS)", which made everything possible and was definitely a great honour for me.

The deepest appreciation would go to my supervisors, **Professor Allan Bretag** and **Dr. Grigori Rychkov**, who led my way patiently to this exciting ion channel research field and supervised me enthusiastically in every respect of my PhD study from experiment design to paper writing. From my supervisors, I learned not only how to do research, but also how to think and behave like a scientist, which, I believe, will be a lifetime benefit for me. Especially, so many thanks to Allan and your gorgeous wife **Mrs. Lesley Bretag**, who have been acting as my English-speaking parents in Australia and have been looking after me and my family so circumspectly in the past four years.

People in the CLC Cl^- channel group have made my research life so much easier and fun. Big thanks to **Mr. Andrew Beck** for your technical assistance, your help in physiology practicals, many lovely chats, and for sharing beautiful things in your life and **Assoc Professor Bernie Hughes**, who always spirits me up with your smiles, for your warm encouragement, wise suggestions and inspiring discussions. Many thanks to **Dr. Paul Bartley** for your help in molecular biology at the beginning which has saved me from being a lost child. My fellow research postgraduates, **Dr. Jennie Cederholm** and **Ms. Peony Fung**, I appreciated everyday being accompanied by you in the lab and many fun discussions and chats. Thank you so much Jennie, for teaching me how to do patch clamp and hosting me in Sydney.

A special thanks to many brilliant scientists around me, who were not from the CLC group but have helped me so much in terms of technologies, trouble shootings, many important suggestions and helpful discussions. **Dr. Benjamin Roberts** has been "the last chance" for me for so many times. It's amazing how you can always easily figure out a solution and save me from sufferings. Also, I was really impressed to see you, as a PI, working so hard in the lab everyday. Thank you for setting such an excellent role model for me. **Mr. Steve Paltoglou**, I have always been so happy to know that you are working in the next door, so I have never felt lonely or scared even when it was midnight because I know that your helpful hands are there forever. **Dr. Frank Madaras**, my dear mentor and friend. It was so much fun

to talk with you about science, culture and life. Your profound knowledge has been a source of wisdom for me. I appreciated so much for your guidance, your solicitude and your help. Another favourite scientist is **Dr. Tom Litjens** from the University of Adelaide. Thank you for those helpful discussions, brilliant suggestions and interesting chats. I was so lucky to share with you the joy to be a parent and to enjoy how lovely your son Simon is. Many thanks to **Assoc Prof. Sandra Orgeig**, **Mrs. Ceilidh Marchant** and **Mrs. Tamara Crittenden** for sharing equipments, research experience and good ideas.

Life has been very busy during my PhD study because of so many highlights. Teaching experience was definitely one of them. I appreciated deeply the teaching opportunities in Physiology and Biological Science, which I have enjoyed greatly. Many thanks to everyone I have worked with in teaching, especially **Prof. Allan Bretag**, **Assoc Prof. Pat Buckley**, **Mr. Clive Watts**, **Dr. Michael Kokkinn**, **Dr. Michael Venning**, **Dr. Tim Smeaton**, **Dr. Jenny Hiscock**, **Dr. Sheridan Gentili**. **Mr. Andrew Beck** and **Mr. Shaun O'Sullivan**. I have learned so much from each of you and had great fun from working with you. Particularly, **Assoc Prof. Pat Buckley**, I have regarded you as another mentor for me, not only because I enjoyed your lectures so much, but also because I know you are someone who I can fully trust and can always learn something from.

Another highlight in my PhD were my buddies in Reid building: **Mr. Jiping Wang**, **Mrs. Jing Ma**, **Ms. Xiaoxin Qi**, **Mr. Zheng Ma**, **Ms. Hongping Jin**, **Ms. Lv Wang**, **Mrs. Yunmei Song** and **Ms. Shasha Rao**. Being away from my family in China, I regard you as my sisters and brothers, who I truly love. Thanks for sharing all the happiness and sadness, all the laughs and tears. I will always remember and treasure all our chats and discussions, lovely lunches, fun hot pots and BBQs, short trips and relaxing games. The confidence that any one of you will always be happy to give me a warm hand made me feel so fearless during this journey. I really appreciate your friendship and hope you will be part of my life way beyond these four years. Knowing that most of you will leave Adelaide sooner or later, I will miss you so much and wish you all the best for the future.

As PhD students, we always need different kinds of encouragement to get motivated. I really treasure the Travel Awards, Publication Awards and Career Exploration Awards presented by the **Sansom Institute** and the Travel Awards and Presentation Awards presented by the **Australian Physiology Society**. These inspiring awards not only provided me with the opportunities to broaden my view by attending conferences and cooperating with other scientists, but also motivated me to improve myself all the time.

During my PhD, I was so lucky to have an opportunity to do a collaborative project in UC Davis, Assoc Prof. Jie Zheng's lab. My supervisors are deeply appreciated for providing me with this opportunity and for their strong support scientifically, psychologically and financially. So many thanks to **Assoc Prof. Jie Zheng** for teaching me FRET technique hand by hand, for making many helpful discussions and for looking after me considerately in Davis. People in Jie's lab are all very kind and lovely persons. **Dr. Katerina Bykova**, **Mrs. Wei Cheng**, **Mr. Fan Yang** and **Mr. Ping Liang**, thank you so much for your help, our caring and your friendship. I have been treated so well that I completely forgot I was a visitor there. I'm sorry that I brought so much rain to Davis that winter, but nothing could stop us from having fun trips around Davis and in San Francisco anyway. Those happy lunch time conversations and lovely dinners will be one of the most beautiful memories in my life.

Also, many thanks to my great mother **Jianfeng** and my fantastic parents in law **Ruchao** and **Jingwen** for caring about me so much and believing in me all the time. I appreciate everything you have done for me all these years! And I miss you so much my dear father **Changxin**! You have always been the strongest spiritual support and a perfect idol for me. I know as a child, I could never do enough to pay you back, but I will try my best to practice what you have taught me and make you proud of me one day!

Last, but not least, a big thank you to my beloved husband **Jiashen**. I am so lucky to have you in my life! Thanks for your courage to give up such a good job in Beijing to support my study in Australia! Thanks for facing an uncertain future bravely without any complaint! Thanks for cooking for me and waiting for me to have dinner even until midnight! Thanks for accompanying me when I worked late for countless nights and weekends! Thanks for giving me love, support, inspiration, understanding and for always believing in me! For any achievement I could get, you should claim half of the credit, because I could never have gone so far without you!

For Jiashen

CHAPTER 1:
LITERATURE REVIEW

Anion channels are pores through proteins which traverse biological membranes and allow the passive diffusion of negatively charged ions along their electrochemical gradient (Estévez & Jentsch 2002). Channels/transporters of CLC family control the flow of small monovalent anions, including Cl^-, Br^-, I^-, NO_3^-, SCN^-, but not F^-, across the membrane (Goldberg & Miller 1991; Rychkov et al. 1998; Jentsch et al. 1999). They are often called Cl^- channels/transporters, because as the most abundant anion in organisms, Cl^- is the predominant permeating species under most circumstances for CLC proteins. Featured as being unique in structure and ubiquitous in expression, Cl^- channels/transporters have been found from prokaryotes to eukaryotes including bacteria, fungi, plants and all animals (Estévez & Jentsch 2002; Salas-Casas et al. 2006).

Just as for cation channels, the most important features of Cl^- channels also include: (1) a selectivity filter, which enables them to discriminate between different ions and permits only a restricted class of ions to flow passively down their electrochemical activity gradients (Hille 2001), (2) a pore, which is the pathway for the ions and (3) one or more gating mechanisms which allow the channels to open or close their permeation pathway to regulate ion flow in response to external stimuli (Dutzler 2004). Chloride channels could be grouped according to their gating mechanisms, which may depend on changes in transmembrane electric field (voltage gated Cl^- channels, the CLC family) (Brandt & Jentsch 1995), on intracellular ATP and phosphorylation by cAMP- or cGMP-dependent kinases (cystic fibrosis transmembrane conductance regulator, CFTR) (Seibert et al. 1997), on binding of a ligand (ligand-gated $GABA_A$ and glycine receptors) (Hosie et al. 1997), on an increase in intracellular Ca^{2+} (Ca^{2+} activated Cl^- channels, CaCC) (Eggermont 2004; Hartzell, Putzier & Arreola 2005), or on cell swelling (volume regulated anion channels, VRAC) (Nilius & Droogmans 2003). In addition, a family of putative intracellular Cl^- channels that have a single putative transmembrane domain has been identified as Chloride Intracellular Channel (CLIC) family (Landry et al. 1993; Berryman & Bretscher 2000).

Among these subgroups, the voltage-gated CLC proteins have been well-established based on the discovery of CLC gene family and related hereditary diseases. In this literature review, I will provide a brief background on the CLC family, then concentrate on the major

physiological features of CLC Cl^- channels/transporters and focus, especially, on the research progress in the study of cytoplasmic tails of CLC proteins.

1.1 GENERAL INTRODUCTION TO THE CLC CHLORIDE CHANNEL/ TRANSPORTER FAMILY

Individual voltage-dependent Cl^- channels were discovered accidentally 29 years ago (White & Miller 1979), and the first molecular identification was then achieved by the expression cloning of ClC-0 from the electric organ of the marine electric ray Torpedo marmorata (Jentsch, Steinmeyer & Schwarz 1990). In less than thirty years, great achievements have been made in understanding the physiological features, functions, working mechanisms and the molecular structures of its family members. These CLC proteins turn out to be fascinating in that they show a remarkable homology between family members and have a unique structure unrelated to any other known ion channels/transporters (Pusch & Jentsch 1994; Chen 1998). They play many important roles in cells, including the stabilization of membrane potential, regulation of transepithelial transport, synaptic inhibition, cell volume regulation, extracellular and vesicular acidification and endocytotic trafficking (Chen 2005). Knock-out mouse models have demonstrated the significance of CLC proteins as have various hereditary diseases caused by defects in these channels/transporters. For example, the loss of particular Cl^- channels leads to Bartter's syndrome with or without deafness (Konrad et al. 2000; Hebert 2003), increased muscle excitability in myotonia congenita (Kubisch et al. 1998; Zhang et al. 2000) as well as neurodegeneration and idiopathic epilepsy (Haug et al. 2003), reduced endosomal acidification and impaired endocytosis in Dent's disease (Lloyd et al. 1996; George 1998), and impaired extracellular acidification by osteoclasts and osteopetrosis (Kornak et al. 2001).

Despite strong conservation of their structural framework, the family members show an unusually broad variety of functional behaviours, as some members work as gated Cl^- channels and others as secondary Cl^- transporters (Accardi & Miller 2004; Picollo & Pusch 2005; Scheel et al. 2005). Different CLC channels/transporters exhibit unique functional properties, particularly with respect to the gating mechanisms, but they all seem to share two characteristics that are apparently inherent to this family. One is an anion over cation selectivity, manifest as permeation by the halogen ions Cl^- and Br^-, and block of Cl^- current by larger anions such as I^-, SCN^- and other organic anions (Rychkov et al. 1996a; Rychkov et al. 2001). Another is the strong functional coupling between ion conduction and gating. Chloride is the current-carrying substrate that flows through the pore, and interestingly, a regulator of

the channel's gating at the same time. Apparently by binding in the pore, the Cl^- ion influences the open probability, giving rise to properties such as voltage-dependent gating in some CLC Cl^- channels (Pusch et al. 1995; Chen & Miller 1996).

Nine mammalian members of the CLC family have been molecularly cloned (ClC-1 to ClC-7, ClC-Ka, ClC-Kb), and several members in invertebrate species, such as bacteria (Fujita et al. 1994), fungi (Greene et al. 1993), archaea (Jentsch et al. 1999), protozoa (Salas-Casas et al. 2006), plants (Hechenberger et al. 1996), fish (Jentsch, Steinmeyer & Schwarz 1990) and birds (predicted by automated computational analysis, NCBI accession number: XP_425521) are also known. On the basis of gene sequences and classifications of functional properties, the vertebrate CLC channels are divided into three subfamilies:

Firstly, ClC-0 and its mammalian homologues, ClC-1, ClC-2, ClC-Ka and ClC-Kb are grouped together and called "muscle-type" CLC channels, which share ~50-60% sequence identity. These channels are all present in the plasma membrane where they control the Cl^- flux and membrane potential (Jentsch et al. 1999). As the "founding member" of the family, ClC-0 has become an excellent model for studying the physiological features of CLC proteins, especially the correlation between structures and functions (Ludewig, Pusch & Jentsch 1996, 1997; Pusch, Ludewig & Jentsch 1997; Fong, Rehfeldt & Jentsch 1998; Maduke, Williams & Miller 1998; Pusch et al. 2001; Bisset, Corry & Chung 2005). Its closest homologue, ClC-1, is exclusively expressed in the skeletal muscles and was identified in rat skeletal muscle tissue by homology screening (Steinmeyer, Ortland & Jentsch 1991). With a small single-channel conductance of about 1-1.5 pS, ClC-1 contributes 70~85% of the total membrane conductance under resting conditions in skeletal muscle (Pusch, Steinmeyer & Jentsch 1994). Accordingly, if the Cl^- conductance mediated by ClC-1 is blocked or genetically absent, repetitive firing of action potentials (myotonic runs) will be generated after one single stimulus, and as a result, the muscle can not relax, which characterizes the disease myotonia.

Screening of rat heart and brain using hClC-1 cDNA led to the identification of the third member of the CLC family, ClC-2, which is approximately 49 and 55 % identical to ClC-0 and ClC-1, respectively (Thiemann et al. 1992). It has a small conductance of ~3 pS (Nilius & Droogmans 2003) and is activated by hyperpolarisation, cell swelling and acidic extracellular pH (pH_o). Functionally, it was shown to be involved in epithelial transport, pH regulation and cell volume regulation (Grunder et al. 1992; Thiemann et al. 1992) and mutations in the *CLCN2* gene were found to be associated with idiopathic generalised epilepsy (Haug et al.

2003). Using degenerative primers against conserved regions of CLC channels Kieferle et al. (1994) cloned ClC-Ka and ClC-Kb, which were approximately 90% identical to each other, from human kidney. Requiring a β-subunit (barttin) for efficient transport to the plasma membrane and normal function (Estévez et al. 2001), these two channels are thought to play an important role in transepithelial Cl^- transport since they are found in the ascending limb of the loop of Henle and the collecting ducts of the nephron (Adachi et al. 1994). Not surprisingly then, mutations in the *CLCNKB* gene have been shown to lead to Bartter's syndrome type III (Simon et al. 1997), which is a severe salt-wasting disorder associated with low blood pressure, hypokalemic alkalosis, hypercalciuria, and normal serum magnesium levels. Currents from ClC-Ks have an anion selectivity sequence of $Cl^- \geq Br^- > NO_3^- > I^-$ for ClC-Ka/barttin and $Cl^- > Br^- = NO_3^- > I^-$ for ClC-Kb/barttin. They show only little voltage-dependent gating, consistent with the fact that the gating glutamate that obstructs the pore is replaced by valine in both ClC-Ka and ClC-Kb. Indeed, introducing a glutamate at that position generated voltage-dependent gating (Rai et al. 1999).

Recently, EhClC-A and EhClC-B from *Entamoeba histolytica* protozoa were identified and also grouped into the first branch of the CLC family (Salas-Casas et al. 2006). These two members are 58% identical to each other but only 25-30% identical with other CLC proteins. Currents elicited in *Xenopus* oocytes expressing EhClC-A feature rapid activation upon hyperpolarisation, inward rectification and a permeability sequence of $Cl^- > Br^- > I^- > F^- >> NO_3^-$, similar to ClC-2, and are strongly inhibited by the Cl^- channel blocker 4-acetamido-4'isothiocyanostilbene-2, 2'-disulphonic acid (SITS). Experiments at diverse pHs suggested that EhClC-A is not a Cl^-/H^+ exchanger, but it is an ion channel that could be involved in pH regulation (Salas-Casas et al. 2006). Although no functional characterization has so far been performed on EhClC-B, its similar characteristics to ClC-2 might indicate an analogous function.

The second branch of the family includes ClC-3, ClC-4 and ClC-5, which are located in the membrane of intracellular vesicles and are thought to be important in maintaining the pH of these vesicles (Stobrawa et al. 2001; Gunther, Piwon & Jentsch 2003; Mohammad-Panah et al. 2003). Of these, ClC-3 was the first to be cloned (Kawasaki et al. 1994); (Borsani et al. 1995). Generally speaking, ClC-3 is ubiquitously expressed and cell fractionation and transfection studies localized it to an endosomal/lysosomal compartment (Birkenhager et al. 2001). Synaptic vesicles from $CLCn3^{-/-}$ mice were acidified at slower rates compared with WT (Schlingmann et al. 2004), suggesting that ClC-3 provides an electric shunt for the electrogenic H^+-ATPase. A function of ClC-3 in regulating cell volume was also suggested,

although this issue has been controversial (Duan et al. 1997; Weylandt et al. 2001). Interestingly, members of the ClC-3 cluster, namely ClC-4 and ClC-5, have recently been reported to function as chloride/proton antiporters upon exogenous expression in both Xenopus oocytes and mammalian tsA201 cells (Picollo & Pusch 2005; Scheel et al. 2005). It is not too surprising though, since the vesicular CLC proteins support the acidification of endosomal-lysosomal compartments by compensating currents of vesicular H^+-ATPases, a mechanism that would work with either Cl^- channels or electrogenic Cl^-/H^+ antiporters. Probably as a consequence of defective endosomal acidification, the loss of ClC-5 leads to a stark reduction in proximal tubular endocytosis (Piwon et al. 2000) and to human Dent's disease (Lloyd et al. 1996).

Finally, ClC-6 and ClC-7, which share only ~45% identity, form a distinct branch of the family. An established sequence tag (EST) from the genome project was used to clone ClC-6 and this channel was then employed as the basis for a PCR-based strategy which led to the identification of ClC-7 (Brandt & Jentsch 1995). Upon overexpression in COS or CHO cells, epitope tagged ClC-6 was targeted to structures identified as endoplasmic reticulum (Buyse et al. 1998), but native ClC-6 was shown to reside in late endosomes (Pöet et al. 2006). It was originally reported that both of ClC-6 and ClC-7 were very broadly expressed, e.g. in brain, testes, muscle and kidney (Brandt & Jentsch 1995), however, Poët and colleagues showed that ClC-6 was nearly exclusively expressed in neurons of the central and peripheral nervous system, with a particularly high expression in dorsal root ganglia (Pöet et al. 2006). A progressive neuropathy of the central and peripheral nervous systems was observed from $CLCn6^{-/-}$ mice with features of neuronal ceroid lipofuscinosis (NCL), a subtype of human lysosomal storage disease, showing reduced pain sensitivity and moderate behavioral abnormalities (Pöet et al. 2006). In addition to the already mentioned ClC-Ka and ClC-Kb, ClC-7 also requires a β-subunit (Ostm1) for proper bone resorption and lysosomal function (Lange et al. 2006). It resides in late endosome and lysosomes (Kornak et al. 2001). Similar to the acidification of renal endosomes or synaptic vesicles, which relies on ClC-5 or ClC-3 respectively, it is thought that the electrically neutralizing Cl^- current through ClC-7 is required for an efficient acidification of the resorption lacuna (Kornak et al. 2001). Correspondingly, it has been well demonstrated that disruption of ClC-7 can cause osteopetrosis and lysosomal storage disease in both humans and mice (Kornak et al. 2001; Kasper et al. 2005). A brief comparison of major properties of vertebrate CLC proteins is summarized in table 1.

Table 1: Properties of Vertebrate CLC proteins (modified from Jentsch *et al*. (2005))

		Expression					
Name	Species	Tissue	Membrane	Biophysics	Function	Mouse model	Human disease
ClC-0	Torpedo	Electric Organ	PM (non-innervated membrane)	Cl^- channel common gate: hyperpol activated; protopore gate: depol-activated	Stabilization of membrane V	n.a.	n.a.
ClC-1	Mammals	Skeletal muscle	PM	Cl^- channel common and protopore gates: activated by depol.	Stabilization of membrane V	Myotonia	Myotonia (recessive and dominant)
ClC-2	Mammals	Broad	PM (basolateral in intestine)	Cl^- channel activated by: hyperpol, swelling, acidic pH_o	Epithelial transport, regulation of pH, cell volume	Degeneration of tests and retina	Epilepsy
ClC-Ka +barttin	Mammals	Kidney and ear	PM (basolateral)	Cl^- channel V-independent activated by: alkaline pH_o, $[Ca]_o$	Epithelial transport	Diabetes insipidus	Together: Bartter's syndrome (renal salt loss+ deafness)
ClC-Kb +barttin	Mammals	Kidney and ear	PM (basolateral)	Cl^- channel V-independent activated by: alkaline pH_o, $[Ca]_o$	Epithelial transport	Bartter renal salt loss	
EhClC-A / B	protozoa		PM	Hyperpol activated, inward rectification	Ph regulation		
ClC-3	Mammals	Broad	EndosomesSynaptic vesicles	Cl^- channel or Cl^-/H^+ exchanger?Depol.-activated, pH-sensitive currents	Endosomal and/or synaptic vesicle acidification	CNS degeneration (loss of hippocampus, blindness)	
ClC-4	Mammals	Broad	Endosomes	Cl^-/H^+ exchanger. Depol.-activated, pH- sensitive currents	Endosomal acidification		
ClC-5	Mammals	Kidney intestine	Endosomes	Cl^-/H^+ exchanger. Depol.-activated, pH- sensitive currents	Endosomal acidification, endocytosis	Proteinuria, change in Calciotropic hormones	Dent's disease, proteinuria, kidney stones
ClC-6	Mammals	Neurons	Endosomes	Channel or exchanger? (no currents available)	Endosomal Acidification	progressive neuropathy	
ClC-7 + Ostm1 β-Subunit	Mammals	Broad	Late endosomes, lysosomes	Channel or exchanger? (no currents available)	Lysosomal acidification	Osteopetrosis, blindness, Lysosomal storage disease	Osteopetrosis, lysosomal storage disease

1.2 STRUCTURAL CHARACTERISTICS OF THE CLC PROTEINS

A first hint regarding the structure of CLC proteins was obtained by Miller and colleagues in the early nineteen eighties (Miller 1982; Miller & White 1984). After incorporation of membrane extracts from *Torpedo* electroplaques into planar phospholipid membranes, single-channel currents could be recorded at high time-resolution. They were able to demonstrate a characteristic "bursting" process in which the open channel fluctuated rapidly between three substates, with conductances of 18.5, 9.4 and 0 pS in 150 mM Cl^-. Under various ionic conditions the three substates were always equally spaced in conductance, whereas various voltages led to different probabilities of observing the three substates (Miller 1982). Based on the equal spacing in conductance, a binomially distributed probability of appearance of the substates and "dimeric" transition probabilities among the substates, they proposed the famous "double-barreled shotgun" model for the channel. This model suggested that ClC-0 functions as a complex of two identical subunits, each opening and closing independently on a time scale of milliseconds, while together entering and leaving an inactivated state on a slower time scale (Miller 1982; Miller & White 1984). This double-pore architecture has been overwhelmingly supported by the sum of the experimental evidences even before crystal structures were resolved (Pusch & Jentsch 2005). Firstly, the ratio of the ClC-0 conductance levels does not depend on ionic conditions and is valid over a large voltage range. Secondly, the substates show binomial distribution, exactly as expected from two pores that are gated independently. Finally, stilbenedisulfonate 4,4-diisothiocyanatostilbene-2,2′-disulfonic acid (DIDS) inhibited ClC-0 in a two-hit process, which led at first to the disappearance of the ~20 pS state, then followed by a total inhibition, suggesting that one molecule inhibited one pore at a time (Hanke & Miller 1983). Also, this model was supported later by three substates (0 pS, 9 pS and 18 pS) observed from single channel analysis on heterologously expressed ClC-0 (Bauer et al. 1991; Middleton, Pheasant & Miller 1994). Correspondingly, three equidistant single channel current levels with binomial distribution were also found in ClC-1 (Saviane, Conti & Pusch 1999).

From a physiological point of view, if it is true that each pore is completely contained within one subunit, then each pore should retain its individual properties, such as ion selectivity and single-channel conductance, even when forced together in an artificial heterodimer. Therefore, if heterodimerization occurs, this may change channel localisation, gating and other types of regulation, but it is unlikely to alter the properties of the open pore. Mutations of CLC channels that reduce single-channel conductance of fast gating, thus, should generally not have dominant-negative effects on co-expressed wild-type subunits. After cloning of

ClC-0, this notion was very well proved by protein purification, concatamers and site-directed mutagenesis. For example, Ludewig and colleagues provided corroborating evidence using mutant S123T, which changed rectification, ion selectivity and gating of the channel, but retained the typical bursting behaviour with two identical independent albeit reduced, conductance states (approximately 1.5 pS). Co-expression of S123T with WT ClC-0, either as covalently linked concatamers or as independent proteins, led to bursting channels with two different pores (Ludewig, Pusch & Jentsch 1996). Moreover, when heterodimeric channels were generated by co-expressing ClC-0 and ClC-1, ClC-0 and ClC-2, or ClC-1 and ClC-2, single channels with two nonidentical but independent pores were observed (Weinreich & Jentsch 2001). This is in contrast to some cation channels, such as K^+ channels. In these tetrameric channels, four subunits jointly form the pore, thereby leading to changes in pore properties when different subunits are mixed (Zhorov & Tikhonov 2004).

Ultimately, the three-dimensional structures of StCLC and EcCLC confirmed, beyond doubt, the dimeric architecture implied from functional studies (Dutzler et al. 2002) and, because of the high homology within the family, it is predicted to apply to all CLC proteins.

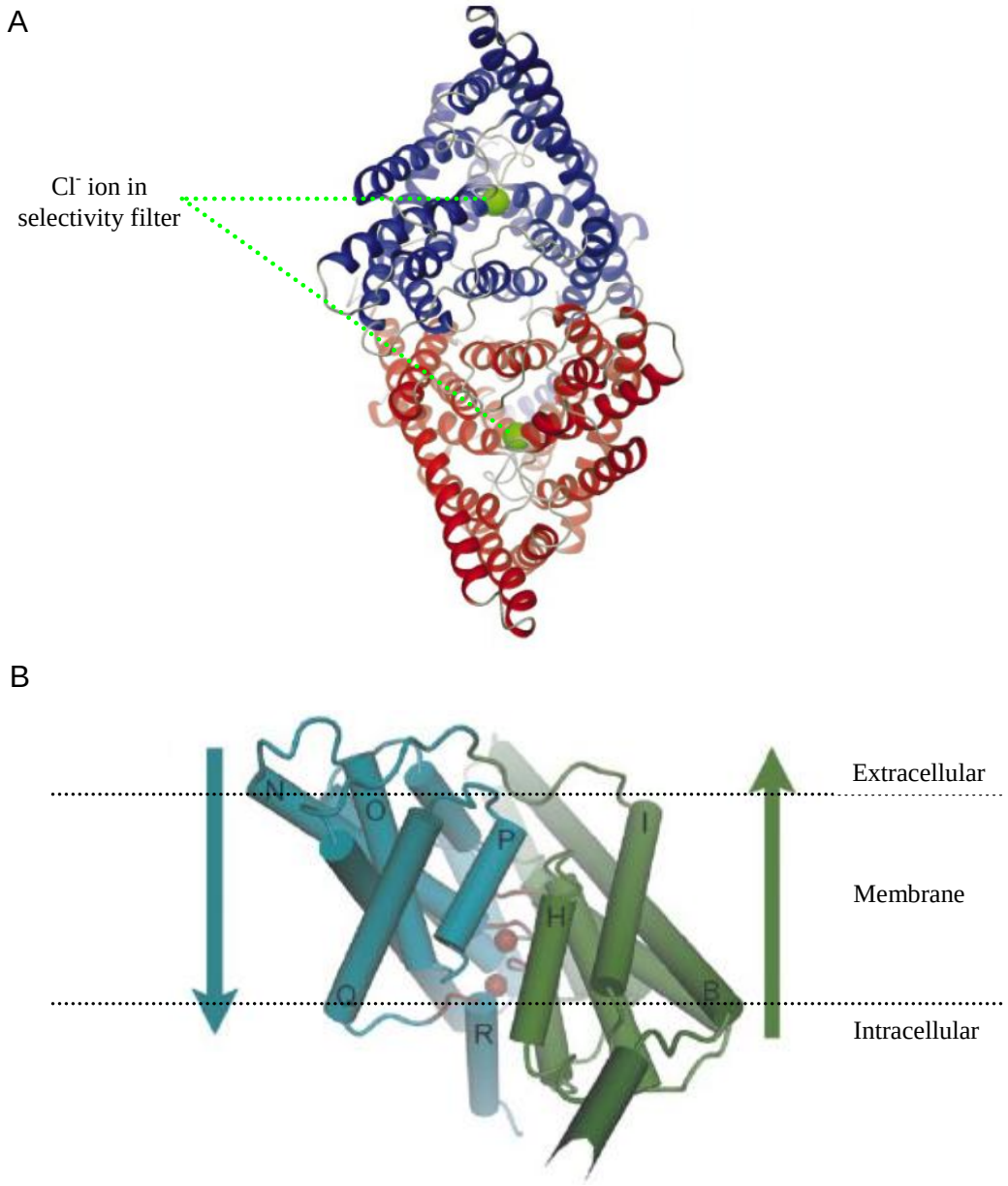
1.2.1 THE GENERAL STRUCTURE OF THE MEMBRANE-RESIDENT DOMAIN

All members of the CLC family share a conserved subunit structural organization consisting of a membrane-resident catalytic domain and, in many cases, a lengthy carboxyl tail that includes cytoplasmic regulatory domains. In many ways, these CLC proteins, like other channels and transporters, resemble enzymes that specifically function to conduct or transport a flow of Cl^- ions through themselves. Hence, I have referred to their "catalytic" domain. Bacterial CLCs (of ~400 amino acids) correspond to the N-terminal half of their vertebrate counterparts, a critical portion of the protein that is embedded in the lipid bilayer and forms the ion-permeation pathway (Dutzler et al. 2002). Therefore the X-ray crystal structures of bacteria CLC transporters, StCLC and EcCLC, serve as an excellent model for the membrane-resident domain of all the CLC members.

According to the structure of StCLC and EcCLC determined by X-ray crystallography at 3.0 Å, each subunit of the homodimeric protein is composed of 18 α-helices (labelled as helix A-R), and looks triangular when viewed along the two-fold axis from outside of the cell. This means that the entire dimeric channel is shaped like a rhombus (Fig.1A) (Dutzler et al. 2002). Between the two subunits, there is a broad interface which involves helices H, I, P, and Q. Rather than consisting of straight membrane-spanning helices of about equal size, helices of each subunit are of variable length with most not spanning the whole membrane but lying

within and at considerable oblique angles to the plane of the membrane. Each subunit consists of an N-terminal half (α-helices B-I) and a C-terminal half (J-Q) that are structurally related to each other and span the membrane with opposite orientations forming an "antiparallel architecture" (Fig.1B). Such an antiparallel architecture had only been observed in the aquaporin superfamily previously (Accardi & Pusch 2000) but has now been found to be a versatile construction principle for several transmembrane transport proteins (Zheng et al. 2004; Hunte et al. 2005; Yamashita et al. 2005). This architecture permits like ends (the same dipole sense) of α-helices to point at the membrane centre from opposite sides of the membrane (with a 180° angular separation) thus forming the Cl^- ion selectivity filter within the membrane to stabilize (or destabilize) ions through electrostatic and chemical interactions (Dutzler et al. 2002).

Figure 1 Structural views of bacterial CLC protein (modified from Dutzler et al. 2002)



(A). Structure of StCLC subunit viewed from the extracellular side. The two subunits of the homodimeric protein are coloured in red and blue respectively. **(B)**. Structure of StCLC subunit viewed from within the plane of the membrane from the dimer interface. The a-helices are drawn as cylinders and loop regions as cords. Arrows indicate the orientation of two halves of the protein in the membrane, and bound ions are shown as red spheres. Regions of the protein contributing to the ion selectivity filter are coloured in red (Dutzler et al. 2002).

1.2.2 THE PORE REGION AND THE SELECTIVITY FILTER

At the interface between the two halves of each subunit, the ion translocation path contains a Cl^- selectivity filter in the neck of an hourglass-shaped pore (Fig. 2A). This narrow 15 Å long selectivity filter is formed by the ends of helices that do not cross the membrane and harbours three selective anion-binding sites, named S_{int}, S_{cen}, and S_{ext} according to their location in the filter (Dutzler, Campbell & MacKinnon 2003). Ions bind with similar affinity to the outer two sites, S_{cen} and S_{ext}, which are approximately 4Å apart (Lobet & Dutzler 2006). A third binding site, S_{int}, is found on the intracellular face of the protein, only about 7Å away from S_{cen}. Ions bind to this intracellular site with lower affinity, because S_{int} is still partly in contact with the solution (Lobet & Dutzler 2006). It is still unclear how ions move between the S_{int} and S_{cen} sites, since the pathway between these two sites appears to be narrowed significantly by neighboring hydrophobic side-chains and by the protein's backbone (Figure 2C). Nonetheless, when the channel opens and the three binding sites are exposed to high extracellular Cl^- concentration, all of them can bind Cl^- ions at the same time with mM (4-40 mM) affinity. The stabilizing effect of the protein arises from hydrogen bonding and longer-range favourable interactions, such as dipole attraction (Faraldo-Gomez & Roux 2004; Lobet & Dutzler 2006). In a cellular environment, however, the binding sites S_{int} and S_{cen} are only exposed to the low intracellular Cl^- concentration ($\sim$5 mM in muscle cells, and up to 40 mM in certain other cells). Consequently S_{cen} would still be occupied, whereas S_{int} would mostly be empty (Lobet & Dutzler 2006).

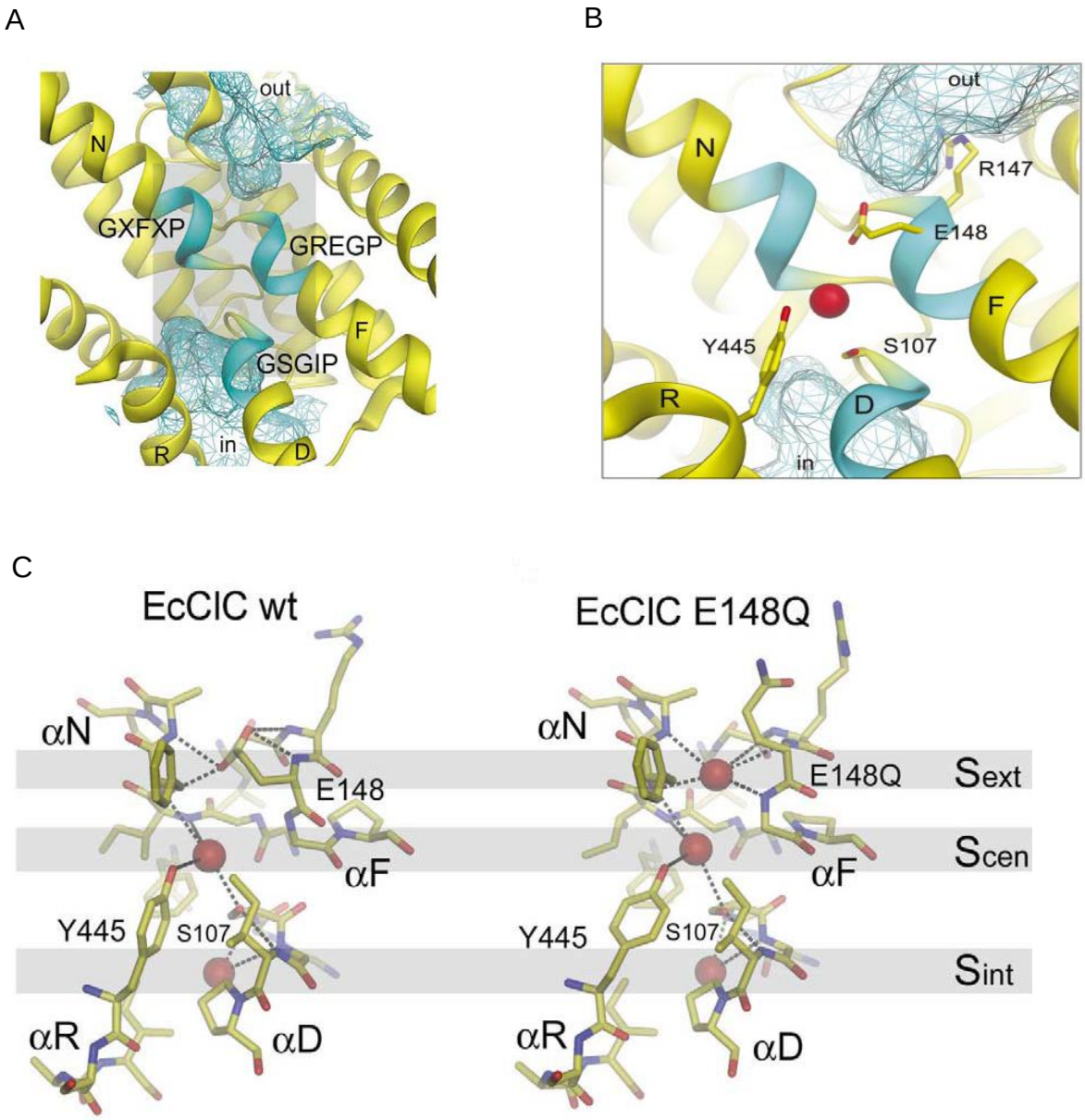
This is in contrast to K^+ channels, in which the four consecutive ion-binding sites are never fully occupied by K^+ but rather a single file of alternating K^+ ions and water molecules bind to the K^+ selectivity filter (Morais-Cabral, Zhou & MacKinnon 2001; Zhou & MacKinnon 2003). Also, the K^+ channel selectivity filter undergoes a conformational change into a nonconducting conformation when the K^+ concentration is lowered to 3 mM. It has been proposed that the energy required to change the selectivity filter into a conducting conformation in K^+ channels weakens its affinity for the ion and, therefore, contributes to an increased conduction rate (Morais-Cabral, Zhou & MacKinnon 2001; Zhou & MacKinnon 2003). In this regard, the CLC selectivity filter again differs from that of K^+ channel by retaining its conformation even in the absence of bound ions, which could contribute to the generally lower conduction rates observed in CLC channels when compared to K^+ channels (Lobet & Dutzler 2006).

Bridging the two aqueous vestibules on either side of the membrane, the CLC selectivity filter is formed by four highly conserved regions (three of these conforming to the consensus

sequence, GXXXP), including the amino terminals of helix D (GSGIP, 106-110), helix F (G(K/R)EGP, 146-150) and its symmetrical partner helix N (GXFXP, 355-359) along with Tyr445 in helix R (Figure. 2B, 2C) (Dutzler et al. 2002; Dutzler, Campbell & MacKinnon 2003; Lobet & Dutzler 2006). It is significant that these sequences occur at the N termini of α-helices, because the helix dipole, or N-terminal positive end charge, creates an electrostatically favourable environment for binding anions and stabilizing them by electrostatic interactions (Figure 2C).

There is only a moderate selectivity for Cl^-/Br^- at these three binding sites which probably reflects the fact that only Cl^- plays a role as a permeant anion in biological systems (Lobet & Dutzler 2006). In the WT protein, two of the binding sites (S_{int} and S_{cen}) are occupied by Cl^- ions, whereas the third site at the extracellular end of the filter is occupied by the sidechain of a conserved glutamate residue E148 (equivalent to E232 in ClC-1), which binds to this site like a tethered anion (Figure 2C left). When this residue is mutated to glutamine, the binding site is emptied and binds a Cl^- ion instead, while leaving the remainder of the filter unchanged (Figure 2C right). Therefore, it has been proposed that for Cl^- conduction to occur, the glutamate side chain has to swing out of the way, permitting the entry of a Cl^- ion in its place (Dutzler, Campbell & MacKinnon 2003). These two conformations of the selectivity filter, the blocked conformation of the WT structure and the opened conformation of the mutant, have important implications for both physiological/functional properties—gating in the ion channels, and coupled transport in the H^+/Cl^- exchangers (Dutzler 2006)— which will be discussed later.

Figure 2. Structure of the ion conducting pore and the selectivity filter in StCLC and EcCLC



(A). Structure of the ion conduction pore of StCLC viewed from the dimer interface along the pseudo two-fold axis. Front α-helices are removed for clarity and the protein is drawn as a ribbon. Aqueous cavities, which approach the selectivity filter from the extracellular side (out) and the intracellular side (in), are shown as a cyan mesh. Structures involved in ion binding are indicated in cyan and the conserved stretches of residues are labelled. Selectivity filter region is highlighted in grey (Dutzler 2004). A closer view of the selectivity filer in (A) is shown in **(B)**, with a Cl^- ion (red sphere) bound in the centre. Selected residues from the

conserved stretches labelled in (A) are shown as sticks (Dutzler et al. 2002). **(C).** Blow-up of the selectivity filters of the WT EcCLC protein and mutant E148Q. Selected residues in the vicinity of the bound ions (red spheres) are shown as sticks. Dashed lines indicate interactions between bound ions and hydrogen bond donors in the protein. Cl^- ion binding sites are labelled (S_{ext}, S_{cen} and S_{int}). Left: the selectivity filter in a closed conformation as seen in the structure of the WT protein. Two Cl^- ions are bound to S_{int} and S_{cen}, whereas the filter is blocked by the sidechain of a conserved glutamate residue E148 (E232 in hClC-1) which occupies S_{ext}. Right: the selectivity filter in an open conformation in mutant E148Q. An additional ion can now bind to the site S_{ext} because the sidechain of mutated Gln (Q) has moved out of the filter (Dutzler 2004). These figures are reproduced by permission from Macmillan Publishers Ltd.: Nature, Dutzler et al. (2002), copyright 2002, http://www.nature.com) and Elsevier Publishers Ltd.: FEBS Letters, Dutzler (2004), copyright 2004, http://www.febsletters.org).

1.3 PHYSIOLOGICAL PROPERTIES OF CLC CHANNELS/TRANSPORTERS

Ion flux across membranes is the basis for many important cellular physiological processes such as electrical signalling, control of the cell volume, ion homeostasis, etc. There are two critical conditions for channels/transporters to carry out their functions accurately and efficiently: the ability to selectively transport a certain kind of ion and to do this at the right time. Of these, the first is dependent on physiological properties called ion selectivity and permeation, whereas the second is fulfilled by another property called gating.

1.3.1 ION SELECTIVITY AND PERMEATION

Unlike many cation channels, selectivity is not very strict in anion channels, as they often allow more than one kind of ion to go through the pore, with one main ion being preferred.

For the CLC channels, Cl^- itself acts as the gating charge as it moves from an external binding site into a filter binding site (Chen & Chen 2001; Dutzler, Campbell & MacKinnon 2003). In addition, a Cl^- in the selectivity filter was suggested to be required for the pH-dependent gating mechanism (Dutzler, Campbell & MacKinnon 2003). Studies on the effect of anions other than Cl^- on hClC-1 channels have divided these ions into three groups according to their ability to gate the channel and to permeate it. Anions that neither permeate nor gate the channel, anions that do not permeate the channel but can gate it and block currents, and those anions which permeate and gate the channel (Rychkov et al. 1998). If the external Cl^- is substituted with anions in the first group, the deactivation curve will shift to more positive potentials, showing that the shift of voltage dependence of the channel is due to the absence of Cl^- instead of the presence of the foreign anion. In contrast to ClC-0, for which only permeant anions are believed to affect channel opening (Pusch et al. 1995), the existence of the second group of ions (impermeant anions which can affect gating) gives a picture of a rather complex interaction between permeation and gating in hClC-1. Despite the identification of the permeation pathway, the mechanism of ion permeation is still not completely clear.

1.3.2 GATING

Gating is a property of ion channels which allows them to open and close their permeation pathway to regulate ion flow in response to external stimuli, such as ligand binding, changes in intracellular Ca^{2+}, or changes in voltage (Weinreich & Jentsch 2001). In voltage-dependent cation channels, such as the K^+ channel, the fourth membrane-spanning segment (S4) which contains four to eight positively charged residues (arginines or lysines, each separated from the next by two hydrophobic residues) is thought to respond to voltage and hence work as a

voltage sensor (Weinreich & Jentsch 2001). Although CLC channels are also voltage-gated, compared with S4-type cation channels, their voltage dependence is ~5 to ~10-fold weaker (Saviane, Conti & Pusch 1999). Moreover, what makes the gating of CLCs unique and complex is that they do not have any structural "voltage sensor" equivalent to S4. Instead, for Cl^- to reach its binding sites in the selectivity filter, it has to go through the transmembrane electric field and gating is therefore dependent on both Cl^- itself and voltage.

A tight link between ion permeation and gating in CLC channels was first demonstrated by Pusch and colleagues (Pusch et al. 1995), who observed a shift of open probability (P_o) vs. voltage curve toward a more hyperpolarised membrane potentials (favouring the open state) upon increasing $[Cl^-]_o$. At single channel level, external Cl^- was shown to increase the opening rate significantly but to have only a very small effect on the closing rate, which was much more sensitive to intracellular Cl^- (Pusch et al. 1995; Chen & Miller 1996; Chen & Chen 2001). As discussed above in 1.2.2, with the elucidation of the X-ray crystal structure of EcCLC and StCLC as well as more elegant experimental and theoretical studies of the ion binding properties of the selectivity filter, it has now been accepted that the three binding sites within the selectivity filter can bind Cl^- ions at the same time with mM affinity (Faraldo-Gomez & Roux 2004; Lobet & Dutzler 2006).

It has been very well accepted for a long time that the gating of ClC-0, ClC-1 and ClC-2 is controlled by multiple mechanisms. For example, direct examination of a single channel current recording trace from ClC-0 already suggests two kinds of gating processes. One of these, within a burst, opens in response to more positive voltages (depolarization) with gating kinetics in millisecond range, is called fast gating. Its open probability is increased by raised extracellular $[Cl^-]_o$ and $[H^+]_o$. The other opens in response to more negative voltages (hyperpolarization) and, when it is closed, leads to long inactivated periods that separate the bursts of channel opening. It has a transition time in the range of seconds, is therefore called slow gating (Pusch & Jentsch 1994). Slow gating can be affected by many factors, which will be discussed later. In hClC-1, these two gating processes also exist, but they both have kinetics in the millisecond range, so one is often called protopore gating (fast gating) and the other is usually called common gating (slow gating) based on their sites of operation. Interestingly, in channel ClC-2, the voltage dependence of gating is reversed, open on hyperpolarization for both fast and slow gating (Zuniga et al. 2004); whereas the prokaryotic CLC homologue, EcClC, does not have any voltage dependent gating (Accardi et al. 2004).

1.3.2.1 FAST GATING

While functional studies using site-directed mutagenesis and electrophysiological recording in the muscle-type CLC channels had partially identified several important residues for gating mechanisms before any crystal structures were available, the critical roles for some of these were immediately apparent after the bacterial CLC structure was resolved. For example, mutation of the critical glutamate in CLC proteins (E148 in StClC, E166 in ClC-0, E232 in ClC-1 and E217 in ClC-2) was already known, or soon found, to have a dramatic effect on channel gating (the fast gating is in the open state most of the time) (Fahlke et al. 1997; Niemeyer et al. 2003; Miloshevsky & Jordan 2004; Traverso et al. 2006). But the molecular basis for these results was clear only when the crystal structure of bacterial CLC revealed the pore lining position of this critical glutamate (Dutzler et al. 2002; Dutzler, Campbell & MacKinnon 2003). Dutzler and his colleagues (2002) then proposed this glutamate to correspond to the fast gate, since both mutants, E148A and E148Q, were observed to have a fast gate that stayed open. This proposal perfectly fits the idea that each pore works independently and that fast gating only has a local effect, so it has been widely accepted.

Once bacterial CLCs had been demonstrated to be H^+/Cl^- anti-porters (Accardi et al. 2004), it seemed that, to some extent, a similar mechanism might also be operating in the ClC-0 channel. The pH-dependence of gating was proposed to be due to a protonation of the gating glutamate, i.e. at high extracellular pH the deprotonated carboxyl sidechain of the glutamate occludes the Cl^- permeation pathway, while upon protonation at low pH, the carboxyl group swings away from the pore and permits unimpeded access of Cl^- to the extracellular solution (Dutzler, Campbell & MacKinnon 2003). This pH-dependence was indeed abolished when the glutamate was mutated in ClC-0 and the known effect of lowered extracellular pH in opening ClC-0 is thus specifically attributed to protonation of the glutamate sidechain (Chen & Chen 2001; Yin et al. 2004). However, other parts of the protein may also contribute to pH-sensitivity, as ClC-K channels are modulated by pH but lack a glutamate at this position (Sauve et al. 2000; Lourdel et al. 2003; Nissant et al. 2006).

This fast gating mechanism is compelling, since it explains the pH dependence of gating and, at the same time, the constitutive activity of a ClC channel isoform in which a neutral residue replaces gating glutamate. But it does not account for voltage or Cl^- dependence and accordingly there are people who thought that this proposal was puzzling in the light of several functional observations (Chen 2003). First, the fast gating of ClC-0 is regulated not only by $[Cl^-]_o$, but also by $[Cl^-]_i$. If the glutamate side chain is the gate opened by the external

Cl^-, what is the mechanism responsible for the internal Cl^- control of the fast gate closure? Second, the apparent affinity for external Cl^- to control fast gating is ~50 mM. When $[Cl^-]_o$> 150-300 mM, this gating effect was nearly saturated (Dutzler, Campbell & MacKinnon 2003; Zuniga et al. 2004). But it seemed doubtful that S_{ext} would have such a high affinity for Cl^- given that Cl^- competes with a fixed negative charge in the pore (Chen 2003). Third, previous mutational studies showed that mutations of K165 and K519 in ClC-0 both affect the fast gating (Dutzler et al. 2002), even though these two residues are separated by more than 25 Å and are facing the extracellular and intracellular solutions respectively. How could two such distant residues regulate the same gating mechanism? These functional observations together raised concerns about the original proposal and led to the suggestion that larger conformational changes are involved in fast gating (Chen 2003).

Actually, there was already other evidence indicating that fast gating might not be as simple as only a residue swinging in and out of S_{ext} in the selectivity filter to open and close the pore. For example, Accardi and Pusch (2003) used a slow gating-deficient mutant of ClC-0, C212S, to study the mechanism of inhibition of ClC-0 by the clofibric acid–derivative p-chlorophenoxy-acetic acid (CPA). Binding site of CPA was mapped to a hydrophobic pocket that overlaps the S_{cen} to some extent (Dutzler et al. 2002; Dutzler, Campbell & MacKinnon 2003). Open channels are blocked by CPA with low affinity (K_D^O = 45 mM at 0 mV) and fast dissociation (k_{off} = 490 s^{-1} at -140 mV). In contrast, the blocker binds to closed channels with higher affinity and much slower kinetics. If the fast gating only involves a small movement of a glutamate side chain, mutations that influence CPA binding should have similar effects on an open and closed channel since the general structure of the pore would remain largely unchanged. However, out of the four point mutations that lie close to the putative selectivity filter, T471S alters CPA binding to closed channels, exclusively, whereas S123T, Y512A and K519Q showed pronounced effects on the open channel block. These results suggested that the structure of the CPA binding site is different in the open and closed state, thus channel opening of the fast gate in ClC-0 involves more than a local conformational change of a side chain. Other parts of the channel and of the selectivity filter are probably also involved (Accardi & Pusch 2003).

At the same time, Traverso and colleagues (2003) tested the blocking effect of CPA on the constitutively open mutants E166A and E166S in ClC-0. This glutamate residue (equivalent to E148 in StClC), which is proposed to be the fast gate, has also previously been proposed to form part of the CPA binding site (Estévez et al. 2003). Traverso et al. (2003) therefore expected that the open mutants E166A and E166S would be blocked by CPA with low

affinity similar to the open channel block of the WT ClC-0. However, results showed that CPA exerted a strong, high affinity block comparable to the closed state block of WT ClC-0. Further analysis indicated that these mutants with a constitutively open fast gate could assume a conformation that closely resembled the closed state of WT ClC-0 and that CPA strongly stabilised this conformation (Traverso, Elia & Pusch 2003). These results contradict those from Dutzler *et al.* (2003), in which E166 mutants cannot undergo any conformational closure since the channel lacks the negatively charged glutamate side chain (Dutzler, Campbell & MacKinnon 2003). This provides additional evidence to suggest that the fast gating of ClC-0 might involve more than the side chain movement of E166, such as a conformational constriction of the pore in addition (Moran et al. 2003).

1.3.2.2 COMMON GATING

Compared to fast gating, common gating of CLC Cl^- channels appears to be mechanistically much more complex, so there is still little known about it. Despite a high degree of similarity between the fast (protopore) gating of ClC-0 and of ClC-1, the slow (common) gating of these two channels has quite different characteristics.

Upon hyperpolarization, the common gate of ClC-0 opens within seconds, and, once opened, closes more slowly at positive voltages, perhaps not closing completely even then (Fahlke et al. 1995; Pusch et al. 1995; Chen & Miller 1996; Chen & Chen 2001). Several factors, such as membrane potential, Cl^-, Zn^{2+}, pH and temperature affect the common gating of ClC-0. For example, early studies on the native ClC-0 channel from the *Torpedo* electric organ indicated that common gating favours a nonconducting, inactivated channel state upon membrane depolarization and low external pH (pH_o) favours the opening of the common gate (Hanke & Miller 1983). Operation of the common gate is also affected by the Cl^- gradient across the channel pore. A reduction of the extracellular Cl^- concentration, $[Cl^-]_o$, favours the inactivated state (Pusch et al. 1995; Chen & Miller 1996). Activation of the common gate at hyperpolarised potentials can, however, also be inhibited by low intracellular Cl^- concentration, $[Cl^-]_i$ (Pusch et al. 1999). Moreover, extracellular Zn^{2+} was shown to reversibly inhibit the ClC-0 by facilitating common gate closure at all temperatures (Chen 1998). Most surprisingly, Pusch and his colleagues found that the common gating of ClC-0 was extremely temperature dependent with a Q_{10} (fold change in the reaction rate in response to a 10°C change in temperature) of ~40 (Pusch, Ludewig & Jentsch 1997), which is comparable to that of the most sensitive temperature-activated transient receptor potential (TRP) channels (Jordt, McKemy & Julius 2003). Such temperature sensitivity of the common gating of ClC-0 is

much more significant than its fast gating, whose Q_{10} is only 2.2 (Pusch, Ludewig & Jentsch 1997).

In ClC-1, the common gating is different from that of ClC-0 in several aspects. First, it opens with depolarization instead of hyperpolarization (Saviane, Conti & Pusch 1999). Second, common gating of ClC-1 is much faster than ClC-0, with transition times on the order of tens of milliseconds, comparable to that of ClC-1 fast gating (Saviane, Conti & Pusch 1999). Third, common gating of ClC-1 is regulated by extracellular Cl^- concentration in a similar way to that of ClC-0, i.e. decreasing the $[Cl^-]_o$ reduces the P_o of the common gating (the curve is shifted to more depolarizing potentials), but change of intracellular Cl^- concentration has no effect on ClC-1 (Rychkov et al. 1996a). Fourth, ClC-1 can also be blocked by extracellular Zn^{2+}, which acts on common gate and favours the closed state, but in this case, in an irreversible way (Duffield et al. 2005). Here, washing off the Zn^{2+} is insufficient and the block can only be reversed by treatments such as acidification and exposure to chelating agents. Fifth, gating and conductance in ClC-1 are also affected by pH, but in a more complex way. When external pH (pH_o) is reduced, the deactivating inward currents of ClC-1 are diminished without change in time constants while the steady-state component is enhanced. At extremely low pH_o, kinetics become independent of the Cl^- concentration in ClC-1 and a current activated by hyperpolarization can be revealed. In contrast, reduced internal pH (pH_i) slows deactivating current kinetics and the P_o curve is shifted in the hyperpolarizing direction (Rychkov et al. 1996a). Finally, common gating of ClC-1 can also be regulated by temperature, but in a much milder way (Q_{10} of ~4) compared with ClC-0. Also, unlike ClC-0, both fast and common gating of ClC-1 show a similar sensitivity to temperature with fast gating having a Q_{10} of ~3 (Bennetts et al. 2001). Apart from being a biophysical tool, the temperature dependence of ClC-1 may also be of physiological or pathophysiological importance, as cooling aggravates myotonic symptoms in some patients (Michel et al. 2007).

Operation of the common gate on both protopores simultaneously and its dependence on the temperature have led to the belief that the mechanisms of common gating must involve subunit-subunit interactions and large conformational rearrangements. These interactions could involve the broad contact interface between the two subunits within the membrane, interactions between the cytosolic tails, or both (Estévez & Jentsch 2002). Interestingly, several relevant mutations have been found in helices at the subunit interface (helices H, I, P, Q). For example, naturally occurring myotonic mutations V286A and I290M change residues in helix H, whereas mutations F307S, A313T and R317Q change residues in helix I (Pusch 2002). Moreover, Cys546 in helix P of ClC-1 appears to have a role in binding Zn^{2+} (Kurz et

al. 1999). What's more, deletions or mutations in the C-terminal intracellular domain have also been shown to affect common gating kinetics (Fong, Rehfeldt & Jentsch 1998; Hryciw et al. 1998; Estévez et al. 2004; Hebeisen et al. 2004; Wu et al. 2006; Accardi 2008). Connecting the C-tail cytoplasmic structures to the membrane-resident domain, is the quite intriguing R-helix. Permeating ion coordination occurs through a tyrosine at its amino terminus, whereas its C terminus protrudes into the cell, potentially providing a mechanism to affect channel function from the cytosol. Some mutations in the R-helix affect common gating, too (Ludewig, Jentsch & Pusch 1997). In general, although we have known that it can be affected by numerous point mutations, little is known about the molecular nature of common gating and just how these mutations modulate it.

On the other hand, considerable efforts have been made to investigate possible structural changes associated with common gating process. A successful example is a recent FRET study showing that the common gating of ClC-0 is associated with a large movement in the C terminus (Bykova et al. 2006). They found that closure of the slow gate is associated with a physical separation of the C termini of the two subunits, causing a large increase in the distance between the fluorophores attached to them. Opening of the slow gate, on the other hand, is accompanied by movements decreasing the distance between the two C termini (Bykova et al. 2006). Now more elegant studies are required to investigate how such movement of the C-tails can be related to the ion translocation and whether the same mechanisms also work for other family members.

To sum up, the fast gating voltage dependence arises from movement of the permeant ion through the transmembrane field (Pusch et al. 1995; Rychkov et al. 1996a; Cohen & Schulten 2004; Corry, O'Mara & Chung 2004); slow gating is also energetically coupled to the transmembrane Cl^- gradient (Pusch et al. 1995; Chen & Miller 1996; Rychkov et al. 1996a; Pusch et al. 1999; Dutzler 2004). Hence, gating, permeation and Cl^- binding are all tightly coupled in CLCs, which makes their gating mechanisms quite complex but very interesting as well.

1.4 CHANNELS vs TRANSPORTERS

Although channel-like properties in transporter families or vice versa have been described before, the CLC proteins are the first family where channels and transporters coexist with a very similar and conserved structural core (Gadsby 2004). This surprising property of CLC proteins was first discovered when EcClC was found to work as secondary active ion transporter in which the flux of Cl^- is stoichiometrically coupled to the flux of H^+ in the

opposite direction. When a sufficient driving force is provided, the protein is therefore able to pump Cl^- uphill against a concentration gradient at the expense of H^+ moving downhill or vice versa (Accardi & Miller 2004). Instead of being restricted to bacteria CLCs, this functional diversity has been demonstrated to be a universal property of eukaryotic family members residing in intracellular membranes, such as ClC-4, ClC-5 and ClC-7 (Picollo & Pusch 2005; Scheel et al. 2005; Graves et al. 2008).

Nevertheless, it is clear that muscle-type CLC members are channels instead of transporters, because firstly, currents from muscle-type CLC channels are understood to be Cl^- fluxes through ion-diffusion pores. This conclusion is based on the fact that reversal potentials for these channels follow faithfully the imposed Cl^- gradients and are not altered by external or internal pH (Rychkov et al. 1996a; Chen & Chen 2001). Secondly, single-channel conductance of these channels is too large for the slow turnover rate of a transporter (Chen 2005). Thirdly, applying the same method as used for ClC-4 and ClC-5, no proton transport activity has been shown in ClC-0 and ClC-Ka, although a small but reproducible proton transport activity was detected for ClC-1 (Picollo & Pusch 2005) and the acidification-dependent activation of ClC-2 has recently be shown to be mediated by protonation of pore gate glutamate 207 (Niemeyer et al. 2009).

1.5 CYTOPLASMIC TAILS

Carboxyl-terminal tails of ion channels and transporters are critical for many plasma membrane-associated functions, such as regulating the trafficking of the proteins to and from recycling endosomes (Kurashima et al. 1998; Weinman, Minkoff & Shenolikar 2000; Kim et al. 2002), targeting the channels for destruction (Staub et al. 1997), forming macromolecular complexes by means of scaffold proteins, or conferring spatial specificity on signal transduction from receptors (Naren et al. 2003). Eukaryotic CLC proteins have quite long cytoplasmic C-tails that range from 155 (ClC-Ka) to 398 amino acids (hClC-1). This intracellular domain has been proposed to play a pivotal role for CLC channel function, because deleting the C-terminal intracellular domain, or making mutations at the specific residues in this domain, can result in poor expression or altered voltage-dependent gating or even lead to nonfunctional channels (Beck, Fahlke & George 1996; Fong, Rehfeldt & Jentsch 1998; Maduke, Williams & Miller 1998; Pusch 2002; Estévez et al. 2004; Hebeisen et al. 2004; Wu et al. 2006; Accardi 2008).

One feature common to these soluble domains of all eukaryotic CLC proteins is the presence of two conserved cystathionine β-synthetase (CBS) domains called CBS1 and CBS2, which are connected by linker sequences and followed by residues at the C-terminus of variable length. Cystathionine β-synthetase domains are evolutionarily conserved protein domains present in the proteome of archaebacteria, prokaryotes, and eukaryotes (Ignoul & Eggermont 2005). Crystal structures of several bacterial proteins containing one or more CBS domains have revealed that a single CBS domain consists of a conserved β1-α1-β2-β3-α2 pattern of about 45-55 aa. Two CBS domains can form a CBS pair in an antiparallel arrangement mediated by β-strands contacting each other within the same protein (Sintchak et al. 1996; Scott et al. 2004). All four α-helices are positioned at one side of the pair whereas the loops connecting the antiparallel β2-β3 sheets are located at the other side of the structure (Zhang et al. 1999). In bacterial proteins, the CBS pairs are always formed by intramolecular association of two CBS domains. Although, at this time, one cannot formally exclude the assembly of intermolecular CBS pairs, the presently available data indicate that the above-described interaction between the CBS domains in a monomer is not a structural determinant for protein multimerization (Ignoul & Eggermont 2005). This is true for CLCs because bacterial CLC proteins dimerize in the absence of CBS domains, so it can be inferred that the CBS domains are not required for their dimerization either (Maduke, Pheasant & Miller 1999; Mindell et al. 2001). Also, experiments with C-tail truncation mutants of mammalian ClC-1 have indeed confirmed that the CBS domains are dispensable for protein dimerization (Estévez et al. 2004).

That CBS domains have other functional significance, however, has been emphasized by the observation that point mutations within them can seriously affect the specific protein function and are responsible for several hereditary diseases in humans, such as (with the protein/gene affected in parentheses), homocystinuria (cystathionine-β-synthase) (Kluijtmans et al. 1996; Shan et al. 2001); retinitis pigmentosa (inosine-5'-monophosphate dehydrogenase-1, IMPDH) (Bowne et al. 2002; Kennan et al. 2002); congenital myotonia, idiopathic generalized epilepsy, hypercalciuric nephrolithiasis and classic Bartter syndrome (ClC-1, ClC-2, ClC-5, and ClC-Kb respectively) (Bowne et al. 2002; Pusch 2002; Haug et al. 2003); and familial hypertrophic cardiomyopathy with Wolff-Parkinson-White syndrome (WPWS) (γ2 subunit of AMP-activated protein kinase (AMPK)) (Blair et al. 2001). In line with the obvious importance indicated by these hereditary diseases, several cellular functions have been proposed for CBS domains. For example, it has been suggested that they play a role in the oligomerization (Jhee, McPhie & Miles 2000), although this has been discounted for CLCs,

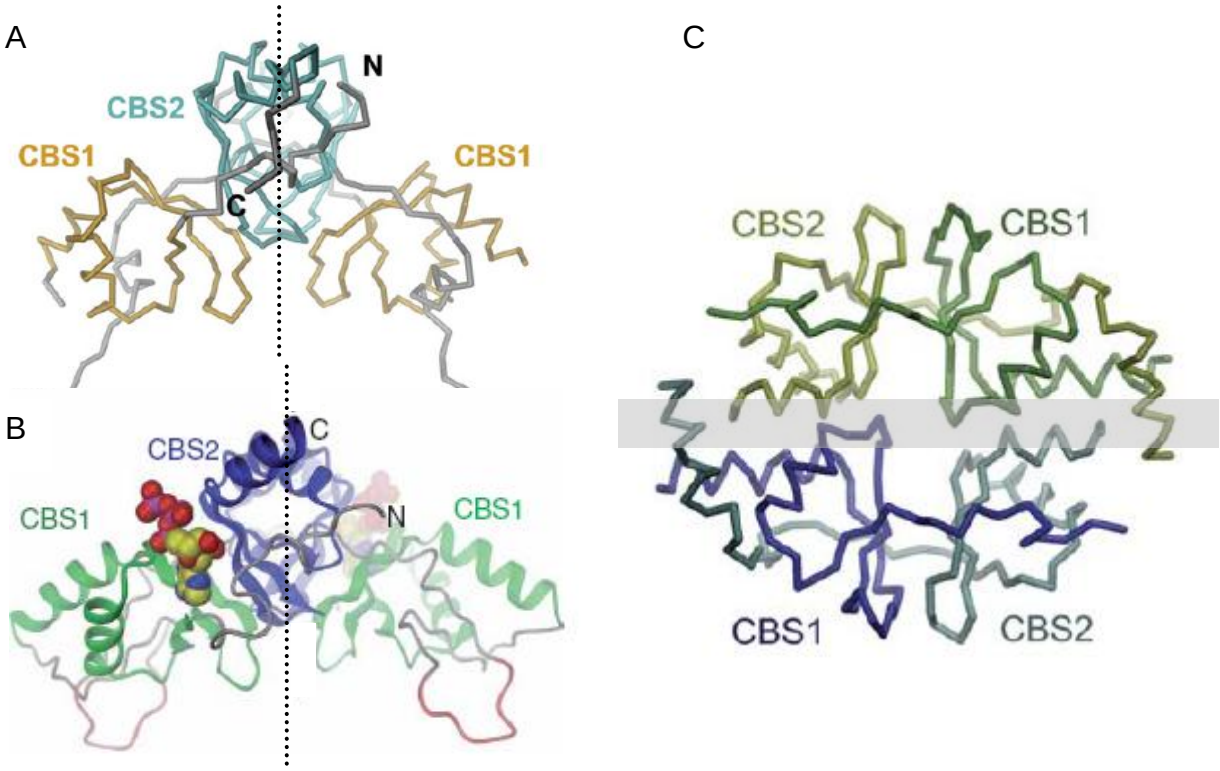
and regulation (Shan et al. 2001) of cystathionine-β-synthase as well as the γ2 subunit of AMP-activated protein kinase (Bowne et al. 2002). Alanine-scanning mutagenesis of the yeast putative CLC Cl^- channel Gef1p suggested that CBS domains influenced the subcellular localization (trafficking) of the channel (Schwappach et al. 1998). Recently, CBS domains in some kinases have been shown to bind nucleotides and might therefore be involved in sensing the energy state in the cell (Scott et al. 2004).

A similar regulation by ATP was also proposed for CBS domains of hClC-1. By mammalian cell transfection and whole-cell patch clamping, a high concentration of ATP in resting muscle was shown to be an effective inhibitor of hClC-1 activity by shifting the voltage gating to more positive potentials. Other nucleotides, ADP and AMP, had similar effects to ATP, but IMP did not (Bennetts et al. 2005). It has also been shown that this inhibition is enhanced by low intracellular pH (Bennetts et al. 2005; Bennetts, Parker & Cromer 2007). A physiologically significant consequence of this could be that when IMP accumulates as ATP is depleted under anaerobic conditions, the activity of hClC-1 would be increased, which would, in turn, reduce muscle excitability, thus contributing to fatigue. Interestingly, another two groups performed the same study by expressing hClC-1 in Xenopus oocytes and patching with the inside-out configuration, but obtained completely contrary results. Tseng and colleagues drew the same conclusion (Tseng, Bennetts & Chen 2007), whereas Zifarelli and Pusch showed that hClC-1 is totally insensitive to intracellular ATP at concentrations up to 10 mM, at neutral pH (pH 7.3) as well as at slightly acidic pH (pH 6.2) (Zifarelli & Pusch 2008). A recent study by Zhang and colleagues addressed this discrepancy by re-examining the ATP effect on ClC-1 in two channel expression systems and they reported that oxidation of ClC-1 may be the reason underlying the controversy. Sensitivity of ClC-1 to ATP could be lost under oxidative conditions, but be retained when treated with reducing agents, suggesting a possible role of cysteine residues on ClC-1 in the ATP inhibition of its common gating (Zhang, Tseng & Chen 2008). This question might be better answered by studies in the skeletal muscle fibres, where ClC-1 can be studied in its original physiological context (Accardi 2008). Structure studies of ATP binding by calculating F_o-F_c difference electron density showed specific interaction of nucleotides with the cytoplasmic domain of ClC-5, but not of ClC-Ka or ClC-0 (Meyer & Dutzler 2006; Alioth et al. 2007; Markovic & Dutzler 2007). Therefore, more concerted efforts would be required to have a complete picture of ATP regulation of ClC proteins.

Although detailed roles of C-tails in CLC function are to date still poorly understood, quite a few functional studies have hinted at their possible involvement in common gating in the voltage-dependent channels ClC-0 and ClC-1 (Beck, Fahlke & George 1996; Fong, Rehfeldt & Jentsch 1998; Maduke, Williams & Miller 1998; Pusch 2002; Estévez et al. 2004; Hebeisen et al. 2004; Wu et al. 2006; Accardi 2008). Crystal structures of some CLC cytoplasmic domains have clarified the structural organization within a single subunit and thus confirmed a number of conclusions from the above functional studies. These include, the interaction between CBS1 and CBS2 domains within each subunit and the dimerization between two subunits in their cytoplasmic tail parts (Meyer & Dutzler 2006; Alioth et al. 2007; Markovic & Dutzler 2007). Nevertheless, it is interesting to notice that although the three-dimensional structures of CBS domains are highly conserved in all the known structures of C-tails, their modes of oligomeric assembly have been proposed to be different. As shown in Figure 3, the dimeric structural arrangement of the cytoplasmic domains of ClC-Ka mainly involves residues on the surface of CBS2 in each chain of the homodimeric protein. These interactions lead to a V-shaped oligomeric structure which puts the two CBS2 subdomains in close proximity with few mutual interactions between the remote CBS1 counterparts (Fig. 3A) (Markovic & Dutzler 2007). A similar dimerization mode was also identified in the structure of the cytoplasmic domain of transporter ClC-5 (Fig. 3B) (Alioth et al. 2007). Different from ClC-Ka and ClC-5, the postulated model of ClC-0 predicted an extended dimerization interface constructed by helices of CBS1 from one subunit forming a four-helix bundle with the equivalent regions in CBS2 of the interacting subunit in a ‘‘head-to-tail’’ arrangement (Figure 3C) (Meyer & Dutzler 2006). Although this is the model that most CBS motif containing proteins take for their dimerization (Miller et al. 2004; Rudolph et al. 2007; Townley & Shapiro 2007), the V-shaped oligomeric structure might be more reasonable for ClC-0 because of the high homology among CLC family members structurally.

A review titled “Structure and function of CLC chloride channels” has been published in “*International Journal of Genetics*” (in Chinese, Appendix C).

Figure 3. A comparison of the dimeric organization of cytoplasmic domains of ClC-Ka, ClC-5 and ClC-0



(A). Ribbon representation of the ClC-Ka cytoplasmic domain. The two CBS subdomains are colored in orange and cyan, respectively. Secondary structure elements are indicated (modified from Markovic & Dutzler 2007). (B). Dimeric organization of two cytoplasmic domains of ClC-5, as observed in the crystal structure. The ATP molecule is shown as CPK model (modified from Meyer et al. 2007). Two-fold axis of symmetry is indicated by a black dashed line in (A) and (B). (C). Proposed quaternary structure of the cytoplasmic domain of ClC-0 using related protein TM0935 (*T. maritima*) as a template. This model is obtained from a least square fit of the two CBS subdomains of ClC-0 onto the respective subunit of TM0935, shown as a Cα-trace. The subunits are coloured in green and blue respectively and the extended dimerization interface between two subunits is highlighted with grey (modified from Meyer & Dutzler 2006).

1.6 PROJECT AIMS

Since the carboxyl tail region contains most of the sequence variations among mammalian members of CLC family, it may represent the molecular basis for the diverse functions of these CLC proteins. This is not to mention the naturally occurring mutations and laboratory mutagenesis/deletion/truncation studies that highlight the importance of the C-tails (Beck, Fahlke & George 1996; Fong, Rehfeldt & Jentsch 1998; Maduke, Williams & Miller 1998; Pusch 2002; Estévez et al. 2004; Hebeisen et al. 2004; Wu et al. 2006). So far, although the three dimensional structure of the cytoplamic domain has been available for some of the CLC family members (Meyer & Dutzler 2006; Alioth et al. 2007; Markovic & Dutzler 2007), their organization in relation to the transmembrane pore domain is still ambiguous (Meyer & Dutzler 2006). Also, there is still no crystal structural study of any part of hClC-1, so the structural arrangement of its C-tail and the relationship between its structure and functions are of great interest. For example, a very challenging question is: How can the C-tails affect the gating since they reside in the cytosol and do not contribute to the core structure of the permeation pathway? Because of its unique characteristics and critical roles in common gating, the C-tail of hClC-1 has become the major focus of my present study.

Previous studies using the split channel strategy have shown that when the channel is cut at specific points, co-expression of the membrane-resident portion and the remaining C-terminal domain could generate functional channels in both ClC-0 and hClC-1 (Schmidt-Rose & Jentsch 1997a; Maduke, Williams & Miller 1998). For this functional complementation to be successful, the split fragments must be able to form structurally independent subdomains or modules and mediate protein-protein interactions strong enough to enable the functional rescue from individual polypeptides in the absence of a covalent link (Schmidt-Rose & Jentsch 1997a). However, there was no direct evidence demonstrating such potential protein-protein interaction between complementary fragments in hClC-1. Thus the first project aim of my study was:

Aim 1: To test whether the physical interaction between split channel fragments of hClC-1 could be detected directly.

My intention was to split the hClC-1 protein between amino acids Ser720 and Gly721 and test for a direct protein-protein interaction between these two fragments by in vitro physical methods, provided that functional rescue could be confirmed by electrophysiology. If a physical interaction could be verified, I would certainly want to know which part/parts of

these two peptides were mediating this interaction. By electrophysiological analysis, previous studies in our laboratory and from other groups had found some important regions within the C-tail of rat ClC-1 (Hryciw et al. 1998) and of hClC-1 in split channel experiments (Estévez et al. 2004; Wu et al. 2006), such as aa800-888 and CBS1, the deletion of which affects expression or gating. However, it remained unclear why these specific regions were important for channel function and exactly which amino acids within the sequence were essential. It is possible that the amino acid sequences making up these regions are indispensable for the interaction between the two complementary split channel fragments which is critical for functional rescue. Thus, when the interaction was disrupted by mutations or deletions in these important regions, no channel function would be restored. Based on this hypothesis, my second aim became:

Aim2: To test the significance of some functionally important peptides in the interaction between hClC-1 split channel fragments. These short peptides include aa800-806, aa807-813, aa863-888, and subdomains CBS1 and CBS2.

Results from this part of my study indicated that it is the CBS1 domain in the membrane resident part (*N*720) and the CBS2 domain in the remaining C-tail (721*C*) that mediate the protein-protein interaction between these two complementary fragments, thus forming the foundation for functional rescue.

Although most of the previous split channel experiments have shown that CBS1 and CBS2 need to be in the N-region and C-region complemented fragments, respectively, to rescue channel function (Schmidt-Rose & Jentsch 1997a; Maduke, Williams & Miller 1998; Estévez et al. 2004; Mo et al. 2004). Are there, however, any other interactions between the C-tail and the membrane-resident domain besides this CBS1-CBS2 interaction? How, for example, could the CBS1-CBS2 pair support common gating, which also involves interacting helices at the dimer interface and the R helix (Duffield et al. 2003; Chen 2005)? To try to answer these questions, my third project aim was established:

Aim 3: To test whether there are other interactions between the C-tail and the membrane-resident domain besides the CBS1-CBS2 interaction.

This question was addressed by designing a new split-channel experiment (*N*720 with CBS1 deleted + 598*C*, which is the whole C-tail with both CBS1 and CBS2 domains) to exclude the effect of the CBS1-CBS2 interaction between the split N- and C-region channel fragments

and to investigate the relationship between the whole C-tail, which contains both CBS1 and CBS2, and the membrane-resident region without any CBS domain.

These first three project aims are addressed in Chapter 3 "Analysis of carboxyl tail function in the skeletal muscle Cl^- channel hClC-1", which constitutes a paper published in "*The Biochemical Journal"* (Appendix C).

By the end of this research stage, I had demonstrated a specific interaction between the membrane-resident region without any CBS domain and the whole cytoplasmic tail with two CBS domains. These results indicate that CBS1-CBS2 binding is not sufficient, in itself, for channel assembly, but rather that this might normally assist in bringing some part of the CBS2/C-tail region into appropriate proximity with the membrane-resident portion of the protein. Then there should be some specific region/regions in the membrane-resident domain which provide(s) interaction sites for the whole C-tail. Loops exposed to the cytoplasm that connect adjacent membrane-embedded helices, such as, loop DE that connects helices D and E, etc., are possible candidates for such interaction sites. Also, since no systematic study had so far been done to investigate the physiological function of these loops, the project aims for the second part of my study became:

Aim 4: To study the possible role of individual cytoplasmic loops of hClC-1 in the interaction between the cytoplasmic tail and the transmembrane pore domain.

Aim 5: To investigate the physiological function of the cytoplasmic loops of hClC-1 by electrophysiological analysis.

These two project aims are addressed in Chapter 4 "Functional study of cytoplasmic loops of human skeletal muscle chloride channel, hClC-1", which has been published in "*The International Journal of Biochemistry & Cell Biology"* (Appendix C).

In 2006, using fluorescence resonance energy transfer (FRET), Bykova and colleagues observed a large backbone movement in the C-terminus of the ClC-0 Cl^- channel which was functionally linked to the common gating (Bykova et al. 2006). This came as a very exciting and enlightening advance with respect to my project, because I had always been interested in the conformational rearrangements predicted to be involved in the common gating process of hClC-1. I, therefore, decided to use the same technique to study possible structural changes in hClC-1 during common gating. My initial aim was:

Aim 6: To test whether there is conformational rearrangement in the C-tails of hClC-1 during its common gating.

Differences between the common gating of ClC-0 and hClC-1, such as opposite voltage dependence and different gating kinetics, different temperature dependence, could, perhaps, be attributed to dissimilarities in the conformational rearrangements of these two channels. So, if there were to be conformational changes in the C-tails of hClC-1 during common gating, the following aim would arise.

Aim 7: To compare the movements in the C-tails of hClC-1 to those of ClC-0 during common gating and analyse the physiological significance of the differences.

Using FRET, I found that there is similar backbone movement at the C-terminus of hClC-1 to that in ClC-0. It then became important to know whether, and how, C-terminal displacement would be disrupted by mutations that interfered with common gating. My next aim was, therefore:

Aim 8: To investigate C-terminal displacement in mutants where there was no common gating and where the common gate was locked in an open state.

While it was interesting and informative to observe C-terminal displacement parallel to the plane of the membrane during common gating, I asked myself, how structural information related to common gating could be communicated between the C-tail and the membrane-resident pore region. My hypothesis is that, as a preliminary condition, the C-terminal of hClC-1 should be very close to the pore domain to make protein-protein interactions, and thus information conduction, possible. Therefore, the last project aim is:

Aim 9: To test whether the C-terminal of hClC-1 is close to its membrane-resident domain using FRET.

Aims six to nine are addressed in Chapter 5 of this thesis. It has been prepared as a manuscript for publication, has been submitted and is currently under review.

CHAPTER 2:
GENERAL METHODS

In this chapter, the basic materials and the common methods used to generate mutant hClC-1 Cl^- channels, express proteins, detect protein-protein interactions, analyse the electrophysiological features of channels and test FRET efficiency will be described in detail.

2.1 CHEMICALS AND WATER

All chemicals were AnalaR or Molecular Biology grade and were purchased from established suppliers. All solutions were prepared with MilliQ (MQ) water obtained from the MilliQ Plus system with an electrical resistance greater than 18 mega ohms (MΩ). MQ water autoclaved at 121 °C, 35 kPa), for 15 min was used for all molecular biology work.

2.2 MATERIALS AND METHODS FOR MOLECULAR BIOLOGY STUDY

2.2.1 POLYMERASE CHAIN REACTIONS (PCR) TO GET DNA SEQUENCE

Normal PCR, overlap extension PCR (Ho et al. 1989) and QuikChange™ Site-Directed Mutagenesis (Stratagene) were used to generate various DNA constructs. Generally speaking, all the insertions, deletions and alanine scanning mutations of short peptides were made using overlap extension PCR, whereas the QuikChange™ Site-Directed Mutagenesis method was used for point mutations. To eliminate read-through, all the truncations were generated by normal PCR using primers targeting appropriate terminating sites with a stop codon in the 3' end primer, instead of site-directed mutagenesis. All the primers used for construct generation are listed in Appendix A, which were designed by myself and purchased from Sigma.

2.2.1.1 Amplification of full-length hClC-1 or hClC-1 fragments (truncations) by PCR

To get full-length hClC-1 or hClC-1 fragments, a plasmid pCI-neohClC-1 was used as the template in all the PCR reactions. This plasmid comprised the mammalian expression vector pCI-neo (Promega) into which WT (wildtype) hClC-1 cDNA had been inserted (Bennetts et al. 2001). All the PCR reactions were performed in 0.2 ml microcentrifuge tubes with a final concentration of 10 to 100 ng of template DNA, 20 ng of each primer, 2 mM $MgSO_4$, 0.2 mM each of dATP, dCTP, dGTP dTTP (Sigma), 1X High Fidelity PCR buffer (60 mM Tris-SO_4 (pH 8.9), 18 mM ammonium sulfate) and one unit of Platinum Taq High Fidelity DNA polymerase (Invitrogen), with water added to a final volume of 50 µl. Reactions were performed in a PCR thermal cycler (Mastercycler® Personal, Eppendorf) using the following protocol: denature the template and activate the polymerase at 94 °C for 2 min, then perform

35 cycles of PCR amplification with denaturation at 94 °C for 30 s, annealing at 55-62 °C for 30 s and primer extension at 68 °C for 1 min per kilobases (kb) of plasmid length, followed by a final cycle at 68 °C for 10 min to allow for full extension and completion. Products from the PCR reactions were then double digested by appropriate endonucleases, ligated into different vectors and verified by sequencing to exclude any possible PCR errors.

2.2.1.2 Overlap extension polymerase chain reaction (PCR)

In general, two pairs of primers were used. One pair of primers is used to amplify the DNA that contains the mutation site together with upstream sequences, whereas the second pair of primers is used to amplify the DNA that contains the mutation site together with downstream sequences. Each 5' primer of the first PCR and 3' primer of the second PCR was designed to cover a restriction enzyme cutting site that would be compatible with a corresponding restriction site in the vector. Desired mutations were designed to lie in the middle of the 3' primer of the first PCR and the 5' primer of the second PCR, which were complementary to each other. In this way, mutation(s) of interest are located in the region of overlap and therefore in both sets of resulting amplified fragments. A third PCR, fusion PCR, used the overlapping PCR products from the first and the second PCR as the template DNA with a molar ratio of one to one. During the PCR amplification cycles, the complementary DNAs were fused and amplified with the 5' primer from the first PCR and the 3' primer from the second PCR.

2.2.1.3 QuikChangeTM Site-Directed Mutagenesis

QuikChange™ allows site-specific mutation in double-stranded plasmids. The basic procedure utilizes a supercoiled, double-stranded DNA vector with an insert of interest and two synthetic oligonucleotide primers, which are complementary to each other and contain the desired mutation(s). During the temperature cycling, each primer is extended and a mutated plasmid is generated.

Primers were designed according to the directions supplied by Stratagene. Both the upstream and downstream primers contained the desired mutation and annealed to the same sequence on opposite strands of the plasmid template. The primers were between 25 and 45 base pairs (bp) in length with a melting temperature (T_m) of ≥ 78 °C. T_m was estimated using the following formula:

$T_m = 81.5 + 0.41\ (GC\%) - [675 / \text{length of primer (bp)}] - \%\ \text{mismatch}$

Where GC% is the number of G and C bases divided by the length of the primer (total number of bp of the primer), % mismatch is the number of bp that do not match the original template DNA within the length of the primer, expressed as a percentage (Derived from the instruction manual of the QuikChange™ Site-Directed Mutagenesis Kit, Stratagene)

The mutagenic reaction mixture contained 10 to 50 ng of template DNA, 5 µl of 10X PCR buffer (100 mM Tris-HCl, 100 mM $(NH_4)_2SO_4$, 200 mM Tris-HCl (pH 8.8), 20 mM $MgSO_4$; 1 % Triton X-100, 1 mg/ml nuclease-free BSA), 125 ng of Fw and Rev oligonuleotide primers respectively, 0.2 mM each of dATP, dCTP, dGTP dTTP (Sigma), 2.5 units of PfuTurbo DNA polymerase (Stratagene) and adjusted with water to a final volume of 50 µl. A positive control reaction was performed occasionally, to assess the mutagenesis efficiency. The PCR reaction was performed in a PCR thermal cycler (Mastercycler® Personal, Eppendorf) with a hot start of 95 °C for 2 min, cycles of denaturation at 95 °C for 30 s, annealing at 55 °C for 1 min and primer extension at 68 °C for 2 min per kilobases (kb) of plasmid length) and a further cycle at 68 °C for 5 min. Cycle number varied according to the type of mutation. In general, point mutations required 12 cycles, single amino acid changes (mutations of two or three base pairs) required 16 cycles, and multiple amino acid mutations required 18 cycles (Stratagene).

Following the thermal cycling, the PCR product was treated with Dpn I, an endonuclease specific for methylated DNA with the target sequence: 5'Gm6ATC-3'. Almost all E. coli strains contain DNA that is dam methylated and therefore susceptible to Dpn I digestion. After the appropriate number of PCR cycles, therefore, Dpn I (20 U) was added directly to the reaction mixture and the tube was gently tapped with a finger to ensure its even distribution. This was then incubated at 37 °C, for 2 to 12 hours (h) during which time the small amount of parental DNA was selectively digested (Nelson & McClelland 1992). The mutation-containing synthesized PCR products, which are not dam methylated, were then transformed into competent *E. coli* cells. All mutants were subsequently verified by sequencing.

2.2.2 DNA PURIFICATION BY GEL EXTRACTION

To extract and purify PCR products and DNA fragments from restriction digestions the QIAquick® Gel Extraction Kit (QAIGEN) was used. Agarose gel slices, which contained the desired DNA fragments, were placed in 1.5 ml centrifuge tubes. Three volumes of Buffer QG* per one gel volume were added to the tube and incubated at 50 °C for ten minutes with mixing (vortex mixer) every two minutes. If the DNA fragments were smaller than 500 bp or

greater than 4 kb, one gel volume of isopropanol was added to the tube after the gel had completely dissolved, to increase the yield of DNA. Samples were then added to QIAquick® spin columns in which the DNA was bound to the resin by centrifugation at 12,000 x g for one minute. An additional 0.5 ml of Buffer QG* was added to each tube to remove all traces of agarose. The DNA was washed by adding 0.75 ml of Buffer PE* to the column, centrifuging at 12,000 x g for one minute and discarding the flow-through. To completely remove the residual ethanol from Buffter PE*, an additional one minute spin was performed at 12,000 x g after which DNA was eluted with 50 µl of Buffer EB (10 mM Tris-HCl, pH 8.5) and collected in a fresh 1.5 ml centrifuge tube.

2.2.3 RESTRICTION DIGESTION

To enable the PCR products and vectors to be ligated with each other, restriction digestion reactions were carried out using appropriate endonucleases. All the reaction mixtures contained DNA (PCR products or plasmid, no more than 2 µg), 10 X appropriate buffer (NEB), 10-20U appropriate endonucleases (NEB), 1 µl 100 X BSA (if required by the endonuclease), and water up to a total volume of 50 µl. To digest PCR products or empty vectors, the samples were usually incubated at 37 °C overnight, whereas digestions of construct DNA were carried out at 37 °C for 3 hours. Restriction digestion products were also gel purified (see Section 2.2.2).

2.2.4 DNA LIGATION

To ligate PCR products containing the desired mutation(s) back into the plasmid, T4 DNA ligase (NEB) was used. After the restriction digestion by the same endonucleases (Section 2.2.3), both the PCR product and the plasmid vector contain complementary DNA overhangs, which are ready for the ligation. Ligation reaction mixtures contained a molar ratio of one to three or five for the vector to the insert, 10 X ligation buffer (1 µl) which consists of 300 mM Tris-HCl, 100 mM $MgCl_2$, 100 mM DTT, 10 mM ATP, pH 7.8, T4 DNA ligase (1 U) and water to a total volume of 10 µl. Ligation reactions were conducted at 16 °C, for 16 h, or at room temperature for two hours. After the restriction enzymes were inactivated at 65-70 °C for 15 min, the ligation products were transformed into competent *E. coli* cells. Vectors used to make the various constructs employed in this study are described in chapters three to five.

2.2.5 BACTERIA STRAINS

2.2.5.1 *E. coli* MC-1061

MC-1061 competent cells were initially purchased from New England Biolabs and were used at the beginning of this project. They have the advantages of being more reliable with respect

to transformation efficiency and requiring a shorter incubation (12-14 hours compared to the 20-24 hours for most *E. coli* strains).

2.2.5.2 *E. coli* DH 5α

The *E. coli* bacteria strain DH 5α was used in this study for all the molecular cloning studies. In this strain a recA (homologous recombination deficient) mutation helps ensure insertion stability, and an endA1 (nonspecific endonuclease1 deficient) mutation greatly improves the quality of plasmid miniprep DNA. Cleavage of cloned DNA by the EcoKI or EcoBI (coded by hsdRMS) endonuclease system is prevented by hsdR17 (rk-, mk+). Also the cells contain the φ80dlacZΔM15 gene on the F prime (F') episome and lack laqIq gene, which allows blue-white colour screening of recombinant plasmids by α-complementation of the β-galactosidase gene. Consequently, the DH 5α strain was preferred over the MC-1061 because of its advantageous genetic characteristics, especially the recA and endA1 genotypes.

2.2.6 BACTERIAL CULTIVATION

Solutions used to cultivate bacteria are defined below. All media were sterilized by autoclaving at 121 °C, 35 kPa for 15 min.

2.2.6.1 Luria-Bertani medium (LB)

For all bacteria cultivation, except during transformation, the general Luria-Bertani (LB) medium was used. It consists of 1 % (w/v) Bacto tryptone, 0.5 % (w/v) Bacto yeast extract, 1 % (w/v) NaCl, pH 7.4 (Sambrook & Gething 1989). To cultivate those bacteria containing recombinant plasmids, relevant antibiotics were freshly added to LB before use. Final concentrations of antibiotics were: ampicillin, 100 μg/ml; kanamycin, 50 μg/ml.

2.2.6.2 LB-Agar

In general, the solid medium used to culture *E. coli* cells was LB agar, which is made of LB broth containing 1.5 % (w/v) Bacto agar (Difco Laboratories, Detroit, Michigan, USA). In this case, the plating medium consisted of 42.3 mM Na_2HPO_4, 22 mM KH_2PO_4, 9.2 mM NaCl, 18.7 mM NH_4Cl, 1.5 % (w/v) agarose, 1 mM thiamine HCl, 2 mM $MgSO_4$, 0.1 mM $CaCl_2$ and 11.5 mM glucose. When used to culture bacteria containing the inoculated recombinant plasmids, the relevant antibiotics were added to sterilized medium that had been allowed to cool down to 50 °C with the same concentration as in LB medium (Section 2.2.2.1).

2.2.6.3 SOC medium

To recover bacteria after the transformation of plasmid DNA into the bacteria, SOC medium was used. Final concentrations of each ingredient in SOC medium were as follows: 2 % (w/v) bacto tryptone, 0.5 % (w/v) yeast extract, 10 mM NaCl, 2.5 mM KCl, 10 mM $MgCl_2$, 10 mM $MgSO_4$ and 20 mM glucose. The solution was filter sterilized with a 0.22 μm gamma sterilized syringe filter (JRH Biosciences Pty Ltd, Brooklyn, VIC).

2.2.6.4 Super-Broth medium

Super-Broth media was used to culture bacteria cells before they were made competent. It contained Bacto Tryptone 3.2 % (w/v), Yeast Extract 2.0 % (w/v) and NaCl 1.0 % (w/v)).

2.2.7 PREPARATION OF COMPETENT CELLS

Competent *E. coli* cells were made with $CaCl_2$ method, a method which can yield $5x10^6$ to $2x10^7$ transformed colonies/μg of supercoiled plasmid DNA (Cohen et al. 1973). Briefly, a LB agar plate was streaked with a bacterial strain and incubated 12-16 hours at 37 ºC. A single bacterial colony (2-3 mm in diameter) was then picked from the plate and incubated in 5 ml of LB broth over night with vigorous shaking. Then the 5 ml starter culture was poured into 400 ml of super-broth media next morning and incubated again at 37 ºC with vigorous shaking for about 90-120 min allowing the cells to reach the optical density of OD_{600} = 0.4-0.5 (by measuring the absorbance at 600 nm). Cells were then kept on ice for 30 min in 50 ml tubes and centrifuged at 4,000 x g for 15 min. Pellets were suspended in 1 ml of chilled 0.1 M $MgCl_2$ and transferred to two 50 ml tubes, which were then filled to the top with chilled 0.1 M $MgCl_2$ and incubated on ice for approximately 10 min. After this, cells were again centrifuged at 4000 g for 15 min. Pellets were resuspended in 1 ml 0.1 M $CaCl_2$ after which a further 3.5 ml of 0.1 M $CaCl_2$ was added to each tube. Cells were then transferred to a chilled 10 ml tube and $CaCl_2$ was added to a final volume of 9.5 ml. Glycerol was then added to a final concentration of 15 % (v/v). Cells were left on ice for 2 hours before they were finally dispensed into 200 μl aliquots and stored at -80 ºC after having been frozen immediately in liquid nitrogen.

2.2.8 TRANSFORMATION OF COMPETENT CELLS WITH PLASMID DNA

Plasmid DNA (50 ng) or ligation products (5 μl) were mixed gently with 50 μl of MC-1061 or DH 5α subcloning competent cells in sterilized 1.5 ml microcentrifuge tubes. These were incubated on ice for 60 min, heat shocked at 42 °C for 90 s to allow the plasmid to get into the cells, and the tubes immediately placed on ice for a further two minutes to chill. The cells

were suspended in 0.4 ml of SOC (Section 2.2.6.3) and incubated at 37 °C for 1.5 hours with shaking at 100 rpm/min to allow the cells to recover from the heating and chilling cycles. Transformation mixture 100 µl was plated onto an LB agar plate (Section 2.2.6.2), which was supplemented with suitable antibiotics to allow the selection of colonies containing the plasmid. The plate was incubated at 37 °C overnight, with positive (pUC18) and negative (water) transformation controls run in parallel to each reaction. Transformation efficiency was typically 1 x 10^6 to 1 x 10^7 colonies / µg of DNA.

2.2.9 PURIFICATION OF PLASMID DNA FROM BACTERIAL CULTURES

2.2.9.1 Small-scale plasmid purification (mini-prep protocol)

A single (transformed) colony from a LB agar plate (section 2.2.6.2) was inoculated into 2 ml of LB containing appropriate antibiotics (section 2.2.6.1) to get a starter culture and vigorously shaken overnight at 37 °C. From overnight cultures, 1.5 ml was extracted and cells were harvested by centrifugation at 14,000 x g for 1 min at room temperature (RT). Supernatants were discarded and cell pellets were homogeneously suspended in 150 µl of pre-chilled resuspension buffer (50 mM Tris·Cl, pH 8.0; 10 mM EDTA). Cells were then lysed by the addition of 200 µl lysis buffer (200 mM NaOH, 1 % SDS (w/v)), mixed by inverting the tubes 5 times and then incubated at RT for 5 min. Samples were then neutralised with 150 µl of neutralisation buffer (3.0 M potassium acetate, pH 5.5), mixed by inverting 5 times and incubated on ice for 5 min. Precipitated cell debris, proteins and genomic DNA were collected by centrifugation at 14,000 x g for 5 min and supernatants were carefully transferred to fresh 1.5 ml tubes. Chloroform (200 µl) was added and the tubes were thoroughly mixed before they were centrifuged again at 14,000 x g for 5 min. The upper aqueous layer was removed to fresh 1.5 ml tubes. Using 1 ml of cold 100 % ethanol, DNA was precipitated and centrifuged at 14, 000 x g for 5 min, then the pellet was washed with 200 µl of 70 % (v/v) ethanol. Pellets were dried on a 50 °C heat block for 5 min before DNAs could be dissolved in 30-50 µl of water. Plasmid DNA was stored at -20 °C until required.

2.2.9.2 Large-scale plasmid purification (midi-prep protocol)

In order to isolate large quantities of plasmid DNA, the QIAGEN plasmid purification midi kit (QIAGEN) was used. Media (LB, 25 ml) supplemented with appropriate antibiotics (section 2.2.6.1) was inoculated with 25 µl of the previous starter culture and incubated overnight at 37 °C with vigorous shaking (about 300 rpm). Cells were harvested by centrifugation at 4,000 x g for 10 min at 4 °C and the cell pellets were suspended in 4 ml of resuspension buffer (50 mM Tris·Cl, pH 8.0; 10 mM EDTA and 100 µg/ml RNase A) until a

homogeneous suspension was achieved. Then 4 ml of lysis buffer (200 mM NaOH, 1 % SDS (w/v)) was added to the tubes which were inverted 5 times and incubated at RT for 5 min. Cell lysates were then neutralised by adding 4 ml of cold neutralisation buffer (3.0 M potassium acetate, pH 5.5) and incubated on ice for 15 min. Neutralised lysates were centrifuged at 18,000 x g for 30 min at 4 °C and supernatants were transferred to QIAGEN-columns previously equilibrated with 10 ml of equilibration buffer (750 mM NaCl, 50 mM MOPS, pH 7.0; 15 % isopropanol (v/v), 0.15 % Triton® X-100 (v/v)). Cleared lysate was allowed to enter the DNA binding resin in the QIAGEN-column by gravity flow, which was then followed by washing the QIAGEN-column twice with washing buffer (1.0 M NaCl, 50 mM MOPS, pH 7.0; 15 % isopropanol (v/v)). Plasmid DNA was eluted from the QIAGEN-column with 5 ml of elution buffer (1.25 M NaCl, 50 mM Tris·Cl, pH 8.5; 15 % isopropanol (v/v)). Then the plasmid DNA was precipitated from the solution by addition of 3.5 ml isopropanol and pelleted by centrifugation at 18,000 x g for 30 min at 4 °C. After the supernatant was removed, the pellet was washed with 1 ml of cold 70 % (v/v) ethanol and centrifuged at 18,000 x g for 5 min at 4 °C. Finally the pellet was air-dried for 10-15 min before suspension in 100-150 µl of water. Plasmid DNA was stored at -20 °C until required.

2.2.10 QUALIFICATION AND QUANTIFICATION OF PLASMID DNA

Concentrations of DNA were determined by measuring the absorbance at 260 nm using GeneQuant RNA/DNA Calculator (Pharmacia). Quality of purified plasmid DNA was always judged in two ways. One was that the ratio of absorbance at 260 nm and 280 nm of the DNA should be ≥ 1.80. The other way was to visualise the DNA by agarose gel electrophoresis using the Gel Doc system (BioRad Laboratories). Plasmid DNA with good quality should show a strong and clear supercoiled DNA band and a weak nicked circular DNA band. Only plasmid DNA fulfilled above two standards was used for following transfections.

2.3 PROTEIN EXPRESSION IN HEK 293T and HEK 293 CELLS

Mutant and control WT hClC-1 channels or protein fragments were transiently or stably expressed in HEK 293T cells (Human Embryonic Kidney 293T, American Type Culture collection, Rockville, MD) for electrophoretic analysis and functional studies, such as protein-protein interaction detection and patch-clamping and assessment of FRET. This cell line is a derivative of HEK 293 line that stably expresses the large T-antigen of SV40. Plasmids containing the SV40 origin are replicated to a copy number of between 400 - 1000 plasmids per cell within 293T, and therefore express at a higher level. Also, HEK 293T cells are very

reliable and stable, and they are usually easy to transfect with high efficiency. These cells express relatively few native channels and are, therefore, very suitable for *in vitro* function studies of over-expressed channel types. But HEK 293 cells were used for FRET studies.

2.3.1 CELL CULTURE MAINTENANCE OF HEK 293T / HEK 293 cells

Cells were routinely cultured in 25 cm^2 flasks at 37 °C with 5 % (v/v) CO_2 and passaged when 75-90 % confluent, approximately every 2 to 3 days. They were maintained in Dulbecco's modified Eagle's medium (DMEM; Invitrogen), which contains high glucose, L-glutamine, 110 mg/l sodium pyruvate and pyridoxine hydrochloride, supplied with a mixture of 9 % Newborn Calf Serum (NCS) (v/v), 1 % Fetal Calf Serum (FCS) (v/v), 1 % (v/v) MEM Non-essential amino acids (10 mM stock; Invitrogen), 2 mM glutamine (200 mM stock; Sigma) and antibiotics (Penicillin 100 units/ml + streptomycin 100 ug/ml, Sigma). This medium is hereafter referred to as $DMEM^+$, whereas the Dulbecco's modified Eagle's medium without any supplement is referred to as $DMEM^-$.

When the cells were passaged, the cell monolayer was first washed with 4 ml of $DMEM^-$. By adding 1 ml of Trypsin-EDTA (Sigma), the cell monolayer could be removed from the base of the flask. After incubation at 37 °C for 1 min, digestion was stopped by adding 3 ml of $DMEM^+$. An aliquot of the resuspended cells (0.5 to 0.75 ml) were then transferred to a new 25 cm^2 flasks containing 4 ml of $DMEM^+$ and incubated at 37 °C with 5 % (v/v) CO_2.

2.3.2 TRANSIENT AND STABLE TRANSFECTION OF HEK 293T / HEK 293 CELLS

All the transfections in this study were carried out using Lipofectamine 2000 reagent from Invitrogen according to the manufacturer's instructions. Briefly, one day before transfection, 0.8-1.0 x 10^6 cells were plated in 25 cm^2 flasks in 5 ml of $DMEM^+$ so that cells were about 70-80 % confluent at the time of transfection. Mutant or WT cDNA (3.0 to 4.0 μg) and Lipofectamine 2000 reagent (9.0 to 12.0 μl) were diluted in 500 μl $DMEM^-$ and incubated at room temperature for 5 min after gentle mixing. Following the 5 minute incubation, the diluted DNA was combined with diluted Lipofectamine™ 2000 (total volume = 1 ml), again mixed gently and then incubated for 30 minutes at room temperature. During this incubation, the cells were washed with $DMEM^-$ twice and 4 ml fresh $DMEM^+$ without antibiotics was added to each flask. Then the 1 ml of incubated complexes were added and mixed gently by rocking the flask back and forth. Transfected cells were incubated at 37 °C with 5 % CO_2 for 24-48 hours prior to functional studies. For stable transfection, cells were passaged at a 1:10 dilution into fresh growth medium 24 hours after transfection and selection of stable cell

clones was carried out using puromycin dihydrochloride (2 µg/ml, Sigma) the following day. After 2-3 weeks, the untransfected cells were all killed by the selective antibiotic and resistant clones were picked up and expanded separately.

If the cells were transfected for patch clamping, they would then be plated into 35 mm petri dishes or 6-well plates with 3-4 coverslips in each dish/well. Accordingly, the amount of plated cells, DNA, transfection reagent and media volume was all scaled down. Also, WT or mutant hClC-1 DNA was always co-transfected with pEGFP-N1 (Clontech) at a molar ratio of 10:1 to facilitate later identification of transfected cells by reporter plasmid-driven expression of the green fluorescent protein.

2.4 PROTEIN DETECTION AND PROTEIN-PROTEIN INTERACTION TEST

2.4.1 TOTAL PROTEIN EXTRACTION

Transfected cells were harvested and lysed on ice for 30 min in lysis buffer containing 150 mM NaCl, 20 mM Tris-HCl (pH 8.0), 10 % glycerol, 0.2 % Triton X-100, 0.2 mM DTT and protease inhibitor cocktail (1 µg/ml pepstatin, 1 µg/ml leupeptin, 0.5 mM PMSF, 5 µg/ml benzamidine, 0.1 µl/ml aprotinin). After centrifugation at 18,000 x g for 15 min at 4 °C, the supernatant was collected and transferred to a new Eppendorf tube. The proteins were kept on ice until quantified or frozen at -80 °C.

2.4.2 MEMBRANE PROTEIN EXTRACTION

To obtain purified membrane proteins, cell plasma membranes were first prepared by a method using density gradient medium silica colloid Percoll (GE Healthcare) (Belsham, Denton & Tanner 1980). At 24-48 h after transfection, 10^8 cells were washed three times by cold phosphate buffered saline (PBS) and pelleted by centrifugation at 1500 x g for 5 min at 4 °C. Cell pellets were resuspended in fresh PBS at a ratio of 3 vol of PBS to 1 vol of packed cells and the cells were disrupted by repeatedly freezing in a bath of ethanol and dry ice, shaking from time to time and then thawing in a 37 °C water bath until homogenization (routinely monitored by phase-contrast microscopy) was satisfactory. At the same time, Percoll was made isotonic by adding 9 parts (v/v) of 100 % Percoll to 1 part (v/v) of 1.5 M NaCl to get Stock Isotonic Percoll (SIP) solution at an osmolality of 340 mOsm/kg H_2O. Every 200 µl cell suspension was mixed with 2 ml SIP solution, and centrifuged at 20,000 x g for 60 min at 4 °C. Then the upper-most ivory-white layer was carefully separated without any contamination from other layers and collected in a new tube. Purification of this layer was

repeated five times before the membrane proteins were finally extracted by the same method described in section 2.4.1.

2.4.3 PROTEIN QUANTIFICATION

Protein concentration was measured using the BCA™ Protein Assay Kit (Pierce). This method combines the well-known reduction of Cu^{2+} to Cu^{1+} by protein in an alkaline medium (the biuret reaction) with the highly sensitive and selective colorimetric detection of the cuprous cation (Cu^{1+}) using a reagent containing bicinchoninic acid (Adilakshmi & Laine 2002). First of all, to make the standard curve, the standard protein Albumin Standard (BSA) was diluted with H_2O in a set of Eppendorf tubes with the final concentrations being 2000 µg/ml, 1500 µg/ml, 1000 µg/ml, 750 µg/ml, 500 µg/ml, 250 µg/ml, 125 µg/ml, 25 µg/ml and 0 µg/ml. At the same time, test protein samples were also diluted 10-50 times. Then a BCA™ working reagent (WR) was prepared by mixing 50 parts of BCA™ Reagent A with 1 part of BCA™ Reagent B (50:1, Reagent A:B). Each diluted BSA and test protein sample was mixed with 2.0 ml WR and incubated at 37 °C for 30 min. After the tubes had cooled down, absorbance at 562 nm (OD_{562}) was measured in a spectrophotometer DU640 (Beckman) within 10 min. A standard curve was prepared by plotting the average blank-corrected 562 nm measurement for each BSA standard vs. its concentration in µg/ml and was used to determine the protein concentration of each unknown sample.

2.4.4 GST-PULLDOWN ASSAY

This assay is an in vitro method used to determine physical interaction between two or more proteins. It is a form of affinity purification and is very similar to immunoprecipitation except that a bait protein is used instead of an antibody. Availability of a purified and tagged protein (the bait) which will be used to capture and 'pull-down' a protein-binding partner (the prey) forms the minimal requirement for a pull-down assay. Typically, a GST-tagged bait protein is captured on an immobilized affinity ligand specific for the GST tag (I used glutathione-Sepharose 4B beads (GE Healthcare) in this study), thereby generating a 'secondary affinity support' for detecting and purifying other proteins that interact with the bait protein.

After the total protein was extracted from transfected cells and quantified, equal amounts of protein (1 mg) were incubated with 50 µl of glutathione-Sepharose 4B beads (GE Healthcare) for 3 h. They were then collected by short centrifugation and washed four times (10 min each time) in 1 ml lysis buffer. All procedures were carried out at 4 °C. Any bound proteins were finally liberated by heating at 55 °C for 20 min in 2 X Laemmli sample buffer and separated by SDS-PAGE (6 %-12 % polyacrylamide).

2.4.5 SDS-PAGE

Protein separation by SDS-polyacrylamide gel electrophoresis was used as the preliminary step for protein detection. For SDS-PAGE, 4 % (w/v) stacking and 6 %-12 % (w/v) resolving gels, were constructed according to the method of Laemmli (Laemmli 1970). Extracted protein samples were dissolved in 2 X Laemmli sample buffer (100 mM Tris-HCl, 4 % (w/v) SDS, 20 % (v/v) glycerol, 0.2 % (w/v) bromophenol blue, 200 mM DTT) and denatured by heating at 55 °C for 20 min prior to electrophoresis. Equal amounts of protein samples (10 to 20 μg) were loaded into each well and separated at 100 volts (V) initially until proteins entered the resolving gel and then 175 V until bromophenol blue dye moved to the end of the gel.

2.4.6 WESTERN BLOT

Proteins separated on a SDS-PAGE gel (Section 2.4.4) were then transferred to nitrocellulose membranes (Amersham Pharmacia Biotech) for 1 h at 100 V at room temperature using the Mini-Protein® Ⅱ Dual Slab Cell System (Bio-Rad). Blots were then blocked for 1 h in blocking buffer (TBST buffer (150 mM NaCl, 25 mM Tris, pH 7.4, 0.1% Tween-20) containing 5% skim milk) with gentle shaking to ensure that non-specific proteins were evenly blocked. Primary antibodies were diluted with blocking buffer and the membrane was incubated for 1 h at room temperature with the appropriate primary antibody. These included anti-FLAG M_2 Monoclonal Antibody (Sigma), anti-myc antibody 9E10 (culture supernatant from hybridoma cell line 9E10, ATCC), anti-hClC-1 antibody (against residues 974-988 of hClC-1) (Gurnett et al. 1995), and anti-GAPDH antibody (SCBT). After four washes in TBST buffer with vigorous shaking (for 15 min each time), the blot was incubated for 1 h with corresponding secondary antibodies (horseradish peroxidase-conjugated anti-mouse IgG (Sigma) or goat anti-rabbit IgG-HRP-conjugate (SCBT)). After washing four more times reacting protein bands were visualized with an enhanced chemiluminescence detection system (Amersham Biosciences).

2.5 ELECTROPHYSIOLOGICAL STUDY OF hClC-1 CHANNEL

Patch clamp experiments were performed in the whole-cell configuration at RT using an Axopatch 200B patch-clamp amplifier (Axon Instruments, Inc.) and associated standard equipment. Cells were continuously superfused with bath solution containing 140 mM NaCl, 4 mM CsCl, 2 mM $CaCl_2$, 2 mM $MgCl_2$, and 10 mM HEPES, adjusted to pH 7.4 with NaOH. Patch pipettes were pulled from borosilicate glass and typically had a resistance of 1-3 MΩ when filled with the standard pipette solution containing 40 mM CsCl, 85 mM Cs glutamate,

10 mM EGTA-Na, 10 mM HEPES, adjusted to pH 7.2 with NaOH. Cells that showed green colour (i.e. expressing GFP) were subjected to patch clamping. Series resistance did not exceed 3 MΩ and was 75-85 % compensated. Currents obtained were filtered at 3 kHz, collected and analysed using Clampex 9.0 Software (Axon Instruments). Results that are presented graphically in this project were analysed using GraphPad PRISM^{TM} 4.00 software (GraphPad Software Inc.). Potentials listed are pipette potentials expressed as intracellular potentials relative to outside zero.

Basically, three protocols were used for electrophysiological analysis of the channel. First, a deactivation protocol was utilised in order to check on the presence or absence of characteristic hClC-1 currents. Channels were first activated by stepping to +40 mV for 200-1600 ms from a holding potential of -30 mV and then deactivated by stepping to potentials between -120 mV and +100 mV in 20 mV increments for durations of 100-600 ms. When applicable, voltage dependence of overall channel activation (i.e. the opening and closing of both the fast gates and the common gate) and common gating were analysed by two specific tail current protocols. In tail current protocol 1 (named tail_1 protocol), tail-current relaxation was measured from a holding potential of -30 mV using 160 ms conditioning pulses at increasingly hyperpolarizing steps (-20 mV) ranging from +100 to -140 mV followed by test tail pulses at a constant voltage of -100 mV for 40 ms. Tail current protocol 2 (named tail_2 protocol) was the same as tail_1, except that an extra 400 μs conditioning pulse to +180 mV was added immediately before the -100 mV tail pulse. The aim of this very positive step is to fully activate the channel's fast gates (i.e. keep them open) and the tail currents at -100 mV then reflect only common gating (Accardi & Pusch 2000). Between test sweeps the cell membrane was clamped at a holding potential of -30 mV for a period of 2 s.

Extrapolated peak currents during the -100mV tail pulse were determined by fitting the tail current with a double-exponential function (equation 1) and then normalized to the maximal value obtained following the most positive test voltage (Rychkov et al. 1996b). In cases where mutants showed only one kind of gating (e.g. the alanine replacement of loop JK), currents were then fitted with a function with one exponential plus a constant (equation 2).

$$I(t) = A_1 \exp(-t/\tau_1) + A_2 \exp(-t/\tau_2) + C \qquad \text{(Equation 1)}$$

$$I(t) = A \exp(-t/\tau) + C \qquad \text{(Equation 2)}$$

where in Equation 1, A_1 and A_2 represent the amplitude of the fast and slow exponential components, τ_1 and τ_2 are their time constants, C represents the amplitude of the steady state

component, and t is time. Equation 3 is a simplified version of Equation 2 with only one exponential.

Normalised instantaneous currents obtained from the analysis were then used to produce apparent open probability curves for the overall open probability, P_o (data from tail_1 protocol), and the open probability of the common gate, P_o^c (data from tail_2 protocol), by fitting with a Boltzmann distribution of the form:

$$P_o(V) = P_{min} + (1- P_{min}) / (1+ \exp ((V_{1/2} – V)/k)) \qquad \text{(Equation 3)}$$

where P_{min} is an offset or minimum P_o at very negative potentials, V is the membrane potential, $V_{1/2}$ is the potential at which $P_o = (1 + P_{min})/2$ (half maximal activation) and k is the slope factor.

Open probability of the fast gates (P_o^f) could then be calculated by dividing the mean values for overall open probability (P_o) by the mean values for the open probability of the common gate (P_o^c). The $V_{1/2}$ is expressed as the mean plus or minus (±) the standard error of the mean (SEM).

2.6 FLUORESCENCE RESONANCE ENERGY TRANSFER (FRET) STUDY

For FRET measurement, HEK 293 cells were cotransfected with full length hClC-1 channel (or channel fragment) constructs labelled separately with either donor fluorophore (Cerulean) or receptor fluorophore (EYFP). Just prior to fluorescence imaging, the culture medium for the HEK 293 cells in a Lab-Tek™ chamber (Nunc, US) was replaced with cell imaging solution (130 mM NaCl, 5 mM MgCl2, 2 mM CaCl2, 5 mM HEPES and 1 mM EGTA (pH 7.4)).

The spectra FRET system was set up around an inverted fluorescence microscope (Olympus IX-81) equipped with a 100 W mercury lamp and a 60X oil-immersion objective (NA 1.42). Duration of light exposure was controlled by a computer-driven mechanical shutter (Olympus IX2-SHA). For spectroscopic imaging, a spectrograph (Acton SpectraPro 2150i) was used in conjunction with a Hamamatsu HQ CCD camera. Two filter cubes (Chroma) were used, one for Cerulean excitation (excitation filter D436/20, dichroic mirror 455dclp, cube 1) and another for EYFP (excitation filter HQ500/20, dichroic mirror Q515lp, cube 2). No emission filter was used in these cubes. Under this experimental condition, autofluorescence from untransfected cells was negligible.

Fluorescence imaging and analysis were done using MetaMorph software (Universal Imaging). Emission spectra were constructed using the fluorescence intensity values recorded from the plasma membrane of the cell by positioning the spectrograph slit across a cell and recording the fluorescence intensity at a position restricted to the membrane region. Since the same slit position applied to the spectra taken with both Cerulean and EYFP excitation it was possible to obtain reliable quantification of FRET efficiency exclusively from the cell membrane. Spectra were corrected for background light which was estimated from the blank region of the same image.

To quantify FRET efficiency with the spectra FRET method, spectra measurements were made from three cell groups: (1) cells expressing only Cerulean, from which a standard Cerulean spectrum (F_C^C) was collected with cube 1; (2) cells expressing only EYFP, from which the spectrum collected with cube 1 represented the direct excitation of EYFP with Cerulean excitation light (the "cross-talk" component, F_C^Y) and the spectrum collected with cube 2 represented the total EYFP emission (F_Y^Y); and (3) cells expressing both Cerulean and EYFP, from which the spectrum collected with cube 1 represented the total fluorescence emission from both Cerulean and EYFP (F_C^{C+Y}) and the spectrum collected with cube 2 represented the total EYFP emission from these cells (F_Y^Y). After all the required spectra were measured, the apparent FRET efficiency was quantified as the enhanced emission of the acceptor (EYFP) during donor (Cerulean) excitation due to energy transfer.

Modeling of FRET efficiency for hClC-1 was the same as described by Bykova and colleagues for ClC-0 (Bykova et al. 2006) and is repeated here in the following terms:

If we make C and Y represent the total concentration of hClC-1-Cerulean subunit and the total concentration of the hClC-1-EYFP subunit in a cell, respectively, and let r be the concentration ratio between the two fluorophores (i.e. r = C/Y), then, assuming that the assembly between the hClC-1-Cerulean subunit and the hClC-1-EYFP subunit is random:

$P_C = C/(C+Y) = r/(1+r)$ (Equation 4)

$P_Y = 1- P_C = 1/(1+r)$ (Equation 5)

where, P_C and P_Y are the probabilities of incorporating a hClC-1-Cerulean subunit and a hClC-1-EYFP subunit into the channel, respectively. Apparent FRET efficiency (E_{app}), was then quantified as the increase in the acceptor emission along with the fluorescence intensity ratio FC/FY, which is measurable from the cell, according to the following equations:

$$E_{app} = \frac{2P_C P_Y E \frac{\varepsilon_C}{\varepsilon_Y} S_Y}{2P_C P_Y S_Y + 2P_Y^2 S_Y} \cdot \frac{\varepsilon_Y}{\varepsilon_C} = E \cdot \frac{r}{1+r} \qquad \text{(Equation 6)}$$

$$\frac{F_C}{F_Y} = \frac{1+r-E}{1+\frac{1}{r}+E\frac{\varepsilon_C}{\varepsilon_Y}} \cdot \frac{S_C}{S_Y} \qquad \text{(Equation 7)}$$

where S_C and S_Y are system transfer functions for Cerulean and EYFP, respectively; ε_C and ε_Y are molar extinction coefficients of Cerulean and EYFP respectively; and E is FRET efficiency.

When equation 6 and 7 are combined, the unknown concentration ratio r can be eliminated. This leaves us with two free parameters, the true FRET efficiency E and the ratio S_C/S_Y which is a constant that reflects properties of the recording system and of the fluorophores. It can be determined from measurements of a system with a known E value or from a global fit of multiple data sets collected with the same recording system and the same fluorophores. After SC/SY is determined, the intrinsic FRET efficiency can be determined by directly fitting the data to equations 6 and 7 (Bykova et al. 2006).

CHAPTER 3:
ANALYSIS OF CARBOXYL TAIL FUNCTION IN THE SKELETAL MUSCLE CHLORIDE CHANNEL, hClC-1

3.1 INTRODUCTION

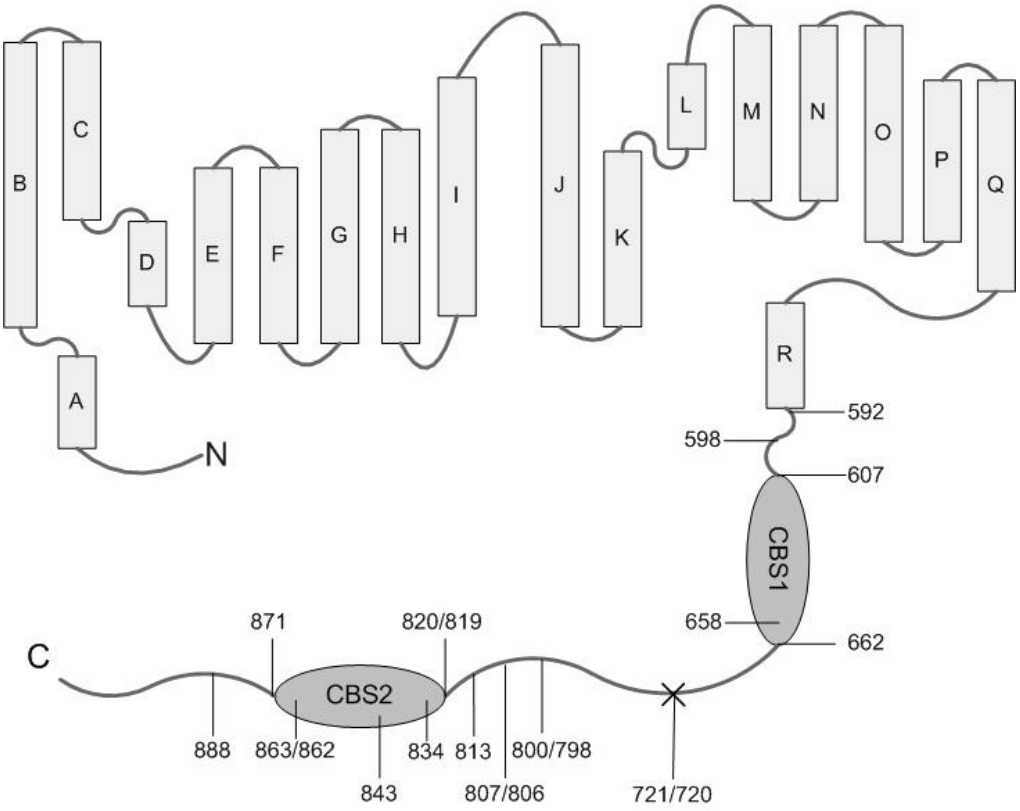
A significant family of proteins that catalyse transmembrane Cl^- flux, the CLC voltage-gated Cl^- channels and transporters, is unrelated to any other ion channel/transporter family but, among its members, is quite conserved with respect to sequence and architecture (Dutzler et al. 2002; Accardi & Miller 2004; Pusch & Jentsch 2005). It is reasonable, therefore, to take the X-ray structures determined for the prokaryotic CLC proteins from *E. coli* and S. enterica serovar typhimurium (EcClC and StClC) (Pusch & Jentsch 2005) as the structural framework for the membrane-resident domain of their eukaryotic, and hence also mammalian, homologs. Accordingly, these membrane-resident proteins are composed of two identical subunits with 18 α-helices (A-R) in each subunit (Fig. 4). In muscle-type CLC channels, an independent ion conduction pathway in each subunit, called a protopore, provides the foundation for two distinct gating mechanisms, protopore (or fast) gating and common (or slow) gating (Rickard 2005). Fast gating regulates protopores individually and independently, and is believed to be mediated by the movement of a glutamate side chain in helix F and Cl^- binding to an external binding site in the pore (Pusch et al. 1995; Rychkov et al. 1996a). On the other hand, common gating regulates both pores simultaneously. It has been suggested that common gating might involve complex higher order, helix-helix or protein-protein interactions based on its unusual temperature sensitivity (Pusch, Ludewig & Jentsch 1997), but the molecular mechanism underlying this process is still far from clear.

Despite the high homology between the membrane-resident domains of eukaryotic and bacterial CLC proteins, one of the most significant differences between them is that the eukaryotic CLCs have long cytoplasmic carboxyl tails (C-tails) containing two CBS domains (CBS1 and CBS2) (Fig. 4). Deletions, truncations, or mutations in the C-tails either resulted in poor expression, altered characteristics or led to nonfunctional channels, demonstrating their physiological significance (Schmidt-Rose & Jentsch 1997a; Hryciw et al. 1998; Haug et al. 2003; Simpson et al. 2004; Wu et al. 2006). For hClC-1, the dysfunction of which leads to myotonic muscle diseases, almost one fifth of over 120 known myotonia-causing mutations are located in its C-tail (Pusch 2002). Most interestingly, the C-tails, which are distant (in primary amino acid sequence) from the membrane-resident pore regions, have been illustrated to be closely associated with the common gating of CLC channels (Estévez et al. 2004;

Bennetts et al. 2005; Wu et al. 2006; Yusef et al. 2006). However, in the absence of structures for whole eukaryotic CLC proteins (complete with their C-tails), just what are the molecular mechanisms underlying the functional roles of these cytoplasmic domains? For example, why are some specific short amino acid (aa) sequences in the C-tail so important for the channel function? So far, the existing evidence is quite controversial with regard to some of these issues, such as whether the C-tails are necessary for trafficking, whether CBS1 and CBS2 interact, and what function this might serve (Hryciw et al. 1998; Schwappach et al. 1998; Carr, Simmons & Sayer 2003; Estévez et al. 2004; Hebeisen et al. 2004; Bennetts et al. 2005).

In the present study, we aimed to learn more about the inherent characteristics of the C-tail of hClC-1 by investigating the physical and functional roles of several specific regions, such as the short sequences aa800-820, aa863-888 and CBS domains (CBS1 and CBS2), in mammalian cells (Fig. 4). These short sequences have been shown to be essential for channel function in split channels, but the underlying molecular mechanisms are still unknown (Estévez et al. 2004; Wu et al. 2006). One of the most likely explanations might be that they are essential for the binding between complementary fragments in split channels. However, we show here that when hClC-1 is cut between the CBS1 and CBS2 domains, binding between the membrane-resident part and the cytoplasmic part is not affected by the absence of any of these short sequences, but seems to rely exclusively on a direct interaction between the two CBS domains. Furthermore, although most of the previous split channel studies rescued channel function using two complementary fragments, each containing one CBS domain (Schmidt-Rose & Jentsch 1997a; Maduke, Williams & Miller 1998; Mo et al. 2004), we have found that this is not a necessary condition. Our study shows, for the first time, that it is possible to restore function to the membrane-resident hClC-1 fragment, aa1-720, even after CBS1 has been deleted, leaving it without a CBS domain. This was achieved by co-expression with a whole C-tail fragment of hClC-1 containing both CBS domains, which is similarly non-functional, if expressed alone. Presumably, an unanticipated, non-covalent, physical interaction between these two fragments lays the foundation for functional rescue in this split channel experiment.

Figure 4 Schematic diagram of hClC-1



The 18 α-helices found in each subunit, are indicated by the blocks labelled A to R with the extracellular region above and the intracellular region below (modified from Dutzler et al. 2002). The CBS1 domain (aa607-662) and CBS2 domain (aa820-871) in the cytoplasmic C-tail are shown as ellipsoids. Amino acid numbers delineating all of the individual domains used in this study are labelled. For the two major hClC-1 fragments, N720 and 721C, employed in our split channel experiments, the position of the split between aa720 and aa721 is indicated by an "X".

3.2 MATERIALS AND METHODS

3.2.1 Plasmid constructs of hClC-1

For convenience, we have labeled our own hClC-1 amino region (N-region) peptide fragments, and those of others, as *N*720 (for aa1-720; i.e. Met 1 to Ser 720), *N*658 (for aa1-658), intermediate fragments as *X*413-720 (for aa413-720; i.e. Phe 413 to Ser 720) and carboxyl-region (C-region) fragments as 721*C* (for aa721-988; i.e. Gly 721 to Leu 988 at the C-terminal), etc. (see Fig. 4). Constructs of hClC-1 cDNA, designed to express the N-region peptides, *N*720, *N*658 and the C-region peptides, typically, 721*C* and 598*C*, etc., were generated by PCR using plasmid pCI-neo-hClC-1 as the template. This plasmid comprised the mammalian expression vector pCI-neo (Promega) into which WT hClC-1 cDNA had been inserted (Bennetts et al. 2001). To facilitate GST-pulldown, particular constructs were labeled at their N-terminal with a FLAG epitope (DYKDDDDK) to express, e.g. FLAG-*N*720 (f-*N*720) and FLAG-721*C* (f-721*C*), while others were tagged at their C-terminal with a c-myc epitope (EQKLISEEDL) to express, e.g., 598*C*-myc (598*C*-m) and 721*C*-myc (721*C*-m). All constructs were then subcloned into mammalian expression vector pEF-IRES-neo to achieve more efficient expression. The cDNA sequence coding for GST was amplified by PCR from prokaryotic GST gene fusion vector pGEX-4T-1 (GE Healthcare) and also inserted into pEF-IRES-neo, forming the mammalian GST fusion vector, pEF-IRES-neo-GST. Where required, our constructs, such as f-*N*720, f-*N*658 and f-721*C* were then subcloned into pEF-IRES-neo-GST to enable expression of the respective GST fusion proteins, GST-f-*N*720 (G-f-*N*720), GST-f-*N*658 (G-f-*N*658) and GST-f-721*C* (G-f-721*C*). These constructs were used as templates for subsequent mutagenesis studies. Green fluorescent protein (GFP) facilitated the visualisation of transfected cells in patch clamp experiments, our 721*C* and 721*C*-m constructs having been subcloned into the pMSCV-IRES-GFP vector (designated pMIG-721*C* and pMIG-721*C*-m, respectively), to allow coordinated expression of GFP and 721*C* or 721*C*-m.

3.2.2 Deletion-scanning and alanine-scanning mutagenesis

Using a method modified from overlap extension PCR (Ho et al. 1989), deletion mutations (where deletion is indicated by Δ) were introduced into G-f-*N*720, 598*C*-m and 721*C*-m to generate the constructs shown in Table 2.

An alanine scanning mutant, 598*C*-m/as = aa598-988-myc/alanine-scan (834-843), was generated in the same way with Gln 834 to Leu 843 being replaced by AAAAAAAAAA. After double digestion by corresponding restriction enzymes and gel purification, the N-

region constructs were ligated into pEF-IRES-neo-GST vector, and those of the C-region were ligated into pEF-IRES-neo. All mutants were subsequently verified by sequencing. In most cases, two independent mutant clones were used for expression and subsequent study.

Table 2 Constructs used in the present study

see Fig. 4 for aa numbers involved

Construct	Details	Notes
G-f-*N*720ΔCBS1	GST-FLAG-aa1-720Δ(607-662)	Deleting CBS1
G-f-*N*720ΔCBS1+	GST-FLAG-aa1-720Δ(592-662)	deleting CBS1 plus the sequence from helix R to CBS1
721*C*-mΔCBS2β	aa721-988-mycΔ(820-862)	deleting the β1β2α1β3 region of CBS2
721*C*-mΔCBS2	aa721-988-mycΔ(820-871)	deleting CBS2
598*C*-mΔpreCBS2	aa598-988Δ-mycΔ(798-819)	deleting the 22 amino acids pre CBS2
598*C*-mΔCBS2α+	aa598-988-mycΔ(863-888)	deleting the α2 region of CBS2 plus the subsequent 17 amino acids
721*C*-ΔpreCBS2a	aa721-988-mycΔ(800-806)	deleting seven amino acids early in the 22 amino acid pre CBS2 sequence
721*C*-ΔpreCBS2b	aa721-988-mycΔ(807-813)	deleting seven amino acids in the middle of the 22 amino acid pre CBS2 sequence
721*C*-mΔCBS2α+	aa721-988-mycΔ(863-888)	deleting the α2 region of CBS2 plus the subsequent 17 amino acids

3.2.3 Cell culture and transfection

HEK 293T cells (American Type Culture collection, Rockville, MD) were maintained in DMEM supplemented with 10% (v/v) of a mixture of Newborn Calf Serum and Fetal Calf Serum (9% (v/v) NCS and 1% (v/v) FCS) (Gibco, Paisley, UK), 2 mM L-glutamine, 1% (v/v) non-essential amino acids, at 37°C, 5% CO_2 atmosphere. For GST-pulldown assays, cells were plated at a density of 1×10^6 per 60-mm dish 24 hours before transfection, and were transfected or co-transfected with various hClC-1 cDNA constructs. All the transient transfections and stable transfections were carried out using Lipofectamine 2000 (Invitrogen) according to the manufacturer's instructions. For each GST-pulldown assay, the same amount of pEF-IRES-neo-GST was transfected as a negative control, from which only GST protein would be expressed.

In case of split channel studies for patch clamping, either HEK 293T cells were transiently co-transfected with *N*720 or G-f-*N*720 and pMIG-721*C* or pMIG-721*C*-m at a molar ratio of 1:1, or HEK 293T-598*C*-m cells, which were HEK 293T cells stably transfected with construct 598*C*-m, were transiently transfected with G-f-*N*720ΔCBS1 and pEGFP-N1 (Clontech) at a molar ratio of 10:1. Transfected cells could be identified by their green fluorescence, in the last case, due to reporter plasmid-driven expression of enhanced green fluorescent protein (EGFP).

3.2.4 GST-Pulldown Assay and Western Blotting

Transfected cells were harvested and lysed on ice for 30 min in lysis buffer containing 150 mM NaCl, 20 mM Tris-HCl (pH 8.0), 10% glycerol, 0.2% Triton X-100, 0.2 mM DTT and protease inhibitor cocktail (1 µg/ml pepstatin, 1 µg/ml leupeptin, 0.5 mM PMSF, 5 µg/ml benzamidine, 0.1 µl/ml aprotinin). After centrifugation at 18,000 x g for 15 min at 4°C, the supernatant was collected and the protein concentration was measured using the BCA Protein Assay Kit (Pierce). Equal amounts of protein (1 mg) were incubated with 50 µl of glutathione-Sepharose 4B beads (GE Healthcare) for 3 h. The beads were then collected by short centrifugation and washed four times (10 min each time) with 1 ml lysis buffer. All procedures were carried out at 4°C. The bound proteins were finally liberated by heating at 55°C for 20 min in 2 x Laemmli sample buffer and separated by SDS-PAGE (6%-12% polyacrylamide).

Proteins on SDS-PAGE gel were transferred to nitrocellulose membranes. The blots were then blocked for 1 h in TBST buffer (150 mM NaCl, 25 mM Tris, pH 7.4, 0.1% Tween-20) containing 5% skim milk powder and incubated for 1 h either with anti-FLAG M2 Monoclonal Antibody (Sigma) or with anti-myc antibody (culture supernatant from hybridoma cell line 9E10, ATCC) in the blocking buffer. After four washes in TBST buffer and 1 h incubation with secondary antibody (horseradish peroxidase-conjugated anti-mouse IgG, Sigma), reacting protein bands were visualized with an enhanced chemiluminescence detection system (Amersham Biosciences, Little Chalfont, UK).

3.2.5 Electrophysiology

Patch-clamp experiments were conducted at room temperature in the whole-cell configuration using an Axopatch 200B patch-clamp amplifier and associated standard equipment (Axon Instruments, Foster City, CA), as described previously (Wu et al. 2006). Cells were continuously superfused with bath solution containing 140 mM NaCl, 4 mM CsCl, 2 mM

$CaCl_2$, 2 mM $MgCl_2$, and 10 mM HEPES, adjusted to pH 7.4 with NaOH. Patch pipettes were pulled from borosilicate glass and typically had a resistance of 1-3 megohms when filled with the standard pipette solution containing 40 mM CsCl, 85 mM Cs glutamate, 10 mM EGTA-Na, 10 mM HEPES, adjusted to pH 7.2 with NaOH. Series resistance did not exceed 3 megohms and was 75-85% compensated. Currents obtained were filtered at 3 kHz, collected and analysed using Clampex 9.0 Software (Axon Instruments).

3.2.6 Data Analysis

The voltage dependence of the apparent overall channel open probability (P_o) was determined by measuring tail-current relaxation at a constant voltage of -100 mV for 40 ms, after 160 ms test pulses at increasingly hyperpolarizing (-20 mV) steps ranging from +100 to -140 mV. To study the voltage dependence of the open probability of common gating (P_o^c), a short prepulse of 400 µs to +180 mV was inserted before the -100 mV tail pulse, to fully activate the fast gate, and the open probability of fast gating (P_o^f) was then calculated by dividing P_o by P_o^c (Accardi & Pusch 2000). Between test sweeps the cell membrane was clamped at a holding potential of -30 mV for a period of 2 s. Apparent P_o curves were obtained by fitting data points with a Boltzmann distribution of the form:

$$P_o(V) = P_{min} + (1- P_{min}) / \{1+ \exp [V_{1/2} - V) / k]\}, \quad (1)$$

where P_{min} is an offset or minimum P_o at very negative potentials, V is the membrane potential, $V_{1/2}$ is the potential at which $P_o = (1 + P_{min})/2$ (half maximal activation) and k is the slope factor. All the data were analyzed by Clampex 9.0 and Graph-Pad Prism 4.0 (GraphPad software, San Diego, CA) software using the same method described previously (Wu et al. 2006). Potentials listed are pipette potentials expressed as intracellular potentials relative to outside zero.

3.3 RESULTS

3.3.1 Investigation of the effects of tags on split channel studies

In a previously reported reconstitution of hClC-1, its N-terminal membrane-resident region including a short length of C-tail, typically aa1-720 (*N*720), co-expressed with its complementary distal C-tail fragment, typically aa721-988 (721*C*), combined to allow the flow of Cl^- currents with WT characteristics (Schmidt-Rose & Jentsch 1997a). However, it is still unclear how these two complementary fragments (indicated by splitting at "X" in Fig. 4) cooperate to produce functional channels.

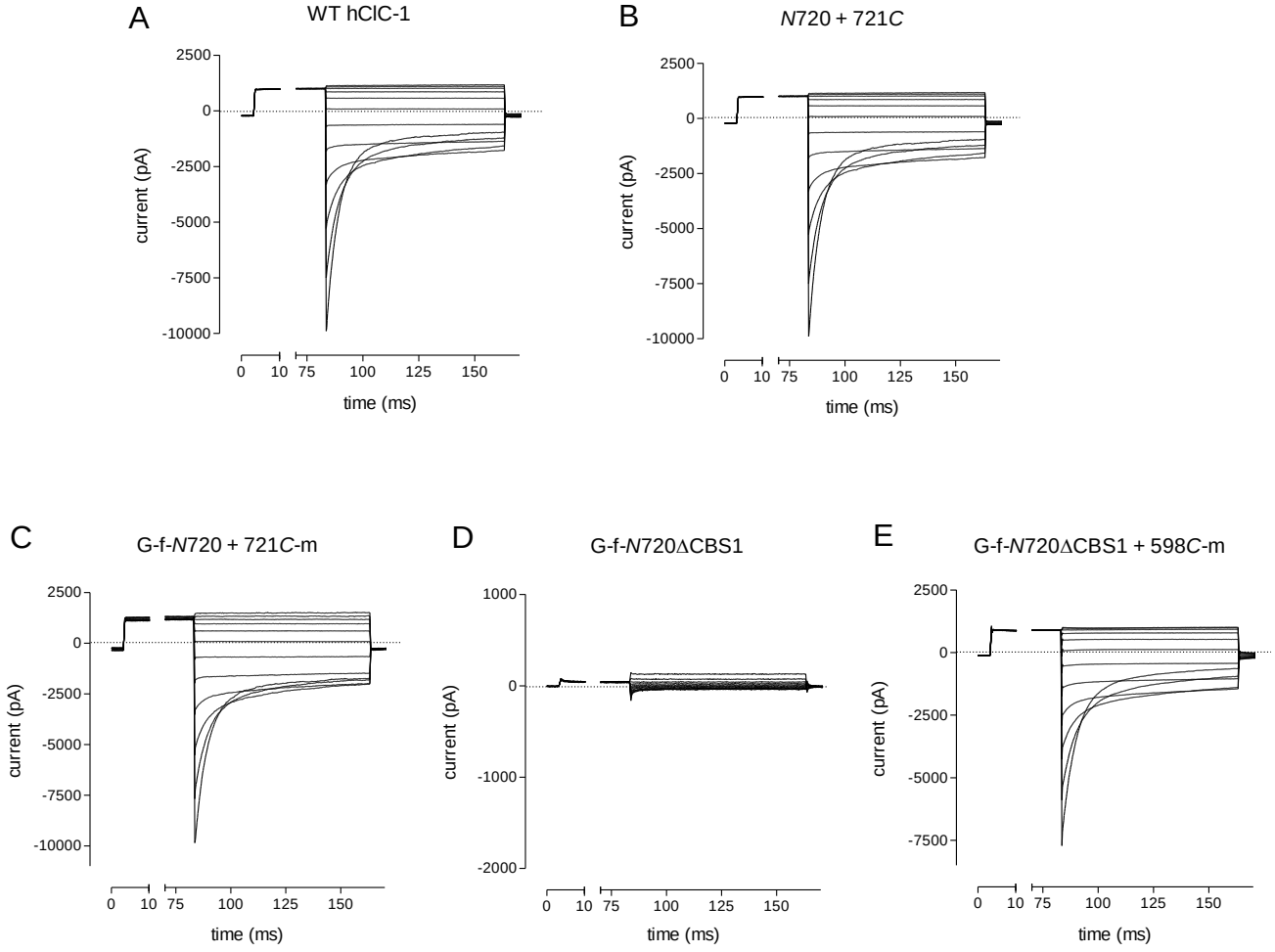
To map the essential interacting parts of these N- and C-region peptides required for this functional rescue a panel of deletion and truncation mutants were constructed and heterologously expressed in HEK 293T cells. As necessary, all N-region constructs were tagged with GST and FLAG epitopes on their N-termini, while C-region constructs were all tagged with c-myc epitopes on their C-termini to facilitate the detection of interactions. Preliminary experiments were conducted to determine whether these tags would affect channel reconstitution by comparing the function of channels composed of fragments with antigenic tags (G-f-*N720* + 721*C*-m) or without them (*N*720 + 721*C*). As shown in Figure 5 and Table 3, according to the patch clamping results, there was no significant difference with both split channels producing WT hClC-1 currents. These featured inward rectification, depolarization-induced activation, a rapid, partial deactivation upon hyperpolarization with a bi-exponential deactivation time course, and the presence of two kinetically distinct gating processes. In this way we were able to exclude any effects of the chosen tags on the expression, targeting or function of either N-region or C-region peptides in our split channel experiments.

3.3.2 Identification of interacting regions in split channel G-f-*N*720 + 721*C*-m

Subsequent to the above verifications, protein-protein interaction studies of different split channels were carried out by GST-pulldown assays, in which split channel G-f-*N*720 + 721*C*-m was used as a positive control, and a construct with only GST protein expressed was used as the negative control to confirm the specificity of the results. In all the GST-pulldown experiments, a reasonable expression level of the N-region peptides, which is a basic requirement to exclude false negative results, was first tested by Western blot using anti-FLAG M2 antibody. As shown in Figure 6A, 7A, 7B and 8A, G-f-721*C* and all of the GST-fused N-region peptides, which were used as bait proteins for GST-pulldown in this study, were very well expressed.

First of all, we found that the shorter C-tail peptide, 721*C*, which contains only CBS2, could bind to itself forming a homodimeric complex in the absence of CBS1 as its normal binding partner (Fig. 6B, lanes 4-6). When some apparently functionally important short aa sequences including aa800-806, aa807-813 (Estévez et al. 2004) and aa863-888 (Wu et al. 2006) were deleted from 721*C*-m (generating 721*C*-mΔpreCBS2a, 721*C*-mΔpreCBS2b and 721*C*-mΔCBS2α+, respectively), there was still strong binding with G-f-*N*720 (Fig. 6C). So, although these short sequences might be essential for channel function, they are unnecessary for binding between the complementary fragments *N*720 and 721*C*.

Figure 5. Electrophysiological analyses of split channels



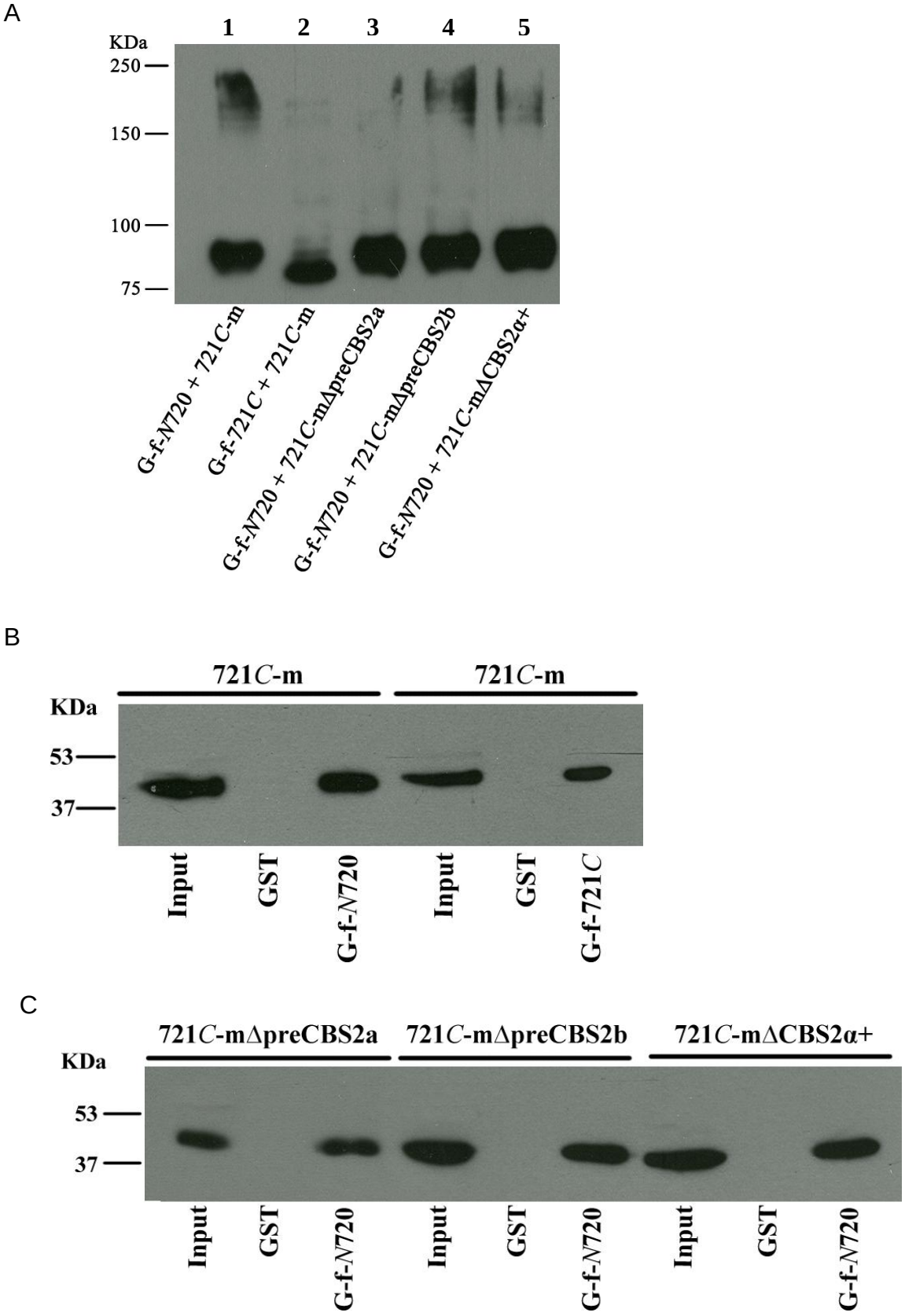
Chloride current traces were obtained by whole-cell patch clamping from HEK293T cells transfected with: (panel A) the positive control WT hClC-1, (panel B) the *N*720 + 721*C* split channel without any tags on the channel fragments, (panel C) the same split channel but now with *N*720 tagged with GST and FLAG (G-f-*N*720), and 721*C* tagged with c-myc (721*C*-m), (panel D) this split channel again but with CBS1 deleted (G-f-*N*720ΔCBS1) and (panel E) a co-expression with CBS1 deleted (G-f-*N*720ΔCBS1) plus the complete C-tail (598*C*-m). As a negative control, cells transfected with (G-f-*N*720ΔCBS1), alone, showed no Cl^- currents. All of these co-expressions support currents indistinguishable from WT. Currents were recorded 24 h after transfection in response to test pulses of 80 ms duration in steps of -20 mV from +80 mV to -140 mV following a conditioning pulse to +40 mV for 80 ms.

Table 3. $V_{1/2}$ of overall channel open probability (P_o) , fast gating (P_o^f) and common gating (P_o^c) for WT hClC-1 and split hClC-1 channels

Peak tail currents, recorded using the protocols described in the experimental procedures, were used to derive P_o values and these were fitted with Boltzmann distribution curves. Fast and common gating parameters were separated using the method of Accardi and Pusch [24]. The truncated mutant, G-f-*N*720ΔCBS1, with CBS1 deleted, showed no Cl^- currents by itself. None of the split channels have characteristics that are significantly different from the WT hClC-1 channel. Values of $V_{1/2}$ in millivolts (mV) are shown as mean ± S.E.

WT/split channel (no. of cells)	$V_{1/2}$ P_o (mV)	$V_{1/2}$ P_o^f (mV)	$V_{1/2}$ P_o^c (mV)
WT hClC-1 (n=15)	-71.7 ± 2.5	-106.4 ± 0.8	-78.0 ± 2.0
*N*720 + 721*C* (n=7)	-72.1 ± 1.3	-102.4 ± 1.2	-64.5 ± 2.1
G-f-*N*720 + 721*C*-m (n=8)	-80.2 ± 1.7	-96.8 ± 2.5	-76.1 ± 1.4
G-f-*N*720ΔCBS1 (n=8)	No currents	No currents	No currents
G-f-*N*720ΔCBS1 + 598*C*-m (n=6)	-69.6 ± 2.2	-84.7 ± 1.8	-73.4 ± 2.3

Figure 6. Interaction between various 721*C*-m mutants and G-f-*N*720



A, Inputs of GST-fusion proteins in each GST-pulldown assay, detected by Western blotting using anti-FLAG M_2 antibody against the FLAG epitope showing that GST-fusion proteins are well expressed. Lane 1 and lanes 3-5 show the expression levels of G-f-*N*720 when it was co-expressed with 721*C*-m variants using 721*C*-m, itself, as positive control, then with 721*C*-mΔpreCBS2a (aa800-806 deleted), 721*C*-mΔpreCBS2b (aa807-813 deleted) and 721*C*-mΔCBS2α+ (aa863-888 deleted), respectively. The lower band in each lane at molecular weight ~ 80KDa corresponds to the monomer of G-f-*N*720, and the upper band in each lane at molecular weight ~ 160KDa is probably an SDS-resistant homodimer. The single band in lane 2 at molecular weight ~ 75KDa shows the expression level of G-f-721*C* when it was co-expressed with 721*C*-m to investigate whether this short tail peptide could form a dimer, independently. B, GST-pulldown shows the direct interaction between G-f-*N*720 and 721*C*-m (lanes 1-3), which serves as a positive control for all of the other GST-pulldown assays. Also, as demonstrated by the binding between G-f-721*C* and 721*C*-m (lanes 4-6), 721*C* can form homodimers *in vitro*. C, GST-pulldown results demonstrate the interaction between G-f-*N*720 and the 721*C*-m variants, 721*C*-mΔpreCBS2a (lanes 1-3), 721*C*-mΔpreCBS2b (lanes 4-6) and 721*C*-mΔCBS2α+ (lanes 7-9), respectively. The Input lanes indicate the input of the 721*C*-m mutants in each pulldown assay, detected by Western blot using 9E10 anti-myc antibody against the c-myc epitope. The GST lanes indicate the GST-pulldown results for the same 721*C*-m mutants using unfused GST protein as negative controls to exclude the possibility that the target proteins could be pulled down by GST protein, itself. The G-f-*N*720 lanes are GST-pulldown results showing the interaction between G-f-*N*720 (as the bait protein) and the 721*C*-m variants (as target proteins). All GST-pulldown assays were carried out using glutathione-Sepharose 4B beads for precipitation and the anti-myc antibody for detection in Western blotting.

However, when CBS1, aa607-662, or CBS1 together with a short sequence leading up to it from the end of helix R, aa592-662, were deleted from G-f-*N*720, generating G-f-*N*720ΔCBS1 and G-f-*N*720ΔCBS1+, respectively, binding with 721*C*-m could no longer be detected (Fig. 7C). Similarly, when the β1 to β3 sequence of CBS2, aa820-862, or the whole of CBS2, aa820-871, was deleted from 721*C*-m, generating 721*C*-mΔCBS2β and 721*C*-mΔCBS2, respectively, interaction with G-f-*N*720 disappeared as well (Fig. 7D-E). Therefore, the coexistence of CBS1 in *N*720 and CBS2 in 721*C* was indispensable for the binding between these two channel fragments.

The more severely truncated N-region construct, *N*658, in which a short sequence at the end of the CBS1 domain is missing, is similar to the naturally occurring myotonic mutation (Q658*X*). We wanted to know whether 721*C* could help to restore the function of *N*658 on co-expression in HEK 293T cells. Unfortunately, *N*658 degraded even when co-expressed with 721*C* (Fig. 7A, lane 3), which explained the absence of interaction between them (Fig. 7C). It had earlier been shown that co-expression of *N*679 + 721*C* could generate WT currents (Estévez et al. 2004), so the sequence between aa659 and aa679 might be important for maintaining the integrity of the membrane-resident N-region of the channel protein in the absence of a CBS2-containing tail. This might also explain why an N-region hClC-1 construct truncated beyond Gln 597 could not be functionally rescued by its complementary C-tail in the co-expression, *N*597 + 598*C* (Schmidt-Rose & Jentsch 1997a). For this reason, we undertook the following experiments keeping this short region, aa659 to aa679 intact within the N-region peptide.

3.3.3 Interaction between the whole C-tail and the membrane-resident domain

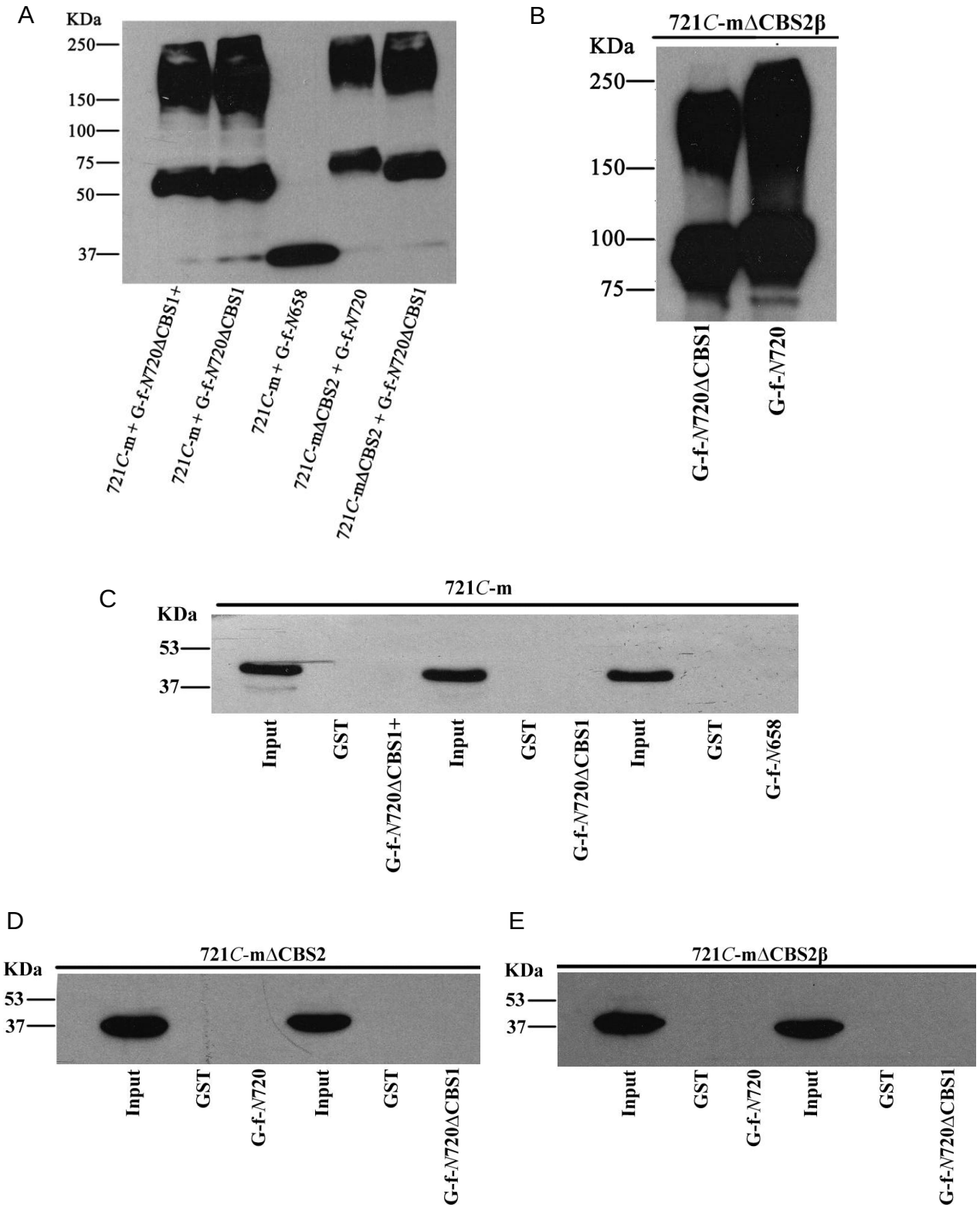
Notice that the above CBS1-CBS2 interaction occurs between CBS1, which exists in the N-region peptide, *N*720, and CBS2 in the C-region peptide**,** 721*C*, respectively. Also, most of the previous split channel experiments have shown that CBS1 and CBS2 need to be in the N-region and C-region complemented fragments, respectively, to rescue channel function (Schmidt-Rose & Jentsch 1997a; Maduke, Williams & Miller 1998; Estévez et al. 2004; Mo et al. 2004). Therefore, it seemed quite reasonable to deduce, based on previous reports and our present results, that the interaction between CBS1 and CBS2 in complemented fragments would be essential for restoring channel function in split channels. Are there, however, any other interactions between the C-tail and the membrane-resident domain besides this CBS1-CBS2 interaction? How, for example, could the CBS1-CBS2 pair support common gating, which also involves interacting helices at the dimer interface and the R-helix (Duffield et al. 2003; Chen 2005)? To try to answer these questions, we designed a new split channel

experiment, in which fragment *N*720 with CBS1 deleted (G-f-*N*720ΔCBS1) was co-expressed with 598*C*-m (Fig. 8A). In this way, we should be able to exclude the effect of CBS1-CBS2 interaction between the split N- and C-region channel fragments and investigate the relationship between the whole C-tail, which contains both CBS1 and CBS2, and the membrane-resident region without any CBS domain. We expected that the N-region channel fragment would be expressed well since most of the aa659-679 sequence is kept intact.

Interestingly, we detected binding between G-f-*N*720ΔCBS1 and 598*C*-m by GST-pulldown, indicating that there is, indeed, protein-protein interaction between the whole C-tail containing the two CBS domains and the membrane-resident N-region with no CBS domain (Fig. 8B,C). To investigate whether such interaction is functionally significant, we also studied the electrophysiological features of this split channel by whole-cell patch clamping. As shown in Figure 5 and Table 3, no Cl^- currents could be obtained when truncated mutant, G-f-*N*720ΔCBS1, was expressed alone in HEK 293T cells. When co-expressed with the whole C-tail, 598*C*-m, however, Cl^- channel function was fully restored, with no significant difference from WT hClC-1 currents.

When we tried to narrow down the essential positions further, with respect to the interactions between the C-tail peptide, 598*C*, and the membrane-resident N-region, we found that, unfortunately, the expression of 598*C*, seemed to be very dependent on its total integrity (no deletions). Deletion of short internal sequences or alanine exchange of the α1 helix of CBS2, Δaa798-819 (598*C*-mΔpreCBS2), Δaa863-888 (598*C*-mΔCBS2α+) and alanine exchange aa834-843 (598*C*-m/as) (Fig. 4) either made this fragment too unstable (for 598*C*-mΔpre CBS2 and 598*C*-mΔCBS2α+) or caused it to be expressed very weakly (for 598*C*-m/as) (data not shown).

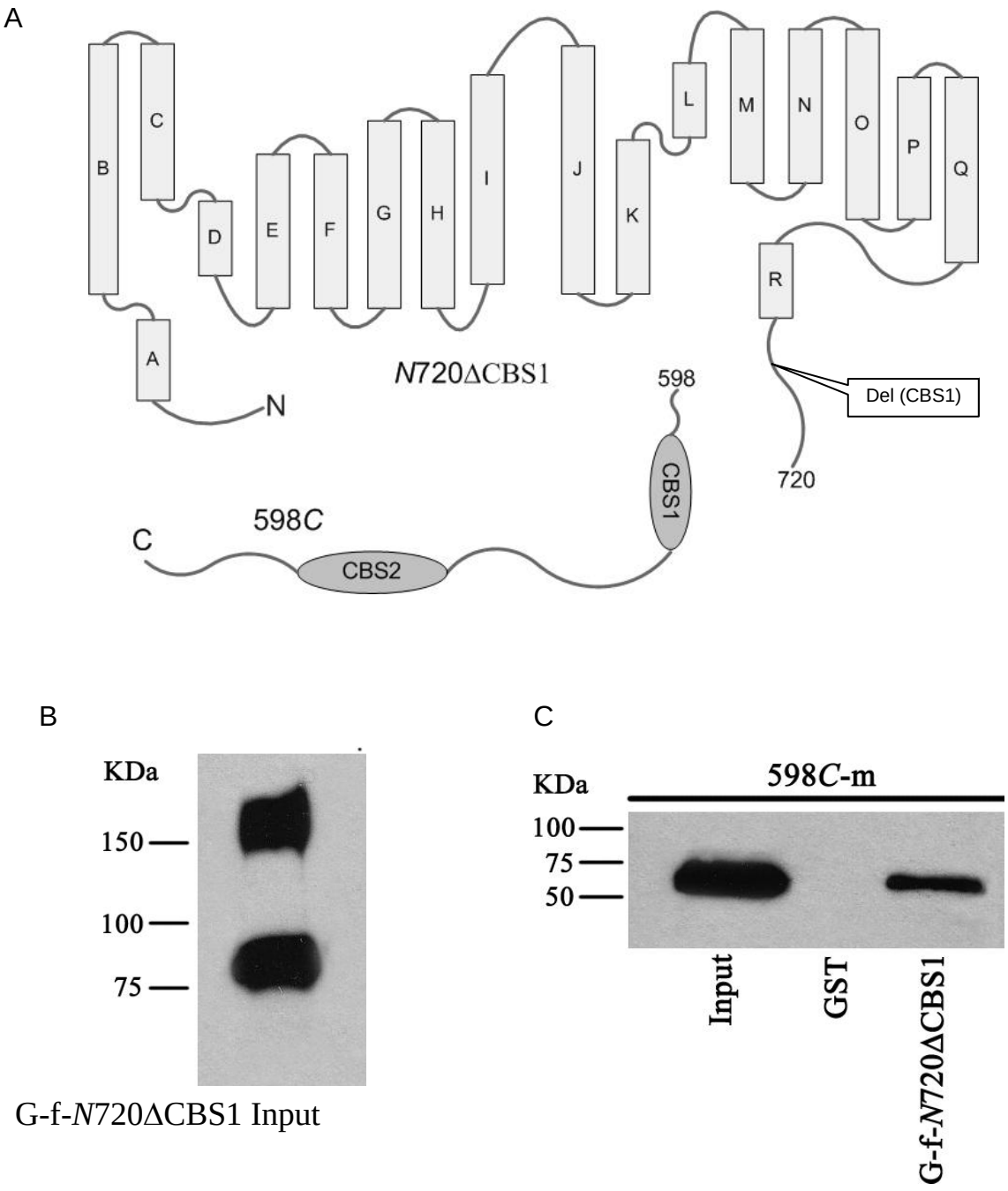
Figure 7. Effects of CBS domains and related regions on the interaction between complemented channel fragments G-f-*N*720 and 721*C*-m



A-B, Inputs of GST-fusion proteins in each GST-pulldown assay, with the lower bands (~75KDa for G-f-*N*720ΔCBS1+ and G-f-*N*720ΔCBS1; ~80KDa for G-f-*N*720) representing

monomers and the upper bands (~150KDa for G-f-*N*720ΔCBS1+ and G-f-*N*720ΔCBS1; ~160KDa for G-f-*N*720) corresponding to SDS-resistant dimers. Degradation of G-f-*N*658 to ~35KDa occurred, even when co-expressed with 721*C*-m (lane 3 of panel A). Detection was by Western Blot using anti-FLAG M_2 antibody against the FLAG epitope. C-E, Results from GST-pulldown assays illustrate that there is no interaction between any of the G-f-*N*720 mutants and the 721*C*-m mutants, including G-f-*N*720ΔCBS1+ + 721*C*-m (C, lanes 1-3), G-f-*N*720ΔCBS1 + 721*C*-m (C, lanes 4-6), G-f-*N*658 + 721*C*-m (C, lanes 7-9), G-f-*N*720 + 721*C*-mΔCBS2 (D, lanes 1-3), G-f-*N*720ΔCBS1 + 721*C*-mΔCBS2 (D, lanes 4-6), G-f-*N*720 + 721*C*-mΔCBS2β (E, lanes 1-3), and G-f-*N*720ΔCBS1 + 721*C*-mΔCBS2β (E, lanes 4-6). All the lanes are labelled in the same way as in Figure 6.

Figure 8. Interaction between 598*C*-m and G-f-*N*720ΔCBS1



A, Schematic representation (modified from Dutzler et al. 2002) of split channel G-f-*N*720ΔCBS1 + 598*C*-m. The N-region peptide has CBS1 deleted, and the C-region peptide contains both CBS1 and CBS2. B, The input of GST fusion protein G-f-*N*720ΔCBS1 in the GST-pulldown assay, detected by Western blotting using anti-FLAG M_2 antibody against the FLAG epitope. C, GST-pulldown result of 598*C*-m + G-f-*N*720ΔCBS1, showing the specific interaction between these two fragments. All the lanes are labelled in the same way as in Figure 6.

3.4 DISCUSSION

The C-tail of eukaryotic CLC channels has been shown to be involved in important channel characteristics such as common gating and sensing cellular energy status (Estévez et al. 2004; Hebeisen et al. 2004; Bennetts et al. 2005; He et al. 2006). In particular, it has been recently demonstrated by solving the crystal structure of the cytoplasmic domain of ClC-5 in complex with ATP and ADP that the C-tail contains a specific binding site for nucleotides, which raises additional interest in this region (Meyer et al. 2007). However, the molecular mechanisms underlying the functional significance of these C-tails are still unclear. In the present study, we have investigated the C-tail of hClC-1, focusing on several functionally important regions using split channel strategies, and revealed that the interaction between CBS1 and CBS2 could form a structural foundation for the whole C-tail to communicate with the membrane-resident pore domain.

According to the crystal structure of the cytoplasmic domain of ClC-0 from the electric ray *Torpedo marmorata*, 25 residues of the linker region prior to CBS2 forms a helix followed by an extended loop, which interacts with CBS1 (Meyer & Dutzler 2006). In hClC-1, the corresponding putative small helix before CBS2 includes the short sequence, aa800-820, which had been found to be necessary in the functional interaction between complementary fragments *N*720 and 721*C* (Estévez et al. 2004). Out of three smaller fragments within this 20aa stretch, aa800-806, aa807-813 and aa814-820, only deletion of aa807-813 from 721*C* completely prevented the recovery of Cl^- currents when co-expressed with *N*720 in *Xenopus* oocytes (Estévez et al. 2004). In the present study, we investigated the physical role of aa807-813 in this interaction, using aa800-806 as a plausible negative control. Also, a short peptide of 26 amino acids from Leu 863 to Arg 888 (aa863-888) had been found to be particularly important, because channel function was restored by co-expressing this peptide with the otherwise inactive truncation, G721*X* (*N*720), in the *Xenopus* oocyte system (Wu et al. 2006). Therefore, aa863-888, another possible candidate sequence for interaction with the membrane-resident pore region, was deleted from 721*C* to investigate its role in the binding between *N*720 and 721*C*. Surprisingly, none of the functionally significant short sequences, whether present or absent, had any obvious effect on the binding. The substantial influences of these short sequences on function might, therefore, reflect relatively weak interactions with the membrane-resident pore domain, rather than, themselves, constituting strong binding sites for the functional rescue of this split channel. Alternatively, their role in the binding between *N*720 and 721*C* could be compensated by some other definable parts of the C-tail when they are deleted individually.

Two CBS domains, each composed of two α-helical and three β-strand segments in the order β1α1β2β3α2, are arranged in tandem within the C-tails of all eukaryotic CLC proteins (Estévez & Jentsch 2002). In CLC channels, the function of CBS domains is still quite controversial (Estévez et al. 2004; Hebeisen et al. 2004; Ignoul & Eggermont 2005). Bacterial CLC proteins dimerize in the absence of CBS domains, so it can be inferred that the CBS domains are not required for dimerization (Dutzler et al. 2002; Estévez et al. 2004). Furthermore, the CBS domains reside in the cytosol and, therefore, they are unlikely to contribute to the core structure of the permeation pathway, which is formed by the membrane-embedded α-helices (Dutzler et al. 2002). Then how do these domains carry out their essential roles in channel function? The present work examines the roles of CBS domains in the split hClC-1 channel by physical interaction assessment, and reveals that the interaction between CBS1 and CBS2 is the primary structural foundation for the functional rescue of the split channel when the channel protein is split between the two CBS domains. Moreover, we find that the CBS1-CBS2 interaction might only be a first step in the complicated conformational rearrangements, which are necessary for the functional reconstitution of split channels. This is demonstrated by the binding of 598*C* to *N*720ΔCBS1 and by the functional channel that is generated from co-expressing these two fragments. The CBS pair, which forms in the whole C-tail (598*C*), probably acts as a structural and functional unit to transfer essential information to the membrane-resident, pore region by close, non-covalent association with some specific sequences in the transmembrane helices or the cytoplasmic loops linking them.

It seems that otherwise-intact, hClC-1 channels remain functional if either individual CBS domain is deleted (Estévez et al. 2004; Hebeisen et al. 2004). Functional reconstitution in split channels, however, requires CBS1-CBS2 interaction, presumably initiating some significant and essential, but presently unknown, conformational change amounting to rather more than just the process of the two CBS domains binding to each other.

For split channel *N*720 + 721*C*, the CBS2 domain might be needed to bring the distal sequence following it into the correct position to confer some necessary tertiary structure by interacting with CBS1; while for split channel *N*720ΔCBS1 + 598*C*, when CBS2 and its distal tail have already positioned correctly with respect to CBS1, the cytoplasmic domain with a specific three-dimensional structure then could interact with the membrane-resident pore domain to support some key attributes of the channel, such as common gating.

For both ClC-0 and hClC-1, common gating has been found to be temperature sensitive, suggesting that it is associated with complex structural rearrangements (Pusch, Ludewig & Jentsch 1997; Bennetts et al. 2001). Besides the broad interface between the two subunits, such changes might also involve the final helix, helix R, and distal C-tail (CBS2 and the sequence that follows CBS2). Many mutations that change gating of different CLC family members are located within this distal part of the C-tail, such as A885P, H835R and H838A in hClC-1 (Beck, Fahlke & George 1996), H736A, E763K, and A783P in ClC-0 (Estévez et al. 2004) and, putatively, since they are dominant mutations, G765D and R767W in ClC-7 (Cleiren et al. 2001). Moreover, several truncations or substitutions of the C-tail after CBS2 show large shifts in the open probability of the channels (Fong, Rehfeldt & Jentsch 1998; Hryciw et al. 1998). Especially, in this region, a conserved sequence, LRPPLASFR, was recently identified as important for the voltage dependence of gating in hClC-1 (where it occurs at aa880-888) and also in ClC-0 (Macías et al. 2007). On the other hand, helix R of the membrane-resident domain, which is directly followed by the C-tail, contributes a tyrosine (Tyr 589) to coordinate a Cl^- ion in the central ion binding site (S_{cen}) of the selectivity filter. This peculiar architecture, along with the possible proximity of CBS2 and the following C-tail sequence to the pore region in the crystal structure, as demonstrated by some studies (Meyer & Dutzler 2006; Markovic & Dutzler 2007), provides a plausible structural explanation for our findings. Thus we suggest that, in the usual split channels, CBS1 and CBS2 might first bind with each other to expose the α-helices of CBS2 to the surface and to bring the distal C-tail close enough to helix R and nearby regions of the membrane-resident domain. This could then trigger a possible interaction between the C-tail and the selectivity filter, which leads to a conformational rearrangement in the ion conduction path and modulates the channel's common gating.

Nevertheless, although in split channels, CBS1 and CBS2 domains could make a cooperative contribution to the rescue of normal channel operation by interacting with each other, each of them still seems to have its own specific role. It was shown that CBS1 could functionally replace the CBS2 domain of 721C in split channel studies, but, when CBS1 was replaced by CBS2 in the uninterrupted hClC-1 protein, no detectable hClC-1 currents could be recorded (Estévez et al. 2004). From the present CBS2-CBS2 binding result (Fig.6B), we are able to deduce that CBS2 could not replace CBS1 in the earlier work (Estévez et al. 2004), probably because of some distinctive requirement for CBS1 within its adjacent sequence environment, rather than because of an interaction failure between the two CBS2 domains.

Our present studies, in conjunction with previous split channel results (Schmidt-Rose & Jentsch 1997a; Maduke, Williams & Miller 1998; Estévez et al. 2004; Hebeisen et al. 2004; Wu et al. 2006), allow us to hypothesize that the short stretch from aa666 to aa679 in ClC-1 might include a trafficking signal. We propose that this signal must be contiguous with at least one membrane-resident component of split hClC-1 channels, instead of being contained solely within a cytoplasmic C-tail fragment. Non-covalent association of the two (or more) components, would then allow transport to the plasma membrane, incorporation and function. Proteins that fail to be trafficked to the plasma membrane might then be degraded. In this way it is possible to explain our present functional reconstitution of **N*720ΔCBS1 + 598*C* and that of previously tested split ClC-1 channels, **N*720 + 721*C*, *N*390 + *369*C*, *N*451 + *413*C*, **N*679 + 801*C*, *N*451 + **X*413-720 + 721*C* and **N*720 + *X*863-888 (Schmidt-Rose & Jentsch 1997a; Estévez et al. 2004; Wu et al. 2006). The asterisks indicate the components in which the putative trafficking signal might reside. If this trafficking signal, however, only exists in the cytoplasmic fragment of a split channel, such as in *N*597 + *598*C* or *N*650 + *590*C*, or if it is missed, as in *N*665 + 721*C*, then, as has been observed (Schmidt-Rose & Jentsch 1997a; Hebeisen et al. 2004), we would expect no functional rescue. The last of these, *N*665 + 721*C*, also serves to underline our contention that the presence of both CBS1 and CBS2 in the split channel is, alone, inadequate for trafficking/functional reconstitution, even though it might be sufficient to establish binding between the two components. Results from in-frame deletions of CBS1 and/or the CBS1-CBS2 inter-linker region up to aa818, within otherwise continuous hClC-1 proteins (Hebeisen et al. 2004), however, suggest that this putative signal region may be unnecessary if the C-tail extends its subsequent full and uninterrupted length.

Clearly, more studies and new methods are required to elucidate the different properties of the CBS1 and CBS2 domains, and to narrow down the sites of significant interaction between the membrane-resident pore region of the channel and its C-tail.

CHAPTER 4:
FUNCTIONAL STUDY OF CYTOPLASMIC LOOPS OF HUMAN SKELETAL MUSCLE CHLORIDE CHANNEL, hClC-1

4.1 INTRODUCTION

Insights into functional regions of CLC family proteins and transporters have been greatly advanced since the determination of their general crystal structure, and confirmation of their dimeric arrangement (Dutzler et al. 2002) (see, e.g. currently accepted topological arrangement of membrane-resident α-helices as illustrated in Figure 9). Although this has identified the amino acid residues lining the conduction pathway, forming the selectivity filter and acting as the protopore or fast gate of each CLC channel monomer, the regions comprising the common or slow gate and many of the peptide sequences involved in the modulation of gating are still to be identified definitively.

Of the two gating processes controlling the permeation pathways of the human ClC-1 (hClC-1) skeletal muscle Cl^- channel, protopore gating regulates conduction through each channel monomer individually and independently (Saviane, Conti & Pusch 1999), as it does in the *Torpedo* electroplaque Cl^- channel, ClC-0 (Miller 1982). It is proposed to be mainly mediated by the movement of a carboxyl side chain at E232 in helix F, which could block the Cl^- pathway by occupying the most external anion-binding site (S_{ext}) in the selectivity filter (Dutzler et al. 2002). Common gating regulates conduction through both protopores simultaneously and is, therefore, believed to rely on subunit interactions, probably involving helices at the dimer interface, the R-helix and the cytoplasmic tail (Pusch, Ludewig & Jentsch 1997; Fong, Rehfeldt & Jentsch 1998; Accardi & Pusch 2000; Duffield et al. 2003; Estévez et al. 2004; Wu et al. 2006).

Existing data suggested that the cytoplasmic domain of CLC proteins might influence gating as a result of complex voltage-dependent conformational rearrangements, triggered by some kind of interaction between the C-tail and the pore pathway of the channel, and this might, secondarily, affect intrinsic pore properties (Hebeisen & Fahlke 2005). Any important interaction between the cytoplasmic amino-tail (N-tail) and the C-tail can probably be discounted because the N-tail can be deleted without significant effect on channel function (Schmidt-Rose & Jentsch 1997a). Cytoplasmic loops with potential exposure to the C-tail might make candidate sites in the membrane-resident domain for this kind of interaction.

Loops connecting adjacent α-helices are likely to be the least constrained regions in the membrane-resident domains of CLC proteins. It is well known that in extracellular loop LM, a glycosylation site is present in all known eukaryotic CLC proteins except ClC-7 (N430 for hClC-1) (Kieferle et al. 1994; Brandt & Jentsch 1995; Schmidt-Rose & Jentsch 1997b). Also, the yeast CLC protein, Gef1p, is proteolytically cleaved in its first extracellular loop during its biogenesis. Functional channels could assemble when the two fragments from the cleavage reaction were co-expressed (Wächter & Schwappach 2005). However, so far there has been little investigation of the physiological features of loop regions in CLC channels. In the present study, we focused on particular cytoplasmic loops of hClC-1 to reveal their possible roles in the interaction between the membrane-resident domain and the C-tail in split channels, as well as the significance of individual loops for channel function.

4.2 MATERIALS AND METHODS

4.2.1 Basic constructs of hClC-1

As described fully in previous work (Ma et al. 2008), we have labeled our hClC-1 amino region (N-region) peptide fragment as *N*720 (for residues 1-720; i.e. Met 1 to Ser 720) and carboxyl-region (C-region) fragments as 598*C* (for residues 598-988; i.e. Leu 598 to Leu 988 at the C-terminus) and 721*C* (accordingly). Constructs of hClC-1 cDNA, designed to express these peptide fragments were generated by PCR using plasmid pCI-neo-hClC-1 as the template. This plasmid comprised the mammalian expression vector pCI-neo (Promega) into which WT hClC-1 cDNA had been inserted (Bennetts et al. 2001). To facilitate GST (glutathione transferase)-pull-down, particular constructs were labeled at their N-terminus with a FLAG epitope (DYKDDDDK) to express, e.g. FLAG-*N*720 (f-*N*720), while others were tagged at their C-terminus with a c-myc epitope (EQKLISEEDL) to express, e.g., 598*C*-myc (598*C*-m). All constructs were then subcloned into mammalian expression vector pEF-IRES-neo to achieve more efficient expression. The cDNA sequence coding for GST was amplified by PCR from prokaryotic GST gene fusion vector pGEX-4T-1 (GE Healthcare) and also inserted into pEF-IRES-neo, forming the mammalian GST fusion vector, pEF-IRES-neo-GST. Where required, our constructs, such as f-*N*720, were then subcloned into pEF-IRES-neo-GST to enable expression of the respective GST fusion protein, eg, GST-f-*N*720 (G-f-*N*720). These constructs were used as templates for subsequent mutagenesis studies.

4.2.2 Deletion and alanine-exchange mutagenesis

By the method modified from overlap extension PCR (Ho et al. 1989), the CBS1 domain (residues 607-662) was deleted from G-f-*N*720 to get a construct G-f-*N*720Δ (where this deletion is indicated by Δ). Alanine-exchange mutations of cytoplasmic loops (loop DE, loop

FG, loop HI and loop JK) were introduced into G-f-*N*720Δ using the same method, generating the set of mutated constructs shown in Table 4 (A).

In the same way, similar alanine-exchange mutations of the above cytoplasmic loops were also introduced into full-length WT hClC-1 (in pCI-neo-hClC-1) for the purpose of electrophysiological studies, generating the constructs shown in Table 4 (B).

All the mutants were subsequently verified by sequencing. For most of the constructs, two independent mutant clones were used for expression studies.

Table 4. Constructs of hClC-1 used in the present study

See Figure 9 for residue numbering

A.

G-f-*N*720 Constructs	**Notes in explanation**
G-f-*N*720Δ	GST-FLAG-hClC-1 residues 1-720, CBS1 (607-662) deleted
G-f-*N*720Δ/aeDE	G-f-*N*720Δ with alanine exchange of loop DE (199-206)
G-f-*N*720Δ/aeFGa	G-f-*N*720Δ with alanine exchange of part loop FG (251-255)
G-f-*N*720Δ/aeFGb	G-f-*N*720Δ with alanine exchange of part loop FG (256-261)
G-f-*N*720Δ/aeHIa	G-f-*N*720Δ with alanine exchange of part loop HI (293-296)
G-f-*N*720Δ/aeHIb	G-f-*N*720Δ with alanine exchange of part loop HI (297-300)
G-f-*N*720Δ/aeJK	G-f-*N*720Δ with alanine exchange of loop JK (380-385)

B.

hClC-1 Constructs	**Notes in explanation**
hClC-1/aeDE	full length hClC-1 with alanine exchange of loop DE (199-206)
hClC-1/aeFGa	full length hClC-1 with alanine exchange of part loop FG (251-255)
hClC-1/aeFGb	full length hClC-1 with alanine exchange of part loop FG (256-261)
hClC-1/aeHI	full length hClC-1 with alanine exchange of loop HI (294-300)
hClC-1/aeJK	full length hClC-1 with alanine exchange of loop JK (380-385)

4.2.3 Cell culture and transfection

Human embryonic kidney 293T cells (HEK 293T, American Type Culture collection, Rockville, MD) were maintained in Dulbecco's modified Eagle's medium supplemented with 10% (v/v) of a mixture of Newborn Calf Serum and Fetal Calf Serum (9% (v/v) NCS and 1% (v/v) FCS) (Gibco, Paisley, UK), 2 mM L-glutamine, 1% (v/v) non-essential amino acids, at 37 °C, 5%CO_2 atmosphere. For GST-pull-down experiment, cells were plated at a density of 1×10^6 per 60-mm dish 24 hours before transfection, and were transiently co-transfected with 598*C*-m and various G-f –*N*720Δ variant constructs. All the transfections were carried out using Lipofectamine 2000 (Invitrogen) according to the manufacturer's instructions. The same amount of pEF-IRES-neo-GST, from which only GST protein would be expressed, was used as a negative control.

For electrophysiological studies by patch-clamping, HEK293T cells were transiently transfected with either wild-type (WT) or an alanine-exchange mutant hClC-1 cDNA and, in a co-transfection at a molar ratio of 10:1, also with pEGFP-N1 (Clontech) in 6-well plates, so that they could later be identified by reporter plasmid-driven expression of the green fluorescent protein. Cells were plated for patch-clamping at least 4 h after transfection, and electrophysiological measurements were commenced approximately 24-48 h after transfections.

4.2.4 GST-pull-down Assay and Western Blot

Transfected cells were harvested and lysed on ice for 30 min in lysis buffer containing 150 mM NaCl, 20 mM Tris-HCl, pH 8.0, 10% glycerol, 0.2% Triton X-100, 0.2 mM DTT and protease inhibitor cocktail (1 µg/ml pepstatin, 1 µg/ml leupeptin, 0.5 mM PMSF, 5 µg/ml benzamidine, 0.1 µl/ml aprotinin). After centrifugation at 18,000 g for 15 min, the supernatant was collected and the protein concentration was measured using the BCA Protein Assay Kit (Pierce). Equal amounts of protein (1 mg) were incubated with 50 µl of glutathione-Sepharose 4B beads (GE Healthcare) for 3 h. The beads were then collected by short centrifugation and washed for four times (10 min each time) in 1 ml lysis buffer. All procedures were carried out at 4 °C. The bound proteins were finally liberated by heating at 55 °C for 20 min in 2 x Laemmli sample buffer and separated by SDS-PAGE (6%-12% polyacrylamide).

Proteins on SDS-PAGE gel were transferred to nitrocellulose membranes. The blots were then blocked for 1 h in TBST buffer (150 mM NaCl, 25 mM Tris, pH 7.4, 0.1% Tween-20) containing 5% non-fat milk powder and incubated in the blocking solution for 1 h with appropriate primary antibody, including anti-FLAG M_2 Monoclonal Antibody (Sigma), anti-

myc antibody 9E10 (culture supernatant from hybridoma cell line 9E10, ATCC), anti-hClC-1 (against residues 974-988 of hClC-1) (Gurnett et al. 1995), and anti-GAPDH (SCBT). After four washes in TBST buffer and 1 h incubation with corresponding second antibodies (horseradish peroxidase-conjugated anti-mouse IgG (Sigma) or goat anti-rabbit IgG-HRP-conjugate (SCBT)), reacting protein bands were visualized with an enhanced chemiluminescence detection system (Amersham Biosciences).

4.2.5 Purification of membrane proteins

To obtain purified membrane proteins, cell plasma membranes were first prepared by a method using density gradient medium silica colloid Percoll (GE Healthcare) (Belsham, Denton & Tanner 1980). At 24-48 h after transfection, 10^8 cells were washed three times by cold PBS and pelleted by centrifugation at 1500 g for 5 min at 4 °C. The cell pellet was then resuspended with fresh PBS at a ratio of 3 vol of PBS to 1 vol of packed cells and the cells were disrupted by repeatedly freezing in a mixture of ethanol and dry ice, shaking from time to time and then thawed in a 37 °C water bath until the homogenization routinely monitored by phase-contrast microscopy was satisfactory. At the same time, Percoll was made isotonic by adding 9 parts (v/v) of 100% Percoll to 1 part (v/v) of 1.5 M NaCl to get Stock Isotonic Percoll (SIP) solution of the osmolality of 340 mOsm/kg H_2O. Every 200 µl cell suspension was mixed with 2 ml SIP solution, and centrifuged at 20,000 g for 60 min at 4 °C. The upper-most ivory-white layer was carefully separated without any contamination from other layers and collected in a new tube. This purification procedure was repeated five times before the membrane proteins were finally extracted by the same method used in the GST-pull-down experiment.

4.2.6 Electrophysiology

Patch-clamp experiments were conducted at room temperature in the whole-cell configuration using an Axopatch 200B patch-clamp amplifier and associated standard equipment (Axon Instruments, Foster City, CA). Cells were continuously superfused with bath solution containing 140 mM NaCl, 4 mM CsCl, 2 mM $CaCl_2$, 2 mM $MgCl_2$, and 10 mM HEPES, adjusted to pH 7.4 with NaOH. Patch pipettes were pulled from borosilicate glass and typically had a resistance of 1-3 MΩ when filled with the standard pipette solution containing 40 mM CsCl, 85 mM Cs glutamate, 10 mM EGTA-Na, 10 mM HEPES, adjusted to pH 7.2 with NaOH. Series resistance did not exceed 3 MΩ and was 75-85% compensated. Currents obtained were filtered at 3 kHz, collected and analysed using Clampex 9.0 Software (Axon Instruments).

4.2.7 Data Analysis

Voltage dependence of overall channel activation was determined by measuring tail-current relaxation at a constant voltage of -100 mV for 40 ms, after 160 ms conditioning pulses at increasingly hyperpolarizing (-20 mV) steps ranging from +100 to -140 mV. To study the voltage dependence of the common gate, a short prepulse of 400 μs to +180 mV was inserted before the -100 mV tail pulse, to fully activate the fast gate (Accardi & Pusch 2000). The initial value of the tail current was determined by fitting the tail current with a double-exponential function, and normalized to the maximal value obtained following the most positive test voltage. All the data were analyzed by software Clampex 9.0 and Graph-Pad Prism 4.0 (GraphPad software, San Diego, CA), and the open probabilities (P_o) were calculated using the same method described previously (Wu et al. 2006). Potentials listed are pipette potentials expressed as intracellular potentials relative to outside zero.

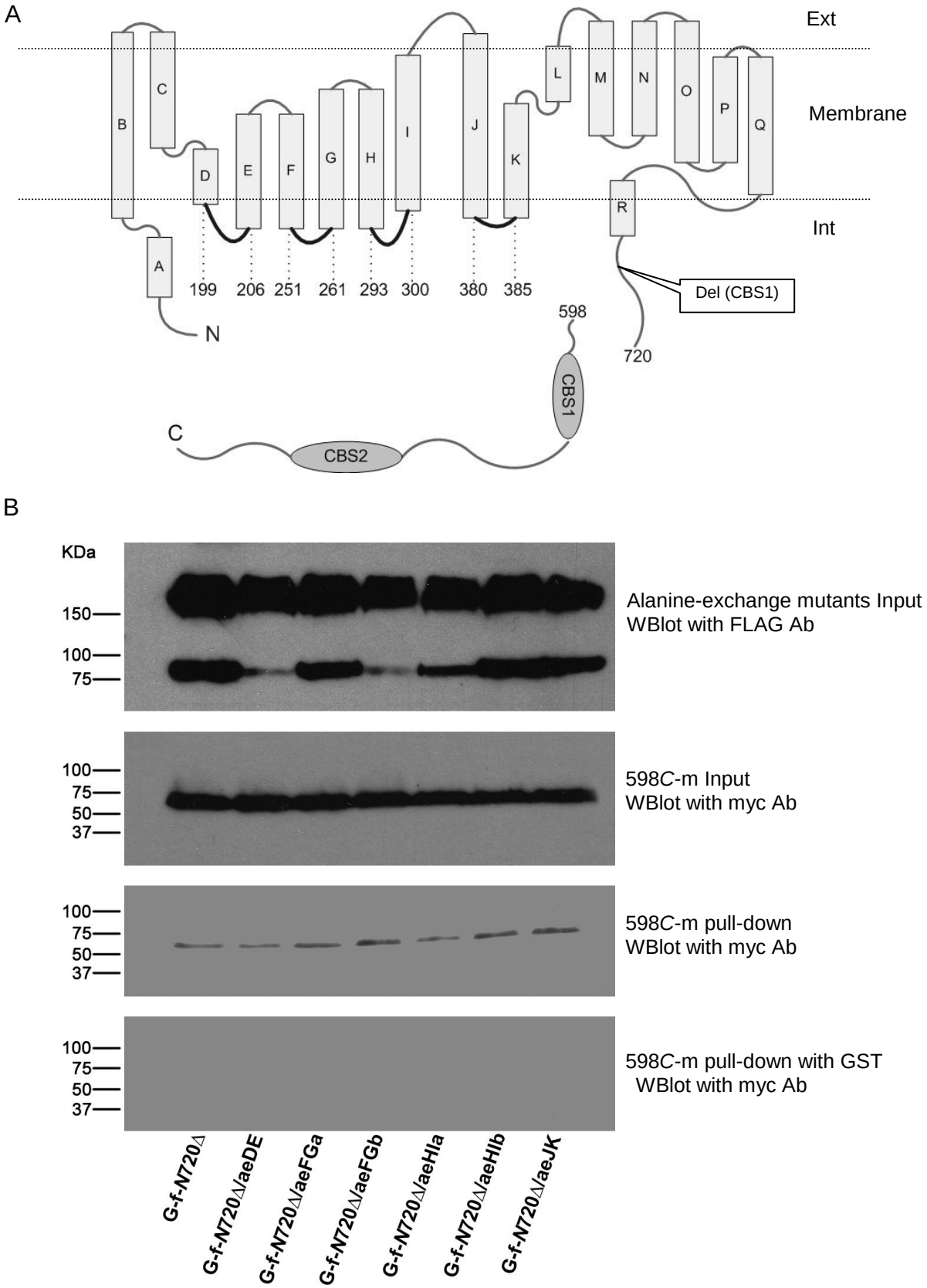
4.3 RESULTS

4.3.1 Roles of cytoplasmic loops in the interaction between the membrane-resident domain and the cytoplasmic tail

Using a split channel strategy, we have previously found that the C-tail of hClC-1 (598*C*) can interact with and complement non-functional *N*720Δ (a membrane-resident construct truncated after Ser 720 and missing CBS1) to rescue function and allow WT hClC-1 currents to be induced (Ma et al. 2008).

To test our prediction that there might be important, non-covalent binding between the C-tail and the membrane-resident domain, we selected several cytoplasmic loop regions of sufficient length to be considered as possible candidates for the interaction (Fig. 9A). These included loop DE (residues 199-206, RGVVLKEY), loop FG (residues 251-261, SVFCGVYEQPY), loop HI (residues 293-300, TSTYFAVR) and loop JK (residues 380-385, KALSQF). All the amino acids in the chosen loops were mutated to alanine in G-f-*N*720Δ generating six constructs, G-f-*N*720Δ/aeDE, G-f-*N*720Δ/aeFGa, G-f-*N*720Δ/aeFGb, G-f-*N*720Δ/aeHIa, G-f-*N*720Δ/aeHIb, G-f-*N*720Δ/aeJK, as described and defined in Materials and Methods. After each of these constructs was co-expressed with 598*C*-m in HEK293T cells, GST-pull-down experiments revealed that there was no less interaction between 598*C*-m and any of the loop alanine-exchange mutants than there was with the positive control, G-f-*N*720Δ (Fig. 9B).

Figure 9. Roles of the cytoplasmic loops in the binding between G-f-*N*720Δ and 598*C*-m.



A: Schematic diagram of split channel *N*720Δ + 598*C* of hClC-1, adapted by permission from Macmillan Publishers Ltd: Nature, Dutzler, R., Campbell, E.B., Cadene, M., Chait, B.T. and MacKinnon, R. (2002) X-ray structure of a ClC Cl^- channel at 3.0 Å reveals the molecular basis of anion selectivity. Nature 415, 287–294, copyright 2002. http://www.nature.com. The 18 α-helices (A-R) of the N-terminal and membrane-resident domain (*N*720Δ**)** are approximated as cylinders with the extracellular region (labelled Ext) above and the intracellular region (labelled Int) below. Two CBS domains in the cytoplasmic C-tail (598*C*) are shown as ellipsoids. The cytoplasmic loops investigated in this study are highlighted by black thick lines with the starting and ending amino acid number labelled. These include loop DE (residues 199-206), loop FG (residues 251-261), loop HI (residues 293-300) and loop JK (residues 380-385). B: GST-pull-down assay showing the binding between loop alanine-exchange mutants of G-f-*N*720Δ and 598*C*-m. Top panel: Western blot analyses of the input level of G-f-*N*720Δ and all its loop alanine-exchange mutants when each of them was co-expressed with 598*C*-m, detected by Anti-FLAG M_2 antibody against FLAG epitope. The lower band in each lane represents protein monomer, and the upper bands are probably SDS-resistant dimers. The expression level of 598*C*-m in each of the above co-expression experiments was detected by Western blot using 9E10 Anti-myc antibody against the c-myc epitope (the second panel). The third panel shows GST-pull-down results using the glutathione-Sepharose 4B beads for precipitation and the Anti-myc antibody for detection in Western blot. No significant differences were detected between any of the mutant and positive control G-f-*N*720Δ variants in their physical interaction with 598*C*-m. The bottom panel shows the GST-pull-down results for the same 598*C*-m mutants using unfused GST protein as negative controls to exclude the possibility that the target proteins could be pulled down by GST protein itself. Molecular masses are labelled in kDa.

4.3.2 Physiological significance of the cytoplasmic loops for the channel function

To investigate the roles of these cytoplasmic loops in channel function, we made similar alanine-exchange mutations of these loops in the full length hClC-1 protein (hClC-1/aeDE, hClC-1/aeFGa, hClC-1/aeFGb, hClC-1/aeHI and hClC-1/aeJK, as described and defined in Methods), and investigated Cl^- currents and gating in these mutants by whole-cell patch-clamping and tail current analysis.

4.3.2.1. Alanine-mutated loop DE (hClC-1/aeDE)

Although all the transfection conditions had been fully optimized, no Cl^- currents were detected from the alanine-exchange mutation of loop DE. Besides the elimination of channel currents by a direct effect of the mutation on the channel pore or gating, there could be two other possible reasons for the absence of currents: either the mutated channel protein could not be expressed well, or the protein could be expressed but with impaired targeting to the plasma membrane. To distinguish between these three possibilities, experiments were first carried out to compare the expression levels of each of the loop alanine-exchange mutants among total cellular proteins. As shown in Fig. 10A, all of the mutants were very well expressed in HEK293T cells, with hClC-1/aeDE mainly existing as SDS-resistant dimers in SDS-PAGE. Then, following purification of membrane proteins from the transfected cells, we investigated the inclusion of these mutants in the plasma membrane. As demonstrated by membrane biotinylation, all the mutants were trafficked to the membrane (Fig. 10B).

4.3.2.2. Alanine-mutated loop FG (hClC-1/aeFGa and hClC-1/aeFGb)

The longest loop in this study, loop FG (251-261) was studied in two adjacent sequences of alanine-exchange in two separate constructs (hClC-1/aeFGa, residues 251-255, and hClC-/aeFGb, residues 256-261), respectively. As shown in Fig. 11, alanine-exchange of the initial segment of the FG loop (hClC-1/aeFGa, SVFCG) produced wild type currents, showing all the typical features of hClC-1, including inward rectification, depolarization-induced activation and a rapid, partial deactivation upon hyperpolarisation with a biexponential deactivation time course indicating the presence of two kinetically distinct gating processes. Although $V_{1/2}$ for P_o^f shifted in a positive direction by ~20 mV, $V_{1/2}$ values for P_o and P_o^c were not significantly different from those of WT hClC-1 (Table 5). In other respects, also, the P_o curves of hClC-/aeFGa were very similar to those of WT (Fig. 12).

Mutation of the C-terminal part of FG loop (hClC-/aeFGb, VYEQPY), however, showed different characteristics. Although hClC-1/aeFGb still retained its basic channel characteristics, there were marked effects on the voltage dependence of gating. For example,

the $V_{1/2}$ value for P_o was shifted in a positive direction by ~30 mV, and the voltage dependence of both P_o^c and P_o^f was shifted to more positive potentials compared with WT. This mutation reduced the P_o^c at any given potential and decreased the fraction of channels that remained open at strongly negative potentials (minimum P_o^c) by about 40% (Table 5, Figs 11,12)

4.3.2.3 Alanine-mutated loop HI (hClC-1/aeHI)

Mutation of the loop HI shifted the P_o curve in a positive direction, much as hClC-1/aeFGb did (Fig. 12). However, in contrast to hClC-1/aeFGb, which imposed almost equal influence on both common gating and fast gating, hClC-1/aeHI predominantly affected fast gating by drastically shifting the voltage dependence of P_o^f in the positive direction by more than 60 mV, but with only a small effect on slow gating (Table 5). Minimum P_o^f values at extremely negative potentials (-140 mV) were not reduced compared to the WT hClC-1 channel (Fig. 12).

4.3.2.4 Alanine-mutated loop JK (hClC-1/aeJK)

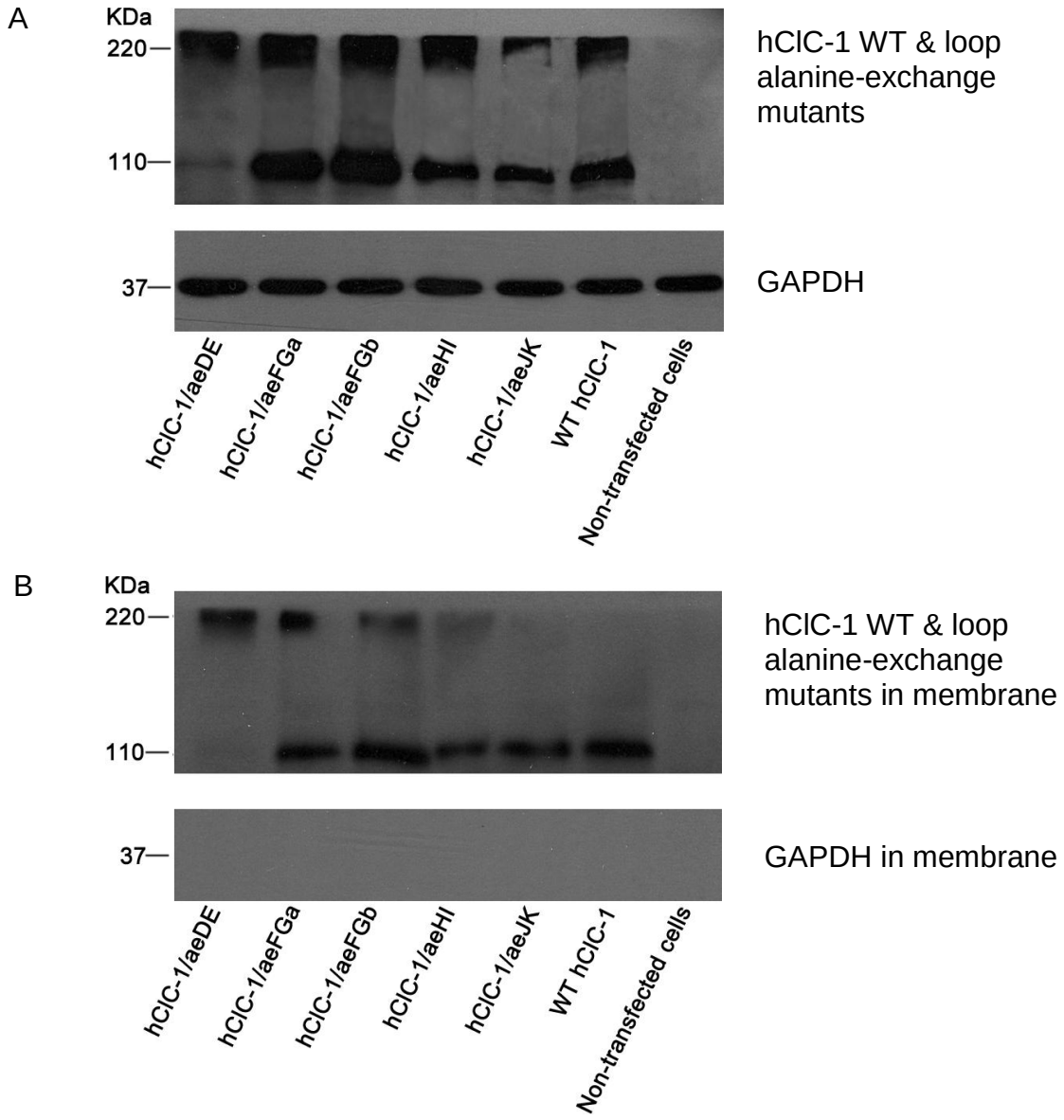
As shown in Fig. 12, the most significant changes in channel function arose from alanine-exchange of loop JK. Unlike all the other mutants, which shifted $V_{1/2}$ for P_o in the positive direction, hClC-1/aeJK changed it to a more negative potential by ~10 mV (Table 5, Fig. 12). Separating common gating from fast gating revealed that the leftward shift in potential was predominantly due to the voltage dependence of common gating being eliminated. This could be well demonstrated by the significant increase of the minimum P_o^c to ~0.78 (~0.4 for WT), which effectively locked the common gating in the open state throughout the physiological voltage range and even at very negative voltages (< -100 mV) (Fig. 12).

Table 5. $V_{1/2}$ of channel open probability (P_o), fast gating (P_o^f) and common gating (P_o^c) for WT hClC-1 and loop alanine-exchange mutants

Peak tail currents, recorded using the protocols described in the experimental procedures, were used to derive P_o values and these were fitted with a Boltzmann distribution curve. Fast and common gating parameters were separated using the method described previously (Accardi & Pusch 2000). $V_{1/2}$ is the potential at which $P_o = (1 + P_{min})/2$ (half maximal activation). Measurements are given in millivolts (mV) as mean ± S.E.

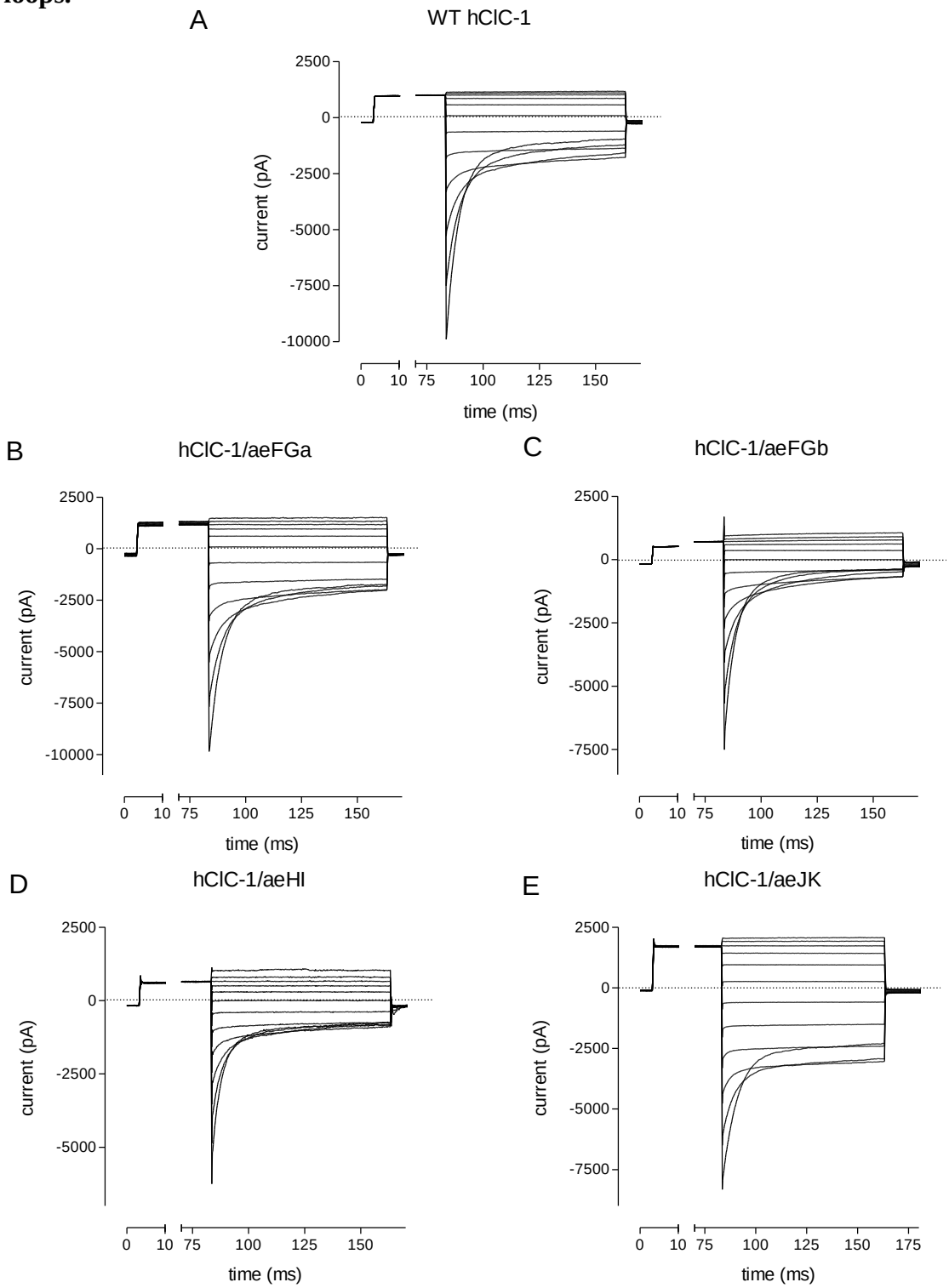
WT / mutated channel (no. of cells)	$V_{1/2}$ P_o (mV)	$V_{1/2}$ P_o^f (mV)	$V_{1/2}$ P_o^c (mV)
WT hClC-1 (n=15)	-71.7 ± 2.5	-106.4 ± 0.8	-77.9 ± 2.0
hClC-1/aeDE (n=23)	no currents	no currents	no currents
hClC-1/aeFGa (n=6)	-68.7 ± 2.4	-82.5 ± 1.6	-72.3 ± 2.1
hClC-1/aeFGb (n=7)	-42.5 ± 2.0	-74.2 ± 1.2	-40.1 ± 2.0
hClC-1/aeHI (n=6)	-37.9 ± 2.2	-39.1 ± 2.5	-58.9 ± 2.3
hClC-1/aeJK (n=8)	-81.8 ± 1.9	-87.5 ± 1.6	n.a

Figure 10. Expression and trafficking study of the loop alanine-exchange mutants of hClC-1.



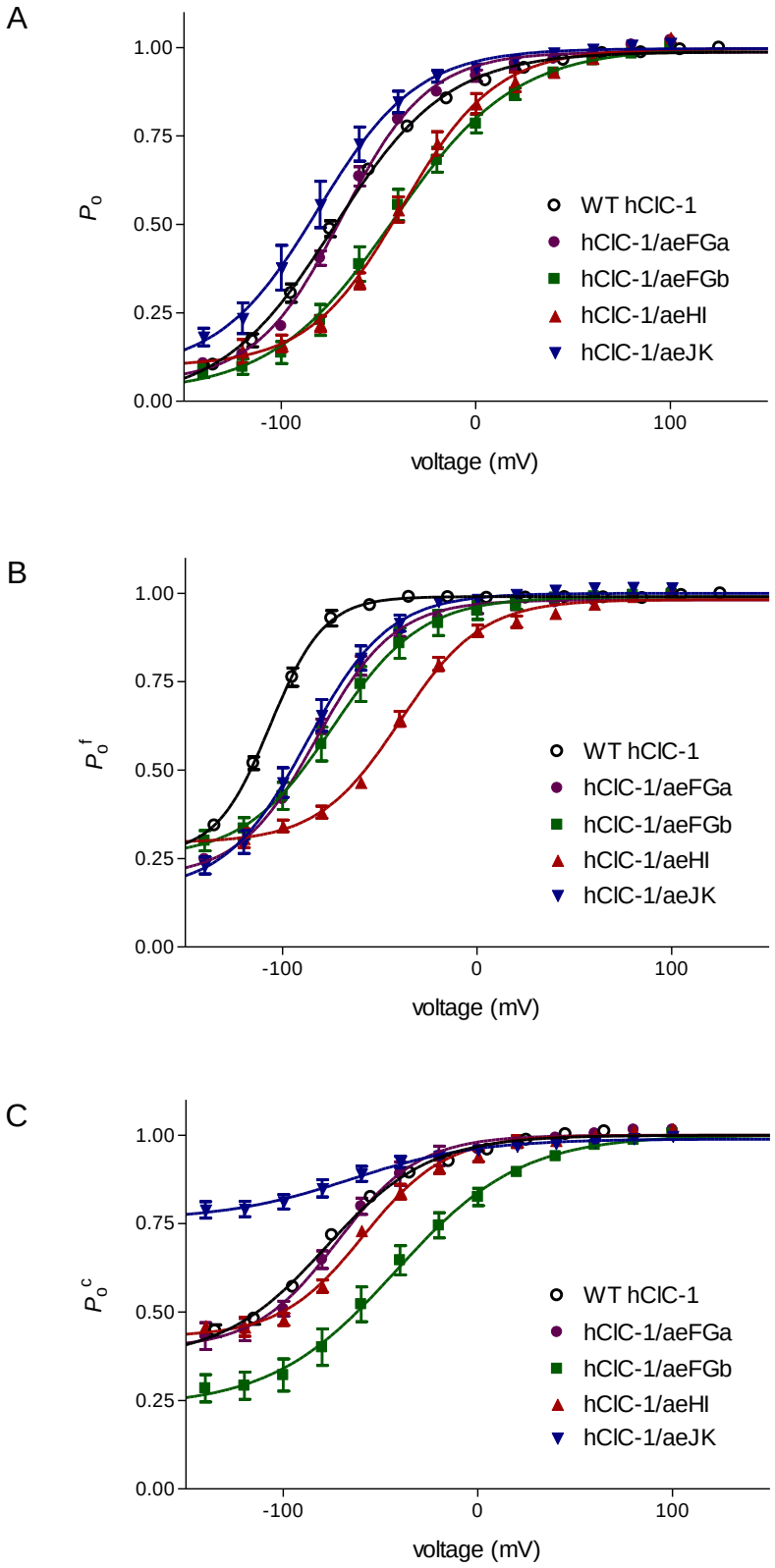
Western blot analyses of protein expression level and trafficking of all the alanine-exchange mutants of cytoplasmic loops in hClC-1. A: Total proteins were extracted from cells transfected with corresponding hClC-1 mutants, then the expression was detected using Anti-hClC-1 antibody, showing that all of the mutants can be very well expressed. B: Membrane proteins were purified from cells transfected with corresponding hClC-1 mutants, then the expression was detected by Anti-hClC-1 antibody, showing that all of the mutants can traffic to the plasma membrane correctly. Each lane was loaded with 10 ug of protein. The lower bands (~110 kDa) represent monomers and the upper bands (~220 kDa) correspond to SDS-resistant dimers of individual hClC-1 mutants. GAPDH protein from the total protein or plasma membrane extracted from the same batch of cells was used as an internal control detected by anti-GAPDH antibody.

Figure 11. Electrophysiological analyses of WT hClC-1 and alanine-exchange mutations of loops.



Chloride current traces were obtained by whole-cell patch-clamping of HEK293T cells transfected with the positive control WT hClC-1 (A) and the alanine-exchange mutants of loop FG (hClC-1/aeFGa, residues 251-255), FG (hClC-1/aeFGb, residues 256-261), HI (hClC-1/aeHI, residues 294-300) and JK (hClC-1/aeJK, residues 380-385) (B-E). Currents were recorded 24 h after transfection in response to voltage steps of 80 ms duration from +80 mV to -140 mV following a conditioning pulse to +40 mV for 80 ms.

Figure 12. A comparison of gating characteristics in cytoplasmic loop alanine-exchange mutants of hClC-1.



From experimentally determined overall open probability values at each voltage (P_o, A), the

equivalent values for fast gating (P_o^f, B) were obtained by dividing by the respective values for common gating (P_o^c, C). Solid lines represent the apparent P_o curves fitted from the experimental data points using the method described by Aromataris *et al*. (Aromataris et al. 2001). In all panels data points are shown as mean ± S.E. In a number of the mutants, slight positive displacements can be seen with respect to the WT curves. For P_o^c in hClC-1/aeFGb, however, there is a more substantial shift in the positive direction, as there is for P_o^f in hClC-1/aeHI, while, in hClC-1/aeJK, P_o^c indicates that the common gates are mainly open, even at very negative potentials.

4.4 DISCUSSION

Intramolecular interactions in CLC proteins have been previously shown to be strong enough to support the proper alignment and functional reconstitution of discrete channel fragments (Schmidt-Rose & Jentsch 1997a; Maduke, Williams & Miller 1998; Estévez et al. 2004). In spite of long-term active research, however, the mechanisms behind this phenomenon have remained poorly understood. For hClC-1, an interaction between CBS1 in a construct consisting of an N-region, membrane-resident domain plus some proximal C-tail (*N*720) and CBS2 in a distal C-tail construct (721*C*) has been proposed to support the functional complementation in split channel *N*720 + 721*C* (Estévez et al. 2004). Then again, we have previously found that split channel *N*720Δ (missing CBS1) + 598*C* could also generate WT hClC-1 currents, suggesting that beside the normal CBS pairing, other interactions between the C-tail and the membrane-resident domain might be supporting such important channel features as common gating (Ma et al. 2008).

By contrast, Hebeisen et al. (2004) found no function and no plasma membrane co-localisation between the C-tail and a complementary membrane-resident domain, using split channel components *N*589 and 590*C*, which might imply that these components cannot associate (Hebeisen et al. 2004). But another explanation (Ma et al. 2008) suggests that these components would not be correctly trafficked to the plasma membrane due to the lack of the appropriate trafficking signal in the membrane-resident component. Having found both interaction and function in the split channel *N*720Δ + 598*C*, we chose to scan the cytoplasmic loops present in the membrane-resident component (*N*720Δ) for possible interactions with the C-tail (598*C*) rather than attempting to scan the mainly-inter-CBS-domain region from amino acid 598 to 720 (CBS1 being deleted). Our reasoning was that the inter-CBS region is disordered in the ClC-0 C-tail crystal structure (Meyer & Dutzler 2006), it varies greatly in length (compare, e.g. hClCKa (Markovic & Dutzler 2007)) and shows little or no sequence similarity between CLC proteins, so that it would seem to be unlikely to constitute a C-tail interaction site.

Our present analysis of alanine-exchange mutations of cytoplasmic loops that could potentially be involved in interactions with the C-tail revealed the following. According to the GST-pull-down results, no single loop could be fully responsible for the interaction. This must mean that none of the selected loops are necessary for the interaction, that more than one loop at a time is involved and each can be individually dispensable or that the C-tail binds with some other site, or sites, accessible from the cytoplasm but not analysed by us. Our

present findings, with support from some other recent results, favour the last two possibilities.

Normally, conformational changes in the membrane–resident subunits of CLC channels and transporters (as relevant to common gating in ClC-0 and hClC-1, for example) might be propagated to and from the C-tail via the R-helix. For mechanical advantage, however, this would require either, that some more distal region of an individual C-tail interacts with another part of the membrane-resident domain, or that the dimer-derived pair of distal C-tails interact with each other. X-ray crystallography of the cytoplasmic domains of ClC-5 and ClC-Ka, and by inference for ClC-0 and, probably, ClC-1, indicates that the cytoplasmic domains do dimerise via a conserved interaction interface, specifically involving a head to tail association between the β1 and α1 regions of CBS2 (Markovic & Dutzler 2007; Meyer et al. 2007). Furthermore, evidence from fluorescence resonance energy transfer (FRET) studies in ClC-0 suggests that C-terminal fluorophore tags move apart significantly when the slow gate closes (Bykova et al. 2006), which implies (because the post CBS2 tail is short and the process has a high Q_{10} in ClC-0) that the CBS2-CBS2 interface dissociates. But we have already shown (Ma et al. 2008) that a direct connection between the C-tail and membrane-resident domain via the R-helix is unnecessary as practically WT function is maintained in the *N*720Δ + 598*C* split channel mentioned above. Nevertheless, conformational movement of the R-helix occurs in a prokaryotic CLC antiporter in conjunction with processes associated with transport and even in the absence of the glutamate residue that has been implicated in both proton-coupled transport in CLC transporters and fast gating in CLC channels (Bell et al. 2006). All of this suggests that the common gating process in hClC-1 and ClC-0 begins in the membrane-resident region and that it relies, for its full expression, on interaction with a C-tail but not necessarily via covalent attachment to it through the R-helix. The alternative, that a transmembrane voltage change could initiate a slow gating conformational change from a site within the C-tail to propagate into the membrane-resident region, seems unlikely. It would be very helpful in the future, though, to mutate all loops simultaneously and to combine the loop mutants in various possible combinations to clarify whether the cytoplasmic loops are in any way involved.

In addition to our study of possible roles of the loops in the interaction between the C-tail and the membrane-resident domain, we also investigated the physiological function of each loop using alanine-exchange mutagenesis and whole-cell patch-clamping. Interestingly, we found some new features of these loop regions as well as consistency with earlier mutagenesis reports. Previously, the only evidence for the physiological significance of cytoplasmic loop

DE was revealed by a dominant myotonic mutation, G200R, which is a missense mutation of a highly conserved amino acid located in that loop. Similar to most dominant mutations, G200R leads to a drastic shift by ~65 mV of the open probability curve to more positive voltages, thus decreasing the Cl^- conductance in the physiological voltage range (Wollnik et al. 1997). In the present study, mutating all the eight amino acids in loop DE to alanine eliminated all currents, possibly because the voltage dependence of channel gating has been shifted too much to make activation of the channel possible. On the other hand, the hClC-1/aeDE extracted from either total proteins, or purified membrane proteins, formed SDS-resistant dimers in SDS-PAGE (Fig. 10), a characteristic typical of very hydrophobic proteins and associated with some diseases. For example, SDS stable oligomers occur in proteolipid protein mutants in Pelizaeus-Merzbacher disease (Swanton et al., 2005). Correspondingly, the absence of hClC-1/aeDE monomers in SDS-PAGE could indicate that an enhanced hydrophobicity prevents this protein from forming normal functional structures in the plasma membrane.

A missense mutation of ClC-5 (S270R, equivalent to S294 in hClC-1), located within the short intracellular loop between helix H and helix I, was identified as being associated with a variant of Dent's disease, characterized by low molecular weight proteinuria, hypercalciuria and nephrocalcinosis (Igarashi et al. 1998). Consistent with this report, mutation of loop HI in hClC-1 in the present study significantly shifted the P_o of fast gating to more positive potentials compared with the WT hClC-1. This would reduce the open probability of fast gating in a wide voltage range, so that at physiological voltages, less channels would be open, leading to a decreased Cl^- conductance, increased skeletal muscle excitability and possibly myotonia.

We show here that alanine-exchange of loop JK drastically reduces the slow component of the macroscopic gating relaxations, apparently locking common gating in the open state at all investigated voltages while having only a minor effect on the fast component. Such a significant effect might occur because loop JK is quite close to the R helix, the N-terminal end of which coordinates the Cl^- ion binding to the centre-most binding site (S_{cen}) in the hClC-1 selectivity filter. For CLC channels, there is strong functional coupling between ion conduction and gating (Pusch et al. 1995; Ludewig, Jentsch & Pusch 1997; Rychkov et al. 1998), so it is conceivable that loop JK plays a role in regulating the channel gating process. Similar evidence has come from an early study of ClC-2. Replacement of, and mutations in, the N-terminal part of the loop between domains D7 and D8 (residues 348-357, including the

loop JK residues 352-357 according to the topology as predicted by the X-ray structure (Dutzler et al. 2002)) also abolished gating, yielding constitutively open channels which were no longer sensitive to voltage, pH and swelling (Jordt & Jentsch 1997). Therefore, loop JK seems to be strongly involved in the common gating process of hClC-1 in a manner similar to mutant C212S in ClC-0 (Lin, Lin & Chen 1999).

Mutation C212S, however, affected only the common gating in ClC-0 leaving fast gating unaltered, while mutation of loop JK slightly changed the fast gating as well, exactly the same as mutant C277S in hClC-1 (equivalent to mutant C212S in ClC-0) (Accardi, Ferrera & Pusch 2001). Also, hClC-1/aeFGb and hClC-1/aeHI had effects on both common gating and protopore gating, too, indicating that coupling between the common gating and fast gating process might be stronger in hClC-1 than in ClC-0.

To some extent, loops in CLC channels have been regarded only as connecting linkers. Our study suggests that, although no single loop could be fully responsible for the interaction between the C-tail and the membrane resident domain of hClC-1, individual loops could, alone, play important functional roles in the regulation of channel activity, especially the common gating. Under normal circumstances, the interaction necessary for complete functional expression is most likely to be that of some essential segment of the C-tail either with the helix-lined, cytoplasmic vestibule of the channel or with multiple cytoplasmic loops simultaneously.

CHAPTER 5:
LATERAL DISPLACEMENT OF hClC-1 CARBOXYL TERMINALS DURING COMMON GATING AND LIMITS ON THEIR CYTOPLASMIC LOCATION

5.1 INTRODUCTION

Like other members of the CLC family of ion channels and transporters, the human skeletal muscle Cl^- channel, hClC-1, occurs as a homodimer. Each subunit in these CLC proteins has its own individual Cl^- permeation pathway with complex exchanging and/or gating mechanisms to catalyse ion flow. For hClC-1 and the *Torpedo* electroplaque Cl^- channel, ClC-0, two distinct gating processes have been identified. One is fast (protopore) gating, which regulates each individual pore independently and the other is slow (common) gating, which operates on both pores simultaneously. It is generally agreed that the basis for fast gating is the movement of a glutamate side-chain carboxyl group moving in or out of the permeation pathway within the selectivity filter (Dutzler et al. 2002; Dutzler, Campbell & MacKinnon 2003). By contrast, the nature of common gating seems to be much more complicated and the picture is, at present, still far from clear.

One major hypothesis, supported by a variety of experimental observations, suggests that alterations in subunit-subunit interaction and large conformational changes are involved. Deactivation kinetics, especially for common gating in ClC-0, is unusually temperature-dependent, pointing to a complex rearrangement of the proteins (Pusch, Ludewig & Jentsch 1997). Again indicative of a large structural reorganisation, extracellular Zn^{2+} inhibition of both ClC-0 and hClC-1 is highly temperature-dependent with common gating being affected but not fast gating (Chen 1998; Duffield et al. 2005). In hClC-1, electrophysiological studies of naturally-occurring, dominant myotonic mutations and similar site-directed mutations reinforce the view that common gating involves helices at the dimer interface (Duffield et al. 2003). Also, certain channel properties known to be dependent on common gating are affected by mutations or truncations in the cytoplasmic tail (C-tail) (Fong, Rehfeldt & Jentsch 1998; Hryciw et al. 1998; Estévez et al. 2004; Hebeisen et al. 2004; Wu et al. 2006; Ma et al. 2008) probably through non-covalent interaction between the C-tail and the membrane-resident pore region (Ma et al. 2008). Progress towards determining the nature of the conformational changes associated with common gating has recently been made by Bykova *et al* (2006) who observed large displacements of the carboxyl termini (C-termini) of the ClC-0 Cl^- channel using fluorescence resonance energy transfer (FRET) (Bykova et al. 2006).

In the present study, we have also used FRET to investigate conformational changes during common gating in hClC-1. Our analyses were confined to spectra FRET measurements from the plasma membrane thereby ensuring that our observations were conducted on correctly trafficked channel proteins. Under the assumption that FRET efficiency reflects distance changes between Cerulean and enhanced Yellow Fluorescent Protein (eYFP) fluorophores at the C-termini of hClC-1, we were able to associate open and closed states of the common gate with changes in the channel's C-terminal separation. Our FRET measurements in channels carrying point mutations that have characteristic effects on gating suggest that fast and common gating are closely coupled. Finally, the extraordinary length of the C-tail in hClC-1 and lack of knowledge about the depth of the C-terminals within the cytoplasm, persuaded us to use FRET to estimate C-terminal position. From a pair of functionally reconstituted split channel constructs, one with an extracellular fluorophore and the other tagged intracellularly, we have been able to gauge approximate C-terminal position and place a limit on the transmembrane distance by which the fluorophores are separated.

5.2 MATERIALS AND METHODS

5.2.1 Constructs of hClC-1

From insertion of full length hClC-1 cDNA into vector pCerulean-N3 or pEYFP-N3, we were able to generate proteins labelled at their C-terminus (Fig. 13) with either donor fluorescent protein Cerulean or fluorescence acceptor eYFP, respectively, including a 2-residue linker (Gly-Ser) between the channel protein and fluorescent label sequences. For our truncation and split channel studies, fragments of hClC-1 cDNA, were amplified by PCR using plasmid pCI-neo-hClC-1 as the template (Bennetts et al. 2001). As shown in Table 6, we termed our hClC-1 amino region (N-region) peptide fragments *N*887 (for amino acid 1-887; i.e. Met 1 to Phe 887) and *N*451 (for amino acid 1-451; i.e. Met 1 to His 451) and our carboxyl-region (C-region) fragment 380*C* (for amino acid 380-988; i.e. Lys 380 to Leu 988). Truncation and mutation sites are depicted in relation to the secondary structure of hClC-1 in Figure 13. Fluorescent tags were attached as for full length hClC-1. Mutations were introduced into our hClC-1 constructs using QuickChange® site-directed mutagenesis kit (Stratagene) according to the manufacturer's instructions. All the mutants were subsequently verified by sequencing.

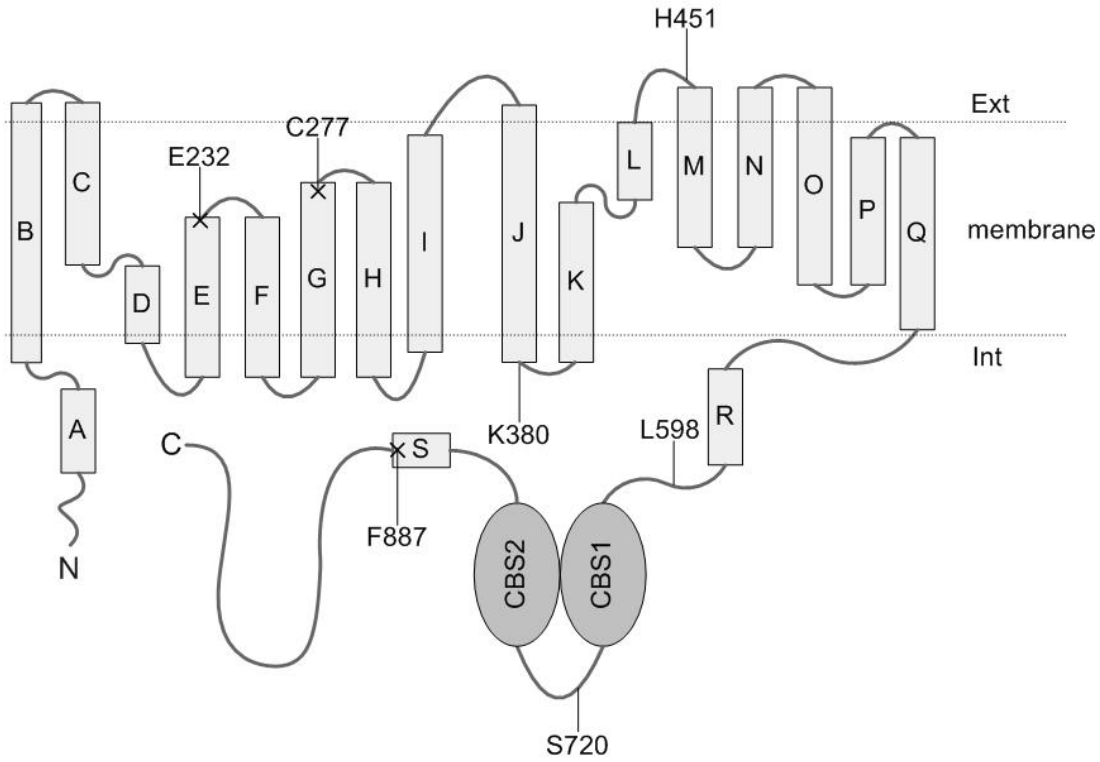
Table 6. Constructs of hClC-1 used and discussed in the present study

hClC-1 Constructs	Residues	Notes in explanation
*N*451	1-451	early part of the membrane-resident region, N terminal to helix L
*N*887	1-887	the membrane-resident region and part of the C-tail, N terminal to end of helix S
380*C*	380-988	part of the membrane-resident region from helix K, including complete C-tail
*N*720Δ	1-720, with 607-662 deleted	a membrane-resident construct truncated between CBS1 and CBS2, after Ser 720, and missing CBS1
598*C*	598-988	the complete cytoplasmic tail containing both CBS1 and CBS2

5.2.2 Cell culture and transfection

Human embryonic kidney 293 cells (HEK 293, American Type Culture collection) were maintained as previously described (Ma et al. 2008). Plasmid DNA was transfected into HEK 293 cells using Lipofectamine 2000 (Invitrogen) 24 h before electrophysiological measurement and 48h before FRET recording. Just before imaging, the culture medium was substituted with a bath solution containing NaCl (130 mM), $MgCl_2$ (5 mM), HEPES (5 mM) and EGTA (1 mM) (pH 7.4). When NaI was used, NaCl (65 mM) was replaced with the same concentration of NaI. For the low $[Cl^-]_e$ condition, the NaCl (130 mM) was replaced with NaCl (4 mM) and sodium glutamate (126 mM). All the Zn^{2+} solutions were freshly made just before the imaging experiments.

Figure 13. Schematic diagram of an hClC-1 monomer



The 19 α-helices found in each subunit (excluding those within the CBS domains), are indicated by the blocks labelled A to S with the extracellular region above and the intracellular region below (adapted by permission from Macmillan Publishers Ltd.: Nature, Dutzler et al. (2002), copyright 2002, http://www.nature.com). The CBS domains are shown as ellipsoids and the S α-helix (Macías et al. 2007) is indicated by the block in the distal cytoplasmic C-tail. In relation to our present study, amino acids delineating individual domains of interest are labelled with numbers while amino acids we have mutated are indicated by an "X". Fluorophores were attached to the C-terminus.

5.2.3 Electrophysiology

Patch-clamp experiments were conducted at room temperature in the whole-cell configuration using an Axopatch 200B patch-clamp amplifier and associated standard equipment (Axon Instruments). Cells were continuously superfused with bath solution containing NaCl (140 mM), CsCl (4 mM), $CaCl_2$ (2 mM), $MgCl_2$ (2 mM) and HEPES (10 mM) (pH 7.4). Patch pipettes were pulled from borosilicate glass and typically had a resistance of 2-3 MΩ when filled with the standard pipette solution containing CsCl (40 mM), Cs glutamate (85 mM), EGTA-Na (10 mM) and HEPES (10 mM) (pH 7.2). Series resistance did not exceed 3 MΩ and was 75-85% compensated. Currents obtained were filtered at 3 kHz.

Voltage dependence of overall channel activation was determined by measuring tail-current relaxation at a constant voltage of -100 mV for 40 ms, after 160 ms conditioning pulses at increasingly hyperpolarizing (-20 mV) steps ranging from +100 to -140 mV. To study the voltage dependence of the common gate, a short prepulse of 400 μs to +180 mV was inserted before the -100 mV tail pulse, to fully activate the fast gate (Accardi & Pusch 2000). Currents were recorded from at least four cells in each case. All the data were analyzed by software Clampex 9.0 (Axon Instruments) and Graph-Pad Prism 4.0 (GraphPad software), using methods described previously (Ma et al. 2008).

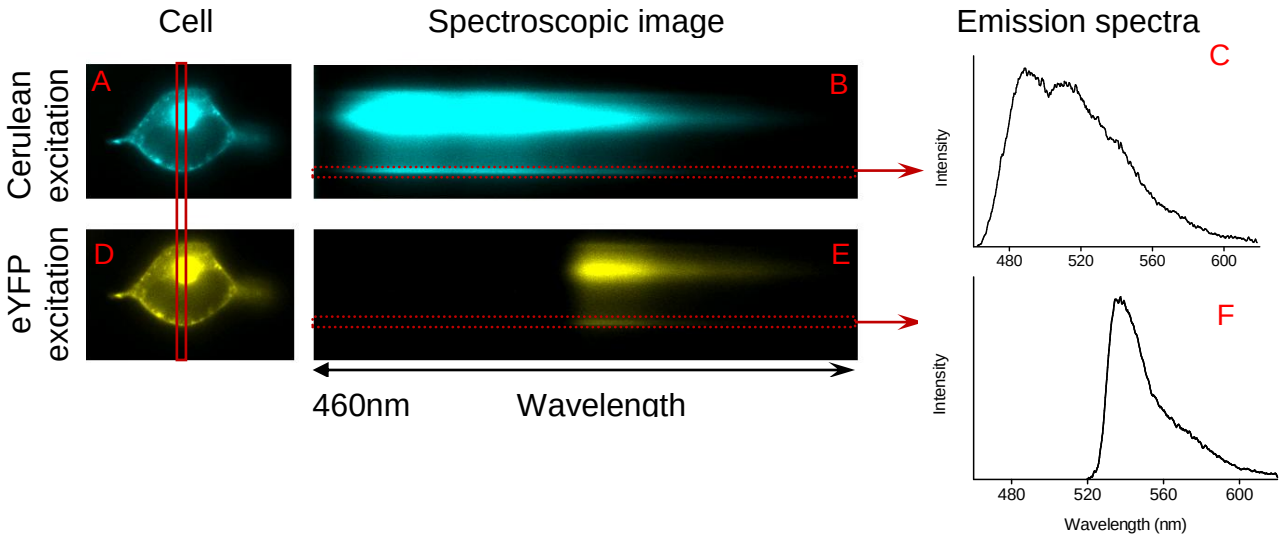
5.2.4 Spectra FRET and FRET efficiency quantification

The spectra FRET system was set up in conjunction with an inverted fluorescence microscope (Olympus IX-81) equipped with a 100 W mercury lamp and a 60×oil-immersion objective (NA 1.42). For spectroscopic imaging, a spectrograph (Acton SpectraPro 2150i) was used in conjunction with a Hamamatsu HQ CCD camera. Two filter cubes (Chroma) were used to excite Cerulean (excitation filter D436/20, dichroic mirror 455dclp) and eYFP (excitation filter HQ500/20, dichroic mirror Q515lp), respectively. No emission filter was used in these cubes. Under these experimental conditions, autofluorescence from untransfected cells was negligible.

As described previously (Bykova et al., 2006), fluorescence imaging and analysis were carried out using MetaMorph software (Universal Imaging). Emission spectra were constructed by positioning the spectrograph input slit across a fluorescent cell (Fig. 14A and D) and recording the resultant spectroscopic images (Fig. 14B and E) in which the X axis represents the wavelength and the Y axis represents the position of the image source. Quantification of the fluorescence intensity from the plasma membrane along the X axis

produces the total emission spectrum (resulting from Cerulean excitation) and the eYFP emission spectrum (resulting from eYFP excitation), respectively (Fig. 14C and F). Spectra were corrected for background light, which was estimated from the blank region of the same image. To eliminate the bleed-through and cross-talk contaminations between Cerulean and eYFP due to donor emission and direct excitation of the acceptor (Takanishi *et al*., 2006), standard emission spectra were also collected from cells expressing only Cerulean-tagged protein or cells expressing only eYFP-tagged protein. Following scaling and subtraction, the FRET efficiency was calculated from the increase in eYFP emission due to energy transfer as described by Zheng *et al (Zheng, Trudeau & Zagotta 2002)*. Modelling of FRET efficiency for hClC-1 was the same as that used for ClC-0 (Bykova et al. 2006). Estimated FRET efficiency was calculated and statistically analysed by GraghPad Prism 5 software (GraphPad Software Inc.) using nonlinear regression fitting of the data points. All the estimated FRET efficiencies were expressed as mean ± SEM and statistic analyses were done by unpaired t-test. To eliminate direct effects of extracellularly applied NaI on fluorescence proteins, exposure of each batch of cells in NaI was not longer than 10 min. Correlation of Spectra FRET with electrophysiological measurements of common gating, as had been achieved in ClC-0 (Bykova et al., 2006), was not feasible in hClC-1 due to the kinetics of its common gating being several orders of magnitude faster than in ClC-0.

Figure 14. Spectra FRET.



Excited by 436 nm (panel A) and 500 nm (panel D), respectively, fluorescent images of a single HEK 293 cell cotransfected with hClC-1-Cerulean and hClC-1-eYFP were collected by a CCD camera connected to an epifluorescence microscope via a spectrograph. From the region restricted by a thin input slit (indicated by the rectangle crossing panel A and panel D), separate spectroscopic images were obtained for Cerulean (panel B) and eYFP (panel E) excitation. To measure FRET exclusively from the plasma membrane, fluorescence signals were only taken from a clearly separated membrane region (indicated by the dashed rectangles in panel B and panel E). Cerulean excitation produces the total emission spectrum shown in panel C, which includes the emission from both Cerulean and eYFP. Panel F shows the emission spectrum of eYFP, alone, obtained by eYFP excitation. From these spectra, FRET efficiencies illustrated in subsequent figures were calculated as the enhanced eYFP emissions due to energy transfer (Zheng, Trudeau & Zagotta 2002).

5.3 RESULTS

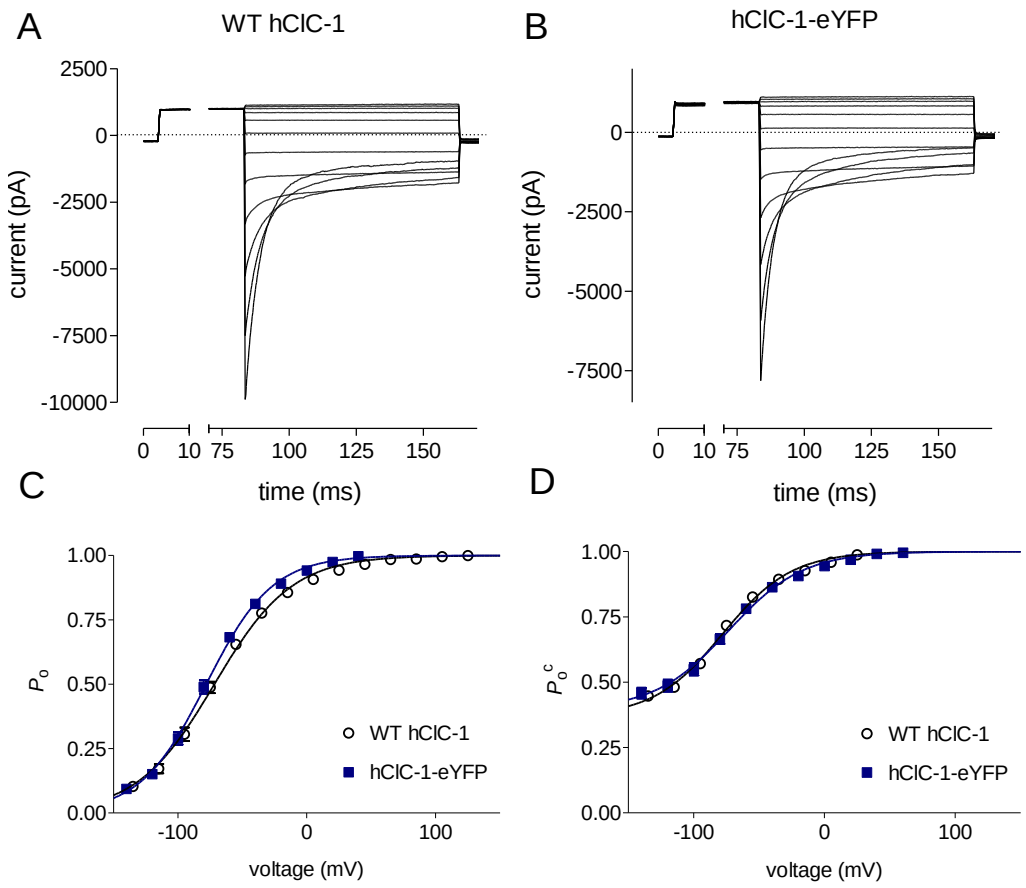
5.3.1 Validation of function and FRET in C-terminal tagged hClC-1 channels

Deactivation currents from whole-cell patch clamp recordings in HEK293T cells expressing hClC-1-eYFP (Fig. 15B) were not significantly different from those in cells expressing WT hClC-1 (Fig. 15A). Apparent open probabilities of overall gating (P_o) and, importantly for the purposes of the present study, common gating (P_o^c) were almost identical to those of WT (Fig. 15C, D).

We next employed spectra FRET in cells expressing fluorescently tagged ClC-0 as our positive control for FRET (Bykova et al. 2006). Apparent FRET efficiency was calculated from individual cells co-expressing ClC-0-Cerulean and ClC-0-eYFP and plotted as a function of the fluorescence intensity ratio between Cerulean and eYFP (Fc/Fy). Data points from the 74 cells analysed were then fitted (solid curve) using a model for dimeric proteins (Bykova et al. 2006) which yielded an estimated true FRET efficiency of 23.7 ± 0.5% (indicated by the upper dotted line in Fig. 16A). As a negative control for FRET, we examined the level of possible non-specific FRET when equivalent amounts of hClC-1-Cerulean and an unrelated protein, TrpV2-eYFP, were co-expressed. In this case, as shown in Fig. 16B, no correlation could be seen between Fc/Fy and apparent FRET.

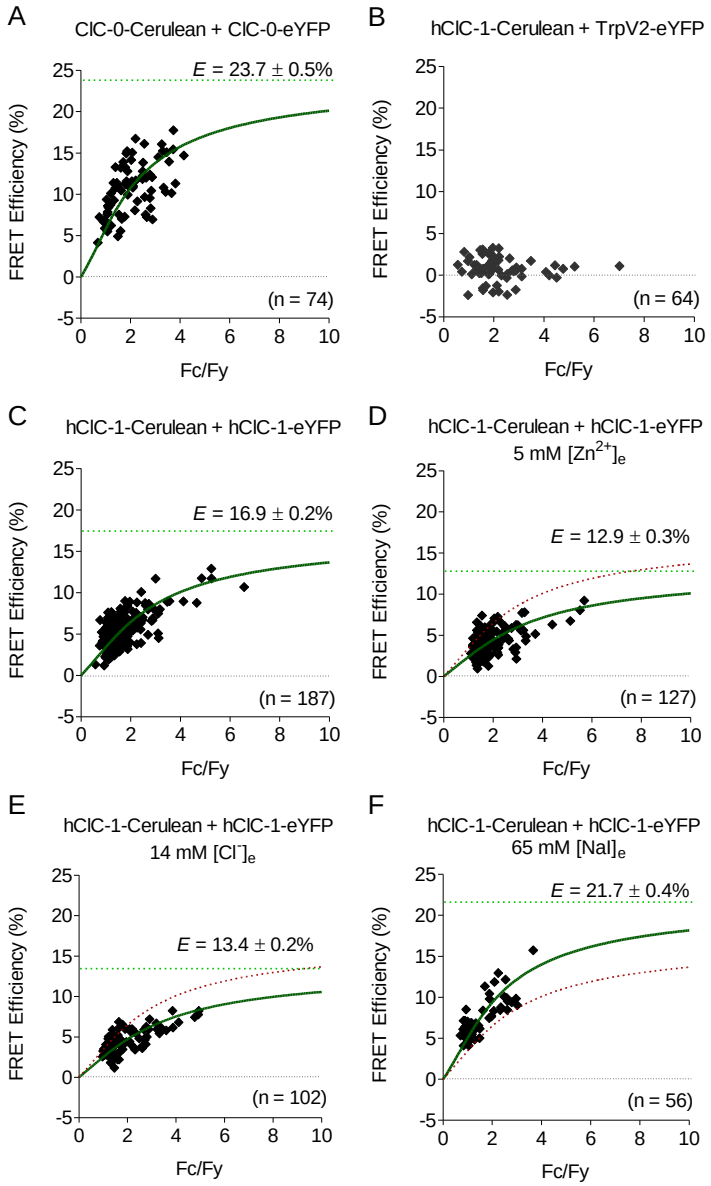
When we applied the same approach to WT hCLC-1 channels formed by co-expressing WT hClC-1-Cerulean and WT hClC-1-eYFP, a clear correlation between Fc/Fy and the apparent FRET efficiency was again observed (Fig. 16C, n = 187). Model fitting now yielded a true FRET efficiency estimate of 16.9 ± 0.2%. In control solution, $[Cl^-]_e$ (140 mM), this probably represents an equilibrium between the closed and open states of the common gate (Bykova et al. 2006). We, therefore, measured FRET under conditions which were designed to hold the common gate either open or closed. As shown in Fig. 16D, when the common gate was closed by $[Zn^{2+}]_e$ (5 mM) (Duffield et al. 2005), FRET efficiency was significantly reduced to 12.9 ± 0.3% (n = 127) ($P < 0.0001$ compared to control, Fig. 16C). Similarly, inhibition of common gating by a low $[Cl^-]_e$ (14 mM) (Rychkov et al. 1996a), caused the FRET efficiency to decrease to 13.4 ± 0.2% (Fig. 16E, n = 102) ($P < 0.0001$ compared to control). By contrast, when the common gate was kept open by replacing $[NaCl]_e$ (64 mM) with the equivalent amount of NaI (Rychkov et al. 1998), FRET efficiency was increased to 21.7 ± 0.4% (Fig. 16F, n = 56) ($P < 0.0001$ compared to control).

Figure 15. Electrophysiological comparison of YFP tagged hClC-1 channel and WT hClC-1



Chloride current traces were obtained by whole-cell patch clamping from HEK 293 cells transfected with: the positive control WT hClC-1 (panel A) and the *e*YFP tagged channel hClC-1-eYFP (panel B). Currents were recorded 24 h after transfection in response to test pulses of 80 ms duration in steps of -20 mV from +80 mV to -140 mV following a conditioning pulse to +40 mV for 80 ms. Tagged hClC-1 channels show currents indistinguishable from WT. From experimentally determined overall open probability values (P_o) at each voltage (panel C), the equivalent values for common gating (P_o^c) were separated (panel D). Apparent P_o curves in panels C and D were fitted to the experimental data points using the methods described previously (Ma et al. 2008). Data points are shown as mean ± S.E. Both P_o curves and P_o^c curves from hClC-1-eYFP and WT hClC-1 closely overlap, indicating, again, that the tag does not affect electrophysiological functions of hClC-1.

Figure 16. FRET efficiency measurements from C-terminal tagged hClC-1 channels



The FRET efficiency measured from cells coexpressing ClC-0-Cerulean + ClC-0-eYFP (panel A, as our positive control for FRET), hClC-1-Cerulean + TrpV2-eYFP (panel B, as our negative control for FRET) and hClC-1-Cerulean + hClC-1-eYFP (panel C), all in our control bathing solution, was plotted as a function of the fluorescence intensity ratio between Cerulean and eYFP. Similarly, FRET efficiency was also measured from cells coexpressing hClC-1-Cerulean and hClC-1-eYFP, which had been exposed to $[Zn^{2+}]_e$ (5 mM) (panel D), low $[Cl^-]_e$ (panel E) and $[NaI]_e$ (65 mM) (panel F). Each symbol shows the FRET efficiency value from a single cell and n represents the number of independent data points from each experiment. Solid curves represent the apparent FRET model fitted to the experimental data points. Lower dotted lines indicate a FRET efficiency level of zero, and upper dotted lines show the estimated true FRET efficiency at high Cerulean to eYFP fluorescence intensity

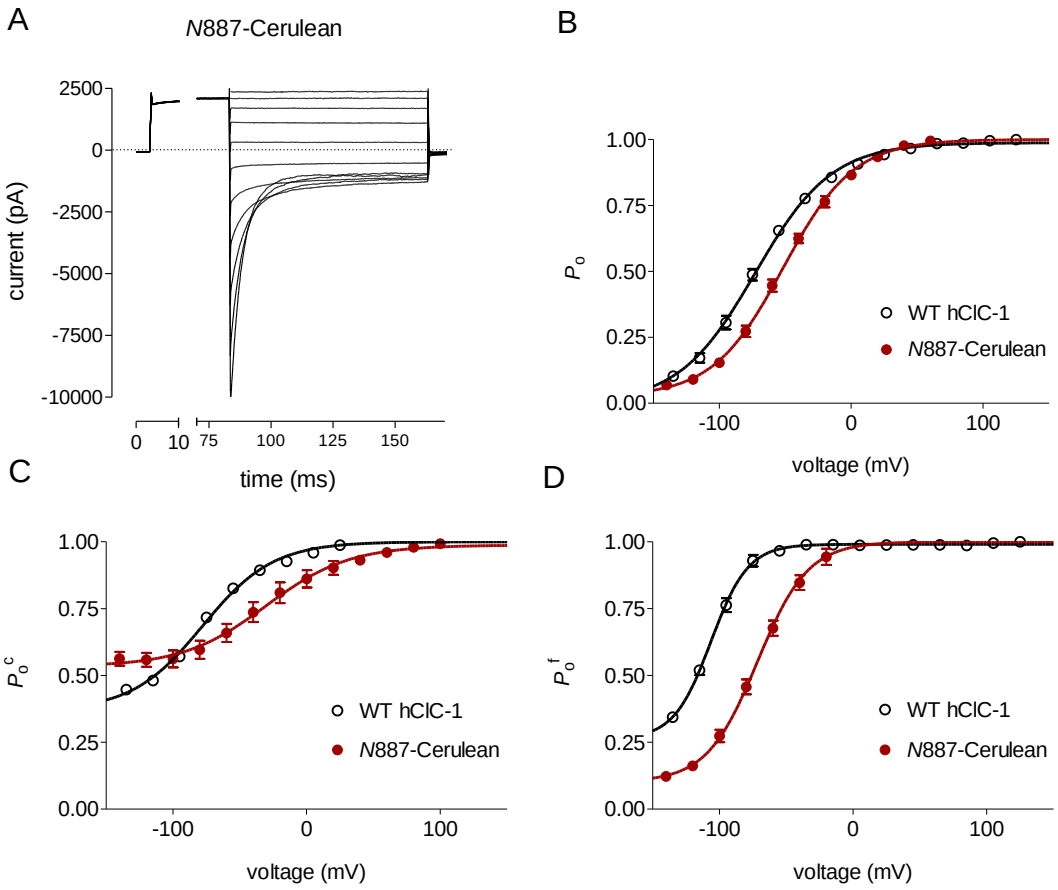
ratio. For easy comparison, FRET efficiency in C-terminal tagged WT hClC-1 channels (hClC-1-Cerulean + hClC-1-eYFP) under control conditions (from panel C) is reproduced as the dotted curves in panels D, E and F.

5.3.2 FRET in truncated hClC-1, *N*887, resembles that in ClC-0

In our experiments, under normal conditions, FRET efficiency of hClC-1 (16.9 ± 0.2%) is lower than that of ClC-0 (23.7 ± 0.5%). Could this be due to the considerably longer C-tail of hClC-1 which causes its two C-termini to be further apart? A previous study of rClC-1 has shown that the final 100 amino acids (fs895X, equivalent to *N*889 in hClC-1), but not the final 125 amino acids (L869X, equivalent to *N*863 in hClC-1), could be removed with only insubstantial changes to the channel function (Hryciw et al. 1998). We assessed FRET in a similarly shortened channel, *N*887, which, based on the observations of Hryciw and colleagues (Hryciw et al. 1998), as well as, those of others, e.g., (Macías et al. 2007), was predicted to have characteristics like WT hClC-1. Also, its C-tail length beyond CBS2 is more like that of ClC-0 (WT hClC-1 = 117 amino acids, *N*887 = 16 amino acids and ClC-0 = 36 amino acids, respectively). Although truncation of around 80 amino acids in hClC-1 would have resulted in a closer approximation to the C-tail length of ClC-0, these channels had been found to have very low conductance when expressed in Xenopus oocytes (Macías et al. 2007) and were, therefore, not chosen for the present study. Electrophysiological analysis of *N*887-Cerulean showed that it retained all the basic channel characteristics of WT hClC-1 (Fig. 17).

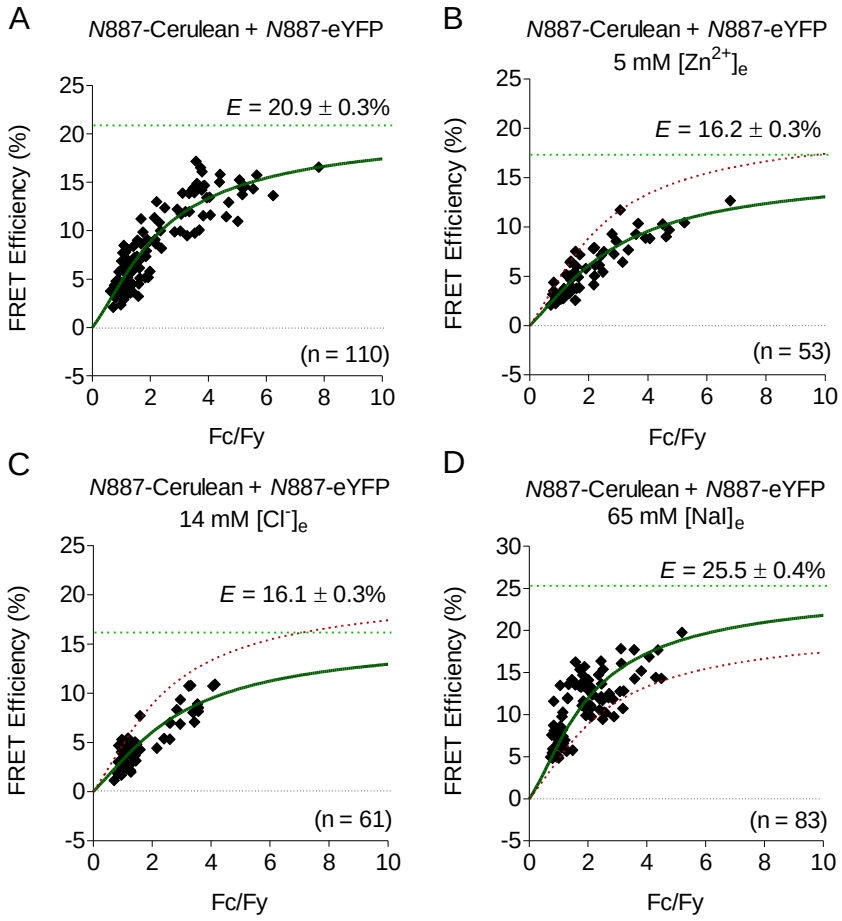
In our control solution, FRET efficiency for *N*887 was estimated to be 20.9 ± 0.3% (Fig. 18A, n = 110), and closer to that of ClC-0. Similar to WT hClC-1, when the common gate of *N*887 was blocked by $[Zn^{2+}]_e$ (5 mM) or inhibited by low $[Cl^-]_e$ (14 mM), FRET efficiency decreased to 16.2 ± 0.3% (Fig. 18B, n = 53) and to 16.1 ± 0.3% (Fig. 18C, n = 61) respectively ($P < 0.0001$ compared to the control condition for both). By contrast, and again similar to WT, FRET efficiency for *N*887 increased to 25.5 ± 0.4% (n = 83) ($P < 0.0001$ compared to control) when the common gate was activated by NaI (Fig. 18D).

Figure 17. Electrophysiological features of truncated hClC-1 channel *N*887-Cerulean



Chloride currents obtained by whole-cell patch clamping HEK 293 cells expressing *N*887-Cerulean (panel A) were very similar to those from cells expressing full length hClC-1, as shown in Figure 14. Overall open probability (P_o) curves, as well as those for common (P_o^c) and fast gating (P_o^f) , as shown in panels B, C and D, respectively, were similar to those for WT hClC-1, although shifted in the depolarizing direction. In all panels data points are shown as mean ± S.E.

Figure 18. FRET efficiency measurements from truncated hClC-1 channel *N*887

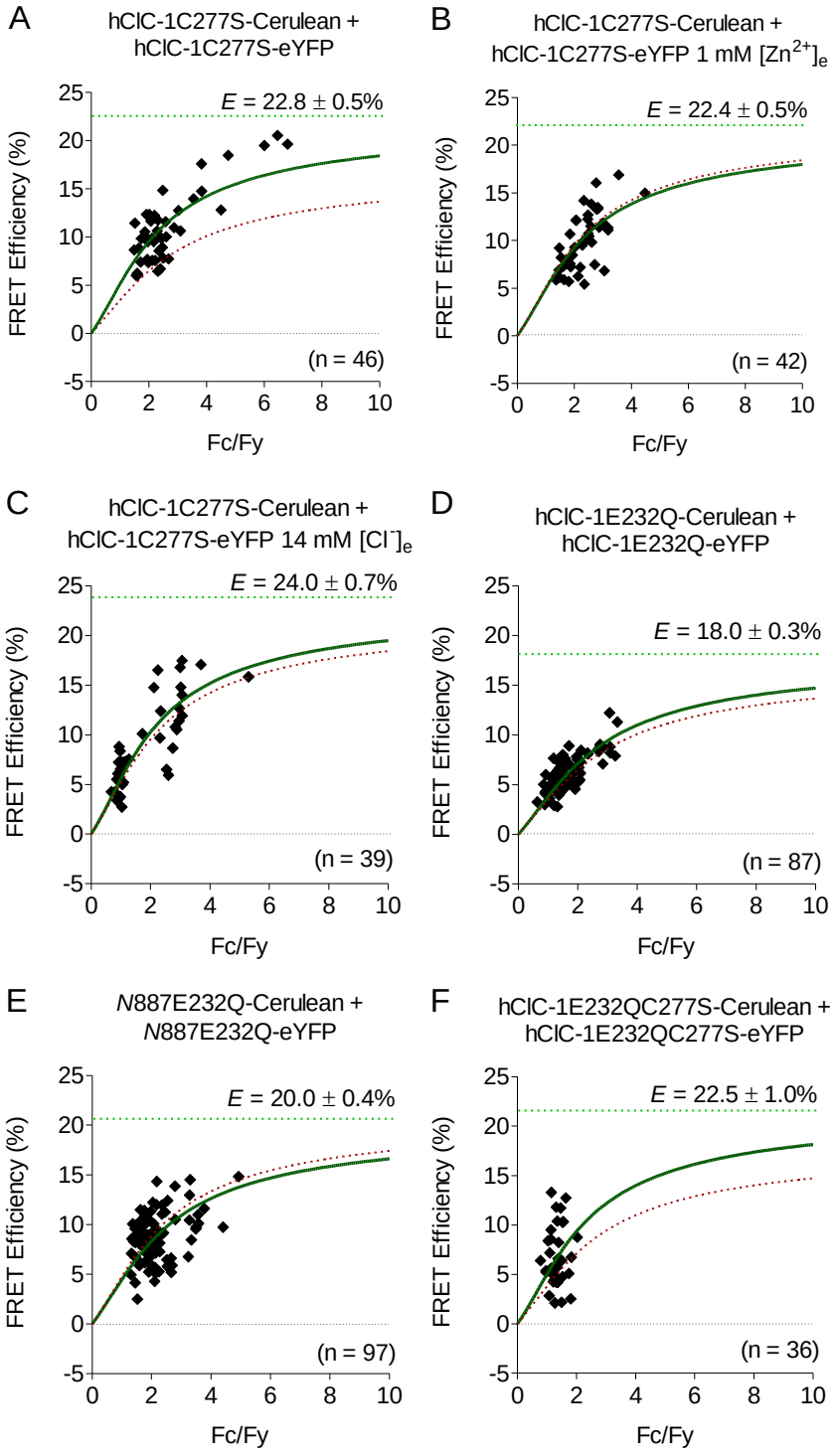


When estimated in the same way as for Figure 16, FRET efficiency in cells coexpressing *N*887-Cerulean + *N*887-eYFP under control conditions was several percent greater than for WT hClC-1 (panel A). As for WT hClC-1, FRET efficiency was then decreased by $[Zn^{2+}]_e$ (5 mM) (panel B) or low $[Cl^-]_e$ (14 mM) (panel C), increased by $[NaI]_e$ (65 mM) (panel D). For comparison, the fitted FRET efficiency curve from panel A is reproduced as the dotted curves in panels B, C and D. Symbols and n as for Figure 16.

5.3.3 FRET study of mutants indicates a strong link between fast gating and common gating in hClC-1

Since FRET efficiency is altered by an effect of Zn^{2+}, low $[Cl^-]_e$ or $[NaI]_e$, on common gating in WT hClC-1, we proposed that site-directed mutations which hold the common gate in an abnormal conformation should also change FRET efficiency. Among such mutations, C277S (equivalent to C212S in ClC-0) is known to lock the common gate in an open and Zn^{2+}-independent state while leaving fast gating intact (Duffield et al. 2005). As we expected, C277S channels showed notably higher FRET efficiency (22.8 ± 0.5%, n = 46, Fig. 19A) than WT hClC-1 (16.9 ± 0.2%, n = 187, Fig. 16C) ($P < 0.0001$) and this was unchanged by Zn^{2+} or low $[Cl^-]_e$ (Fig. 19B, C) ($P > 0.05$ compared to control). In another point mutant, E232Q (equivalent to E166Q in ClC-0), the glutamate side-chain carboxyl group which forms the putative fast gate (Dutzler, Campbell & MacKinnon 2003) has been deleted but both fast and common gating are eliminated (Fahlke et al. 1997) (submitted paper). As distinct from C277S, FRET efficiency measured in E232Q (18.0 ± 0.3%, n = 87, Fig. 19D) was not substantially different from that of WT hClC-1 and when E232Q was introduced into the truncated channel *N*887 background, it showed a FRET efficiency (20.0 ± 0.4%, n = 97, Fig. 19E) that was also quite similar to the WT *N*887 value (20.9 ± 0.3%, n = 110, Fig. 18A) ($P > 0.05$). If the conformational changes associated with the common gate actually occur in E232Q but these are prevented from coupling to the fast gates (because the latter have been deleted) then this could be the reason why functional common gating is eliminated. In this case, insertion of C277S should modify E232Q in the same way that it modifies WT hClC-1. As shown in Figure 19F, FRET efficiency from the double mutant E232QC277S was estimated to be 22.5 ± 1.0% (n = 36), which is indeed close to that of the single C277S mutant (22.8 ± 0.5%, Fig. 19A) ($P > 0.05$), but significantly different from that of single E232Q mutant (18.0 ± 0.3%, Fig. 19D) ($P < 0.0001$).

Figure 19. FRET study of hClC-1 mutants C277S, E232Q and the double mutant E232QC277S



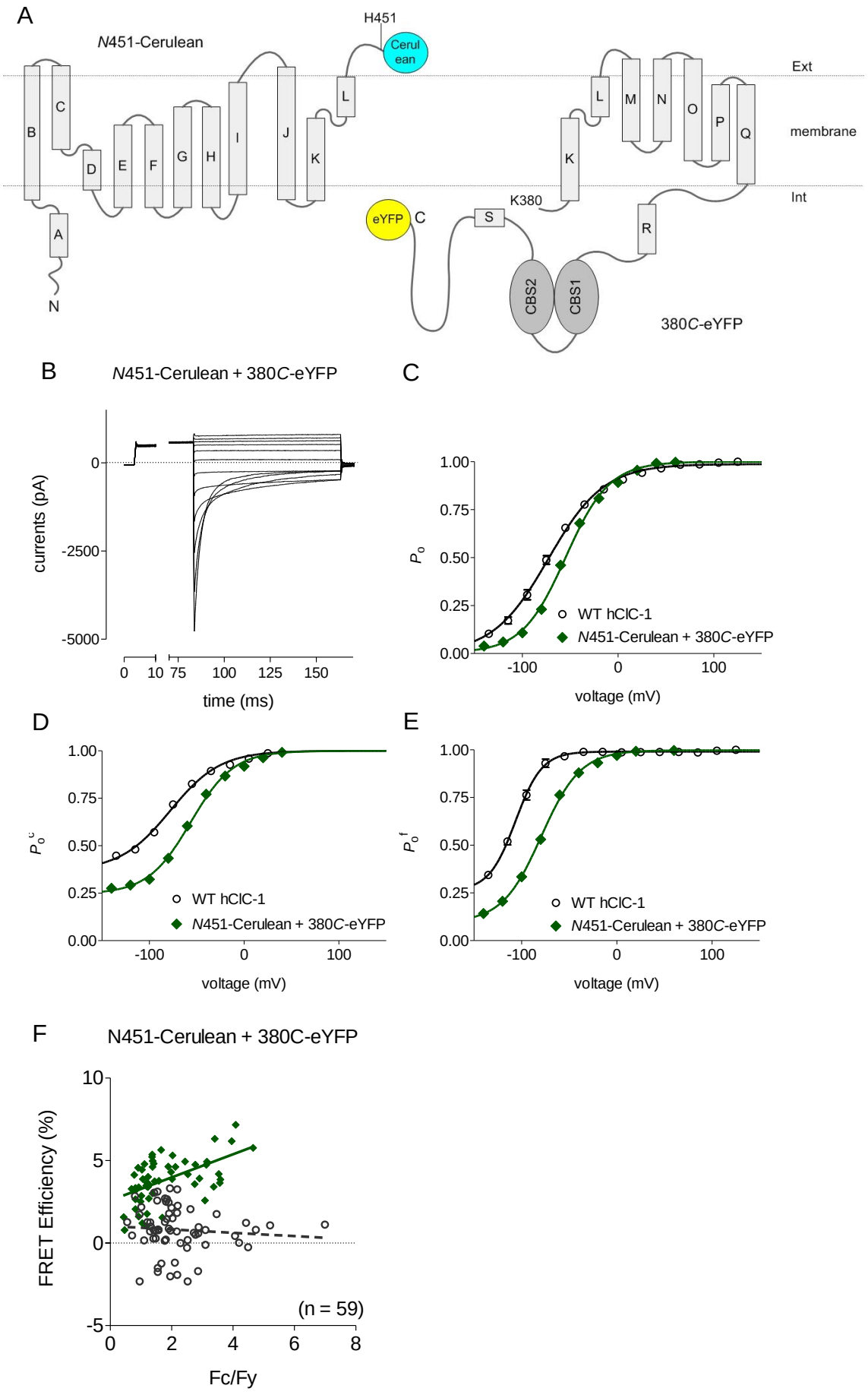
FRET efficiency was also estimated in cells co-expressing hClC-1C277S-Cerulean and hClC-1C277S-eYFP under control conditions (panel A), with $[Zn^{2+}]_e$ (1 mM) (panel B), and with low $[Cl^-]_e$ (14 mM) (panel C). For comparison, the dotted curve in panel A comes from the

fitted FRET efficiency curve for WT hClC-1 shown in Figure 16, panel C (hClC-1-Cerulean + hClC-1-eYFP under control conditions). By contrast with WT and truncated hClC-1 (Figs 16 and 18), FRET efficiency was unaffected by the presence of Zn^{2+} or low [Cl^-]. The dotted curves in panels B and C show FRET efficiency for this mutant under control conditions as in panel A. Mutations E232Q and C277S affect gating of hClC-1 in distinctive ways although both prevent common gate closure (Accardi, Ferrera & Pusch 2001)(submitted paper). We therefore estimated FRET efficiency in cells coexpressing hClC-1E232Q-Cerulean + hClC-1E232Q-eYFP (panel D), *N*887E232Q-Cerulean + *N*887E232Q-eYFP (panel E) and hClC-1E232QC277S-Cerulean + hClC-1E232QC277S-eYFP (panel F) under control conditions. For comparison, the dotted curve in panel D comes from fitted FRET efficiency curve for WT hClC-1 from Figure 16, panel C (hClC-1-Cerulean + hClC-1-eYFP under control conditions), in panel E the dotted curve comes from the fitted FRET efficiency curve for the *N*887 truncation shown in Figure 18, panel A (*N*887-Cerulean + *N*887-eYFP under control conditions), and in panel F reproduces the fitted FRET efficiency curve from panel D (hClC-1E232Q-Cerulean and hClC-1E232Q-eYFP under control conditions). The E232Q mutation has little effect on FRET efficiency in either WT hClC-1 or in the *N*887 truncation backgrounds while C277S has a similar effect in both the full length WT and in the presence of the E232Q mutation. Symbols and n as for Figure 16. Panel A-C and F were reproduced with permission from data collected by a collaborator Dr. Ekaterina Bykova from University of California, Davis.

5.3.4 FRET study of split hClC-1 channel *N*451-Cerulean + 380*C*-eYFP places constraints on the position of the C-terminal perpendicular to the plane of the membrane

Our earlier GST-pulldown experiments (Ma et al. 2008) have shown that the whole C-tail of hClC-1 (598*C*, containing both CBS1 and CBS2 domains) is able to interact with, and restore function to, a non-functional membrane-resident construct (*N*720Δ, containing no CBS domain). In the present study, we constructed another split hClC-1 channel, this time divided within the membrane-resident region (Fig. 20A). Its first (N-terminal) component was tagged with Cerulean at its extracellularly located C-terminal (*N*451-Cerulean) and its second component, extending to the normal cytoplasmic C-terminal of the protein, was tagged there with eYFP (380*C*-eYFP). Co-expression of these fragments allowed functional complementation of the two otherwise nonfunctional components (Fig. 20B-E). Data from our FRET studies on this split channel could not be fitted by the same equation used for our other experiments (Fig. 20F), probably because the FRET efficiency, in this case, depends not only on the ratio between Cerulean and eYFP (Fc/Fy), but also on the probability of forming functional channels in the plasma membrane and thus on the absolute concentration of *N*451-Cerulean and 380*C*-eYFP in each cell. Linear regression analysis of the data from 59 cells co-expressing *N*451-Cerulean and 380*C*-eYFP showed a slope of 0.7 ± 0.1, which deviated significantly from zero ($P < 0.001$). By contrast, the same analysis of a data set from 64 cells co-expressing unrelated proteins hClC-1-Cerulean and TrpV2-eYFP (negative control) presented a slope of -0.1 ± 0.1, which does not significantly deviate from zero ($P = 0.5$).

Figure 20. Electrophysiological analysis and FRET efficiency measurements from split hClC-1 channel *N*451-CFP + 380*C*-YFP



A schematic diagram of split channel *N*451-Cerulean + 380*C*-eYFP (panel A) is shown in a similar way to WT hClC-1 in Figure 13 (adapted by permission from Macmillan Publishers Ltd.: Nature, Dutzler *et al.* (2002), copyright 2002, http://www.nature.com). Using the same protocol as described for Figure 15, Cl^- currents similar to WT indicate functional split channel recombination in HEK293T cells co-expressing *N*451-Cerulean and 380*C*-eYFP (panel B). Overall open probability (P_o) curves, as well as those for common (P_o^c) and fast gating (P_o^f) , as shown in panels C, D and E, respectively, were similar to those for WT hClC-1 (Fig. 15), although shifted by about 20 mV in the depolarizing direction. In all panels data points are shown as mean ± S.E.

FRET efficiency in cells coexpressing *N*451-Cerulean and 380*C*-eYFP are shown in panel F under control conditions (solid rhombus symbols, n = 59) is positive compared with that from cells co-expressing hClC-1-Cerulean + TrpV2-eYFP (hollow circle symbols, negative control from Fig. 16, panel B, n = 64). Otherwise, symbols and n as for Figure 16. The solid and dashed lines represent the linear regression analysis of data from each group of cells, respectively, indicating significant positive FRET efficiency between *N*451-Cerulean and 380*C*-eYFP compared to the negative control.

5.4 DISCUSSION

Internal deletions, truncations or mutations at various sites in the long C-tails of eukaryotic CLC proteins can result in poor expression, nonfunctional channels or dysfunction where it is common gating that is specifically affected (Pusch, Ludewig & Jentsch 1997; Fong, Rehfeldt & Jentsch 1998; Hryciw et al. 1998; Estévez et al. 2004; Hebeisen et al. 2004; Wu et al. 2006). Recently, a FRET study of ClC-0 during common gating demonstrated that its C-termini undergo large displacements from a position close to each other under resting conditions (Bykova et al. 2006). A much longer post-CBS2 tail in hClC-1 than in ClC-0 might be responsible for it having a lower, although comparable, FRET efficiency (~17% versus ~24%, respectively), as we found in our present study. At ~24%, FRET efficiency for ClC-0 was somewhat higher than the ~19% obtained previously (Bykova et al. 2006), due to optimisation of the recording technique. From the Förster equation, $E = 1/(1 + (R/R_0)^6)$, assuming $R_0 = 4.9$ nm, our FRET efficiency values for hClC-1 and ClC-0 translate into spatial separations of 6.4 nm and 6.0 nm, respectively, and when the post-CBS2 C-tail of hClC-1 was truncated to a length more like that of ClC-0, FRET efficiency increased beyond that of WT hClC-1 (from ~17% to ~21%, corresponding to a decrease in separation to 6.1 nm). These results suggest that under normal control conditions the post-CBS2 regions probably assume defined positions similar to each other in these two channels. X-ray crystallography of the cytoplasmic domains of both ClC-5 and ClC-Ka support this view (Markovic & Dutzler 2007; Meyer et al. 2007) although the post-CBS2 region appeared to be unstructured in C-tail crystals of ClC-0 (Meyer & Dutzler 2006). Deletion of ClC-0's last 36 amino acids, however, dramatically affects its common gating properties (Maduke, Williams & Miller 1998)

In both ClC-0 and ClC-1 channels, common gate opening from its equilibrium state increases FRET efficiency, corresponding to closer C-terminal proximity. By contrast, closure induced by the action of $[Zn^{2+}]_e$ reduces FRET efficiency which corresponds to increased separation. Common gate closure from its maximum open position in ClC-0 is associated with a FRET decrease from 23% to 5% (Bykova et al. 2006), whereas, in hClC-1 the decrease is from 22% to 13% (present results). Displacement of the C-terminals associated with closure must, therefore, be considerably greater in ClC-0 than in ClC-1. According to the Förster equation, an increase in separation by more than 2 nm would be required to reduce FRET from 23% (slow gate open state) to less than 5% (closed state) in ClC-0 (Bykova et al. 2006) while, to reduce FRET from 22% to 13% in hClC-1, the increase in separation could not be more than about 0.7 nm (approximately 1/3 of that in ClC-0).

While qualitatively similar conformational changes in the two channels are consistent with their predicted structural homology, a close correspondence might not have been anticipated since the common gate of ClC-0 has an opposite voltage dependence to that of hClC-1, the ClC-0 common gate closing with depolarisation. Conversely, some differences might have been expected because of the significant disparity in temperature dependence of their gating relaxations, the Q_{10} values for the common gating of ClC-0 and hClC-1 being approximately 40 and 4, respectively (Pusch, Ludewig & Jentsch 1997; Bennetts et al. 2001). Conformational rearrangements during common gating in ClC-0, therefore, are likely to be considerably greater than in hClC-1. Indeed, time constants for common gating are of the order of seconds to minutes for ClC-0 (Ludewig, Jentsch & Pusch 1997), and just tens of milliseconds for hClC-1 (Accardi & Pusch 2000), consistent with a larger movement in ClC-0.

In the E232Q mutant, common gate closure is eliminated along with fast gating, as can be discerned from the raw current records of Fahlke *et al.* (Fahlke et al. 1997) and from analysis of the apparent open probabilities of the two gating processes (submitted paper). Notwithstanding the total absence of gating, FRET is unchanged by E232Q in either the full-length hClC-1 or *N*887 truncated channel (Fig. 19D, E). By contrast, fast gating is maintained in the C277S mutant, although its common gate is effectively locked open (Accardi, Ferrera & Pusch 2001), and its FRET efficiency is increased above that of WT hClC-1 (Fig. 16C). Most interestingly, when these two mutations are combined in a double mutant construct (E232QC277S), FRET efficiency is enhanced (Fig. 19F). This suggests that C277S is capable of locking the common gate in its open conformational state even in the E232Q background that otherwise exhibits the common gate conformation of WT hClC-1.

Although fast and common gating have been described as “not necessarily independent” (Accardi & Pusch 2000), independence has generally been assumed. Our present conclusions depart significantly from this common presumption, which is: (a) that fast gate transitions occur independently of each other within each pore and independently of the common gate, (b) that common gate transitions occur independently of the fast gates and (c) that the common gate is a separate structural entity that physically obstructs the two pores, simultaneously. Based on our findings, where deletion of the fast gates also abolishes common gating, we propose, instead that fast and common gating must be closely coupled in the following way: (a) that fast gate transitions occur independently of each other within each pore depending on the common gate being in an open (permissive) state, (b) that common

gate transitions occur independently of the fast gates and (c) that the common gate is not a structural entity that causes concurrent obstruction of both pores, but rather a conformational change that simultaneously permits or prevents the operation of both fast gates, alternately allowing their freely independent action or locking both closed (Fig. 21A, B). So common gating is manifested exclusively through synchronised switching (coupling) that affects both fast gates at once, the associated conformational change being reflected at the C-terminals. We also propose that the rearrangements normally associated with common gating can still occur in the E232Q mutant but, because the fast gate is absent, there can no longer be any coupling of the gating to the conformation (Fig. 21C). Common gating is eliminated by C277S because this mutation prevents the common gate from switching out of its open configuration where the channel's two fast gates remain permissive (Fig. 21D, E). That fast and common gating are closely coupled is supported by a number of hClC-1 mutations in which both the fast and common gating are affected, such as I290M (Accardi & Pusch 2000), F307S, A313T (Aromataris et al. 2001), T268M, T539A and S541A (Duffield et al. 2003).

Conformational changes throughout helix R are associated with the ion transport process in ClC-ec1 (Bell et al. 2006). This could help to explain why a connection from the C-tail through helix R to the membrane-resident region in eukaryotic CLCs can appear to have relevance to common gating. At least in hClC-1, however, direct connectivity through helix R does not appear to be necessary, or likely, because we have shown in a previous paper that approximately WT function is maintained in a split channel reconstitution where there is no connection from the C-tail via the R helix (Ma et al. 2008).

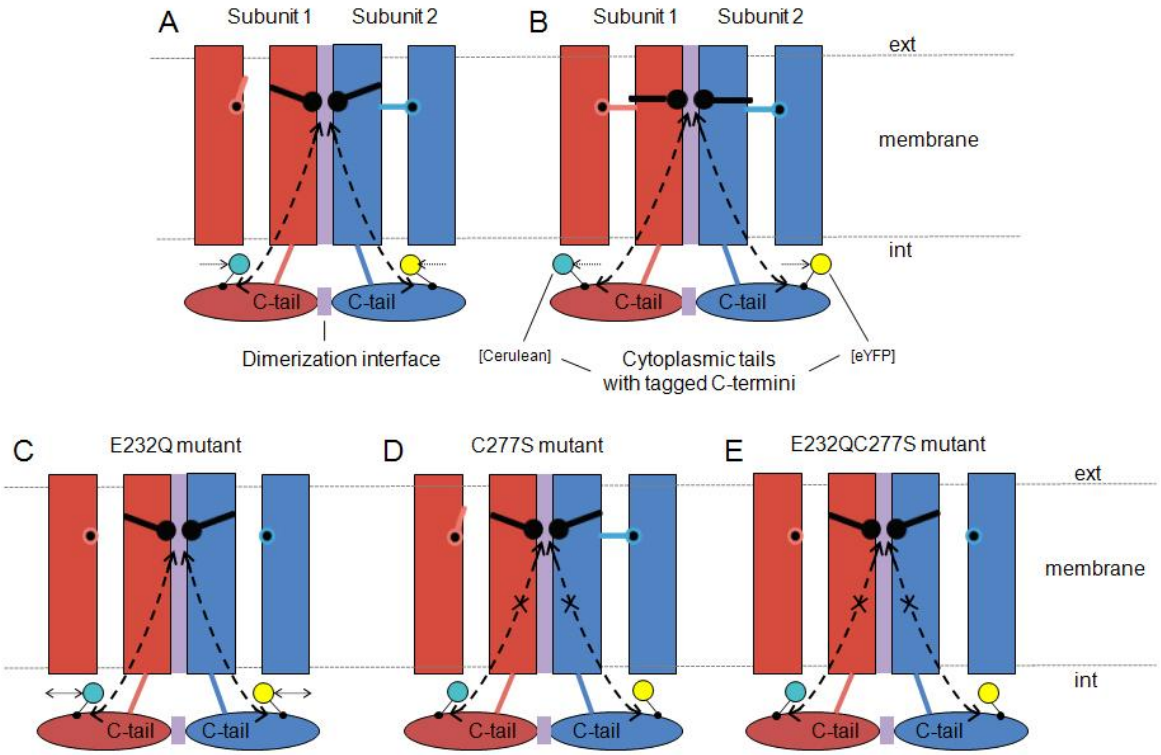
To try to understand the structural relationship between the C-tail and the membrane-resident region of hClC-1, especially with respect to the position of the C-terminals perpendicular to the plane of the membrane, we split the channel into two fragments, *N*451 + 380*C*, and labelled their C-terminals extracellularly with Cerulean in the first fragment and intracellularly with eYFP in the second. When co-expressed, these fragments recombined to form functional channels and exhibited positive FRET between the extracellular and intracellular fluorophore.

Although each of the split channel components might separately be trafficked into the plasma membrane, only a single form of functional reconstitution is possible between them where one fluorescent tag is located on the extracellular side of the membrane (on *N*451) and the other on the intracellular side (on 380*C*). Positive FRET obtained from co-expression of these

constructs suggests that the donor and acceptor fluorophores probably have a transmembrane separation of not more than ~8 nm perpendicular to the membrane. If the membrane-resident region of hClC-1 is structurally similar to its prokaryotic homolog, ClC-ec1, it should have a transmembane thickness of ~3.5 nm (Dutzler et al. 2002) and this would constitute a minimum fluorophore separation. Additional spatial separation due to effective fluorophore radius, and likely lateral displacement of the extracellular Cerulean fluorophore with respect to the intracellular eYFP, makes it likely that the C-terminal of hClC-1 is located at quite a shallow depth within the cytoplasm and close to the cytoplasmic surface of its membrane-resident region.

Since the lateral distance between the two C-termini in hClC-1 under normal conditions is of the order of 6.5 nm, the structural space able to be occupied by each C-terminus is quite constrained. A poly-proline helix (helix S in Fig. 13) has recently been identified in the C-tail of hClC-1 (amino acid 880-888), just distal to CBS2 (Macías et al. 2007). While this could act as a site for interaction with other (regulatory) cytoplasmic proteins (Adzhubei & Sternberg 1993) it might also bind the terminal portion of the C-tail onto the cytoplasmic loop region of the membrane-resident domain. The latter interaction could explain how the C-terminal is kept close to the membrane-resident region and how A885P can be a dominant myotonic mutation (Beck, Fahlke & George 1996).

Figure 21. Diagrammatic representation of coupling between fast and common gating in hClC-1.



The dimeric structure of the channel is shown in transmembrane section with Cerulean and eYFP tags attached to the C-termini of subunit 1 and 2, respectively. In panel A, fast gating is illustrated with the fast gate in subunit 1 in the open position and that in subunit 2 in the closed position. Open and closed states will be distributed through the channel population in an equilibrium that is dependent on membrane potential and other factors, such as $[Cl^-]_e$ and pH. Panel B shows common gating. A concerted conformation change, indicated by the curved dashed lines in panel B, latches both fast gates simultaneously in their non-permissive condition. At equilibrium, dependent again on membrane potential and other factors, there will be a distribution of the conformations shown in panel A (common gate open) and panel B (common gate closed). One aspect of the conformation change, with common gate closure, is separation of the C-termini of the channel dimer, a movement detectable by FRET. In panel C, the condition of the E232Q mutant is illustrated, in which the fast gate is eliminated. Conformational changes normally associated with common gating may still occur but functional common gating is not possible. By contrast, in a C277S mutant (panel D), the conformational change associated with common gate closure is somehow prevented (broken dashed lines with crosses) thus restricting the common gate to the open condition. A combination of the condition in E232Q and in C277S is shown in panel E for double mutant E232QC277S in panel E. Both the fast gate and conformational changes associated with the common gate are eliminated, so the common gate is kept open.

CHAPTER 6:
GENERAL DISCUSSION, CONCLUSIONS AND FUTURE DIRECTIONS

Since the structure of a bacterial CLC protein was resolved by X-ray crystallography (Dutzler et al. 2002), great progress has been made towards understanding structural and functional features of the CLC channel/transporter family. With the structure of its α-helices across the membrane and the nature of its selectivity filter/binding sites now being clear, gating mechanisms have become a focus of interest. Especially for common gating in the channels, ClC-0, ClC-1 and ClC-2, little is yet known about its complex working mechanisms. Therefore, an overall aim of this study was to clarify some functional characteristics of common gating using hClC-1 as a model and in this way to contribute to a better understanding of CLC proteins on the whole.

As an important member of the CLC chloride channel/transport family in humans, hClC-1 shares common features with other family members (especially ClC-0). It is functional only as the dimer, its membrane-resident domain consists of eighteen α helices with an ion conduction pathway in the centre of each, it has multiple gating mechanisms and complex coupling of gating, permeation and chloride binding. On the other hand, hClC-1 also has its own special characteristics to support its fundamental role in stabilizing the membrane potential of skeletal muscles. One of these is its much longer cytoplasmic tail compared to other family members. The 397 amino acid C-tail of hClC-1 affects the common gating in a complex way, which has been the focus of the present study.

6.1 GENERAL DISCUSSION

6.1.1 SPLIT CHANNEL STRATEGY AND TRAFFICKING SIGNAL

Split channel strategies are popular and powerful tools to study channel function, where the channel protein is split at a specific position and the channel fragments are coexpressed to investigate the expression, trafficking and physiological function of certain parts of the protein. For example, using a split channel method, Lewarchik *et al*. demonstrated that the NEG2 region in the R domain of CFTR (cystic fibrosis transmembrane conductance regulator) allows the channel to be stabilized in a regulated intracellular compartment before trafficking to the plasma membrane in response to cAMP/PKA stimulation (Lewarchik et al. 2008). Similarly, by coexpressing different split channel fragments, Becker *et al*. found that in the ATP-gated cation channel P2X7 receptor, non-covalent association of crucial functional

importance exists between the carboxyl end of the channel core fragment and the complementary tail extension (Becker et al. 2008).

In this study, I used the split channel strategy to investigate how the C-tail of hClC-1 might contribute to the common gating process. Although co-expression of membrane-resident portions and their complementary cytoplasmic domains have previously been shown to generate functional channels in both ClC-0 and hClC-1 (Schmidt-Rose & Jentsch 1997a; Maduke, Williams & Miller 1998), no further study was done to illuminate the underlying mechanism. My results from Chapter 3 first demonstrated that functional recue could be gained by co-expressing split channel fragments G-f-*N*720 and 721*C*-m when hClC-1 was cut between the CBS1 and CBS2 domains in its cytoplasmic tail. This is in accordance with previous reports (Schmidt-Rose & Jentsch 1997a; Estévez et al. 2004), again verifying the belief that some regions in hClC-1 are structurally autonomous. It has been proposed that they can form individual subdomains or modules with similar tertiary structure to the one found within the native protein, which can insert and fold independently and then mediate protein-protein interactions to enable the functional expression of hClC-1 channels. I was able to confirm this putative protein-protein interaction directly (as decribed in Chapter 3) by demonstrating strong binding between G-f-*N*720 and 721*C*-m using the GST-pull-down method. It clearly illustrates that the distal C-tail of hClC-1 regulates channel function by interacting non-covalently with some part/parts of its complementary partner, thus providing a good foundation for further studies on how this could affect common gating.

In the regulatory sulfonylurea receptor subunits of ATP-sensitive K^+ channels, the location of the "splitting point" in the vicinity of the nucleotide binding folds 1 domain has marked effects on the MgADP stimulation of resulting channels (Masia, Caputa & Nichols 2007). Similarly, the fact that combination *N*597 + 598*C* could not reconstitute channel function (Chapter 3) demonstrated that independent folding and trafficking of channel fragments require specific signal(s) or subdomain(s) (Schmidt-Rose & Jentsch 1997a). For example, in the present study, a short peptide from aa666 to aa679 was hypothesized to be important for keeping the integrity or trafficking ability of hClC-1 fragments in split channels. As discussed in Chapter 3, I proposed that this short stretch must be contiguous with at least one membrane-resident component of split hClC-1 channels, instead of being contained solely within a cytoplasmic C-tail fragment. This hypothesis is supported, on the one hand, by the successful functional rescue from split channels with the membrane-resident component containing the putative trafficking signal and on the other hand, by the failed reconstitution

from split channels with the putative trafficking signal existing only in the cytoplasmic fragment (Schmidt-Rose & Jentsch 1997a; Estévez et al. 2004; Hebeisen et al. 2004; Wu et al. 2006). Also, in this short peptide (aa666-679), a myotonic mutation R669C was identified from a sporadic myotonia patient (de Diego et al. 1999). This region of the inter CBS linker is otherwise both unremarkable in the lack of conservation of its amino acid sequence and in its apparent lack of structure in X-ray crystals of several CLC proteins (Meyer & Dutzler 2006; Markovic & Dutzler 2007; Meyer et al. 2007).

Mutations affecting protein trafficking, which then lead to genetic diseases, have been reported in different channels. For example, the vesicular trafficking mechanism of ATP-sensitive potassium channels was shown to be inhibited by genetic mutations in its subunit Kir6.2, resulting in the loss of channel function and hence genetic diseases (Sivaprasadarao et al. 2007). Mutation E282K, as an example of these mutations, was found to disrupt a di-acidic ER-exit signal (DXE), preventing subsequent endoplasmic reticulum (ER) exit. Accordingly, people with mutation E282K would have congenital hyperinsulinism (Christesen et al. 2007). Mutations Y330C and F333I, reported in patients with neonatal diabetes mellitus, disrupted an endocytic traffic signal, thereby impairing clathrin-coated vesicle formation and endocytosis (Sagen et al. 2004).

It would be interesting to test whether myotonic mutation R669C would affect the trafficking of hClC-1 in some way, especially in the sarcolemma. Nevertheless, more studies are required to verify the role of this putative trafficking signal or to find out the real trafficking signal for hClC-1.

6.1.2 CBS DOMAINS AND THEIR PHYSIOLOGICAL FUNCTIONS

Protein domains are evolutionarily conserved units with shared structural (sequence and folding pattern) and functional properties. Therefore, it is generally assumed that each domain performs a specific function unique to it no matter what the overall function of the protein in which it is present. A major challenge, then, is to relate the domain function to the overall protein function. As a good example, various cytosolic and membrane proteins performing different functions, including, the CLC family of channels/transporters, all contain CBS domains but the functional role of these domains remains largely unresolved and even controversial.

An open question about CBS domains in CLC proteins is whether they play a role in the intracellular trafficking. As discussed above, I hypothesized that the short peptide, aa666-679,

instead of the CBS domains, might be indispensable for protein trafficking in split channel configurations in hClC-1. Other data, however, have implicated CBS2 in the intracellular trafficking of some CLC proteins. One example is that disruption of the CBS2 domain by alanine scanning led to mislocalization of the *Saccharomyces cerevisiae* CLC (Gef1p) (Schwappach et al. 1998). Wild-type Gef1p is normally sorted to the Golgi apparatus, but Gef1p with a mutated CBS2 is retained in a compartment that also stains for Kar2p, a marker for the endoplasmic reticulum. Another example comes from functional studies of ClC-5. When expressing mouse ClC-5 mutants in CHO-K1 and IMCD-3 cells, it was found that truncation mutants with a disrupted second CBS domain were retained in a perinuclear compartment instead of being delivered to acidic endosomes as was the fate of wild-type ClC-5 (Carr, Simmons & Sayer 2003). Nevertheless, we can not deduce from these data that CBS2 contains a sorting signal for plasma membrane delivery. Indeed, in agreement with my results in Chapter 3, in-frame deletion of CBS2 did not affect the functional expression of ClC-1 channels, indicating that CBS2 itself is dispensable for membrane sorting and channel function (Hryciw et al. 1998; Estévez et al. 2004). Mo and colleagues also showed that truncated CLC-5 channels missing large portions of the C-tail or even some of the transmembrane domains were able to insert into the plasma membrane (Mo et al. 2004). Most recently, a study on the C-tail domains of hClC-2 demonstrated that surface membrane insertions of R751X (truncated before the CBS2 domain) and H573X (truncated before the CBS1 domain) are comparable to WT channels. In contrast, S551X, that lacks the R helix and the complete C-tail, results in intracellular retention of mutant channels (Garcia-Olivares et al. 2008).

A possible interpretation of these data is that CLC proteins contain as yet uncharacterized sorting signals for plasma membrane insertion that do not reside in CBS domains and that function both in the complete channel and in the split channel configuration. However, in split channels, the CBS1-CBS2 interaction within a single C-tail fragment, or between two C-tail fragments, might be necessary to bring the sorting signal of, for example, a membrane-resident fragment into the correct position. In the complete channel, however, the sorting signal could be correctly positioned independently of the CBS interaction. Finally, we should also be aware that the missorting of a mutant protein does not necessarily reflect the loss of a sorting signal but could be due to malfolding of the mutant protein and retention of the malfolded protein by the quality control system in the endoplasmic reticulum.

There is no doubt, however, that CBS domains in human CLCs are very important for protein function and/or expression. Using GST-pull-down, I found that the strong interaction between

G-f-*N*720 and 721*C*-m was totally interrupted when CBS1 was deleted from G-f-*N*720 or when CBS2 was deleted from 721*C*-m (Chapter 3). This result demonstrated the substantial role of CBS domains physically and their physiological significance has been illustrated by many functional studies. For example, specific point mutations have been identified in the CBS2 domain that changed the characteristics of the common gate of ClC-1 and ClC-0. In particular, mutation of E763, which corresponds to a conserved acidic residue in many CBS domains, abolished common gating in ClC-0 without interfering with fast gating (Estévez et al. 2004). These experiments are consistent with previous observations, which revealed that exchanging the CBS domains between, ClC-0 and ClC-1 or ClC-2, modified the common gating (Fong, Rehfeldt & Jentsch 1998). Garcia-Olivares and colleagues (2008) recently showed that ClC-2 channels with only one CBS domain are permanently closed and can be opened by a point mutation (E205Q) that affects fast and slow gating. Also, mutations in CBS domains of ClC-1, -2, -5, -7 and ClC-Kb have been shown to result in specific diseases caused by CLC dysfunction (Lloyd et al. 1997; Kornak et al. 2001; Bowne et al. 2002; Pusch 2002; Haug et al. 2003; Jentsch et al. 2005).

My present study (Chapter 3) clearly demonstrates that the interaction between CBS1 and CBS2 domains is precisely the primary structural foundation for the functional rescue of the split channel when the channel protein is split between the two CBS domains. Apparently, heterodimerization of CBS domains is not essential for, but rather appears to enhance protein expression and function at the cell surface (Simon et al. 1996; Sintchak et al. 1996; Schwappach et al. 1998; Estévez et al. 2004; Scott et al. 2004). In fact, I hypothesized that this dimerization might provide an optimal molecular platform for presentation of key parts of the CBS-CBS dimer surface or of the intervening sequence between the CBS domains to complementary interacting regions. Importantly, I was then able to confirm such an interaction between 598*C* (containing both CBS domains) and *N*720ΔCBS1 (without any CBS domain). This is an interesting extension of existing knowledge of CBS domain function, not only because the physiological significance of the binding was demonstrated by WT hClC-1 currents that were generated from co-expressing these two fragments (Chapter 3), but also because it broadens the view of how the C-tail of CLC proteins could communicate with the membrane-resident pore region.

Previous studies from our lab on rat ClC-1 expressed in Sf9 insect cells showed that most of the CBS2 domain (aa840-870) could be deleted without significantly affecting channel function (Hryciw et al. 1998). A later study of hClC-1 in *Xenopus* oocytes even indicated that

only 26 amino acids from Leu^{863} to Arg^{888} were enough to substitute for the 721*C* cytoplasmic fragment in channels split at *N*720, since channel function was restored by co-expressing this peptide with the otherwise inactive *N*720 (Wu et al. 2006). However, as shown by the GST-pulldown results (Figure 3, Chapter 3), when this short peptide (aa863-888), as well as another two functionally significant peptides aa800-806 and aa807-813, were deleted from 721*C*, the interaction between CBS1 and CBS2 was still intact. It is possible that these peptide segments are not involved in the major binding sites between CBS1 and CBS2, or they are involved and when individually deleted, their role could be compensated for by some other parts of the C-tail.

6.1.3 LOOPS IN CLC PROTEINS

Loops connecting adjacent transmembrane α helices in channels are usually regarded as less significant than other secondary structures such as α helices or β sheets in channel function. They cannot be compared with the cytosolic tails either, because the latter often play important roles including mediating protein-protein interactions, regulating the trafficking of the protein, targeting the channels for destruction and sensing the energy state in the cell. As I have shown in Chapter 4, however, the loops in CLC proteins are more than just structural linkers in terms of channel function.

Although no single loop studied in this project proved to be fully responsible for the interaction between the C-tail 598*C* and the membrane-resident region *N*720ΔCBS1, alanine-exchange of loops DE, FG, HI and JK of hClC-1 has been shown to have different effects on channel function. All the loop mutants were demonstrated to be able to be well expressed and trafficked correctly to the plasma membrane (Fig.2, Chapter 4). Mutating all the eight amino acids in loop DE to alanine eliminated hClC-1 currents completely, possibly because the voltage dependence of channel gating has been shifted too far in the depolarizing direction to make activation of the channel possible or the channel is totally nonfunctional due to the influence of loop DE on the adjacent helix R. A large depolarizing voltage shift gains support from an earlier study on G200R, which is a missense mutation of a highly conserved amino acid located in loop DE and which has been associated with dominant myotonia congenita. When this mutant is heterologously expressed, it leads to a drastic shift by ~+65 mV of the open probability curve, thus decreasing the chloride conductance in the physiological voltage range (Wollnik et al. 1997).

An alanine-exchange of loop FG did not affect channel function, but mutation of loop HI significantly shifted the P_o of fast gating to more positive potentials compared with the WT

hClC-1. This shift reduces the open probability of fast gating in a wide voltage range, so that at physiological voltages, less channels would be open, leading to a decreased chloride conductance, increased skeletal muscle excitability and possibly myotonia. Quite a surprising effect on channel gating arose from alanine-exchange of loop JK. At all investigated voltages there was a drastic reduction in the slow component of the macroscopic gating relaxations, consistent with the common gate being locked in an open state whereas there was only a minor effect on the fast component.

Apparently, the functional significance of loops in CLC proteins is not limited to hClC-1. Igarashi and colleagues investigated five unrelated, non-consanguinous Japanese families with Dent's disease and found five new mutations in ClC-5. One of them, a missense mutation, S270R (equivalent to S294 in hClC-1), located within the short intracellular loop between helix H and helix I, was shown to abolish currents completely (Igarashi et al. 1998). In 2005, a study of yeast CLC channel, Gef1p, demonstrated that the channel is proteolytically processed in the secretary pathway. Proteolytic cleavage occurs in the first extracellular loop of the protein at residues KR136/137. Activation of proteins by proteolytic processing events late in the secretory pathway is a common regulatory mechanism, hence loop BC might be involved in the specific regulation of Gef1p channel (Wächter & Schwappach 2005). Most recently, Osteen and colleagues found that Zn^{2+} inhibits the currents of hClC-4 with an apparent affinity of approximately 50 mM, which is minimally voltage-dependent, suggesting an extracellular binding site for the ion. Out of nine candidate external residues they tested, only mutations of three consecutive histidine residues located in loop NO (H493A, H494A, H495A) significantly reduced the effect of Zn^{2+}. Therefore, loop NO provides the binding site for zinc in hClC-4 (Osteen & Mindell 2008).

It is thus reasonable to believe that loops in CLC proteins are also significant in carrying out normal channel functions, especially, in communicating between channel subunits, e.g. C-tail to membrane-resident region, or with other binding proteins or in conducting information changes from the surrounding environment to the pore region.

6.1.4 COMMON GATING

No structure has yet been identified that fully represents the common gate, however, more and more properties of the common gating are being identified. In the present study, I have shown that the common gating process in hClC-1 is functionally associated with a significant backbone movement in its C-termini. Closure of the common gate is accompanied by a physical separation of the C-termini, whereas opening is associated with them moving closer

to each other (Chapter 5). This adds another characteristic shared between the common gating in hClC-1 and in ClC-0, as there is a similar conformational rearrangement in the C-tail of ClC-0 (Bykova et al. 2006). Besides this, common gating of hClC-1 and ClC-0, are alike in many other ways.

First of all, both of them have significant temperature dependence (Pusch, Ludewig & Jentsch 1997; Bennetts et al. 2001). Second, it is also clear that the interactions between the two subunits of the channel dimer are involved in the common gating process. For example, mutations in ClC-1 that affect common gating have been found in different parts of the protein, but there is clustering of these mutations at the dimerization interface where inter-subunit interaction would occur (Duffield et al. 2003). Third, they are both inhibited by extracellular zinc (Zn^{2+}) or cadmium (Cd^{2+}) ions, which have an allosteric stabilization of the closed conformation of the common gate and the inhibition could be reduced by several mutations that eliminate the common gating, such as C212S in ClC-0, or C277S in ClC-1 (Chen 1998; Duffield et al. 2005). Fourth, mutations in the C-tails of both ClC-0 and hClC-1 have been demonstrated to affect the open probability or voltage dependence of common gating (Fong, Rehfeldt & Jentsch 1998; Maduke, Williams & Miller 1998; Estévez et al. 2004; Macías et al. 2006). Fifth, lower external pH favors the opening of the common gate in both ClC-0 and hClC-1, whereas a reduction of the extracellular chloride concentration favors the inactivated state (Pusch et al. 1995; Rychkov et al. 1996a; Pusch et al. 1999).

On the other hand, common gating in hClC-1 is also significantly different from ClC-0 in several aspects. For example, my analysis of FRET efficiency associated with common gating, suggested that the change in the distance between the two C-termini of the channel, is much smaller during common gating in hClC-1 compared to that in ClC-0 (Chapter 5). Secondly, the common gate of ClC-0 opens with hyperpolarization within seconds, and, once open, closes even more slowly at positive voltages (Pusch et al. 1995; Chen & Miller 1996). In hClC-1, the open probability of common gating increases upon membrane depolarization. Also, it is much faster than in ClC-0, with transition times on the order of tens of milliseconds, only ~threefold slower than the hClC-1 fast gating (Accardi & Pusch 2000). Most interestingly, the temperature dependence of relaxation of common gating is unusually large in ClC-0 compared with that in hClC-1, which was clearly demonstrated by a $Q_{10} = 40$ for ClC-0 versus a $Q_{10} = 4$ for hClC-1 (Pusch, Ludewig & Jentsch 1997; Bennetts et al. 2001). It might be deduced from this remarkably difference in temperature sensitivity that the conformational change/s associated with common gating in hClC-1are much smaller than those in ClC-0. Indeed, this hypothesis is supported by the evidence from my FRET study of

relative C-terminal displacement associated with common gating in the two channels (above and Chapter 5).

Another interesting finding that comes from my project is that common gating and fast gating seem to be closely coupled in hClC-1. Mutation C277S, which eliminates common gating but keeps fast gating intact, shows higher FRET efficiency between the two fluorophores labeled on its C-termini compared to WT hClC-1. Unlike WT hClC-1, however, this level of FRET efficiency is not reduced by either extracellular zinc or low chloride concentration (Chapter 5). By contrast, mutation E232Q, which keeps both the common gate and fast gate in hClC-1 open all the time, has a similar FRET efficiency to that of WT hClC-1 in either the full-length protein or truncated channel (Chapter 5). This means that the loss of common gating (maintenance of the common gate in its open state) in E232Q is not coupled with the conformational change, a closer approach, of the C-termini. The difference between C277S and E232Q seems to arise because of the absence of the fast gate in E232Q, but not in C277S. I have therefore hypothesized that E232Q might retain its mechanical basis for common gating. Although currents recorded electrophysiologically from cells expressing E232Q show neither fast nor common gating, this might be because the mutual effector of both types of gating is normally the carboxyl side chain of E232, which is absent in E232Q. This is different from the situation for the C277S mutant. In C277S, common gating is eliminated probably because the conformational changes associated with it are prevented.

If my hypotheses about these two mutants were right, the FRET efficiency of double mutant E232Q/C277S should be quite like that of C277S, because the mechanical basis for common gating in E232Q/C277S should be abolished by the existence of mutation C277S. A FRET efficiency of 21.8% from this double mutant is indeed close to that of the single C277S mutant (22.8%, Chapter 5) and therefore provides supporting evidence for my proposal that common gating is functionally linked to fast gating in hClC-1.

As discussed previously, I have shown in Chapter 3 that the whole cytoplasmic tail of hClC-1 (598*C*) can bind to its complemetary membrane-resident fragment (*N*720ΔCBS1), indicating a possible communication pathway between these separate domains, although the interacting sites are still unknown. I then tried to obtain more details about this interaction by testing whether the C-terminals could be close enough to the pore region to participate in the interaction. Positive FRET between an extracellular fluorophore attached to the C-terminal of loop LM on *N*451 and an intracellular fluorophore attached to the C-terminal of the protein on 380*C* indicate that they lie in close proximity across the membrane. If, in the future, a change

of this FRET could be associated with the common gating process, we ought to be able to obtain common gating-related conformational rearrangements perpendicular to the membrane. These, together with the now well characterized movements of the cytoplasmic C-terminals (presumably parallel to the membrane) should eventually help to provide a three dimensional view of the conformational changes associated with common gating.

6.2 CONCLUSIONS

Based on the three parts of my project and the 9 Aims set out in Chapter 1, the following conclusions can be drawn:

Aim 1: To test whether the physical interaction between split channel fragments of hClC-1 could be detected directly.

Conclusion 1: There is strong binding between an N-terminal membrane-resident fragment (terminating mid-C-tail at Ser720 and containing CBS1) and its complement (containing CBS2). This interaction is functionally significant because co-expression of the same otherwise nonfunctional protein fragments rescues channel function. This satisfies Aim 1. by providing the first direct evidence for physical protein-protein binding in this situation.

Aim2: To test the significance of some functionally important peptides in the interaction between hClC-1 split channel fragments. These short peptides include aa800-806, aa807-813, aa863-888, and subdomains CBS1 and CBS2.

Conclusion 2: With respect to Aim 2., short peptides aa800-806, aa807-813 and aa863-888, which have been demonstrated to be important for channel functions, especially for the channel gating, can be deleted without affecting the apparent strength of binding between *N*720 and 721*C*. This is a novel and unanticipated finding.

Conclusion 3: Also in regard to Aim 2., interaction between the membrane-resident *N*720 and the C-tail fragment, 721*C*, could be eliminated by either deleting CBS1 from *N*720 or deleting CBS2 from 721*C*. This suggests that contact between CBS1 and CBS2 might make a major contribution to assembly of functional channels from such co-expressed complements. That C-tail fragments could, in addition, bind to other parts of the membrane-resident component, however, remain as a possibility.

Aim 3: To test whether there are other interactions between the C-tail and the membrane-resident domain besides the CBS1-CBS2 interaction.

Conclusion 4: There is interaction between a membrane-resident component terminating at Ser720 (but with CBS1 deleted, *N*720Δ) and a complete C-tail beginning at Leu598 (598*C*). Channel function is rescued in patch-clamped HEK-293T cells co-expressing these same fragments indicating that their interaction has operational significance. Thus the CBS1-CBS2 interaction is not sufficient, in itself, for channel assembly, but rather this might normally assist in bringing some part of the CBS2/post-CBS2-C-tail region into appropriate proximity with the membrane-resident portion of the protein. My goal, set out in Aim 3., has therefore been achieved.

Aim 4: To study the possible role of individual cytoplasmic loops of hClC-1 in the interaction between the cytoplasmic tail and the transmembrane pore domain.

Conclusion 5: In completing Aim 4., I have found that there is unlikely to be significant binding between the C-tail and any one of individual cytoplasmic loops among loop DE, FG, HI and JK. While apparently a negative set of results, this raises many possibilities that are discussed, below, under Future Directions.

Aim 5: To investigate the physiological function of the cytoplasmic loops of hClC-1 by electrophysiological analysis.

Conclusion 6: In part, Aim 5. arose out of achieving my goal for Aim 4. If individual loop sequence could be disrupted by alanine-exchange, without any effect on binding, would the same be true for channel function? I can now conclude that the gating mechanisms of hClC-1 might not only involve the helices and the C-tail, but also involve some of the loops, because alanine-exchange mutation of the loop linking helix D to E, completely eliminated channel currents; of the loop linking helix H to I, caused a significant shift of the open probability of fast gating towards more positive voltages and of the loop linking helix J to K, locked the common gate of hClC-1 open.

Aim 6: To test whether there is conformational rearrangement in the C-tails of hClC-1 during its common gating.

Conclusion 7: My goal as set out in Aim 6. has also been attained. There are, indeed, significant displacements of the C-termini associated with the common gating process in both full-length hClC-1 and in a shorter version, *N*887. Closure of the common gate is accompanied by a physical separation of the two C-termini of the dimer, whereas, on opening, the C-termini move closer to each other.

Aim 7: To compare the movements in the C-tails of hClC-1 to those of ClC-0 during common gating and analyse the physiological significance of the differences.

Conclusion 8: These movements and, presumably, the conformational changes that accompany common gating in hClC-1, are considerably smaller than in ClC-0, which might underlie some of the differing properties of common gating in these two channels. Aim7. has therefore been realized and valuable new understanding obtained in doing so.

Aim 8: To investigate C-terminal displacement in mutants where there was no common gating and where the common gate was locked in an open state.

Conclusion 9: In achieving Aim 8., I have not only found that C-tail displacement is modified by mutations that disrupt common gating but have also made the novel and unexpected discovery that fast gating and common gating may be closely coupled in hClC-1. This is quite different from what is generally accepted, that is, that (1) fast gating in one pore occurs independently of that in the other and independently of the common gate and that (2) common gating occurs independently of the fast gates but that (3) the common gate is a separate physical structure that obstructs both pores simultaneously. My conclusion, instead, is that (1) fast gating in one pore occurs independently of that in the other but that this gating is only possible when the common gate is open (in a permissive state), that (2) common gating occurs independently of the fast gates and that (3) the common gate is not a physical structure that obstructs both pores separately from the fast gates but, rather, a conformational change that locks both fast gates in a closed (non-permissive) state.

Aim 9: To test whether the C-terminal of hClC-1 is close to its membrane-resident domain using FRET.

Conclusion 10: In relation to Aim 9., I have made the first ever observation that there is positive FRET between split channel fragments *N*451-Cerulean and 380*C*-eYFP, which were able to combine appropriately for functional reconstitution of channel. Perpendicular transmembrane separation of the cytoplasmic C-terminal of hClC-1 from its extracellular helix L-helix M loop is therefore constrained to ~8 nm.

6.3 FUTURE DIRECTIONS

6.3.1 Further dissect the physical and physiological roles of loops in hClC-1

Attempt to determine which part from the membrane-resident region is the target for binding by the cytoplasmic tail in the absence of covalent attachment through helix R (Chapter 3), since none of the single cytoplasmic loops studied were fully responsible for the interaction (Chapter 4). There are three possibilities here: either none of the selected loops are necessary for the interaction, or more than one loop at a time is involved and each can be individually dispensable, or, besides the loops, the C-tail binds with some other site, or sites, accessible from the cytoplasm but not analysed by me. Therefore, if I had the chance to continue this project, I would mutate the cytoplasmic loops in various possible combinations to clarify whether they are in any way involved.

Also, for loop JK, which completely eliminates common gating, it would be interesting to further narrow down the critical region for such an effect, perhaps to only one or two amino acids. If I could study other cytoplasmic or extracelluar loops using electrophysiological methods, I would be able to achieve a more comprehensive understanding of hClC-1.

6.3.2 Further study on the short peptide L863 to R888

Previous study from our lab in *Xenopus* oocytes identified a short peptide of 26 amino acids (aa863-888) which was able to rescue channel function when co-expressed with the otherwise non-functional truncated protein, *N*720 (Wu et al. 2006). This successful assembly indicates that the interaction between these two independent regions must be strong enough to allow their stable association to form the active channel. However, in the present study, when aa863-888 was deleted from 721*C*, the binding between *N*720 and 721*C* was not noticeably affected (Chapter 3). It is possible that when the aa863-888 peptide is completely independent, it is able to change the tertiary structure of *N*720 so that the quaternary relationship between itself and *N*720 is different from that between 721*C* and *N*720. It is also possible that the discrepancy is because of the different experimental systems used in these two studies, electrophysiological analysis of co-expression in *Xenopus* oocytes versus protein biding of co-expressed proteins in HEK293T cells. It would be very interesting to repeat the co-expression study of *N*720 + aa863-888 in mammalian cells. If the functional rescue were still successful, I would like to investigate how this short peptide could reconstitute the channel function using some new techniques, such as Surface Plasmon Resonance, which can identify and monitor protein-protein interaction dynamically.

6.3.3 Locate the interacting sites between the membrane-resident pore region and the C-tail of hClC-1 by FRET

In chapter 5, I demonstrated that the cytoplasmic end of hClC-1 is so close to the membrane-resident pore region (loop LM) that an interaction, which might provide the information transfer pathway between the C-tail and the pore domain, is predicable. However, is this the only way that the C-tail communicates with the membrane-resident pore? What are the other interacting site/sites on the C-tail and on the membrane-resident region? And how does such an interaction contribute to channel properties such as common gating? These are the more critical questions to answer.

A straightforward way to locate the interacting sites is to label the C-tail and the pore region at different positions with fluorescent proteins or fluorescent chemical groups or intrinsic fluorescent amino acid residues (tryptophan, tyrosine, phenylalanine) respectively (the selection of the fluorescent tags depends on the position to label), and test FRET between the two fluorophores (Zal 2008). For the positive fluorescent pairs, changes of the FRET efficiency between the labeled sites of interest during the gating processes might be able to be observed by opening up or closing down the gates. For example, the effect of Zn^{2+}, low Cl^- and NaI on the channel could be tested. In that case, some ideas about the conformational changes in various dimensions could be obtained during common gating to make modeling of the channel behaviour much more accurate. Of course, the best way to gain this kind of knowledge of hClC-1 would be to determine the crystal structure of the whole protein. But even then, crystal structures usually only provide static information and complex dynamic functional rearrangements are difficult to predict.

6.3.4 Further study of the common gating mechanism by chimeras using FRET

Similar conformational rearrangements during common gating have been detected in both ClC-0 (Bykova et al. 2006) and hClC-1 (Chapter 5), so is there the same kind of movement in the C-tail of ClC-2 during its common gating? Also, since a chimera of different CLC subunits would result in changed common gating features from the parent channels (Fong, Rehfeldt & Jentsch 1998), what would the movement in the C-tail be like in a chimera of ClC-0/ClC-1, ClC-0/ClC-2 or ClC-1/ClC-2? How would that movement (if there is any) be affected by different factors that could influence common gating, such as Zn^{2+}, Cl^-, pH and mutations?

An interesting conclusion coming from my present study is that there is close coupling between common and fast gating in hClC-1. This could be further extended by investigating the effects of Zn^{2+}, low Cl^- and NaI on FRET in hClC-1 mutants that affect common gating such as E232Q (Fahlke et al. 1997; Cederholm 2007), C277S (Duffield et al. 2003), I290M (Accardi & Pusch 2000), V292L (Cederholm 2007), the alanine-exchange of loop JK mutant (Chapter 4) and in corresponding mutants in ClC-0 and ClC-2. These questions can be answered using the same method as in this study and would help to gain a better understanding of structure-function relationships in the CLC family.

6.3.5 Find other proteins that interact with hClC-1

Except for ClC-K and ClC-7 (Estévez et al. 2001; Lange et al. 2006), it is thought that CLC proteins can function as a channels or transporters independently, without the participation of ancillary proteins. However, several CLC family members have been found to associate in some way with cytoskeletal elements, kinases, phosphatases and chaperones. For example, disruption of the actin cytoskeleton results in significant activation of ClC-2 currents, supporting a role for actin remodeling in modulating the functional properties of ClC-2 (Ahmed et al. 2000). Biochemical studies further revealed that the N-terminus of ClC-2 (residues 31-74) can associate directly with the actin cytoskeleton via electrostatic interactions (Ahmed et al. 2000). The endosome-associated ClC-5 was also reported to interact directly with a cytoskeletal protein, cofilin, via its C-tail (Hryciw et al. 2003). As an actin-binding protein, cofilin promotes disassembly of actin filaments, and has been implicated in actin remodeling (Bamburg & Wiggan 2002). These findings thus suggest that the function and/or trafficking of ClC-5, as well as ClC-2, may be mediated through associations with the actin cytoskeleton.

Electrophysiological studies suggested that kinase- and phosphatase-mediated reactions significantly modulate the functional properties of several members of the CLC family. Agonists that enhance cellular kinase activity usually suppress Cl^- flux through CLC proteins, whereas those that promote phosphatase activity boost CLC function at the cell surface (Fritsch & Edelman 1996; Kajita, Whitwell & Brown 2000; Rutledge, Denton & Strange 2002; Cuppoletti et al. 2004). In 2005, Hsp70 and Hsp90 were identified as possible ClC-2 interacting partners. An association of Hsp90 with ClC-2 results in greater channel activity due to increased cell surface channel expression, facilitation of channel opening and enhanced channel sensitivity to intracellular [Cl^-] (Hinzpeter et al. 2005). Investigation of the functional consequences of these interactions has provided considerable insight into the functional modulation of these channels. Although closely related and in the same sub-family with ClC-

2, hClC-1 has not been reported to interact directly with any other proteins. But it would be interesting to find out whether hClC-1 also has chaperones and how these partners might affect the physiological function of ClC-1.

Extensive investigations have proven that a protein's subcellular localization is highly dependent on "localization motifs", which dictate interactions with specific organelle-resident proteins. For example, ClC-3B localizes to the Golgi compartment. This protein has an extended C-terminal cytosolic domain that contains a unique PDZ domain-binding motif, which enables ClC-3B to interact with a second PDZ-binding domain motif of several scaffolding proteins including EBP50 and the Golgi-associated protein, GOPC (Golgi-associated PDZ and coiled-coil motif-containing protein). Interaction between ClC-3B and GOPC via its carboxyl terminus possibly accounts for its Golgi localization (Gentzsch et al. 2003) while ClC-3A lacks this PDZ domain-binding motif which might explain its distinct localization in the late endosomal compartment. Therefore, questions about membrane trafficking of hClC-1 might also be able to be answered by identification of interacting protein partners.

6.3.6 Study of myotonic mutations in hClC-1

Until Lipicky and Bryant (1966) found that the Cl^- conductance in skeletal muscles was lower in the autosomal dominant form of myotonic goats compared to normal goats, the molecular mechanism of myotonia was completely unknown. Their results were later verified by in vitro studies showing that a reduced chloride conductance in skeletal muscle fibers led to electrical instability (Rüdel & Lehmann-Horn 1985). It is now known that both of the two forms of pure nonsyndromic myotonia, the autosomal dominant form myotonia congenita (MC) or Thomsen's disease (MIM# 160800) (Thomsen 1876) and the autosomal recessive form generalized myotonia (GM) or Becker's disease (MIM# 255700) (Becker 1977), are due to mutations on the same gene, *CLCN1*, on chromosome 7q35 (Abdalla et al. 1992; Koch et al. 1992; Koch et al. 1993).

Myotonic mutations identified so far have been shown to be spread throughout the whole hClC-1 sequence (Pusch 2002), but not all of them have had their electrophysiological characteristics analysed and the mechanism by which many of them cause myotonia is not known. It would be interesting to know why mutations in various positions could have the same effects and why mutations which are not in obviously important positions can still cause myotonia whereas some others, which are in pivotal positions in terms of ion permeation, do not.

An understanding of common gating would be particularly important with respect to drug mining for a possible cure for dominant myotonia. In this disease and in contrast to recessive myotonia, it is usual for full length functional protein subunits to be expressed, it is just that 50% of these subunits tend to have a voltage dependence of common gating that is shifted far in the depolarizing direction. Even more importantly, when dimerized with a WT subunit, they confer much or all of their abnormal voltage dependence onto their WT partner via a dominant negative effect. This leaves the majority of channels closed at normal membrane potentials and greatly diminishes the large Cl^- shunt that normally damps the excessive membrane potential fluctuations responsible for myotonic muscle contractions. It is possible that an appropriate small chemical agent could have the pharmacological properties necessary to bind to the mutant subunits and to reverse their abnormal voltage dependence.

BIBLIOGRAPHY

Abdalla, JA, Casley, WL, Cousin, HK, Hudson, AJ, Murphy, EG, Cornelis, FC, Hashimoto, L & Ebers, GC 1992, 'Linkage of Thomsen disease to the T-cell-receptor beta (TCRB) locus on chromosome 7q35', *Am J Hum Genet,* vol. 51, no. 3, Sep, pp. 579-84.

Accardi, A 2008, 'To ATP or not to ATP: this is the question', *J Gen Physiol,* vol. 131, no. 2, Feb, pp. 105-8.

Accardi, A, Ferrera, L & Pusch, M 2001, 'Drastic reduction of the slow gate of human muscle chloride channel (ClC-1) by mutation C277S', *J Physiol,* vol. 534, no. Pt 3, Aug 1, pp. 745-52.

Accardi, A, Kolmakova-Partensky, L, Williams, C & Miller, C 2004, 'Ionic currents mediated by a prokaryotic homologue of CLC Cl- channels', *J Gen Physiol,* vol. 123, no. 2, Feb, pp. 109-19.

Accardi, A & Miller, C 2004, 'Secondary active transport mediated by a prokaryotic homologue of ClC Cl- channels', *Nature,* vol. 427, no. 6977, Feb 26, pp. 803-7.

Accardi, A & Pusch, M 2003, 'Conformational changes in the pore of CLC-0', *J Gen Physiol,* vol. 122, no. 3, Sep, pp. 277-93.

Accardi, A & Pusch, M 2000, 'Fast and slow gating relaxations in the muscle chloride channel CLC-1', *J Gen Physiol,* vol. 116, no. 3, Sep, pp. 433-44.

Adachi, S, Uchida, S, Ito, H, Hata, M, Hiroe, M, Marumo, F & Sasaki, S 1994, 'Two isoforms of a chloride channel predominantly expressed in thick ascending limb of Henle's loop and collecting ducts of rat kidney', *J Biol Chem,* vol. 269, no. 26, Jul 1, pp. 17677-83.

Adilakshmi, T & Laine, RO 2002, 'Ribosomal protein S25 mRNA partners with MTF-1 and La to provide a p53-mediated mechanism for survival or death', *J Biol Chem,* vol. 277, no. 6, Feb 8, pp. 4147-51.

Adzhubei, AA & Sternberg, MJ 1993, 'Left-handed polyproline II helices commonly occur in globular proteins', *J Mol Biol,* vol. 229, no. 2, Jan 20, pp. 472-93.

Ahmed, N, Ramjeesingh, M, Wong, S, Varga, A, Garami, E & Bear, CE 2000, 'Chloride channel activity of ClC-2 is modified by the actin cytoskeleton', *Biochem J,* vol. 352 Pt 3, Dec 15, pp. 789-94.

Alioth, S, Meyer, S, Dutzler, R & Pervushin, K 2007, 'The cytoplasmic domain of the chloride channel ClC-0: structural and dynamic characterization of flexible regions', *J Mol Biol,* vol. 369, no. 5, Jun 22, pp. 1163-9.

Aromataris, EC, Rychkov, GY, Bennetts, B, Hughes, BP, Bretag, AH & Roberts, ML 2001, 'Fast and slow gating of CLC-1: differential effects of 2-(4-chlorophenoxy) propionic acid and dominant negative mutations', *Mol Pharmacol,* vol. 60, no. 1, Jul, pp. 200-8.

Bamburg, JR & Wiggan, OP 2002, 'ADF/cofilin and actin dynamics in disease', *Trends Cell Biol,* vol. 12, no. 12, Dec, pp. 598-605.

Bauer, CK, Steinmeyer, K, Schwarz, JR & Jentsch, TJ 1991, 'Completely functional double-barreled chloride channel expressed from a single Torpedo cDNA', *Proc Natl Acad Sci U S A*, vol. 88, no. 24, Dec 15, pp. 11052-6.

Beck, CL, Fahlke, C & George, AL, Jr. 1996, 'Molecular basis for decreased muscle chloride conductance in the myotonic goat', *Proc Natl Acad Sci U S A*, vol. 93, no. 20, Oct 1, pp. 11248-52.

Becker, D, Woltersdorf, R, Boldt, W, Schmitz, S, Braam, U, Schmalzing, G & Markwardt, F 2008, 'The P2X7 carboxyl tail is a regulatory module of P2X7 receptor channel activity', *J Biol Chem*, vol. 283, no. 37, Sep 12, pp. 25725-34.

Becker, P 1977, *Myotonia congenita and syndromes associated with myotonia*, Thieme, Stuttgart,

Bell, SP, Curran, PK, Choi, S & Mindell, JA 2006, 'Site-directed fluorescence studies of a prokaryotic ClC antiporter', *Biochemistry*, vol. 45, no. 22, Jun 6, pp. 6773-82.

Belsham, GJ, Denton, RM & Tanner, MJ 1980, 'Use of a novel rapid preparation of fat-cell plasma membranes employing Percoll to investigate the effects of insulin and adrenaline on membrane protein phosphorylation within intact fat-cells', *Biochem J*, vol. 192, no. 2, Nov 15, pp. 457-67.

Bennetts, B, Parker, MW & Cromer, BA 2007, 'Inhibition of skeletal muscle ClC-1 chloride channels by low intracellular pH and ATP', *J Biol Chem*, vol. 282, no. 45, Nov 9, pp. 32780-91.

Bennetts, B, Roberts, ML, Bretag, AH & Rychkov, GY 2001, 'Temperature dependence of human muscle ClC-1 chloride channel', *J Physiol*, vol. 535, no. Pt 1, Aug 15, pp. 83-93.

Bennetts, B, Rychkov, GY, Ng, HL, Morton, CJ, Stapleton, D, Parker, MW & Cromer, BA 2005, 'Cytoplasmic ATP-sensing domains regulate gating of skeletal muscle ClC-1 chloride channels', *J Biol Chem*, vol. 280, no. 37, Sep 16, pp. 32452-8.

Berryman, M & Bretscher, A 2000, 'Identification of a novel member of the chloride intracellular channel gene family (CLIC5) that associates with the actin cytoskeleton of placental microvilli', *Mol Biol Cell*, vol. 11, no. 5, May, pp. 1509-21.

Birkenhager, R, Otto, E, Schurmann, MJ, Vollmer, M, Ruf, EM, Maier-Lutz, I, Beekmann, F, Fekete, A, Omran, H, Feldmann, D, Milford, DV, Jeck, N, Konrad, M, Landau, D, Knoers, NV, Antignac, C, Sudbrak, R, Kispert, A & Hildebrandt, F 2001, 'Mutation of BSND causes Bartter syndrome with sensorineural deafness and kidney failure', *Nat Genet*, vol. 29, no. 3, Nov, pp. 310-4.

Bisset, D, Corry, B & Chung, SH 2005, 'The fast gating mechanism in ClC-0 channels', *Biophys J*, vol. 89, no. 1, Jul, pp. 179-86.

Blair, E, Redwood, C, Ashrafian, H, Oliveira, M, Broxholme, J, Kerr, B, Salmon, A, Ostman-Smith, I & Watkins, H 2001, 'Mutations in the gamma(2) subunit of AMP-activated protein kinase cause familial hypertrophic cardiomyopathy: evidence for the central role of energy compromise in disease pathogenesis', *Hum Mol Genet*, vol. 10, no. 11, May 15, pp. 1215-20.

Borsani, G, Rugarli, EI, Taglialatela, M, Wong, C & Ballabio, A 1995, 'Characterization of a human and murine gene (CLCN3) sharing similarities to voltage-gated chloride channels and to a yeast integral membrane protein', *Genomics,* vol. 27, no. 1, May 1, pp. 131-41.

Bowne, SJ, Sullivan, LS, Blanton, SH, Cepko, CL, Blackshaw, S, Birch, DG, Hughbanks-Wheaton, D, Heckenlively, JR & Daiger, SP 2002, 'Mutations in the inosine monophosphate dehydrogenase 1 gene (IMPDH1) cause the RP10 form of autosomal dominant retinitis pigmentosa', *Hum Mol Genet,* vol. 11, no. 5, Mar 1, pp. 559-68.

Brandt, S & Jentsch, TJ 1995, 'ClC-6 and ClC-7 are two novel broadly expressed members of the CLC chloride channel family', *FEBS Lett,* vol. 377, no. 1, Dec 11, pp. 15-20.

Buyse, G, Trouet, D, Voets, T, Missiaen, L, Droogmans, G, Nilius, B & Eggermont, J 1998, 'Evidence for the intracellular location of chloride channel (ClC)-type proteins: co-localization of ClC-6a and ClC-6c with the sarco/endoplasmic-reticulum Ca2+ pump SERCA2b', *Biochem J,* vol. 330 (Pt 2), Mar 1, pp. 1015-21.

Bykova, EA, Zhang, XD, Chen, TY & Zheng, J 2006, 'Large movement in the C terminus of CLC-0 chloride channel during slow gating', *Nat Struct Mol Biol,* vol. 13, no. 12, Dec, pp. 1115-9.

Carr, G, Simmons, N & Sayer, J 2003, 'A role for CBS domain 2 in trafficking of chloride channel CLC-5', *Biochem Biophys Res Commun,* vol. 310, no. 2, Oct 17, pp. 600-5.

Cederholm, J 2007, 'Common gating of the skeletal muscle chloride channel involved in dominant myotonia congenita', Doctoral Dissertation thesis, University of South Australia.

Chen, MF & Chen, TY 2001, 'Different fast-gate regulation by external Cl(-) and H(+) of the muscle-type ClC chloride channels', *J Gen Physiol,* vol. 118, no. 1, Jul, pp. 23-32.

Chen, TY 2003, 'Coupling gating with ion permeation in ClC channels', *Sci STKE,* vol. 2003, no. 188, Jun 24, p. pe23.

Chen, TY 1998, 'Extracellular zinc ion inhibits ClC-0 chloride channels by facilitating slow gating', *J Gen Physiol,* vol. 112, no. 6, Dec, pp. 715-26.

Chen, TY 2005, 'Structure and function of clc channels', *Annu Rev Physiol,* vol. 67, pp. 809-39.

Chen, TY & Miller, C 1996, 'Nonequilibrium gating and voltage dependence of the ClC-0 Cl- channel', *J Gen Physiol,* vol. 108, no. 4, Oct, pp. 237-50.

Christesen, HB, Brusgaard, K, Alm, J, Sjöblad, S, Hussain, K, Fenger, C, Rasmussen, L, Hovendal, C, Otonkoski, T & Jacobsen, BB 2007, 'Rapid genetic analysis in congenital hyperinsulinism', *Horm Res,* vol. 67, no. 4, pp. 184-8.

Cleiren, E, Bénichou, O, Van Hul, E, Gram, J, Bollerslev, J, Singer, FR, Beaverson, K, Aledo, A, Whyte, MP, Yoneyama, T, deVernejoul, MC & Van Hul, W 2001, 'Albers-Schönberg disease (autosomal dominant osteopetrosis, type II) results from mutations in the ClCN7 chloride channel gene', *Hum Mol Genet,* vol. 10, no. 25, Dec 1, pp. 2861-7.

Cohen, J & Schulten, K 2004, 'Mechanism of anionic conduction across ClC', *Biophys J,* vol. 86, no. 2, Feb, pp. 836-45.

Cohen, SN, Chang, AC, Boyer, HW & Helling, RB 1973, 'Construction of biologically functional bacterial plasmids in vitro', *Proc Natl Acad Sci U S A*, vol. 70, no. 11, Nov, pp. 3240-4.

Corry, B, O'Mara, M & Chung, SH 2004, 'Conduction mechanisms of chloride ions in ClC-type channels', *Biophys J*, vol. 86, no. 2, Feb, pp. 846-60.

Cuppoletti, J, Tewari, KP, Sherry, AM, Ferrante, CJ & Malinowska, DH 2004, 'Sites of protein kinase A activation of the human ClC-2 Cl(-) channel', *J Biol Chem*, vol. 279, no. 21, May 21, pp. 21849-56.

de Diego, C, Gamez, J, Plassart-Schiess, E, Lasa, A, Del Rio, E, Cervera, C, Baiget, M, Gallano, P & Fontaine, B 1999, 'Novel mutations in the muscle chloride channel CLCN1 gene causing myotonia congenita in Spanish families', *J Neurol*, vol. 246, no. 9, Sep, pp. 825-9.

Duan, D, Winter, C, Cowley, S, Hume, JR & Horowitz, B 1997, 'Molecular identification of a volume-regulated chloride channel', *Nature*, vol. 390, no. 6658, Nov 27, pp. 417-21.

Duffield, M, Rychkov, G, Bretag, A & Roberts, M 2003, 'Involvement of helices at the dimer interface in ClC-1 common gating', *J Gen Physiol*, vol. 121, no. 2, Feb, pp. 149-61.

Duffield, MD, Rychkov, GY, Bretag, AH & Roberts, ML 2005, 'Zinc inhibits human ClC-1 muscle chloride channel by interacting with its common gating mechanism', *J Physiol*, vol. 568, no. Pt 1, Oct 1, pp. 5-12.

Dutzler, R 2006, 'The ClC family of chloride channels and transporters', *Curr Opin Struct Biol*, vol. 16, no. 4, Aug, pp. 439-46.

Dutzler, R 2004, 'Structural basis for ion conduction and gating in ClC chloride channels', *FEBS Lett*, vol. 564, no. 3, Apr 30, pp. 229-33.

Dutzler, R, Campbell, EB, Cadene, M, Chait, BT & MacKinnon, R 2002, 'X-ray structure of a ClC chloride channel at 3.0 Å reveals the molecular basis of anion selectivity', *Nature*, vol. 415, no. 6869, Jan 17, pp. 287-94.

Dutzler, R, Campbell, EB & MacKinnon, R 2003, 'Gating the selectivity filter in ClC chloride channels', *Science*, vol. 300, no. 5616, Apr 4, pp. 108-12.

Eggermont, J 2004, 'Calcium-activated chloride channels: (un)known, (un)loved?', *Proc Am Thorac Soc*, vol. 1, no. 1, pp. 22-7.

Estévez, R, Boettger, T, Stein, V, Birkenhager, R, Otto, E, Hildebrandt, F & Jentsch, TJ 2001, 'Barttin is a Cl- channel beta-subunit crucial for renal Cl- reabsorption and inner ear K+ secretion', *Nature*, vol. 414, no. 6863, Nov 29, pp. 558-61.

Estévez, R & Jentsch, TJ 2002, 'CLC chloride channels: correlating structure with function', *Curr Opin Struct Biol*, vol. 12, no. 4, Aug, pp. 531-9.

Estévez, R, Pusch, M, Ferrer-Costa, C, Orozco, M & Jentsch, TJ 2004, 'Functional and structural conservation of CBS domains from CLC chloride channels', *J Physiol*, vol. 557, no. Pt 2, Jun 1, pp. 363-78.

Estévez, R, Schroeder, BC, Accardi, A, Jentsch, TJ & Pusch, M 2003, 'Conservation of chloride channel structure revealed by an inhibitor binding site in ClC-1', *Neuron,* vol. 38, no. 1, Apr 10, pp. 47-59.

Fahlke, C, Rudel, R, Mitrovic, N, Zhou, M & George, AL, Jr. 1995, 'An aspartic acid residue important for voltage-dependent gating of human muscle chloride channels', *Neuron,* vol. 15, no. 2, Aug, pp. 463-72.

Fahlke, C, Yu, HT, Beck, CL, Rhodes, TH & George, AL, Jr. 1997, 'Pore-forming segments in voltage-gated chloride channels', *Nature,* vol. 390, no. 6659, Dec 4, pp. 529-32.

Faraldo-Gomez, JD & Roux, B 2004, 'Electrostatics of ion stabilization in a ClC chloride channel homologue from Escherichia coli', *J Mol Biol,* vol. 339, no. 4, Jun 11, pp. 981-1000.

Fong, P, Rehfeldt, A & Jentsch, TJ 1998, 'Determinants of slow gating in ClC-0, the voltage-gated chloride channel of Torpedo marmorata', *Am J Physiol,* vol. 274, no. 4 Pt 1, Apr, pp. C966-73.

Fritsch, J & Edelman, A 1996, 'Modulation of the hyperpolarization-activated Cl- current in human intestinal T84 epithelial cells by phosphorylation', *J Physiol,* vol. 490 (Pt 1), Jan 1, pp. 115-28.

Fujita, N, Mori, H, Yura, T & Ishihama, A 1994, 'Systematic sequencing of the Escherichia coli genome: analysis of the 2.4-4.1 min (110,917-193,643 bp) region', *Nucleic Acids Res,* vol. 22, no. 9, May 11, pp. 1637-9.

Gadsby, DC 2004, 'Ion transport: spot the difference', *Nature,* vol. 427, no. 6977, Feb 26, pp. 795-7.

Garcia-Olivares, J, Alekov, A, Boroumand, MR, Begemann, B, Hidalgo, P & Fahlke, C 2008, 'Gating of human ClC-2 chloride channels and regulation by carboxy-terminal domains', *J Physiol,* vol. 586, no. Pt 22, Nov 15, pp. 5325-36.

Gentzsch, M, Cui, L, Mengos, A, Chang, XB, Chen, JH & Riordan, JR 2003, 'The PDZ-binding chloride channel ClC-3B localizes to the Golgi and associates with cystic fibrosis transmembrane conductance regulator-interacting PDZ proteins', *J Biol Chem,* vol. 278, no. 8, Feb 21, pp. 6440-9.

George, AL, Jr. 1998, 'Chloride channels and endocytosis: ClC-5 makes a dent', *Proc Natl Acad Sci U S A,* vol. 95, no. 14, Jul 7, pp. 7843-5.

Goldberg, AF & Miller, C 1991, 'Solubilization and functional reconstitution of a chloride channel from Torpedo californica electroplax', *J Membr Biol,* vol. 124, no. 3, Dec, pp. 199-206.

Graves, AR, Curran, PK, Smith, CL & Mindell, JA 2008, 'The Cl-/H+ antiporter ClC-7 is the primary chloride permeation pathway in lysosomes', *Nature,* vol. 453, no. 7196, Jun 5, pp. 788-92.

Greene, JR, Brown, NH, DiDomenico, BJ, Kaplan, J & Eide, DJ 1993, 'The GEF1 gene of Saccharomyces cerevisiae encodes an integral membrane protein; mutations in which have effects on respiration and iron-limited growth', *Mol Gen Genet,* vol. 241, no. 5-6, Dec, pp. 542-53.

Grunder, S, Thiemann, A, Pusch, M & Jentsch, TJ 1992, 'Regions involved in the opening of CIC-2 chloride channel by voltage and cell volume', *Nature,* vol. 360, no. 6406, Dec 24-31, pp. 759-62.

Gunther, W, Piwon, N & Jentsch, TJ 2003, 'The ClC-5 chloride channel knock-out mouse - an animal model for Dent's disease', *Pflugers Arch,* vol. 445, no. 4, Jan, pp. 456-62.

Gurnett, CA, Kahl, SD, Anderson, RD & Campbell, KP 1995, 'Absence of the skeletal muscle sarcolemma chloride channel ClC-1 in myotonic mice', *J Biol Chem,* vol. 270, no. 16, Apr 21, pp. 9035-8.

Hanke, W & Miller, C 1983, 'Single chloride channels from Torpedo electroplax. Activation by protons', *J Gen Physiol,* vol. 82, no. 1, Jul, pp. 25-45.

Hartzell, C, Putzier, I & Arreola, J 2005, 'Calcium-activated chloride channels', *Annu Rev Physiol,* vol. 67, pp. 719-58.

Haug, K, Warnstedt, M, Alekov, AK, Sander, T, Ramirez, A, Poser, B, Maljevic, S, Hebeisen, S, Kubisch, C, Rebstock, J, Horvath, S, Hallmann, K, Dullinger, JS, Rau, B, Haverkamp, F, Beyenburg, S, Schulz, H, Janz, D, Giese, B, Muller-Newen, G, Propping, P, Elger, CE, Fahlke, C, Lerche, H & Heils, A 2003, 'Mutations in CLCN2 encoding a voltage-gated chloride channel are associated with idiopathic generalized epilepsies', *Nat Genet,* vol. 33, no. 4, Apr, pp. 527-32.

He, L, Denton, J, Nehrke, K & Strange, K 2006, 'Carboxy terminus splice variation alters ClC channel gating and extracellular cysteine reactivity', *Biophys J,* vol. 90, no. 10, May 15, pp. 3570-81.

Hebeisen, S, Biela, A, Giese, B, Müller-Newen, G, Hidalgo, P & Fahlke, C 2004, 'The role of the carboxyl terminus in ClC chloride channel function', *J Biol Chem,* vol. 279, no. 13, Mar 26, pp. 13140-7.

Hebeisen, S & Fahlke, C 2005, 'Carboxy-terminal truncations modify the outer pore vestibule of muscle chloride channels', *Biophys J,* Jun 24.

Hebert, SC 2003, 'Bartter syndrome', *Curr Opin Nephrol Hypertens,* vol. 12, no. 5, Sep, pp. 527-32.

Hechenberger, M, Schwappach, B, Fischer, WN, Frommer, WB, Jentsch, TJ & Steinmeyer, K 1996, 'A family of putative chloride channels from Arabidopsis and functional complementation of a yeast strain with a CLC gene disruption', *J Biol Chem,* vol. 271, no. 52, Dec 27, pp. 33632-8.

Hille, B 2001, *Ion channels of excitable membranes,* Sinauer Associates Inc., Sunderland.

Hinzpeter, A, Lipecka, J, Brouillard, F, Baudouin-Legros, M, Dadlez, M, Edelman, A & Fritsch, J 2005, 'ASSOCIATION BETWEEN HSP90 AND THE ClC-2 CHLORIDE CHANNEL UPREGULATES CHANNEL FUNCTION', *Am J Physiol Cell Physiol,* Jul 27.

Ho, SN, Hunt, HD, Horton, RM, Pullen, JK & Pease, LR 1989, 'Site-directed mutagenesis by overlap extension using the polymerase chain reaction', *Gene,* vol. 77, no. 1, Apr 15, pp. 51-9.

Hosie, AM, Aronstein, K, Sattelle, DB & ffrench-Constant, RH 1997, 'Molecular biology of insect neuronal GABA receptors', *Trends Neurosci*, vol. 20, no. 12, Dec, pp. 578-83.

Hryciw, DH, Rychkov, GY, Hughes, BP & Bretag, AH 1998, 'Relevance of the D13 region to the function of the skeletal muscle chloride channel, ClC-1', *J Biol Chem*, vol. 273, no. 8, Feb 20, pp. 4304-7.

Hryciw, DH, Wang, Y, Devuyst, O, Pollock, CA, Poronnik, P & Guggino, WB 2003, 'Cofilin interacts with ClC-5 and regulates albumin uptake in proximal tubule cell lines', *J Biol Chem*, vol. 278, no. 41, Oct 10, pp. 40169-76.

Hunte, C, Screpanti, E, Venturi, M, Rimon, A, Padan, E & Michel, H 2005, 'Structure of a Na+/H+ antiporter and insights into mechanism of action and regulation by pH', *Nature*, vol. 435, no. 7046, Jun 30, pp. 1197-202.

Igarashi, T, Gunther, W, Sekine, T, Inatomi, J, Shiraga, H, Takahashi, S, Suzuki, J, Tsuru, N, Yanagihara, T, Shimazu, M, Jentsch, TJ & Thakker, RV 1998, 'Functional characterization of renal chloride channel, CLCN5, mutations associated with Dent'sJapan disease', *Kidney Int*, vol. 54, no. 6, Dec, pp. 1850-6.

Ignoul, S & Eggermont, J 2005, 'CBS domains: structure, function, and pathology in human proteins', *Am J Physiol Cell Physiol*, vol. 289, no. 6, Dec, pp. C1369-78.

Jentsch, TJ, Friedrich, T, Schriever, A & Yamada, H 1999, 'The CLC chloride channel family', *Pflugers Arch*, vol. 437, no. 6, May, pp. 783-95.

Jentsch, TJ, Poet, M, Fuhrmann, JC & Zdebik, AA 2005, 'Physiological functions of ClC Cl^- channel gleaned from human genetic disease and mouse models', *Annu Rev Physiol*, vol. 67, pp. 779-807.

Jentsch, TJ, Steinmeyer, K & Schwarz, G 1990, 'Primary structure of Torpedo marmorata chloride channel isolated by expression cloning in Xenopus oocytes', *Nature*, vol. 348, no. 6301, Dec 6, pp. 510-4.

Jhee, KH, McPhie, P & Miles, EW 2000, 'Domain architecture of the heme-independent yeast cystathionine beta-synthase provides insights into mechanisms of catalysis and regulation', *Biochemistry*, vol. 39, no. 34, Aug 29, pp. 10548-56.

Jordt, SE & Jentsch, TJ 1997, 'Molecular dissection of gating in the ClC-2 chloride channel', *Embo J*, vol. 16, no. 7, Apr 1, pp. 1582-92.

Jordt, SE, McKemy, DD & Julius, D 2003, 'Lessons from peppers and peppermint: the molecular logic of thermosensation', *Curr Opin Neurobiol*, vol. 13, no. 4, Aug, pp. 487-92.

Kajita, H, Whitwell, C & Brown, PD 2000, 'Properties of the inward-rectifying Cl- channel in rat choroid plexus: regulation by intracellular messengers and inhibition by divalent cations', *Pflugers Arch*, vol. 440, no. 6, Oct, pp. 933-40.

Kasper, D, Planells-Cases, R, Fuhrmann, JC, Scheel, O, Zeitz, O, Ruether, K, Schmitt, A, Poet, M, Steinfeld, R, Schweizer, M, Kornak, U & Jentsch, TJ 2005, 'Loss of the chloride channel ClC-7 leads to lysosomal storage disease and neurodegeneration', *EMBO J*, vol. 24, no. 5, Mar 9, pp. 1079-91.

Kawasaki, M, Uchida, S, Monkawa, T, Miyawaki, A, Mikoshiba, K, Marumo, F & Sasaki, S 1994, 'Cloning and expression of a protein kinase C-regulated chloride channel abundantly expressed in rat brain neuronal cells', *Neuron*, vol. 12, no. 3, Mar, pp. 597-604.

Kennan, A, Aherne, A, Palfi, A, Humphries, M, McKee, A, Stitt, A, Simpson, DA, Demtroder, K, Orntoft, T, Ayuso, C, Kenna, PF, Farrar, GJ & Humphries, P 2002, 'Identification of an IMPDH1 mutation in autosomal dominant retinitis pigmentosa (RP10) revealed following comparative microarray analysis of transcripts derived from retinas of wild-type and Rho(-/-) mice', *Hum Mol Genet*, vol. 11, no. 5, Mar 1, pp. 547-57.

Kieferle, S, Fong, P, Bens, M, Vandewalle, A & Jentsch, TJ 1994, 'Two highly homologous members of the ClC chloride channel family in both rat and human kidney', *Proc Natl Acad Sci U S A*, vol. 91, no. 15, Jul 19, pp. 6943-7.

Kim, JH, Lee-Kwon, W, Park, JB, Ryu, SH, Yun, CH & Donowitz, M 2002, 'Ca(2+)-dependent inhibition of Na+/H+ exchanger 3 (NHE3) requires an NHE3-E3KARP-alpha-actinin-4 complex for oligomerization and endocytosis', *J Biol Chem*, vol. 277, no. 26, Jun 28, pp. 23714-24.

Kluijtmans, LA, Boers, GH, Stevens, EM, Renier, WO, Kraus, JP, Trijbels, FJ, van den Heuvel, LP & Blom, HJ 1996, 'Defective cystathionine beta-synthase regulation by S-adenosylmethionine in a partially pyridoxine responsive homocystinuria patient', *J Clin Invest*, vol. 98, no. 2, Jul 15, pp. 285-9.

Koch, MC, Ricker, K, Otto, M, Wolf, F, Zoll, B, Lorenz, C, Steinmeyer, K & Jentsch, TJ 1993, 'Evidence for genetic homogeneity in autosomal recessive generalised myotonia (Becker)', *J Med Genet*, vol. 30, no. 11, Nov, pp. 914-7.

Koch, MC, Steinmeyer, K, Lorenz, C, Ricker, K, Wolf, F, Otto, M, Zoll, B, Lehmann-Horn, F, Grzeschik, KH & Jentsch, TJ 1992, 'The skeletal muscle chloride channel in dominant and recessive human myotonia', *Science*, vol. 257, no. 5071, Aug 7, pp. 797-800.

Konrad, M, Vollmer, M, Lemmink, HH, van den Heuvel, LP, Jeck, N, Vargas-Poussou, R, Lakings, A, Ruf, R, Deschenes, G, Antignac, C, Guay-Woodford, L, Knoers, NV, Seyberth, HW, Feldmann, D & Hildebrandt, F 2000, 'Mutations in the chloride channel gene CLCNKB as a cause of classic Bartter syndrome', *J Am Soc Nephrol*, vol. 11, no. 8, Aug, pp. 1449-59.

Kornak, U, Kasper, D, Bosl, MR, Kaiser, E, Schweizer, M, Schulz, A, Friedrich, W, Delling, G & Jentsch, TJ 2001, 'Loss of the ClC-7 chloride channel leads to osteopetrosis in mice and man', *Cell*, vol. 104, no. 2, Jan 26, pp. 205-15.

Kubisch, C, Schmidt-Rose, T, Fontaine, B, Bretag, AH & Jentsch, TJ 1998, 'ClC-1 chloride channel mutations in myotonia congenita: variable penetrance of mutations shifting the voltage dependence', *Hum Mol Genet*, vol. 7, no. 11, Oct, pp. 1753-60.

Kurashima, K, Szabo, EZ, Lukacs, G, Orlowski, J & Grinstein, S 1998, 'Endosomal recycling of the Na+/H+ exchanger NHE3 isoform is regulated by the phosphatidylinositol 3-kinase pathway', *J Biol Chem*, vol. 273, no. 33, Aug 14, pp. 20828-36.

Kurz, LL, Klink, H, Jakob, I, Kuchenbecker, M, Benz, S, Lehmann-Horn, F & Rudel, R 1999, 'Identification of three cysteines as targets for the Zn2+ blockade of the human skeletal muscle chloride channel', *J Biol Chem*, vol. 274, no. 17, Apr 23, pp. 11687-92.

Laemmli, UK 1970, 'Cleavage of structural proteins during the assembly of the head of bacteriophage T4', *Nature,* vol. 227, no. 5259, Aug 15, pp. 680-5.

Landry, D, Sullivan, S, Nicolaides, M, Redhead, C, Edelman, A, Field, M, al-Awqati, Q & Edwards, J 1993, 'Molecular cloning and characterization of p64, a chloride channel protein from kidney microsomes', *J Biol Chem,* vol. 268, no. 20, Jul 15, pp. 14948-55.

Lange, PF, Wartosch, L, Jentsch, TJ & Fuhrmann, JC 2006, 'ClC-7 requires Ostm1 as a beta-subunit to support bone resorption and lysosomal function', *Nature,* vol. 440, no. 7081, Mar 9, pp. 220-3.

Lewarchik, CM, Peters, KW, Qi, J & Frizzell, RA 2008, 'Regulation of CFTR Trafficking by Its R Domain', *J Biol Chem,* vol. 283, no. 42, Oct 17, pp. 28401-12.

Lin, YW, Lin, CW & Chen, TY 1999, 'Elimination of the slow gating of ClC-0 chloride channel by a point mutation', *J Gen Physiol,* vol. 114, no. 1, Jul, pp. 1-12.

Lloyd, SE, Gunther, W, Pearce, SH, Thomson, A, Bianchi, ML, Bosio, M, Craig, IW, Fisher, SE, Scheinman, SJ, Wrong, O, Jentsch, TJ & Thakker, RV 1997, 'Characterisation of renal chloride channel, CLCN5, mutations in hypercalciuric nephrolithiasis (kidney stones) disorders', *Hum Mol Genet,* vol. 6, no. 8, Aug, pp. 1233-9.

Lloyd, SE, Pearce, SH, Fisher, SE, Steinmeyer, K, Schwappach, B, Scheinman, SJ, Harding, B, Bolino, A, Devoto, M, Goodyer, P, Rigden, SP, Wrong, O, Jentsch, TJ, Craig, IW & Thakker, RV 1996, 'A common molecular basis for three inherited kidney stone diseases', *Nature,* vol. 379, no. 6564, Feb 1, pp. 445-9.

Lobet, S & Dutzler, R 2006, 'Ion-binding properties of the ClC chloride selectivity filter', *Embo J,* vol. 25, no. 1, Jan 11, pp. 24-33.

Lourdel, S, Paulais, M, Marvao, P, Nissant, A & Teulon, J 2003, 'A chloride channel at the basolateral membrane of the distal-convoluted tubule: a candidate ClC-K channel', *J Gen Physiol,* vol. 121, no. 4, Apr, pp. 287-300.

Ludewig, U, Jentsch, TJ & Pusch, M 1997, 'Analysis of a protein region involved in permeation and gating of the voltage-gated Torpedo chloride channel ClC-0', *J Physiol,* vol. 498 (Pt 3), Feb 1, pp. 691-702.

Ludewig, U, Pusch, M & Jentsch, TJ 1997, 'Independent gating of single pores in CLC-0 chloride channels', *Biophys J,* vol. 73, no. 2, Aug, pp. 789-97.

Ludewig, U, Pusch, M & Jentsch, TJ 1996, 'Two physically distinct pores in the dimeric ClC-0 chloride channel', *Nature,* vol. 383, no. 6598, Sep 26, pp. 340-3.

Ma, L, Rychkov, GY, Hughes, BP & Bretag, AH 2008, 'Analysis of carboxyl tail function in the skeletal muscle Cl(-) channel hClC-1', *Biochem J,* vol. 413, no. 1, Jul 1, pp. 61-9.

Macías, MJ, Teijido, O, Zifarelli, G, Martin, P, Ramirez-Espain, X, Zorzano, A, Palacín, M, Pusch, M & Estévez, R 2007, 'Myotonia-related mutations in the distal C-terminus of ClC-1 and ClC-0 chloride channels affect the structure of a poly-proline helix', *Biochem J,* vol. 403, no. 1, Apr 1, pp. 79-87.

Macías, MJ, Teijido, O, Zifarelli, G, Martin, P, Ramirez-Espain, X, Zorzano, A, Palacín, M, Pusch, M & Estévez, R 2006, 'Myotonia-related mutations in the distal C-terminus of ClC-1 and ClC-0 chloride channels affect the structure of a poly-proline helix', *Biochem J*, Nov 15.

Maduke, M, Pheasant, DJ & Miller, C 1999, 'High-level expression, functional reconstitution, and quaternary structure of a prokaryotic ClC-type chloride channel', *J Gen Physiol*, vol. 114, no. 5, Nov, pp. 713-22.

Maduke, M, Williams, C & Miller, C 1998, 'Formation of CLC-0 chloride channels from separated transmembrane and cytoplasmic domains', *Biochemistry*, vol. 37, no. 5, Feb 3, pp. 1315-21.

Markovic, S & Dutzler, R 2007, 'The structure of the cytoplasmic domain of the chloride channel ClC-Ka reveals a conserved interaction interface', *Structure*, vol. 15, no. 6, Jun, pp. 715-25.

Masia, R, Caputa, G & Nichols, CG 2007, 'Regulation of KATP channel expression and activity by the SUR1 nucleotide binding fold 1', *Channels (Austin)*, vol. 1, no. 4, Jul-Aug, pp. 315-23.

Meyer, S & Dutzler, R 2006, 'Crystal Structure of the Cytoplasmic Domain of the Chloride Channel ClC-0', *Structure*, vol. 14, no. 2, Feb, pp. 299-307.

Meyer, S, Savaresi, S, Forster, IC & Dutzler, R 2007, 'Nucleotide recognition by the cytoplasmic domain of the human chloride transporter ClC-5', *Nat Struct Mol Biol*, vol. 14, no. 1, Jan, pp. 60-7.

Michel, P, Sternberg, D, Jeannet, PY, Dunand, M, Thonney, F, Kress, W, Fontaine, B, Fournier, E & Kuntzer, T 2007, 'Comparative efficacy of repetitive nerve stimulation, exercise, and cold in differentiating myotonic disorders', *Muscle Nerve*, vol. 36, no. 5, Nov, pp. 643-50.

Middleton, RE, Pheasant, DJ & Miller, C 1994, 'Purification, reconstitution, and subunit composition of a voltage-gated chloride channel from Torpedo electroplax', *Biochemistry*, vol. 33, no. 45, Nov 15, pp. 13189-98.

Miller, C 1982, 'Open-state substructure of single chloride channels from Torpedo electroplax', *Philos Trans R Soc Lond B Biol Sci*, vol. 299, no. 1097, Dec 1, pp. 401-11.

Miller, C & White, MM 1984, 'Dimeric structure of single chloride channels from Torpedo electroplax', *Proc Natl Acad Sci U S A*, vol. 81, no. 9, May, pp. 2772-5.

Miller, MD, Schwarzenbacher, R, von Delft, F, Abdubek, P, Ambing, E, Biorac, T, Brinen, LS, Canaves, JM, Cambell, J, Chiu, HJ, Dai, X, Deacon, AM, DiDonato, M, Elsliger, MA, Eshagi, S, Floyd, R, Godzik, A, Grittini, C, Grzechnik, SK, Hampton, E, Jaroszewski, L, Karlak, C, Klock, HE, Koesema, E, Kovarik, JS, Kreusch, A, Kuhn, P, Lesley, SA, Levin, I, McMullan, D, McPhillips, TM, Morse, A, Moy, K, Ouyang, J, Page, R, Quijano, K, Robb, A, Spraggon, G, Stevens, RC, van den Bedem, H, Velasquez, J, Vincent, J, Wang, X, West, B, Wolf, G, Xu, Q, Hodgson, KO, Wooley, J & Wilson, IA 2004, 'Crystal structure of a tandem cystathionine-beta-synthase (CBS) domain protein (TM0935) from Thermotoga maritima at 1.87 A resolution', *Proteins*, vol. 57, no. 1, Oct 1, pp. 213-7.

Miloshevsky, GV & Jordan, PC 2004, 'Anion pathway and potential energy profiles along curvilinear bacterial ClC Cl- pores: electrostatic effects of charged residues', *Biophys J,* vol. 86, no. 2, Feb, pp. 825-35.

Mindell, JA, Maduke, M, Miller, C & Grigorieff, N 2001, 'Projection structure of a ClC-type chloride channel at 6.5 A resolution', *Nature,* vol. 409, no. 6817, Jan 11, pp. 219-23.

Mo, L, Xiong, W, Qian, T, Sun, H & Wills, NK 2004, 'Coexpression of complementary fragments of ClC-5 and restoration of chloride channel function in a Dent's disease mutation', *Am J Physiol Cell Physiol,* vol. 286, no. 1, Jan, pp. C79-89.

Mohammad-Panah, R, Harrison, R, Dhani, S, Ackerley, C, Huan, LJ, Wang, Y & Bear, CE 2003, 'The chloride channel ClC-4 contributes to endosomal acidification and trafficking', *J Biol Chem,* vol. 278, no. 31, Aug 1, pp. 29267-77.

Morais-Cabral, JH, Zhou, Y & MacKinnon, R 2001, 'Energetic optimization of ion conduction rate by the K+ selectivity filter', *Nature,* vol. 414, no. 6859, Nov 1, pp. 37-42.

Moran, O, Traverso, S, Elia, L & Pusch, M 2003, 'Molecular modeling of p-chlorophenoxyacetic acid binding to the CLC-0 channel', *Biochemistry,* vol. 42, no. 18, May 13, pp. 5176-85.

Naren, AP, Cobb, B, Li, C, Roy, K, Nelson, D, Heda, GD, Liao, J, Kirk, KL, Sorscher, EJ, Hanrahan, J & Clancy, JP 2003, 'A macromolecular complex of beta 2 adrenergic receptor, CFTR, and ezrin/radixin/moesin-binding phosphoprotein 50 is regulated by PKA', *Proc Natl Acad Sci U S A,* vol. 100, no. 1, Jan 7, pp. 342-6.

Nelson, M & McClelland, M 1992, 'Use of DNA methyltransferase/endonuclease enzyme combinations for megabase mapping of chromosomes', *Methods Enzymol,* vol. 216, pp. 279-303.

Niemeyer, MI, Cid, LP, Yusef, YR, Briones, R & Sepulveda, FV 2009, 'Voltage-dependent and -independent titration of specific residues accounts for complex gating of a ClC chloride channel by extracellular protons', *J Physiol,* vol. 587, no. Pt 7, Apr 1, pp. 1387-400.

Niemeyer, MI, Cid, LP, Zuniga, L, Catalan, M & Sepulveda, FV 2003, 'A conserved pore-lining glutamate as a voltage- and chloride-dependent gate in the ClC-2 chloride channel', *J Physiol,* vol. 553, no. Pt 3, Dec 15, pp. 873-9.

Nilius, B & Droogmans, G 2003, 'Amazing chloride channels: an overview', *Acta Physiol Scand,* vol. 177, no. 2, Feb, pp. 119-47.

Nissant, A, Paulais, M, Lachheb, S, Lourdel, S & Teulon, J 2006, 'Similar chloride channels in the connecting tubule and cortical collecting duct of the mouse kidney', *Am J Physiol Renal Physiol,* vol. 290, no. 6, Jun, pp. F1421-9.

Osteen, JD & Mindell, JA 2008, 'Insights into the ClC-4 transport mechanism from studies of Zn2+ inhibition', *Biophys J,* vol. 95, no. 10, Nov 15, pp. 4668-75.

Picollo, A & Pusch, M 2005, 'Chloride/proton antiporter activity of mammalian CLC proteins ClC-4 and ClC-5', *Nature,* vol. 436, no. 7049, Jul 21, pp. 420-3.

Piwon, N, Gunther, W, Schwake, M, Bosl, MR & Jentsch, TJ 2000, 'ClC-5 Cl- -channel disruption impairs endocytosis in a mouse model for Dent's disease', *Nature,* vol. 408, no. 6810, Nov 16, pp. 369-73.

Pöet, M, Kornak, U, Schweizer, M, Zdebik, AA, Scheel, O, Hoelter, S, Wurst, W, Schmitt, A, Fuhrmann, JC, Planells-Cases, R, Mole, SE, Hubner, CA & Jentsch, TJ 2006, 'Lysosomal storage disease upon disruption of the neuronal chloride transport protein ClC-6', *Proc Natl Acad Sci U S A,* vol. 103, no. 37, Sep 12, pp. 13854-9.

Pusch, M 2002, 'Myotonia caused by mutations in the muscle chloride channel gene *CLCN1*', *Hum Mutat,* vol. 19, no. 4, Apr, pp. 423-34.

Pusch, M, Accardi, A, Liantonio, A, Ferrera, L, De Luca, A, Camerino, DC & Conti, F 2001, 'Mechanism of block of single protopores of the Torpedo chloride channel ClC-0 by 2-(p-chlorophenoxy)butyric acid (CPB)', *J Gen Physiol,* vol. 118, no. 1, Jul, pp. 45-62.

Pusch, M & Jentsch, TJ 1994, 'Molecular physiology of voltage-gated chloride channels', *Physiol Rev,* vol. 74, no. 4, Oct, pp. 813-27.

Pusch, M & Jentsch, TJ 2005, 'Unique structure and function of chloride transporting CLC proteins', *IEEE Trans Nanobioscience,* vol. 4, no. 1, Mar, pp. 49-57.

Pusch, M, Jordt, SE, Stein, V & Jentsch, TJ 1999, 'Chloride dependence of hyperpolarization-activated chloride channel gates', *J Physiol,* vol. 515 (Pt 2), Mar 1, pp. 341-53.

Pusch, M, Ludewig, U & Jentsch, TJ 1997, 'Temperature dependence of fast and slow gating relaxations of ClC-0 chloride channels', *J Gen Physiol,* vol. 109, no. 1, Jan, pp. 105-16.

Pusch, M, Ludewig, U, Rehfeldt, A & Jentsch, TJ 1995, 'Gating of the voltage-dependent chloride channel CIC-0 by the permeant anion', *Nature,* vol. 373, no. 6514, Feb 9, pp. 527-31.

Pusch, M, Steinmeyer, K & Jentsch, TJ 1994, 'Low single channel conductance of the major skeletal muscle chloride channel, ClC-1', *Biophys J,* vol. 66, no. 1, Jan, pp. 149-52.

Rai, T, Uchida, S, Sasaki, S & Marumo, F 1999, 'Isolation and characterization of kidney-specific CLC-K2 chloride channel gene promoter', *Biochem Biophys Res Commun,* vol. 261, no. 2, Aug 2, pp. 432-8.

Rickard, HR, Bartley, P.A., Bagley, C.J. and Bretag, A.H. 2005, 'The CLC family of proteins: chloride transporters and channels. ', in *Bacteiral Ion Channels and their Eukaryotic Homologs*, ed. AaM Kubalski, B., eds., ASM Press, Washington.

Rudolph, MJ, Amodeo, GA, Iram, SH, Hong, SP, Pirino, G, Carlson, M & Tong, L 2007, 'Structure of the Bateman2 domain of yeast Snf4: dimeric association and relevance for AMP binding', *Structure,* vol. 15, no. 1, Jan, pp. 65-74.

Rüdel, R & Lehmann-Horn, F 1985, 'Membrane changes in cells from myotonia patients', *Physiol Rev,* vol. 65, no. 2, Apr, pp. 310-56.

Rutledge, E, Denton, J & Strange, K 2002, 'Cell cycle- and swelling-induced activation of a Caenorhabditis elegans ClC channel is mediated by CeGLC-7alpha/beta phosphatases', *J Cell Biol,* vol. 158, no. 3, Aug 5, pp. 435-44.

Rychkov, GY, Pusch, M, Astill, DS, Roberts, ML, Jentsch, TJ & Bretag, AH 1996a, 'Concentration and pH dependence of skeletal muscle chloride channel ClC-1', *J Physiol*, vol. 497 (Pt 2), Dec 1, pp. 423-35.

Rychkov, GY, Pusch, M, Astill, DS, Roberts, ML, Jentsch, TJ & Bretag, AH 1996b, 'Concentration and pH dependence of skeletal muscle chloride channel ClC-1', *J Physiol*, vol. 497 (Pt 2), Dec 1, pp. 423-35.

Rychkov, GY, Pusch, M, Roberts, ML & Bretag, AH 2001, 'Interaction of hydrophobic anions with the rat skeletal muscle chloride channel ClC-1: effects on permeation and gating', *J Physiol*, vol. 530, no. Pt 3, Feb 1, pp. 379-93.

Rychkov, GY, Pusch, M, Roberts, ML, Jentsch, TJ & Bretag, AH 1998, 'Permeation and block of the skeletal muscle chloride channel, ClC-1, by foreign anions', *J Gen Physiol*, vol. 111, no. 5, May, pp. 653-65.

Sagen, JV, Raeder, H, Hathout, E, Shehadeh, N, Gudmundsson, K, Baevre, H, Abuelo, D, Phornphutkul, C, Molnes, J, Bell, GI, Gloyn, AL, Hattersley, AT, Molven, A, Sovik, O & Njolstad, PR 2004, 'Permanent neonatal diabetes due to mutations in KCNJ11 encoding Kir6.2: patient characteristics and initial response to sulfonylurea therapy', *Diabetes*, vol. 53, no. 10, Oct, pp. 2713-8.

Salas-Casas, A, Ponce-Balderas, A, Garcia-Perez, RM, Cortes-Reynosa, P, Gamba, G, Orozco, E & Rodriguez, MA 2006, 'Identification and functional characterization of EhClC-A, an Entamoeba histolytica ClC chloride channel located at plasma membrane', *Mol Microbiol*, vol. 59, no. 4, Feb, pp. 1249-61.

Sambrook, J & Gething, MJ 1989, 'Protein structure. Chaperones, paperones', *Nature*, vol. 342, no. 6247, Nov 16, pp. 224-5.

Sauve, R, Cai, S, Garneau, L, Klein, H & Parent, L 2000, 'pH and external Ca(2+) regulation of a small conductance Cl(-) channel in kidney distal tubule', *Biochim Biophys Acta*, vol. 1509, no. 1-2, Dec 20, pp. 73-85.

Saviane, C, Conti, F & Pusch, M 1999, 'The muscle chloride channel ClC-1 has a double-barreled appearance that is differentially affected in dominant and recessive myotonia', *J Gen Physiol*, vol. 113, no. 3, Mar, pp. 457-68.

Scheel, O, Zdebik, AA, Lourdel, S & Jentsch, TJ 2005, 'Voltage-dependent electrogenic chloride/proton exchange by endosomal CLC proteins', *Nature*, vol. 436, no. 7049, Jul 21, pp. 424-7.

Schlingmann, KP, Konrad, M, Jeck, N, Waldegger, P, Reinalter, SC, Holder, M, Seyberth, HW & Waldegger, S 2004, 'Salt wasting and deafness resulting from mutations in two chloride channels', *N Engl J Med*, vol. 350, no. 13, Mar 25, pp. 1314-9.

Schmidt-Rose, T & Jentsch, TJ 1997a, 'Reconstitution of functional voltage-gated chloride channels from complementary fragments of CLC-1', *J Biol Chem*, vol. 272, no. 33, Aug 15, pp. 20515-21.

Schmidt-Rose, T & Jentsch, TJ 1997b, 'Transmembrane topology of a CLC chloride channel', *Proc Natl Acad Sci U S A*, vol. 94, no. 14, Jul 8, pp. 7633-8.

Schwappach, B, Stobrawa, S, Hechenberger, M, Steinmeyer, K & Jentsch, TJ 1998, 'Golgi localization and functionally important domains in the NH2 and COOH terminus of the yeast CLC putative chloride channel Gef1p', *J Biol Chem,* vol. 273, no. 24, Jun 12, pp. 15110-8.

Scott, JW, Hawley, SA, Green, KA, Anis, M, Stewart, G, Scullion, GA, Norman, DG & Hardie, DG 2004, 'CBS domains form energy-sensing modules whose binding of adenosine ligands is disrupted by disease mutations', *J Clin Invest,* vol. 113, no. 2, Jan, pp. 274-84.

Seibert, FS, Loo, TW, Clarke, DM & Riordan, JR 1997, 'Cystic fibrosis: channel, catalytic, and folding properties of the CFTR protein', *J Bioenerg Biomembr,* vol. 29, no. 5, Oct, pp. 429-42.

Shan, X, Dunbrack, RL, Jr., Christopher, SA & Kruger, WD 2001, 'Mutations in the regulatory domain of cystathionine beta synthase can functionally suppress patient-derived mutations in cis', *Hum Mol Genet,* vol. 10, no. 6, Mar 15, pp. 635-43.

Simon, DB, Bindra, RS, Mansfield, TA, Nelson-Williams, C, Mendonca, E, Stone, R, Schurman, S, Nayir, A, Alpay, H, Bakkaloglu, A, Rodriguez-Soriano, J, Morales, JM, Sanjad, SA, Taylor, CM, Pilz, D, Brem, A, Trachtman, H, Griswold, W, Richard, GA, John, E & Lifton, RP 1997, 'Mutations in the chloride channel gene, CLCNKB, cause Bartter's syndrome type III', *Nat Genet,* vol. 17, no. 2, Oct, pp. 171-8.

Simon, DB, Karet, FE, Hamdan, JM, DiPietro, A, Sanjad, SA & Lifton, RP 1996, 'Bartter's syndrome, hypokalaemic alkalosis with hypercalciuria, is caused by mutations in the Na-K-2Cl cotransporter NKCC2', *Nat Genet,* vol. 13, no. 2, Jun, pp. 183-8.

Simpson, BJ, Height, TA, Rychkov, GY, Nowak, KJ, Laing, NG, Hughes, BP & Bretag, AH 2004, 'Characterization of three myotonia-associated mutations of the *CLCN1* chloride channel gene via heterologous expression', *Hum Mutat,* vol. 24, no. 2, Aug, p. 185.

Sintchak, MD, Fleming, MA, Futer, O, Raybuck, SA, Chambers, SP, Caron, PR, Murcko, MA & Wilson, KP 1996, 'Structure and mechanism of inosine monophosphate dehydrogenase in complex with the immunosuppressant mycophenolic acid', *Cell,* vol. 85, no. 6, Jun 14, pp. 921-30.

Sivaprasadarao, A, Taneja, TK, Mankouri, J & Smith, AJ 2007, 'Trafficking of ATP-sensitive potassium channels in health and disease', *Biochem Soc Trans,* vol. 35, no. Pt 5, Nov, pp. 1055-9.

Staub, O, Gautschi, I, Ishikawa, T, Breitschopf, K, Ciechanover, A, Schild, L & Rotin, D 1997, 'Regulation of stability and function of the epithelial Na+ channel (ENaC) by ubiquitination', *Embo J,* vol. 16, no. 21, Nov 3, pp. 6325-36.

Steinmeyer, K, Ortland, C & Jentsch, TJ 1991, 'Primary structure and functional expression of a developmentally regulated skeletal muscle chloride channel', *Nature,* vol. 354, no. 6351, Nov 28, pp. 301-4.

Stobrawa, SM, Breiderhoff, T, Takamori, S, Engel, D, Schweizer, M, Zdebik, AA, Bosl, MR, Ruether, K, Jahn, H, Draguhn, A, Jahn, R & Jentsch, TJ 2001, 'Disruption of ClC-3, a chloride channel expressed on synaptic vesicles, leads to a loss of the hippocampus', *Neuron,* vol. 29, no. 1, Jan, pp. 185-96.

Thiemann, A, Grunder, S, Pusch, M & Jentsch, TJ 1992, 'A chloride channel widely expressed in epithelial and non-epithelial cells', *Nature,* vol. 356, no. 6364, Mar 5, pp. 57-60.

Thomsen, J 1876, 'Tonische Krämpfe in willkürlich beweglichen Muskeln in Folge von ererbter psychischer Disposition', *Arch Psychiatr Nervenkr,* vol. 6, pp. 702-718.

Townley, R & Shapiro, L 2007, 'Crystal structures of the adenylate sensor from fission yeast AMP-activated protein kinase', *Science,* vol. 315, no. 5819, Mar 23, pp. 1726-9.

Traverso, S, Elia, L & Pusch, M 2003, 'Gating competence of constitutively open CLC-0 mutants revealed by the interaction with a small organic Inhibitor', *J Gen Physiol,* vol. 122, no. 3, Sep, pp. 295-306.

Traverso, S, Zifarelli, G, Aiello, R & Pusch, M 2006, 'Proton sensing of CLC-0 mutant E166D', *J Gen Physiol,* vol. 127, no. 1, Jan, pp. 51-65.

Tseng, PY, Bennetts, B & Chen, TY 2007, 'Cytoplasmic ATP inhibition of CLC-1 is enhanced by low pH', *J Gen Physiol,* vol. 130, no. 2, Aug, pp. 217-21.

Wächter, A & Schwappach, B 2005, 'The yeast CLC chloride channel is proteolytically processed by the furin-like protease Kex2p in the first extracellular loop', *FEBS Lett,* vol. 579, no. 5, Feb 14, pp. 1149-53.

Weinman, EJ, Minkoff, C & Shenolikar, S 2000, 'Signal complex regulation of renal transport proteins: NHERF and regulation of NHE3 by PKA', *Am J Physiol Renal Physiol,* vol. 279, no. 3, Sep, pp. F393-9.

Weinreich, F & Jentsch, TJ 2001, 'Pores formed by single subunits in mixed dimers of different CLC chloride channels', *J Biol Chem,* vol. 276, no. 4, Jan 26, pp. 2347-53.

Weylandt, KH, Valverde, MA, Nobles, M, Raguz, S, Amey, JS, Diaz, M, Nastrucci, C, Higgins, CF & Sardini, A 2001, 'Human ClC-3 is not the swelling-activated chloride channel involved in cell volume regulation', *J Biol Chem,* vol. 276, no. 20, May 18, pp. 17461-7.

White, MM & Miller, C 1979, 'A voltage-gated anion channel from the electric organ of Torpedo californica', *J Biol Chem,* vol. 254, no. 20, Oct 25, pp. 10161-6.

Wollnik, B, Kubisch, C, Steinmeyer, K & Pusch, M 1997, 'Identification of functionally important regions of the muscular chloride channel ClC-1 by analysis of recessive and dominant myotonic mutations', *Hum Mol Genet,* vol. 6, no. 5, May, pp. 805-11.

Wu, W, Rychkov, GY, Hughes, BP & Bretag, AH 2006, 'Functional complementation of truncated human skeletal-muscle chloride channel (hClC-1) using carboxyl tail fragments', *Biochem J,* vol. 395, no. 1, Apr 1, pp. 89-97.

Yamashita, A, Singh, SK, Kawate, T, Jin, Y & Gouaux, E 2005, 'Crystal structure of a bacterial homologue of Na+/Cl--dependent neurotransmitter transporters', *Nature,* vol. 437, no. 7056, Sep 8, pp. 215-23.

Yin, J, Kuang, Z, Mahankali, U & Beck, TL 2004, 'Ion transit pathways and gating in ClC chloride channels', *Proteins,* vol. 57, no. 2, Nov 1, pp. 414-21.

Yusef, YR, Zúñiga, L, Catalán, M, Niemeyer, MI, Cid, LP & Sepúlveda, FV 2006, 'Removal of gating in voltage-dependent ClC-2 chloride channel by point mutations affecting the pore and C-terminus CBS-2 domain', *J Physiol*, vol. 572, no. Pt 1, Apr 1, pp. 173-81.

Zal, T 2008, 'Visualization of protein interactions in living cells', *Adv Exp Med Biol*, vol. 640, pp. 183-97.

Zhang, J, Bendahhou, S, Sanguinetti, MC & Ptacek, LJ 2000, 'Functional consequences of chloride channel gene (CLCN1) mutations causing myotonia congenita', *Neurology*, vol. 54, no. 4, Feb 22, pp. 937-42.

Zhang, R, Evans, G, Rotella, FJ, Westbrook, EM, Beno, D, Huberman, E, Joachimiak, A & Collart, FR 1999, 'Characteristics and crystal structure of bacterial inosine-5'-monophosphate dehydrogenase', *Biochemistry*, vol. 38, no. 15, Apr 13, pp. 4691-700.

Zhang, XD, Tseng, PY & Chen, TY 2008, 'ATP inhibition of CLC-1 is controlled by oxidation and reduction', *J Gen Physiol*, vol. 132, no. 4, Oct, pp. 421-8.

Zheng, J, Trudeau, MC & Zagotta, WN 2002, 'Rod cyclic nucleotide-gated channels have a stoichiometry of three CNGA1 subunits and one CNGB1 subunit', *Neuron*, vol. 36, no. 5, Dec 5, pp. 891-6.

Zheng, L, Kostrewa, D, Berneche, S, Winkler, FK & Li, XD 2004, 'The mechanism of ammonia transport based on the crystal structure of AmtB of Escherichia coli', *Proc Natl Acad Sci U S A*, vol. 101, no. 49, Dec 7, pp. 17090-5.

Zhorov, BS & Tikhonov, DB 2004, 'Potassium, sodium, calcium and glutamate-gated channels: pore architecture and ligand action', *J Neurochem*, vol. 88, no. 4, Feb, pp. 782-99.

Zhou, Y & MacKinnon, R 2003, 'The occupancy of ions in the K+ selectivity filter: charge balance and coupling of ion binding to a protein conformational change underlie high conduction rates', *J Mol Biol*, vol. 333, no. 5, Nov 7, pp. 965-75.

Zifarelli, G & Pusch, M 2008, 'The muscle chloride channel ClC-1 is not directly regulated by intracellular ATP', *J Gen Physiol*, vol. 131, no. 2, Feb, pp. 109-16.

Zuniga, L, Niemeyer, MI, Varela, D, Catalan, M, Cid, LP & Sepulveda, FV 2004, 'The voltage-dependent ClC-2 chloride channel has a dual gating mechanism', *J Physiol*, vol. 555, no. Pt 3, Mar 16, pp. 671-82.

APPENDIX A:

SEQUENCES OF PRIMERS

All primers are written in the 5' to 3' direction. All primers were designed using Primer Premier 5.0 and were purchased from Sigma Genosys, Australia.

Table A-1 Primers for amplifying full-length hClC-1 or hClC-1 fragments

Designation	Sequence 5' to 3'
hClC-1-Fw (EcoRI)	TT CCG GAA TTC ACC ATG GAG CAA TCC CGG TCA CAG
hClC-1-Rev (XbaI)	GC TCT AGA CTA TCA AAG GAT CAG TTC ATC CTC
N658-Rev (Not I)	ATA AGA ATG CGG CCG CTA TCA CTG CAG TTC CGA CCG CTC C
N720-Fw (BamHI)	CGC GGA TCC ATG GAT TAT AAA GAT GAT GAT GAT AAA ATG GAG CAA TCC CGG TCA CAG
N720-Rev (EcoRI)	TT CCG GAA TTC AGA GAG ATC TTC GTC CTC ATC C
N720-Rev (Not I)	ATA AGA ATG CGG CCG CTA TCA AGA GAG ATC TTC GTC CTC ATC C
C598-Fw (XhoI)	CCG CTC GAG ACC ATG GAG CTC AGC AAA TAT ACC ATC TTT GTT G
C721-Fw (EcoR I)	TT CCG GAA TTC GGC AAG AGC GAG CTT CCT CC
C721-Rev (Not I)	ATA AGA ATG CGG CCG CTA TCA AAG GAT CAG TTC ATC C
C721-Fw (Nhe I)	CG GGA TCC GCT AGC ACC ATG GAG GGC AAG AGC GAG CTT CCT CC
C721-Rev (Xho I)	GCC CGC TCG AGC AAG GAT CAG TTC ATC CTC ATC C
C721-Fw (Xho I)	CCG CTC GAG ACC ATG GAG GGC AAG AGC GAG CTT CCT C
C721-Rev (EcoRI)-c-myc (XbaI)	GC TCT AGA TCA CAG ATC CTC TTC TGA GAT GAG TTT TTG TTC GAA TTC AAG GAT CAG TTC ATC CTC ATC C
C721-Fw (Flag)	TT CCG GAA TTC ATG GAT TAT AAA GAT GAT GAT GAT AAA GGC AAG AGC GAG CTT CCT C
C807-Fw (Xho I)	CCG CTC GAG ACC ATG GAG CAG GAG CAG CTG AGC CAG
C863-Fw (Xho I)	CCG CTC GAG ACC ATG GAG CTG GAG GAG CTA CAG AAG GCC
C889-Fw (Xho I)	CCG CTC GAG ACC ATG GAG AAC ACG ACT TCA ACT CGA AAG AG

Table A-2 Sequencing primers

Designation	Sequence 5' to 3'
hCLC-1 F360	G CTC CTG GGA GCT GTA TTT GTG
hCLC-1 F527	CC CTC TTC TGC CAC CTC ATC TC
hCLC-1 F590	TTG CCT GAC CTT GGC TGG AAC
hClC-1 P7 Fw	CCT GAC CTT GGC TGG AAC CAG CTC AGC
hClC-1 P8 Rev	GCT AAA TAG CAC TCC TCC AAG TGG
hClC-1 P9 Fw	C CCA CTA GTC CTC ATC CTC TTC
hClC-1 P10 Fw	CTG GGC CAG TCA GCT GTG TGG ATT CAC
pIRES Fw (952)	TGG TCT TAC TGA CAT CCA CTT TG
pIRES Rev (1164)	AAG CGG CTT CGG CCA GTA AC
HTa-Rev	TTG GTA CCG CAT GCC TCG AGA CTG

Table A-3 Primers for deletion mutagenesis

Designation	Sequence 5' to 3'
Del (592-662)R	C TAC TTG CCT CGC CAC CTG TGT CCT GAG
Del (592-662)F	A CAG GTG GCG AGG CAA GTA GGG TAG CTT CTT GAC C
Del (607-662)R	C TTT GTT GAG CGC CAC CTG TGT CCT GAG
Del (607-662)F	A CAG GTG GCG CTC AAC AAA GAT GGT ATA TTT G
Del (800-806)R	C ATG TCA CCT CAG GAG CAG CTG AGC CAG
Del (800-806)F	G CTG CTC CTG AGG TGA CAT GTT ATC CAC TAA ATC TG
Del (807-813)R	G GCC TGG GAG GTC TGT TTT GAT TCC TGC TGT ATT G
Del (807-813)F	C AAA ACA GAC CTC CCA GGC CTC AAT CTC TTC
Del (820-862)R	TGA TTC CTG CCT GGA GGA GCT ACA GAA GGC C
Del (820-862)F	GCT CCT CCA GGC AGG AAT CAA AAC AGA CAG G
Del (820-870)R	T GAT TCC TGC GAG GGG CAC ACC AAG TCT GG
Del (820-870)F	T GTG CCC CTC GCA GGA ATC AAA ACA GAC AGG
Del (863-888)R	C GTC CTG GCC AAC ACG ACT TCA ACT CGA AAG AG

Table A-3 Primers for deletion mutagenesis (continued)

Designation	Sequence 5' to 3'
Del (863-888)F	A AGT CGT GTT GGC CAG GAC GCC CCT G
C598Δ(798-819)R(NotI)	GCG GCC GCT TGT ATT GAC CAG TCT CCC TTC C
C598Δ(798-819)F (NotI)	GC GGC CGC CAT GTT ATC CAC TAA ATC TGT GGA ATC CTG GG
C598Δ(863-888)R (NotI)	GCG GCC GCT AAC ACG ACT TCA ACT CGA AAG AG
C598Δ(863-888)F (NotI)	GC GGC CGC GGC CAG GAC GCC CCT GAG CTT C

Table A-4 Primers for alanine-exchange mutagenesis

Designation	Sequence 5' to 3'
Alanine DE (199-206)R	GCT GCA GCT GCA GCT GCA GCC CTC ACA ATG AAA GCC TTT GTG G
Alanine DE (199-206)F	GGC TGC AGC TGC AGC TGC AGC AAG TAT TGT CTT CAT TTC GGG
Alanine FG (251-255)R	TTC ATG GCT GCA GCT GCA GCG GTA TAT GAG CAG CCA TAC TAC TAC TC
Alanine FG (251-255)F	ATA TAC CGC TGC AGC TGC AGC CAT GAA TTT GCT GAG GAC AG
Alanine FG (257-261)R	GGG GTA GCA GCT GCA GCT GCC TAC TAC TCT GAT ATC CTG ACG GTG GG
Alanine FG (257-261)F	GTA GTA GGC AGC TGC AGC TGC TAC CCC GCA GAA CAC AGA C
Alanine HI (293-296)R	ATC GAG GTC GCT GCA GCT GCC TTT GCT GTT CGG AAC TAC TGG AG
Alanine HI (293-296)F	AAC AGC AAA GGC AGC TGC AGC GAC CTC GAT GCT AAA TAG CAC TC
Alanine HI (297-300)R	TCC ACC TAC GCT GCA GCT GCG AAC TAC TGG AGA GGA TTC TTT GCA G
Alanine HI (297-300)F	CCA GTA GTT CGC AGC TGC AGC GTA GGT GGA GGT GAC CTC GAT G
Alanine JK (380-385)R	CAC GCT GCA GCT GCA GCT GCT CTT GCT AAG CAC CGC CTG

Table A-4 Primers for alanine-exchange mutagenesis (continued)

Designation	Sequence 5' to 3'
Alanine JK(380-385)F	AAG AGC AGC TGC AGC TGC AGC GTG CTT TCG GAC ACC GAG
DE Not (199-206)R	GCG GCC GCT GCA GCC CTC ACA ATG AAA GCC TTT GTG G
DE Not (199-206)F	GC GGC CGC AGC TGC AGC AAG TAT TGT CTT CAT TTC GGG
FG Not (251-255)R	GCG GCC GCT GCG GTA TAT GAG CAG CCA TAC TAC
FG Not (251-255)F	GC GGC CGC AGC CAT GAA TTT GCT GAG GAC AGC AG
FG Not (256-261)R	GCG GCC GCA GCT GCC TAC TAC TCT GAT ATC CTG ACG G
FG Not (256-261)F	GC GGC CGC TGC CCC GCA GAA CAC AGA CAT GAA TTT G
HI Not (294-300)R	GCG GCC GCT GCG AAC TAC TGG AGA GGA TTC TTT G
HI Not (294-300)F	GC GGC CGC AGC TGC AGC GGT GAC CTC GAT GCT AAA TAG
Jk Not (380-385)R	GCG GCC GCA GCT CTT GCT AAG CAC CGC CTG CTG
Jk Not (380-385)F	GC GGC CGC TGC AGC GTG CTT TCG GAC ACC GAG CAT G
C598 AE (834-843)R (NotI)	GCG GCC GCT GCA GCT GCA GCC CTT GGC CTC CAC CTC GCT TAC
C598 AE (834-843)F (NotI)	GC GGC CGC AGC TGC AGC GGT TGT CTG CTC CAC CAG CTG G

APPENDIX B:

cDNA AND PROTEIN SEQUENCE OF HUMAN ClC-1

```
5'ATG GAG CAA TCC CGG TCA CAG CAG CGT GGG GGT GAA CAA AGC TGG TGG GGT
  Met Glu Gln Ser Arg Ser Gln Gln Arg Gly Gly Glu Gln Ser Trp Trp Gly

  AGT GAC CCC CAG TAC CAG TAT ATG CCC TTT GAA CAC TGC ACC AGC TAC GGA
  Ser Asp Pro Gln Tyr Gln Tyr Met Pro Phe Glu His Cys Thr Ser Tyr Gly

  CTG CCC TCT GAG AAT GGG GGC CTC CAG CAC AGG CTC CGG AAG GAT GCA GGC
  Leu Pro Ser Glu Asn Gly Gly Leu Gln His Arg Leu Arg Lys Asp Ala Gly

  CCC CGC CAC AAC GTC CAC CCC ACA CAG ATT TAT GGC CAT CAC AAA GAA CAA
  Pro Arg His Asn Val His Pro Thr Gln Ile Tyr Gly His His Lys Glu Gln

  TTC TCA GAC AGG GAG CAG GAC ATA GGG ATG CCC AAG AAG ACA GGC TCC AGT
  Phe Ser Asp Arg Glu Gln Asp Ile Gly Met Pro Lys Lys Thr Gly Ser Ser

  TCT ACC GTG GAC AGC AAG GAT GAG GAT CAC TAT TCT AAA TGT CAA GAT TGT
  Ser Thr Val Asp Ser Lys Asp Glu Asp His Tyr Ser Lys Cys Gln Asp Cys
                                 Helix A
  ATC CAC CGC CTG GGA CAG GTG GTG AGA AGA AAA TTA GGG GAA GAC TGG ATC
  Ile His Arg Leu Gly Gln Val Val Arg Arg Lys Leu Gly Glu Asp Trp Ile
          105                                     Helix B
  TTT CTG GTG CTT CTG GGA CTG CTG ATG GCT CTG GTC AGC TGG AGC ATG GAC
  Phe Leu Val Leu Leu Gly Leu Leu Met Ala Leu Val Ser Trp Ser Met Asp

  TAC GTC AGT GCC AAA AGC CTT CAG GCC TAC AAG TGG TCC TAC GCG CAG ATG
  Tyr Val Ser Ala Lys Ser Leu Gln Ala Tyr Lys Trp Ser Tyr Ala Gln Met
                                                          152
  CAG CCC AGC CTT CCT CTG CAG TTC CTG GTC TGG GTC ACC TTC CCA CTA GTC
  Gln Pro Ser Leu Pro Leu Gln Phe Leu Val Trp Val Thr Phe Pro Leu Val
                        Helix C
  CTC ATC CTC TTC AGC GCC CTC TTC TGC CAC CTC ATC TCT CCC CAG GCT GTT
  Leu Ile Leu Phe Ser Ala Leu Phe Cys His Leu Ile Ser Pro Gln Ala Val
                                          181
  GGC TCT GGA ATC CCC GAA ATG AAG ACA ATA CTT CGT GGG GTT GTC CTG AAG
  Gly Ser Gly Ile Pro Glu Met Lys Thr Ile Leu Arg Gly Val Val Leu Lys
          Helix D                         198 199
  GAA TAC CTC ACA ATG AAA GCC TTT GTG GCC AAG GTT GTC GCC CTG ACT GCG
  Glu Tyr Leu Thr Met Lys Ala Phe Val Ala Lys Val Val Ala Leu Thr Ala
      206 Helix E
  GGC CTG GGC AGT GGC ATC CCC GTG GGG AAA GAG GGC CCC TTC GTC CAC ATT
  Gly Leu Gly Ser Gly Ile Pro Val Gly Lys Glu Gly Pro Phe Val His Ile
                225                       Helix F
  GCC AGC ATC TGT GCT GCT GTC CTC AGC AAA TTC ATG TCT GTG TTC TGC GGG
  Ala Ser Ile Cys Ala Ala Val Leu Ser Lys Phe Met Ser Val Phe Cys Gly
                                          250 251             255
  GTA TAT GAG CAG CCA TAC TAC TAC TCT GAT ATC CTG ACG GTG GGC TGT GCT
  Val Tyr Glu Gln Pro Tyr Tyr Tyr Try Ser Asp Ile Leu Thr Val Gly Cys Ala
  256                 261 Helix G
  GTG GGA GTC GGC TGT TGT TTT GGG ACA CCA CTT GGA GGA GTG CTA TTT AGC
  Val Gly Val Gly Cys Cys Phe Gly Thr Pro Leu Gly Gly Val Leu Phe Ser
                      278             Helix H
```

```
ATC GAG GTC ACC TCC ACC TAC TTT GCT GTT CGG AAC TAC TGG AGA GGA TTC
Ile Glu Val Thr Ser Thr Tyr Phe Ala Val Arg Asn Tyr Trp Arg Gly Phe
        292 293         296             300 Helix I

TTT GCA GCC ACG TTC AGC GCC TTT GTG TTT CGA GTG CTG GCA GTG TGG AAC
Phe Ala Ala Thr Phe Ser Ala Phe Val Phe Arg Val Leu Ala Val Trp Asn
                                                    320
AAG GAT GCT GTC ACC ATC ACT GCT CTG TTC AGA ACC AAT TTC CGA ATG GAT
Lys Asp Ala Val Thr Ile Thr Ala Leu Phe Arg Thr Asn Phe Arg Met Asp

TTC CCC TTT GAC CTG AAG GAA CTA CCA GCT TTT GCT GCC ATC GGG ATT TGC
Phe Pro Phe Asp Leu Lys Glu Leu Pro Ala Phe Ala Ala Ile Gly Ile Cys
                           Helix J
TGT GGG CTC CTG GGA GCT GTA TTT GTG TAT CTG CAT CGC CAA GTC ATG CTC
Cys Gly Leu Leu Gly Ala Val Phe Val Tyr Leu His Arg Gln Val Met Leu

GGT GTC CGA AAG CAC AAG GCC CTC AGC CAG TTT CTT GCT AAG CAC CGC CTG
Gly Val Arg Lys His Lys Ala Leu Ser Gln Phe Leu Ala Lys His Arg Leu
                379 380             385 Helix K
CTG TAT CCT GGA ATT GTT ACC TTT GTC ATT GCC TCA TTC ACC TTC CCA CCA
Leu Tyr Pro Gly Ile Val Thr Phe Val Ile Ala Ser Phe Thr Phe Pro Pro
                                                    405
GGA ATG GGT CAA TTC ATG GCT GGA GAG TTG ATG CCC CGC GAA GCC ATC AGT
Gly Met Gly Gln Phe Met Ala Gly Glu Leu Met Pro Arg Glu Ala Ile Ser
                                    Helix L         422
ACT TTG TTT GAC AAC AAT ACA TGG GTG AAA CAC GCG GGT GAT CCT GAG AGC
Thr Leu Phe Asp Asn Asn Thr Trp Val Lys His Ala Gly Asp Pro Glu Ser

CTG GGC CAG TCA GCT GTG TGG ATT CAC CCC CGG GTC AAC GTT GTC ATC ATC
Leu Gly Gln Ser Ala Val Trp Ile His Pro Arg Val Asn Val Val Ile Ile
                                            Helix M
ATC TTT CTC TTC TTC GTC ATG AAG TTC TGG ATG TCC ATC GTG GCC ACC ACT
Ile Phe Leu Phe Phe Val Met Lys Phe Trp Met Ser Ile Val Ala Thr Thr

ATG CCC ATA CCC TGC GGA GGC TTC ATG CCT GTG TTT GTG CTA GGA GCT GCA
Met Pro Ile Pro Cys Gly Gly Phe Met Pro Val Phe Val Leu Gly Ala Ala
477                     Helix N
TTT GGA AGG CTG GTA GGA GAA ATC ATG GCC ATG CTC TTT CCT GAT GGT ATT
Phe Gly Arg Leu Val Gly Glu Ile Met Ala Met Leu Phe Pro Asp Gly Ile
                                        504
TTG TTT GAT GAC ATC ATC TAC AAG ATC CTA CCT GGG GGC TAT GCA GTA ATT
Leu Phe Asp Asp Ile Ile Tyr Lys Ile Leu Pro Gly Gly Tyr Ala Val Ile
                                    Helix O
GGA GCA GCA GCG CTG ACT GGT GCC GTT TCC CAC ACA GTC TCC ACA GCT GTG
Gly Ala Ala Ala Leu Thr Gly Ala Val Ser His Thr Val Ser Thr Ala Val
                                        537 Helix P
ATT TGC TTC GAA TTA ACG GGT CAG ATT GCT CAC ATC CTG CCC ATG ATG GTG
Ile Cys Phe Glu Leu Thr Gly Gln Ile Ala His Ile Leu Pro Met Met Val
                        550             Helix Q
GCT GTT ATC TTG GCC AAC ATG GTG GCC CAG AGC CTG CAG CCC TCT CTC TAT
Ala Val Ile Leu Ala Asn Met Val Ala Gln Ser Leu Gln Pro Ser Leu Tyr
                                        573     Helix R
GAC AGC ATC ATC CAG GTC AAG AAG CTA CCC TAC TTG CCT GAC CTT GGC TGG
Asp Ser Ile Ile Gln Val Lys Lys Leu Pro Tyr Leu Pro Asp Leu Gly Trp
                                            591
```

```
AAC CAG CTC AGC AAA TAT ACC ATC TTT GTT GAG GAC ATC ATG GTA CGT GAT
  Asn Gln Leu Ser Lys Tyr Thr Ile Phe Val Glu Asp Ile Met Val Arg Asp
                                             CBS1
  GTG AAG TTT GTT TCA GCT TCT TAC ACA TAT GGG GAG TTG CGA ACC CTG CTC
  Val Lys Phe Val Ser Ala Ser Tyr Thr Tyr Gly Glu Leu Arg Thr Leu Leu


  CAG ACC ACC ACA GTC AAG ACT TTA CCA CTG GTT GAC TCA AAA GAT TCA ATG
  Gln Thr Thr Thr Val Lys Thr Leu Pro Leu Val Asp Ser Lys Asp Ser Met

  ATC CTG CTG GGC TCG GTG GAG CGG TCG GAA CTG CAG GCC CTC CTG CAG CGC
  Ile Leu Leu Gly Ser Val Glu Arg Ser Glu Leu Gln Ala Leu Leu Gln Arg
                                                              662
  CAC CTG TGT CCT GAG CGC AGG CTG CGC GCA GCC CAA GAG ATG GCG CGG AAG
  His Leu Cys Pro Glu Arg Arg Leu Arg Ala Ala Gln Glu Met Ala Arg Lys

  TTG TCG GAG CTG CCT TAC GAC GGG AAG GCG CGG CTG GCT GGG GAG GGG CCC
  Leu Ser Glu Leu Pro Tyr Asp Gly Lys Ala Arg Leu Ala Gly Glu Gly Pro

  CCC GGC GCG CCT CCA GGC CGG CCC GAG TCC TTC GCC TTT GTG GAT GAG GAT
  Pro Gly Ala Pro Pro Gly Arg Pro Glu Ser Phe Ala Phe Val Asp Glu Asp

  GAG GAC GAA GAT CTC TCT GGC AAG AGC GAG CTT CCT CCT TCC CTT GCT CTC
  Glu Asp Glu Asp Leu Ser Gly Lys Ser Glu Leu Pro Pro Ser Leu Ala Leu

  CAC CCC TCT ACT ACT GCC CCT CTG TCC CCA GAA GAG CCC AAT GGG CCT CTG
  His Pro Ser Thr Thr Ala Pro Leu Ser Pro Glu Glu Pro Asn Gly Pro Leu

  CCT GGC CAC AAA CAG CAG CCG GAA GCA CCA GAG CCT GCA GGT CAA AGA CCC
  Pro Gly His Lys Gln Gln Pro Glu Ala Pro Glu Pro Ala Gly Gln Arg Pro

  TCC ATC TTC CAG TCC CTG CTT CAC TGC TTG CTG GGC AGA GCT CGC CCC ACA
  Ser Ile Phe Gln Ser Leu Leu His Cys Leu Leu Gly Arg Ala Arg Pro Thr

  AAG AAG AAA ACA ACC CAG GAT TCC ACA GAT TTA GTG GAT AAC ATG TCA CCT
  Lys Lys Lys Thr Thr Gln Asp Ser Thr Asp Leu Val Asp Asn Met Ser Pro
                                                              798
  GAA GAG ATT GAG GCC TGG GAG CAG GAG CAG CTG AGC CAG CCT GTC TGT TTT
  Glu Glu Ile Glu Ala Trp Glu Gln Glu Gln Leu Ser Gln Pro Val Cys Phe
  800                         806 807                     813
  GAT TCC TGC TGT ATT GAC CAG TCT CCC TTC CAG CTG GTG GAG CAG ACA ACC
  Asp Ser Cys Cys Ile Asp Gln Ser Pro Phe Gln Leu Val Glu Gln Thr Thr
           819     CBS2
  CTG CAC AAG ACT CAT ACC CTG TTT TCA CTC CTT GGC CTC CAC CTC GCT TAC
  Leu His Lys Thr His Thr Leu Phe Ser Leu Leu Gly Leu His Leu Ala Tyr
  834                               843
  GTG ACC AGC ATG GGG AAG CTC AGG GGC GTC CTG GCC CTG GAG GAG CTA CAG
  Val Thr Ser Met Gly Lys Leu Arg Gly Val Leu Ala Leu Glu Glu Leu Gln
                                                  862 863
  AAG GCC ATT GAG GGG CAC ACC AAG TCT GGG GTG CAG CTC CGC CCT CCC CTT
  Lys Ala Ile Glu Gly His Thr Lys Ser Gly Val Gln Leu Arg Pro Pro Leu
           870 871
  GCC AGC TTC CGG AAC ACG ACT TCA ACT CGA AAG AGT ACC GGG GCA CCT CCA
  Ala Ser Phe Arg Asn Thr Thr Ser Thr Arg Lys Ser Thr Gly Ala Pro Pro
              888
```

```
TCT TCT GCA GAG AAC TGG AAC CTG CCT GAG GAC AGG CCT GGG GCC ACT GGA
 Ser Ser Ala Glu Asn Trp Asn Leu Pro Glu Asp Arg Pro Gly Ala Thr Gly

 ACA GGG GAT GTG ATT GCT GCC TCC CCA GAG ACC CCT GTG CCA TCT CCT TCC
 Thr Gly Asp Val Ile Ala Ala Ser Pro Glu Thr Pro Val Pro Ser Pro Ser

 CCA GAG CCC CCT CTC TCC CTG GCC CCA GGC AAG GTA GAG GGC GAG TTG GAG
 Pro Glu Pro Pro Leu Ser Leu Ala Pro Gly Lys Val Glu Gly Glu Leu Glu

 GAG CTG GAG CTG GTG GAG AGT CCA GGG CTG GAA GAG GAG CTG GCC GAC ATC
 Glu Leu Glu Leu Val Glu Ser Pro Gly Leu Glu Glu Glu Leu Ala Asp Ile

 TTG CAG GGC CCC AGC CTG CGA TCC ACA GAC GAG GAG GAT GAG GAT GAA CTG
 Leu Gln Gly Pro Ser Leu Arg Ser Thr Asp Glu Glu Asp Glu Asp Glu Leu

 ATC CTT TGA 3′
 Ile Leu Stop
```

Note:

1. The hClC-1 cDNA sequence is given using the standard 5'to 3'convention.
2. α-helices A-R are in green and bold, whereas CBS1 and CBS2 domains are shown in dark red and bold. Labels are shown underneath.
3. The locations of deletion and alanine-exchange mutations in the present study are highlighted in yellow. Labels are shown underneath.

APPENDIX C:

PUBLISHED PAPERS

国际遗传学杂志 2008 年 2 月 15 日第 31 卷第 1 期 Int J Genet Feb. 15,2008,Vol. 31,No. 1

· 综述 ·

CLC 氯离子通道结构与功能研究进展

马琳琳 傅松滨 Bretag AH

【摘要】 电压门控的 CLC 氯离子通道(及转运蛋白)家族广泛存在于从细菌到人类的各种生物中,负责调控氯离子等阴离子的跨膜转运。CLC 通道蛋白皆为菱形的同源二聚体,每个三角形的单体由 18 个 α 螺旋构成,有各自独立的孔道(pore)和选择性过滤器(selectivity filter),且其内部呈双重对称性反向平行结构。CLC 通道及转运蛋白(ClC-0, -1, -2)的门控机制(gating)与渗透机制(permeation)及氯离子在孔道内的结合能力(binding)紧密相关,使这个家族表现出与众不同的电生理学特性。其哺乳动物中的家族成员肩负着调控肌肉细胞膜兴奋性及跨上皮细胞转运、调节细胞容积和胞内细胞器的酸化等使命,所以其功能缺陷会导致肌强直、Bartter 综合征、Dent 病及骨骼石化症等多种遗传性疾病。

【关键词】 CLC 氯离子通道; 门控机制; 选择性过滤器; CBS 结构域

Structure and Function of CLC Chloride Channels *MA Lin-lin*[1,2], *FU Song-bin*[1,3], *Bretag AH*[2]. ([1]*Laboratory of Medical Genetics, Harbin Medical University, Harbin* 150081, *China*; [2]*Sansom Institute, University of South Australia, Adelaide, SA* 5000, *Australia*; [3]*Bio-pharmaceutical Key Laboratory of Heilongjiang Province, Harbin* 150081, *China*)

Corresponding authors: *Bretag AH. E-mail*: *Allan. Bretag@ unisa. edu. au*; *FU Song-bin. E-mail*: *fusb@ ems. hrbmu. edu. cn*

【**Abstract**】 Voltage-gated CLC chloride channels and transporters are ubiquitously expressed from bacteria to mammals, performing their functions in the plasma membrane or in intracellular organelles such as vesicles of the endosomal/lysosomal pathway or in synaptic vesicles. According to the crystal structural models from bacterial CLC transporters EcCLC and StCLC, the CLC channels are homodimeric proteins composed of two identical subunits. Each of these monomers contains its own chloride pore, and each is composed, in turn, of a pair of pseudo symmetrical peptide domains with the chloride selectivity filter located at the interface of these two domains. CLC channel (transporter) gating (for ClC-0, -1, and -2) is strictly regulated by Cl? itself, so a remarkable property of CLC channels (transporters) is that their gating, permeation and ion binding are closely coupled. The major function of CLC channels is to modulate chloride ion flux across cell membranes, with different family members playing many pivotal roles in cells as a consequence, including stabilization of membrane potential, facilitation of transepithelial transport, synaptic inhibition, cell volume regulation, extracellular and vesicular acidification and endocytotic trafficking. Correspondingly, it has been well established by animal models and mutation studies that loss of distinct mammalian ClC chloride channels results in different hereditary diseases, such as myotonia, Bartter's syndrome; Dent's disease, and osteopetrosis.

【**Key words**】 CLC chloride channels; Gating; Selectivity filter; CBS domain

CLC 通道为氯离子通道蛋白中的一个大家族,广泛分布于从细菌到人类的各种生物中,为氯离子沿电化学梯度的跨膜移动提供通路和途径。其表达于哺乳动物中的九大家族成员存在于各种细胞的细胞质膜或细胞器膜上,承担着各自不同的生理功能,包括稳定骨骼肌细胞的膜电位并调控其电兴奋性;调控跨上皮细胞的转运和水盐重吸收;调节内涵体和突触小泡的酸化;调控细胞容积和胞内定位等[1-2]。CLC 通道是极为特别的一类通道蛋白,因为他们在结构上与其他任何一种离子通道都迥然不同,所以在选择性滤过机制,门控机制以及功能上都

作者单位:150081,哈尔滨医科大学医学遗传学研究室(马琳琳、傅松滨);SA5000 阿德莱德,南澳大学 Sansom 学院(马琳琳,Bretag AH);150081 哈尔滨,黑龙江省生物医药重点实验室(傅松滨)

通讯作者:Bretag AH(E-mail:Allan. Bretag@ unisa. edu. au);傅松滨(E-mail:fusb@ ems. hrbmu. edu. cn)

表现出独特而鲜明的特征。本文将主要以 CLC 通道蛋白晶体结构研究方面的最新进展为基础,简要概述其上述各方面的特性。

1 CLC 氯离子通道蛋白的结构

对于 CLC 通道蛋白结构的最初推测来源于对 ClC-0 单通道电流的定量分析。研究者发现 ClC-0 呈现三等分的通道电流水平,并且通道处于某种开放状态的几率符合二项式分布规律,因此推断此类通道蛋白为含有两个离子通透孔道(pore)的同源二聚体,此即著名的"双管结构"(double-barreled architecture)[3]。随后对于通道的克隆、蛋白纯化、定点突变及嵌合体的研究不断地为这一推断提供新的证据,并证明每一个孔道存在于一个单体(subunit)中,并独立地行使各自的功能[4~6]。

1999 年,Maduke 等[7]发现了细菌中的 CLC 蛋白。虽然最新的研究表明,细菌 CLC 蛋白是作为协同转运蛋白(cotransporter)或离子交换器(exchanger)在发挥功能,而不是真正的离子通道[8],但众多突变分析显示,其结构在哺乳动物的 CLC 离子通道中也是高度保守的[9]。所以细菌 *Escherichia coli* 和 *Salmonella typhimurium* 中 CLC 蛋白(EcCLC 和 StCLC)的三维晶体结构就成了所有 CLC 蛋白主体结构的权威代表[10]。EcCLC 和 StCLC 的晶体结构完全证实了双管结构的推测,并显示:CLC 通道皆为由两个三角形单体构成的同源二聚体,两个选择性滤过阴离子的孔道(pore)分别位于两个单体的中心,彼此之间的距离约 39Å(见图 1A)。就其拓扑结构而言,每个单体由 18 个 α 螺旋(螺旋 A-R)构成,各个螺旋长短不一,并以不同的倾斜角度及深度嵌入细胞膜内。α 螺旋 H、I、P、Q 参与构成了两个单体之间广阔的交界面。每个单体内,α 螺旋 B-I 和 J-Q 又分别构成两个结构域(domain),以双重对称且反向平行的方式跨越细胞膜,形成所谓的"反向平行结构(antiparallel architecture)"(见图 1B、1C)。这种构型使得 4 个高度保守的区域(GXXXP)——α 螺旋 D 的氨基端环(GSGIP)、螺旋 F 的氨基端环(GREGP)及其对称结构螺旋 N 的氨基端环(GIFAP)和螺旋 R 内的一个酪氨酸分别从膜的两侧伸向单体的中心而形成选择性过滤器(selectivity filter)[10,11]。

真核生物 CLC 通道与细菌 CLC 通道之间最显著的区别在于,他们虽然具有极为相似的跨膜结构域,但绝大部分真核生物 CLC 通道都拥有 EcCLC 和 StCLC 所没有的位于胞质内的羧基末端尾巴(carboxyl-tail)。在脊椎动物中,此 C 末端结构域的长度由 155 个氨基酸(ClC-Ks)至 398 个氨基酸(ClC-1)不等,但其共同的特征是,他们都含有一对胱硫醚-β-合成酶(CBS)结构域(CBS1 和 CBS2)。最近,Meyer 和 Dutzler[12]成功地实现了对 ClC-0 胞质内羧基末端晶体结构的检测和分析,从而为所有真核生物 CLC 通道的羧基末端结构域建立了一个具有极高参考价值的结构模型。根据这一模型,羧基末端内的两个三角形 CBS 结构域(CBS1 和 CBS2)分别严格遵守 β1-α1-β2-β3-α2 的构型,并通过各自的 β 片层(由 β2 和 β3 折叠形成)之间的相互作用而结合成 CBS 对。而且超速离心和沉降平衡实验表明,此胞内羧基末端结构域在溶液中以二聚体形态存在,可见 CLC 通道跨膜结构域的同源二聚体化结构模式很可能适用于整个蛋白[12]。此 C 末端结构域虽然与通道的孔道相距甚远,却显然对通道的功能有着巨大的影响。因为该区域内的突变或缺失会改变通道的传导和门控特性,甚至会导致通道丧失正常功能而引发各种遗传病[13,14]。

2 CLC 氯离子通道的孔道(pore)和选择性过滤器(selectivity filter)

CLC 通道供阴离子选择性通过的孔道(pore)位于每个单体的中心,两个反向平行对称的结构域相交界处。整个孔道呈沙漏形,分别从胞外和胞内延伸过来的水性通道(vestibules)形成了上下两个圆锥型的沙池,而中间约 15Å 宽的狭长的颈部即为选择性过滤器(selectivity filter)所在处[10,11]。作为所有离子通道最重要的特性之一,选择性过滤器使离子通道能够分辨各种不同的离子并仅允许特定的离子顺着电化学梯度被动跨膜转移[15]。

选择性过滤器内由外向内顺序分布着 3 个氯离子结合位点(S_{ext}、S_{cen}、S_{int}),由分别位于螺旋 D、F、N、R 氨基端环内的一些在进化上极其保守的氨基酸残基构成。其特有的构成方式使得这几个螺旋带正电荷的一端都伸向进入孔道的阴离子并能够通过静电相互作用维持其稳定性[10,11]。在正常通道中,S_{cen} 和 S_{int} 总是处于被阴离子占据的状态。最外侧的结合位点 S_{ext} 在通道非活动状态下被螺旋 F 氨基末端的一个谷氨酸的侧链所封闭。当 CLC 通道被激活时,这个谷氨酸的侧链会让出 S_{ext} 的位置供第 3 个氯离子结合[11,16]。

3　CLC 氯离子通道的门控机制（gating）

门控机制（gating）是离子通道的另外一个重要特性，它是指通道在接受内外环境中的刺激信号后开放或关闭其通透通路的机制。CLC 通道的门控机制是电压依赖性的，在细胞膜去极化（内正外负）时通道开放，超极化（内负外正）时通道关闭[16]。目前已知 CLC 通道受两种迥然不同的门控机制调控，其中之一在细胞膜去极化时激活，能在毫秒的时间范围内分别打开或关闭单个孔道（pore），故称之为快门控机制（fast gating）或单孔门控机制（protopore gating）；另外一个，对于 ClC-0 而言，在细胞膜超极化时激活，以秒为时间尺度同时打开或关闭两个孔道，故通常称之为慢门控机制（slow gating）[1]；对于 ClC-1 而言，则在膜去极化时激活且能以与快门控相似的速度开放或关闭通道，所以人们放弃了习惯上的慢门控的叫法，而称之为共同门控机制（common gating）[1,14]。

3.1　单孔门控机制（protopore gating）：虽然总体而言，CLC 通道属于电压门控性离子通道，但包括 ClC-0在内的一些成员同时也被称为“氯离子激活的氯离子通道”，这是因为细胞外的氯离子浓度的升高可以促进通道的开放[17]；而细胞内氯离子浓度的升高会抑制通道的关闭[18]。人们根据细菌 CLC 蛋白的晶体结构推测，这种“细胞外氯离子浓度依赖性单孔门控”的机制可能是，细胞外的氯离子通过从胞外延伸至孔道的水性通道进入孔道内，引起通道蛋白构象的变化，使本来占据 S_{ext} 的谷氨酸羧基侧链移开，让位给这个氯离子，通道的单孔门控由此被激活[10]。所以这个特别位置上的谷氨酸侧链被认为是单孔门控的闸门（gate）。这一推断获得了一些证据的支持[11,19~21]，但也有人提出一些质疑[18]。我们显然需要更深入的研究和更充分的证据才可能有所定论。

对于 ClC-0 和 ClC-1 而言，在上述细胞外氯离子浓度依赖性，去极化激活的单孔门控机制的控制下，膜电位越低，单孔门控的开放率也越低；但有趣的是，当膜电位低于 -140mV 或 -150mV 的时候，单孔门控的开放率反而会大幅度提高。但这种超极化激活的单孔门控机制并不依赖于细胞外的氯离子浓度，而是受 H^+ 浓度调节——胞外 pH 值越低，通道开放率越高；而胞内 pH 值越低，通道失活得越慢[17,18,21]。目前认为，其机制可能在于起闸门作用的这个谷氨酸的质子化状态，因为当该谷氨酸在 ClC-0 中发生突变时，其门控对于 pH 的依赖性也随之丧失了[11]。综上所述，ClC 通道的单孔门控似乎拥有两种不同的开放机制，而其独特之处和复杂之处就在于，该门控机制（孔道开放的过程）与传导机制（离子通过开放的孔道的过程），以及孔道内氯离子的结合能力是密切相关的。

3.2　共同门控机制（common gating）：共同门控或慢门控的具体作用机制及其与单孔门控之间的关系目前都尚无定论，但因为它可以同时关闭分别位于两个单体内的两个孔道，所以很可能与两个单体之间的相互作用有关[22]；而且其高度温度依赖性的动力学特性使人们相信，这是一个涉及巨大构型变化的复杂过程[23,24]。能够影响共同门控机制的生理因素很多，除膜电位和温度之外，细胞外的锌离子（Zn^{2+}）或镉离子（Cd^{2+}）具有封闭作用[25]；而细胞外氯离子浓度的增高或 pH 值的降低则具有激活作用[22,24]。

4　哺乳动物 CLC 氯离子通道家族及其主要功能

目前已知的 CLC 通道蛋白在哺乳动物中的家族成员共有 9 个（ClC-1 至 ClC-7、ClC-Ka、ClC-Kb）。不同成员功能的缺陷会分别导致显性或隐形遗传的肌强直、Bartter 综合征、癫痫症、Dent 病及骨骼石化症等各种遗传病[1,14]，充分体现出其生理功能的重要性。根据基因序列的同源性和功能特性的相似性，这 9 个成员加上 ClC-0 通常被归类为三个亚家族。

4.1　第一亚家族——肌肉型 CLC 通道蛋白：ClC-0 及其哺乳动物中的同源体 ClC-1、ClC-2、ClC-Ka 和 ClC-Kb 在序列上有 50% ~60% 的同源性，且都表达于细胞质膜上并调控 Cl^- 的跨膜移动及膜电位；由于其中最具代表性的 ClC-1 仅表达于骨骼肌细胞中，因此这一亚家族被共同归类为肌肉型 CLC 通道蛋白[26]。其主要功能包括调节细胞质膜的兴奋性、维持细胞内外离子的稳态、调节细胞容积等。

4.1.1　调节细胞兴奋性　我们知道，绝大多数哺乳动物细胞的静息电位是靠 K^+ 来维持的，但骨骼肌细胞比较特别，他们的静息电位是由 Cl^- 来控制的。仅在骨骼肌细胞中表达的 ClC-1，虽然其单通道电导只有 1 ~1.5 pS，却占了骨骼肌细胞静息状态下总膜电导的 70% ~85%，所以 ClC-1 对于骨骼肌细胞静息电位的维持和电兴奋性的调控起着举足轻重的作用。当 ClC-1 功能缺陷的时候，骨骼肌细胞在去极化后不能及时复极，钠通道从而获得充分的时间从失活状态恢复过来；而此时细胞膜电位仍高于钠通

道开放的域值，Na^+ 的内流便诱发另一个动作电位，其结果是单一刺激会诱发动作电位的反复发生，肌肉在主动性收缩后不能正常松弛。这种骨骼肌细胞电兴奋性异常增高所导致的遗传性疾病即为肌强直（myotonia）[14,26]。迄今为止，研究者们已经在肌强直患者中发现了 80 多种 ClC-1 的突变[1]。

4.1.2　维持细胞内外离子的稳态，调节细胞容积　Cl^- 通道通过与各种泵，协同转运器以及其他离子通道相互协调，共同调控细胞内的离子组成及细胞容积。例如，对于绝大多数细胞而言，由于 Na^+/H^+ 交换器及 HCO_3^-/Cl^- 交换器的存在，其细胞内 pH 值都比按照电化学平衡预期的 pH 值要高一些，而这些离子交换作用都需要 Cl^- 通道来保证 Cl^- 的再循环，从而维持细胞的电中性。此外，当细胞外渗透压降低时，细胞必须通过膨胀激活的 K^+ 和 Cl^- 通道的开放来实现盐离子的外流[1,14]。所以当相关氯离子通道发生功能障碍时，会引发水盐代谢失调性疾病。例如，ClC-Kb的突变会导致Ⅲ型Bartter综合征，一种以低血压，低钾性碱中毒和高钙血症为主要表现的严重的盐代谢紊乱，主要由髓袢升支粗段的NaCl

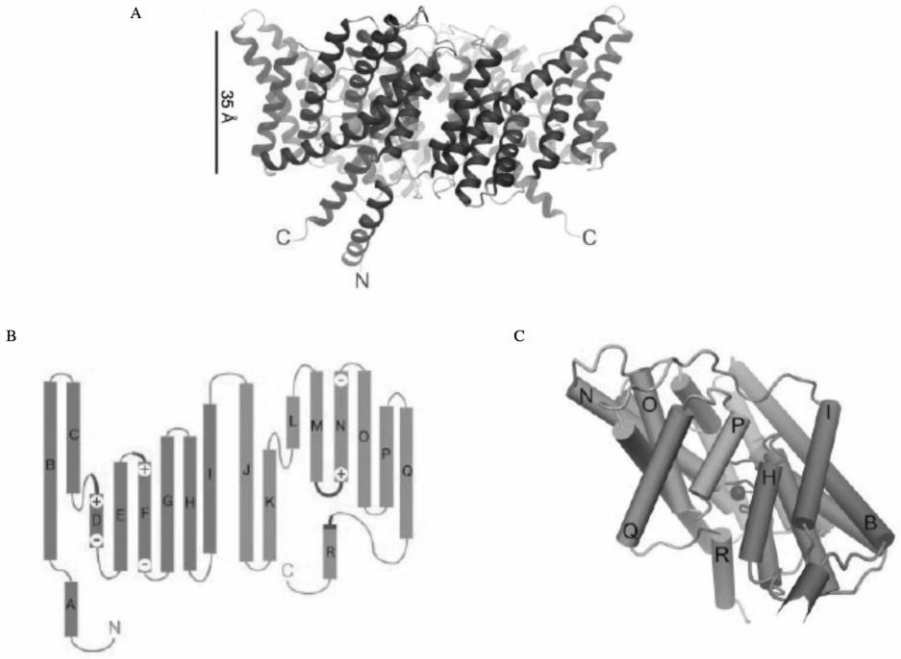


图 1　StClC 蛋白结构示意图

Fig. 1 Structure of the StClC protein

A：从细胞膜内角度观察到的 StClC 二聚体三维立体结构图。两个单体分别以蓝色和红色表示，每个单体中心的绿色小球为位于选择性过滤器内的氯离子。黑色标尺线（35 Å）示细胞膜的大致厚度，上为胞外侧，下为胞质侧。B：StClC 蛋白单体的拓扑结构模型。每个单体由 18 个 α 螺旋（螺旋 A-R）构成；参与构成选择性过滤器的区域以红色显示，与氯离子结合相关的螺旋末端以 + 和 - 分别标示该螺旋末端的极性。C：从细胞膜内角度观察到 StClC 蛋白单体的柱形立体结构示意图，展现 18 个 α 螺旋（螺旋 A-R）的相对位置。上为胞外侧，下为胞质侧；中心的红色小球为位于选择性过滤器内的氯离子[10]。

A: Three-dimensional structure of the StClC dimer viewed from within the membrane with the extracellular solution above. The two subunits are blue and red. A Cl^- ion in the selectivity filter is represented as a green sphere. The black line (35Å) indicates the approximate thickness of the membrane. B: Topology structure of the StClC subunit. Each subunit contains 18 α-helices (A-R). The regions forming the Cl^- selectivity filter are shown in red. Partial charges at the end of helices involved in Cl^- binding are indicated by + and - (end charges) to indicate the sense of the helix dipole. C: Stereo view of the StClC subunit showing the relative positions of the α-helices. It is viewed from within the plane of the membrane with the extracellular solution above and the Cl^- ion in the selectivity filter as a red sphere[10].

重吸收障碍造成[27]。

4.2　第二亚家族——调节酸化功能的 ClC-3、ClC-4 和 ClC-5：这 3 个 CLC 通道家族成员在序列上有 80% 左右的同源性，都位于胞内小泡（intracellular vesicles），如突触小泡和其他内涵体/溶酶体途径细胞器的膜上。当生电性 H^+-ATPase 或 Ca^{2+}-ATPase 将质子或钙离子摄入细胞器内时，会迅速导致细胞器内电荷的失衡，并阻碍质子或钙离子的进一步摄取。为了建立细胞所必需的质子或钙离子浓度梯度，这些细胞器内过多的正电荷必须被有效地中和掉。原则上，这可以通过氯离子的内流或钾离子的外流而实现，因此当氯离子通道功能障碍的时候，这些细胞器的酸化就会发生异常，并导致相应的疾病。例如，保障内噬通路实现有效酸化的 ClC-5，其功能缺陷会引起 Dent 病（Dent's disease），以低相对分子质量蛋白尿，高磷尿症和高钙尿症为特征，最终会导致肾结石、糖尿和氨基酸尿症[28]。

最新的研究显示，外源性表达于爪蟾卵母细胞（Xenopus oocytes）或哺乳动物细胞系 tsA201 时，ClC-4 和 ClC-5（有可能也包括 ClC-3）是作为 Cl^-/H^+ 逆转运蛋白（antiporters）在发挥功能，而不是离子通道[29,30]。显然我们需要更多的研究来支持这一论断，并验证是否还有其他家族成员也应被归类为 Cl^-/H^+ 逆转运蛋白。

4.3　第三亚家族——广泛表达的细胞内 CLC 通道蛋白 ClC-6 和 ClC-7：最后一个亚家族的这 2 个成员，ClC-6 和 ClC-7 是 CLC 通道蛋白中表达得最为广泛的两个成员，分布于各种组织的内质网、溶酶体、内涵体等细胞器的膜上。正如肾脏内涵体和突触小泡的酸化分别依赖于 ClC-5 和 ClC-3 一样，ClC-7 为骨吸收陷窝的酸化所必需[31]，所以，ClC-7 功能的缺失会导致骨骼石化症（osteopetrosis），说明该通道对于骨的重吸收起着重要的作用；此外，ClC-$7^{-/-}$ 的老鼠还会发生光感受器细胞和视网膜神经元的大量丧失而最终导致失明[14]。ClC-6 的生理功能目前还不清楚。

从 Miller 首次在电鳐（torpedo ray）电器官内发现了第一个 CLC 氯离子通道（ClC-0）至今，人们对于 CLC 通道蛋白的研究历史不过 20 多年而已。逐步深入的研究进展令人欣慰，但文中众多“未可知”的领域也让我们看到，目前已知的这些功能和特性大概只是冰山一角，不同专业的研究者们需要跨专业合作，综合应用复杂动物模型，以及生理学，生物物理学，细胞生物学，分子生物学的各种方法和技术，才有可能全面解读这一独特的离子通道家族。而我们最终的目的在于，通过设计小分子靶向药物，反义分子，高效拮抗剂或激活剂来实现对各种 CLC 通道相关遗传病的有效药物治疗和/或基因治疗。

参 考 文 献

[1] Jentsch TJ, Stein V, Weinreich F, *et al*. Molecular structure and physiological function of chloride channels. Physiol Rev, 2002, 82: 503-568.

[2] Chen TY. Structure and function of clc channels. Annu Rev Physiol, 2005, 67: 809-839.

[3] Saviane C, Conti F, Pusch M. The muscle chloride channel ClC-1 has a double-barreled appearance that is differentially affected in dominant and recessive myotonia. J Gen Physiol, 1999, 113: 457-468.

[4] Ludewig U, Pusch M, Jentsch TJ. Two physically distinct pores in the dimeric ClC-0 chloride channel. Nature, 1996, 383: 340-343.

[5] Middleton RE, Pheasant DJ, Miller C. Homodimeric architecture of a ClC-type chloride ion channel. Nature, 1996, 383 : 337-340.

[6] Weinreich F, Jentsch TJ. Pores formed by single subunits in mixed dimers of different CLC chloride channels. J Biol Chem, 2001, 276: 2347-2353.

[7] Maduke M, Pheasant DJ, Miller C. High-level expression, functional reconstitution, and quaternary structure of a prokaryotic ClC-type chloride channel. J Gen Physiol, 1999, 114: 713-722.

[8] Accardi A, Miller C. Secondary active transport mediated by a prokaryotic homologue of ClC Cl- channels. Nature, 2004, 427: 803-807.

[9] Estevez R, Schroeder BC, Accardi A, *et al*. Conservation of chloride channel structure revealed by an inhibitor binding site in ClC-1. Neuron, 2003, 38: 47-59.

[10] Dutzler R, Campbell EB, Cadene M, *et al*. X-ray structure of a ClC chloride channel at 3.0 A reveals the molecular basis of anion selectivity. Nature, 2002, 415:287-294.

[11] Dutzler R, Campbell EB, MacKinnon R. Gating the selectivity filter in ClC chloride channels. Science, 2003, 300:108-112.

[12] Meyer S, Dutzler R. Crystal structure of the cytoplasmic domain of the chloride channel ClC-0. Structure, 2006, 14: 299-307.

[13] Estevez R, Pusch M, Ferrer-Costa C, *et al*. Functional and structural conservation of CBS domains from CLC chloride channels. J Physiol, 2004, 557: 363-378.

[14] Jentsch TJ, Poet M, Fuhrmann JC, *et al*. Physiological functions of CLC Cl^- channels gleaned from human genetic disease and mouse models. Annu Rev Physiol, 2005, 67: 779-807.

[15] Hilber K, Sandtner W, Kudlacek O, *et al*. The selectivity filter of the voltage-gated sodium channel is involved in channel activation. J Biol Chem, 2001, 276: 27831-27839.

[16] Maduke M, Miller C, Mindell JA. A decade of CLC chloride channels: structure, mechanism, and many unsettled questions. Annu Rev Biophys Biomol Struct, 2000, 29: 411-438.

（下转 52 页）

5-hydroxytryptamine 1A receptor gene polymorphism associated with major depression and suicide. J Neuraci, 2003, 23:8788-8799.

[12] Du L, Bakish D, Lapierre YD, *et al*. Association of polymorphism of serotonin 2A receptor gene with suicidal ideation in major depressive disorder. Am J Med Genet, 2000, 96:56-60.

[13] Arias B , Gasto C, Catalán R, *et al*. The 5-HT2A receptor gene 102T/C polymorphism is associated with suicidal behavior in depressed patients. Am J Med Genet, 2001, 105:801-804.

[14] Arias B, Gutierrez B, Pintor L, *et al*. Variability in the 5-HT(2A) receptor gene is associated with seasonal pattern in major depression. Mol Psychiatry, 2001, 6: 239-242.

[15] Tsai SJ, Hong CJ, Yu YW, *et al*. Association study of serotonin 1B receptor (A-161T) genetic polymorphism and suicidal behaviors and response to fluoxetine in major depressive disorder. Neuropsychobiology, 2004, 50:235-238.

[16] Huang YY, Grailhe R, Arango V, *et al*. Relationship of psychopathology to the human serotonin1B genotype and receptor binding kinetics in postmortem brain tissue. Neuropsychopharmacology, 1999, 21:238-46.

[17] Lan NC, Heinzmann C, Gal A, *et al*. Human monoamine oxidase A and B genes map to Xp11.23 and are deleted in a patient with Nerrie disease. Genomics, 1989, 4:552-559.

[18] Sabol SZ, Hu S, Hamer D. A functional polymorphism in the monoamine oxidase A gene promoter. Hum Genet, 1998, 103:273-279.

[19] Hotamisligil GS, Brekefield XO. Human monoamine oxidase A gene determines levels of enzyme activity. Am J Hum Genet, 1991, 49:383-392.

[20] Du L, Bakish D, Ravindran A, *et al*. MAO-A gene polymorphisms are associated with major depression and sleep disturbance in males. Neuroreport, 2004, 15: 2097-101.

[21] Jiang HY, Xu XF. Schizophrenia and polymorphism of catechol-O-methyltransferase gene. Section Genet Foreign Med Sci, 2005, 28: 309-312.
[姜红燕,许秀峰. 精神分裂症与儿茶酚胺甲基转移酶基因多态性. 国外医学遗传学分册,2005,28:309-312.]

[22] Massat I, Souery D, Del-Favero J, *et al*. Association between COMT(Val158Met) functional polymorphism and early onset in patients with major depressive disorder in a European multicenter genetic association study. Mol Psychiatry, 2005, 10:598-605.

[23] Cubells JF, VanKammen DP, Kelley ME, *et al*. Dopamine beta-hydroxylase: two polymorphisms in linkage disequilibrium at the structural gene DβH associate with biochemical phenotypic variation. Hum Genet, 1998, 102:533-540.

[24] Wei J, Ramchand CN, Hemmings GP. TaqI polymorphic sites at the human dopamine beta-hydroxylase gene possibly associated with biochemical alterations of the catecholamine pathway in schizophrenia. Psychiatr Genet, 1998, 8:19-24.

[25] Wood JG, Joyce PR, Miller AL, *et al*. A polymorphism in the dopamine beta-hydroxylase gene is associated with " paranoid ideation" in patients with major depression. Biol Psychiatry, 2002, 51: 365-369.

[26] Guo S, Guo KF. Research progress on depression. Chin J Clin Rehabilitat, 2005, 9:131-133.
[郭珊,郭克锋. 抑郁症的研究进展. 中国临床康复,2005,9: 131-133.]

(收稿日期:2006-11-20)

(上接 40 页)

[17] Chen MF, Chen TY. Different fast-gate regulation by external Cl (-) and H(+) of the muscle-type ClC chloride channels. J Gen Physiol, 2001, 118: 23-32.

[18] Chen TY, Chen MF, Lin CW. Electrostatic control and chloride regulation of the fast gating of ClC-0 chloride channels. J Gen Physiol, 2003, 122: 641-651.

[19] Fahlke C, Yu HT, Beck CL, *et al*. Pore-forming segments in voltage-gated chloride channels. Nature, 1997, 390: 529-532.

[20] Niemeyer MI, Cid LP, Zuniga L, *et al*. A conserved pore-lining glutamate as a voltage- and chloride-dependent gate in the ClC-2 chloride channel. J Physiol, 2003, 553: 873-879.

[21] Rychkov GY, Pusch M, Astill DS, *et al*. Concentration and pH dependence of skeletal muscle chloride channel ClC-1. J Physiol, 1996, 497: 423-435.

[22] Estevez R, Jentsch TJ. CLC chloride channels: correlating structure with function. Curr Opin Struct Biol, 2002, 12: 531-539.

[23] Pusch M, Ludewig U, Jentsch TJ. Temperature dependence of fast and slow gating relaxations of ClC-0 chloride channels. J Gen Physiol, 1997, 109: 105-116.

[24] Bennetts B, Roberts ML, Bretag AH, *et al*. Temperature dependence of human muscle ClC-1 chloride channel. J Physiol, 2001, 535: 83-93.

[25] Chen TY. Extracellular zinc ion inhibits ClC-0 chloride channels by facilitating slow gating. J Gen Physiol, 1998, 112: 715-726.

[26] Jentsch TJ, Friedrich T, Schriever A, *et al*. The CLC chloride channel family. Pflugers Arch, 1999, 437: 783-795.

[27] Simon DB, Bindra RS, Mansfield TA, *et al*. Mutations in the chloride channel gene, CLCNKB, cause Bartter´s syndrome type III. Nat Genet, 1997, 17: 171-178.

[28] Piwon N, Gunther W, Schwake M, *et al*. ClC-5 Cl^--channel disruption impairs endocytosis in a mouse model for Dent's disease. Nature, 2000, 408: 369-373.

[29] Picollo A, Pusch M. Chloride/proton antiporter activity of mammalian CLC proteins ClC-4 and ClC-5. Nature, 2005, 436: 420-423.

[30] Scheel O, Zdebik AA, Lourdel S, *et al*. Voltage-dependent electrogenic chloride/proton exchange by endosomal CLC proteins. Nature, 2005, 436: 424-427.

[31] Kornak U, Mundlos S. Genetic disorders of the skeleton: a developmental approach. Am J Hum Genet, 2003, 73: 447-474.

(收稿日期:2007-01-08)

BJ www.biochemj.org

BJ Cell

Biochem. J. (2008) **413**, 61–69 (Printed in Great Britain) doi:10.1042/BJ20071489

Analysis of carboxyl tail function in the skeletal muscle Cl^- channel hClC-1

Linlin MA*, Grigori Y. RYCHKOV*†, Bernard P. HUGHES* and Allan H. BRETAG*[1]

*Sansom Institute, School of Pharmacy and Medical Sciences, University of South Australia, North Terrace, Adelaide, SA 5000, Australia, and †Discipline of Physiology, School of Molecular and Biomedical Science, University of Adelaide, Adelaide, SA 5005, Australia

Human ClC-1 (skeletal muscle Cl^- channel) has a long cytoplasmic C-tail (carboxyl tail), containing two CBS (cystathionine β-synthase) domains, which is very important for channel function. We have now investigated its significance further, using deletion and alanine-scanning mutagenesis, split channels, GST (glutathione transferase)-pull-down and whole-cell patch-clamping. In tagged split-channel experiments, we have demonstrated strong binding between an N-terminal membrane-resident fragment (terminating mid-C-tail at Ser^{720} and containing CBS1) and its complement (containing CBS2). This interaction is not affected by deletion of some sequences, suggested previously to be important, particularly in channel gating. Contact between CBS1 and CBS2, however, may make a major contribution to assembly of functional channels from such co-expressed complements, although the possibility that C-tail fragments could, in addition, bind to other parts of the membrane-resident component has not been eliminated. We now show such an interaction between a membrane-resident component terminating at Ser^{720} (but with CBS1 deleted) and a complete C-tail beginning at Leu^{598}. Channel function is rescued in patch-clamped HEK-293T (human embryonic kidney) cells co-expressing these same fragments. From our own results and those of others, we conclude that the CBS1–CBS2 interaction is not sufficient, in itself, for channel assembly, but rather that this might normally assist in bringing some part of the CBS2/C-tail region into appropriate proximity with the membrane-resident portion of the protein. Previously conflicting and anomalous results can now be explained by an hypothesis that, for split channels to be functional, at least one membrane-resident component must include a plasma membrane trafficking signal between Leu^{665} and Lys^{680}.

Key words: carboxyl tail, common gating, cystathionine β-synthase domain (CBS domain), functional reconstitution, human skeletal muscle Cl^- channel (hClC-1).

INTRODUCTION

A significant family of proteins that catalyse transmembrane Cl^- flux, the CLC voltage-gated Cl^- channels and transporters, is unrelated to any other ion channel/transporter family, but, among its members, is quite conserved with respect to sequence and architecture [1–3]. It is therefore reasonable to take the X-ray structures determined for the prokaryotic CLC proteins from *Escherichia coli* and *Salmonella enterica* serovar Typhimurium (EcClC and StClC) [1] as the structural framework for the membrane-resident domain of their eukaryotic, and hence also mammalian, homologues. Accordingly, these membrane-resident proteins are composed of two identical subunits with 18 α-helices (A–R) in each subunit (Figure 1). In muscle-type CLC channels, an independent ion-conduction pathway in each subunit, called a protopore, provides the foundation for two distinct gating mechanisms, protopore (or fast) gating and common (or slow) gating [4]. Fast gating regulates protopores individually and independently, and is believed to be mediated by the movement of a glutamate side chain in helix F and Cl^- binding to an external binding site in the pore [5,6]. On the other hand, common gating regulates both pores simultaneously. It has been suggested that common gating might involve complex higher-order, helix–helix or protein–protein interactions based on its unusual temperature-sensitivity [7,8], but the molecular mechanism underlying this process is still far from clear.

Despite the high homology between the membrane-resident domains of eukaryotic and bacterial CLC proteins, one of the most significant differences between them is that the eukaryotic CLCs have long cytoplasmic C-tails (carboxyl tails) containing two CBS (cystathionine β-synthase) domains (CBS1 and CBS2) (Figure 1). Deletions, truncations or mutations in the C-tails resulted in poor expression, altered characteristics or non-functional channels, demonstrating their physiological significance [9–13]. For hClC-1 (human skeletal muscle Cl^- channel), the dysfunction of which leads to myotonic muscle diseases, almost one-fifth of over 120 known myotonia-causing mutations are located in its C-tail [14]. Most interestingly, the C-tails, which are distant (in primary amino acid sequence) from the membrane-resident pore regions, have been illustrated to be closely associated with the common gating of CLC channels [11,15–17]. However, in the absence of structures for whole eukaryotic CLC proteins (complete with their C-tails), just what are the molecular mechanisms underlying the functional roles of these cytoplasmic domains? For example, why are some specific short amino acid sequences in the C-tail so important for the channel function? So far, the existing evidence is quite controversial with regard to some of these issues, such as whether the C-tails are necessary for trafficking, whether CBS1 and CBS2 interact, and what function this might serve [12,15,16,18–20].

In the present study, we aimed to learn more about the inherent characteristics of the C-tail of hClC-1 by investigating the physical and functional roles of several specific regions, such as the short sequences consisting of amino acids 800–820, amino acids 863–888 and CBS domains (CBS1 and CBS2), in mammalian cells (Figure 1). These short sequences have been shown to be essential for channel function in split channels, but the underlying

Abbreviations used: CBS, cystathionine β-synthase; CLC, voltage-gated Cl^- channel family; C-region, C-terminal region; C-tail, carboxyl tail; f-, N-terminal FLAG tag; FCS, fetal calf serum; GFP, green fluorescent protein; GST, glutathione transferase; G-, GST-fusion; hClC-1, human skeletal muscle Cl^- channel; HEK-293T, human embryonic kidney; -m, C-terminal c-Myc tag; NCS, newborn calf serum; N-region, N-terminal region; TBST, Tris-buffered saline with Tween 20; WT, wild-type.

[1] To whom correspondence should be addressed (a.bretag@unisa.edu.au).

© The Authors Journal compilation © 2008 Biochemical Society

Biochemical Journal

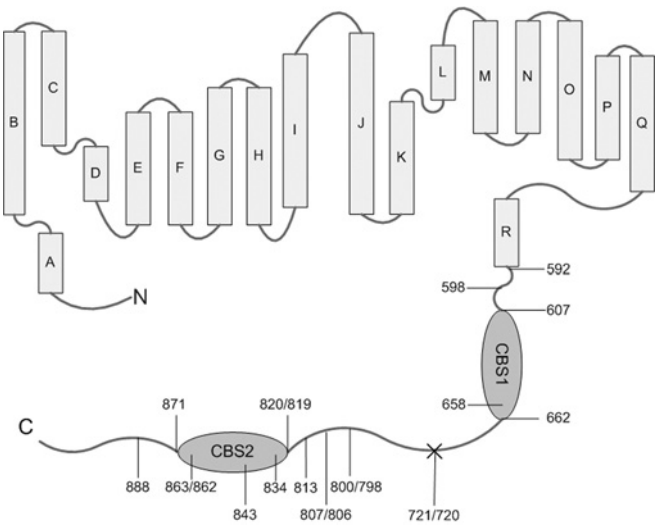


Figure 1 Schematic diagram of hClC-1

The 18 α-helices found in each subunit, are indicated by the blocks labelled A–R with the extracellular region above and the intracellular region below. Adapted by permission from Macmillan Publishers Ltd: *Nature*, Dutzler, R., Campbell, E.B., Cadene, M., Chait, B.T. and MacKinnon, R. (2002) X-ray structure of a CIC chloride channel at 3.0 Å reveals the molecular basis of anion selectivity. Nature **415**, 287–294, copyright 2002. http://www.nature.com. The CBS1 domain (amino acids 607–662) and CBS2 domain (amino acids 820–871) in the cytoplasmic C-tail are shown as ellipsoids. Amino acid numbers delineating all of the individual domains used in the present study are labelled. For the two major hClC-1 fragments, *N*720 and 721*C*, employed in our split-channel experiments, the position of the split between amino acids 720 and 721 is indicated by an X.

molecular mechanisms are still unknown [11,16]. One of the most likely explanations might be that they are essential for the binding between complementary fragments in split channels. However, we show in the present study that, when hClC-1 is cut between the CBS1 and CBS2 domains, binding between the membrane-resident part and the cytoplasmic part is not affected by the absence of any of these short sequences, but seems to rely exclusively on a direct interaction between the two CBS domains. Furthermore, although most of the previous split-channel studies rescued channel function using two complementary fragments, each containing one CBS domain [13,21,22], we have found that this is not a necessary condition. The present study shows, for the first time, that it is possible to restore function to the membrane-resident hClC-1 fragment, amino acids 1–720, even after CBS1 has been deleted, leaving it without a CBS domain. This was achieved by co-expression with a whole C-tail fragment of hClC-1 containing both CBS domains, which is similarly non-functional, if expressed alone. Presumably, an unanticipated non-covalent physical interaction between these two fragments lays the foundation for functional rescue in this split-channel experiment.

EXPERIMENTAL

Plasmid constructs of hClC-1

For convenience, we have labelled our own hClC-1 N-region (N-terminal region) peptide fragments, and those of others, as *N*720 (for amino acids 1–720, i.e. Met^{1}–Ser^{720}), *N*658 (for amino acids 1–658, i.e. Met^{1}–Glu^{658}), intermediate fragments as *X*413–720 (for amino acids 413–720, i.e. Phe^{413}–Ser^{720}) and C-region (carboxyl-region) fragments as 721*C* (for amino acids 721–988, i.e. Gly^{721}–Leu^{988} at the C-terminus), etc. (see Figure 1). Constructs of hClC-1 cDNA, designed to express the N-region peptides, *N*720 and *N*658 and the C-region peptides, typically 721*C* and 598*C*, were generated by PCR using plasmid pCI-neo-hClC-1 as the template. This plasmid comprised the mammalian expression vector pCI-neo (Promega) into which WT (wild-type) hClC-1 cDNA had been inserted [7]. To facilitate GST (glutathione transferase)-pull-down, particular constructs were labelled at their N-terminus with a FLAG epitope (DYKDDDDK) to express, e.g., FLAG–*N*720 (f-*N*720) and FLAG–721*C* (f-721*C*), whereas others were tagged at their C-terminus with a c-Myc epitope (EQKLISEEDL) to express, e.g., 598*C*–Myc (598*C*-m) and 721*C*–Myc (721*C*-m). All constructs were then subcloned into mammalian expression vector pEF-IRES-neo to achieve more efficient expression. The cDNA sequence coding for GST was amplified by PCR from the prokaryotic GST-gene-fusion vector pGEX-4T-1 (GE Healthcare) and also inserted into pEF-IRES-neo, forming the mammalian GST-fusion vector, pEF-IRES-neo-GST. Where required, our constructs, such as f-*N*720, f-*N*658 and f-721*C* were then subcloned into pEF-IRES-neo-GST to enable expression of the respective GST fusion proteins, GST–f-*N*720 (G-f-*N*720), GST–f-*N*658 (G–f-*N*658) and GST–f-721*C* (G-f-721*C*). These constructs were used as templates for subsequent mutagenesis studies. GFP (green fluorescent protein) facilitated the visualization of transfected cells in patch-clamp experiments, our 721*C* and 721*C*-m constructs having been subcloned into the pMSCV-IRES-GFP vector (designated pMIG-721*C* and pMIG-721*C*-m respectively), to allow co-ordinated expression of GFP and 721*C* or 721*C*-m.

Deletion-scanning and alanine-scanning mutagenesis

Using a method modified from overlap extension PCR [23], deletion mutations (where deletion is indicated by Δ) were introduced into G-f-*N*720, 598*C*-m and 721*C*-m to generate the constructs shown in Table 1.

Table 1 Constructs used in the present study

See Figure 1 for amino acid numbers involved.

Construct	Details	Notes
G-f-*N*720ΔCBS1	GST–FLAG–(1–720)Δ(607–662)	Deleting CBS1
G-f-*N*720ΔCBS1+	GST–FLAG–(1–720)Δ(592–662)	Deleting CBS1 plus the sequence from helix R to CBS1
721*C*-mΔCBS2β	(721–988)–MycΔ(820–862)	Deleting the $\beta_1\beta_2\alpha_1\beta_3$ region of CBS2
721*C*-mΔCBS2	(721–988)–MycΔ(820–871)	Deleting CBS2
598*C*-mΔpreCBS2	(598–988)–MycΔ(798–819)	Deleting the 22 amino acids before CBS2
598*C*-mΔCBS2α+	(598–988)–MycΔ(863–888)	Deleting the α_2 region of CBS2 plus the subsequent 17 amino acids
721*C*-mΔpreCBS2a	(721–988)–MycΔ(800–806)	Deleting seven amino acids early in the 22-amino-acid pre-CBS2 sequence
721*C*-mΔpreCBS2b	(721–988)–MycΔ(807–813)	Deleting seven amino acids in the middle of the 22-amino-acid pre-CBS2 sequence
721*C*-mΔCBS2α+	(721–988)–MycΔ(863–888)	Deleting the α_2 region of CBS2 plus the subsequent 17 amino acids

© The Authors Journal compilation © 2008 Biochemical Society

An alanine-scanning mutant, 598*C*-m/as [(598–988)–Myc/alanine-scan(834–843)], was generated in the same way with Gln^{834}–Leu^{843} being replaced by Ala_{10} (AAAAAAAAAA). After double digestion by corresponding restriction enzymes and gel purification, the N-region constructs were ligated into pEF-IRES-neo-GST vector, and those of the C-region were ligated into pEF-IRES-neo. All mutants were subsequently verified by sequencing. In most cases, two independent mutant clones were used for expression and subsequent study.

Cell culture and transfection

HEK-293T (human embryonic kidney) cells (A.T.C.C., Manassas, VA, U.S.A.) were maintained in DMEM (Dulbecco's modified Eagle's medium) supplemented with 10 % (v/v) of a mixture of NCS (newborn calf serum) and FCS (fetal calf serum) [9 % (v/v) NCS and 1 % (v/v) FCS] (Gibco), 2 mM L-glutamine and 1 % (v/v) non-essential amino acids, at 37 °C under a 5 % CO_2 atmosphere. For GST-pull-down assays, cells were plated at a density of 10^6 cells per 60-mm dish 24 h before transfection, and were transfected or co-transfected with various hClC-1 cDNA constructs. All the transient transfections and stable transfections were carried out using Lipofectamine™ 2000 (Invitrogen) according to the manufacturer's instructions. For each GST-pull-down assay, the same amount of pEF-IRES-neo-GST was transfected as a negative control, from which only GST protein would be expressed.

In the case of split-channel studies for patch-clamping, either HEK-293T cells were transiently co-transfected with *N*720 or G-f-*N*720 and pMIG-721*C* or pMIG-721*C*-m at a molar ratio of 1:1, or HEK-293T-598*C*-m cells, which were HEK-293T cells stably transfected with construct 598*C*-m, were transiently transfected with G-f-*N*720ΔCBS1 and pEGFP-N1 (Clontech) at a molar ratio of 10:1. Transfected cells could be identified by their green fluorescence, in the last case, owing to reporter-plasmid-driven expression of EGFP (enhanced GFP).

GST-pull-down assay and Western blotting

Transfected cells were harvested and lysed on ice for 30 min in lysis buffer containing 150 mM NaCl, 20 mM Tris/HCl (pH 8.0), 10 % (v/v) glycerol, 0.2 % Triton X-100, 0.2 mM DTT (dithiothreitol) and protease inhibitor cocktail (1 μg/ml pepstatin, 1 μg/ml leupeptin, 0.5 mM PMSF, 5 μg/ml benzamidine and 0.1 μl/ml aprotinin). After centrifugation at 18 000 ***g*** for 15 min at 4 °C, the supernatant was collected and the protein concentration was measured using the BCA (bicinchoninic acid) Protein Assay Kit (Pierce). Equal amounts of protein (1 mg) were incubated with 50 μl of glutathione–Sepharose 4B beads (GE Healthcare) for 3 h. The beads were then collected by short (10 s) centrifugation at 12 000 ***g*** and washed four times (10 min each time) with 1 ml of lysis buffer. All procedures were carried out at 4 °C. The bound proteins were finally liberated by heating at 55 °C for 20 min in 2× Laemmli sample buffer and separated by SDS/PAGE (6–12 % polyacrylamide).

Proteins on SDS/PAGE gels were transferred on to nitrocellulose membranes. The blots were then blocked for 1 h in TBST (Tris-buffered saline with Tween 20: 150 mM NaCl, 25 mM Tris/HCl, pH 7.4, and 0.1 % Tween 20) containing 5 % (w/v) non-fat dried skimmed milk powder and incubated for 1 h either with anti-FLAG M2 monoclonal antibody (Sigma) or with anti-Myc antibody (culture supernatant from hybridoma cell line 9E10, A.T.C.C.) in the blocking buffer. After four washes in TBST and 1 h of incubation with secondary antibody (horseradish-peroxidase-conjugated anti-mouse IgG; Sigma), reacting protein bands were visualized with an ECL® (enhanced chemiluminescence) detection system (GE Healthcare).

Electrophysiology

Patch-clamp experiments were conducted at room temperature (22–24 °C) in the whole-cell configuration using an Axopatch 200B patch-clamp amplifier and associated standard equipment (Axon Instruments), as described previously [11]. Cells were superfused continuously with bath solution containing 140 mM NaCl, 4 mM CsCl, 2 mM $CaCl_2$, 2 mM $MgCl_2$ and 10 mM Hepes, adjusted to pH 7.4 with NaOH. Patch pipettes were pulled from borosilicate glass and typically had a resistance of 1–3 MΩ when filled with the standard pipette solution containing 40 mM CsCl, 85 mM Cs glutamate, 10 mM sodium EGTA and 10 mM Hepes, adjusted to pH 7.2 with NaOH. Series resistance did not exceed 3 MΩ and was 75–85 % compensated. Currents obtained were filtered at 3 kHz, collected and analysed using Clampex 9.0 Software (Axon Instruments).

Data analysis

The voltage-dependence of the apparent overall channel open probability (P_o) was determined by measuring tail-current relaxation at a constant voltage of −100 mV for 40 ms, after 160 ms test pulses at increasingly hyperpolarizing (−20 mV) steps ranging from +100 to −140 mV. To study the voltage-dependence of the open probability of common gating (P_o^c), a short prepulse of 400 μs to +180 mV was inserted before the −100 mV tail pulse, to fully activate the fast gate, and the open probability of fast gating (P_o^f) was then calculated by dividing P_o by P_o^c [24]. Between test sweeps, the cell membrane was clamped at a holding potential of −30 mV for a period of 2 s. Apparent P_o curves were obtained by fitting data points with a Boltzmann distribution of the form:

$$P_o(V) = P_{min} + (1 - P_{min}) / \{1 + \exp[V_{½} - V)/k]\}, \quad (1)$$

where P_{min} is an offset or minimum P_o at very negative potentials, V is the membrane potential, $V_{½}$ is the potential at which $P_o = (1 + P_{min})/2$ (half-maximal activation) and k is the slope factor. All the data were analysed by Clampex 9.0 and GraphPad Prism 4.0 software using the same method described previously [11]. Potentials listed are pipette potentials expressed as intracellular potentials relative to outside zero.

RESULTS

Investigation of the effects of tags on split-channel studies

In a previously reported reconstitution of hClC-1, its N-terminal and membrane-resident region, including a short length of C-tail, typically amino acids 1–720 (*N*720), co-expressed with its complementary distal C-tail fragment, typically amino acids 721–988 (721*C*), combined to allow the flow of Cl^- currents with WT characteristics [13]. However, it is still unclear how these two complementary fragments (indicated by splitting at X in Figure 1) co-operate to produce functional channels.

To map the essential interacting parts of these N- and C-region peptides, required for this functional rescue, a panel of deletion and truncation mutants were constructed and heterologously expressed in HEK-293T cells. As necessary, all N-region constructs were tagged with GST and FLAG epitopes on their N-termini, whereas C-region constructs were all tagged with c-Myc epitopes on their C-termini to facilitate the detection of interactions. Preliminary experiments were conducted to determine whether

© The Authors Journal compilation © 2008 Biochemical Society

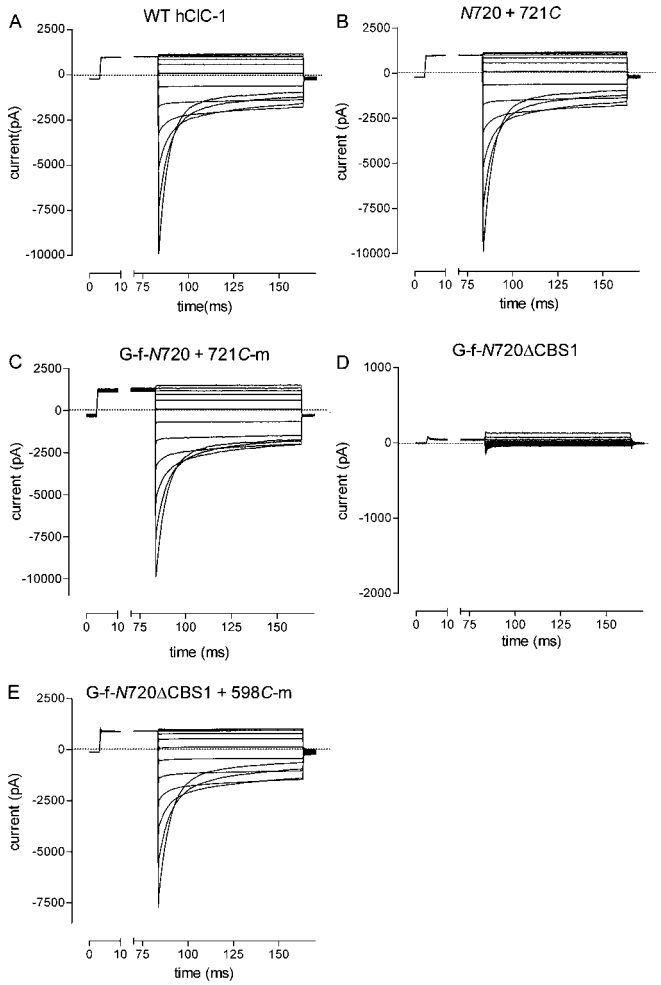


Figure 2 Electrophysiological analyses of split channels

Cl^- current traces were obtained by whole-cell patch-clamping from HEK-293T cells transfected with (**A**) the positive control WT hClC-1, (**B**) the *N*720 + 721*C* split channel without any tags on the channel fragments, (**C**) the same split channel, but now with *N*720 tagged with GST and FLAG (G-f-*N*720) and *721C* tagged with c-Myc (721*C*-m), (**D**) the same N-region component (G-f-*N*720), but with CBS1 deleted (G-f-*N*720ΔCBS1), and (**E**) a co-expression of the CBS1-deleted N-region component (G-f-*N*720ΔCBS1) plus the complete C-tail (598*C*-m). As the negative control, cells transfected with G-f-*N*720ΔCBS1 alone show no Cl^- currents (**D**). In contrast, all of the co-expressions with or without tags supported currents indistinguishable from the WT control. Currents were recorded 24 h after transfection in response to test pulses of 80 ms duration in steps of − 20 mV from + 80 mV to − 140 mV following a conditioning pulse to + 40 mV for 80 ms.

these tags would affect channel reconstitution by comparing the function of channels composed of fragments with antigenic tags (G-f-*N*720+721*C*-m) or without them (*N*720+721*C*). As shown in Figure 2 and Table 2, according to our patch-clamp results, there was no significant difference from WT hClC-1, with both split channels producing similar currents (as opposed to the situation in which N-region or C-region peptides were expressed alone, where there were no currents; see, e.g., Figure 2D). Typical WT currents featured inward rectification, depolarization-induced activation, a rapid partial deactivation upon hyperpolarization with a bi-exponential deactivation time course, and the presence of two kinetically distinct gating processes. In this way, we were able to exclude any effects of the chosen tags on the expression, targeting or function of either N-region or C-region peptides in our split-channel experiments.

Table 2 $V_{½}$ of overall channel open probability (P_o), fast gating (P_o^f) and common gating (P_o^c) for WT hClC-1 and split hClC-1 channels

Peak tail currents, recorded using the protocols described in the Experimental section, were used to derive P_o values, and these were fitted with Boltzmann distribution curves. Fast and common gating parameters were separated using the method of Accardi and Pusch [24]. The truncated mutant, G-f-*N*720ΔCBS1, with CBS1 deleted, showed no Cl^- currents by itself. None of the split channels has characteristics that are significantly different from the WT hClC-1 channel. Values of $V_{½}$ in millivolts (mV) are shown as means ± S.E.M.

WT/split channel (no. of cells)	$V_{½}$ P_o (mV)	$V_{½}$ P_o^f (mV)	$V_{½}$ P_o^c (mV)
WT hClC-1 (n = 15)	− 71.7 ± 2.5	− 106.4 ± 0.8	− 78.0 ± 2.0
*N*720 + 721*C* (n = 7)	− 72.1 ± 1.3	− 102.4 ± 1.2	− 64.5 ± 2.1
G-f-*N*720 + 721*C*-m (n = 8)	− 80.2 ± 1.7	− 96.8 ± 2.5	− 76.1 ± 1.4
G-f-*N*720ΔCBS1 (n = 8)	No currents	No currents	No currents
G-f-*N*720ΔCBS1 + 598*C*-m (n = 6)	− 69.6 ± 2.2	− 84.7 ± 1.8	− 73.4 ± 2.3

Identification of interacting regions in split-channel G-f-*N*720 + 721*C*-m

Subsequent to the above verifications, protein–protein interaction studies of different split channels were carried out by GST-pull-down assays, in which split-channel G-f-*N*720 + 721*C*-m was used as a positive control, and a construct with only GST protein expressed was used as the negative control to confirm the specificity of the results. In all of the GST-pull-down experiments, a reasonable expression level of the N-region peptides, which is a basic requirement to exclude false negative results, was first tested by Western blot using anti-FLAG M2 antibody. As shown in Figures 3(A), 4(A), 4(B) and 5(B), G-f-721*C* and all of the GST-fused N-region peptides, which were used as bait proteins for GST-pull-down in the present study, were very well expressed.

First of all, we found that the shorter C-tail peptide, 721*C*, which contains only CBS2, could bind to itself, forming a homodimeric complex in the absence of CBS1 as its normal binding partner (Figure 3B, lanes 4–6).

When some apparently functionally important short amino acid sequences, including amino acids 800–806, amino acids 807–813 [16] and amino acids 863–888 [11], were deleted from 721*C*-m (generating 721*C*-mΔpreCBS2a, 721*C*-mΔpreCBS2b and 721*C*-mΔCBS2α+ respectively), there was still strong binding with G-f-*N*720 (Figure 3C). So, although these short sequences might be essential for channel function, they are unnecessary for binding between the complementary fragments *N*720 and 721*C*.

However, when CBS1 (amino acids 607–662) or CBS1 together with a short sequence leading up to it from the end of helix R (amino acids 592–662) was deleted from G-f-N720, generating G-f-*N*720ΔCBS1 and G-f-*N*720ΔCBS1+ respectively, binding with 721*C*-m could no longer be detected (Figure 4C). Similarly, when the β1–β3 sequence of CBS2 (amino acids 820–862) or the whole of CBS2 (amino acids 820–871) was deleted from 721*C*-m, generating 721*C*-mΔCBS2β and 721*C*-mΔCBS2 respectively, interaction with G-f-*N*720 disappeared as well (Figures 4D–4E). Therefore the coexistence of CBS1 in *N*720 and CBS2 in 721*C* was indispensable for the binding between these two channel fragments.

The more severely truncated N-region construct, *N*658, in which a short sequence at the end of the CBS1 domain is missing, is similar to the naturally occurring myotonic mutation (Q658Stop). We wanted to know whether 721*C* could help to restore its function on co-expression in HEK-293T cells. Unfortunately, *N*658 degraded even when co-expressed with 721*C* (Figure 4A, lane 3), which obviously explained very well the absence of interaction between them (Figure 4C). It had earlier been shown that an *N*679 + 721*C* co-expression could generate

© The Authors Journal compilation © 2008 Biochemical Society

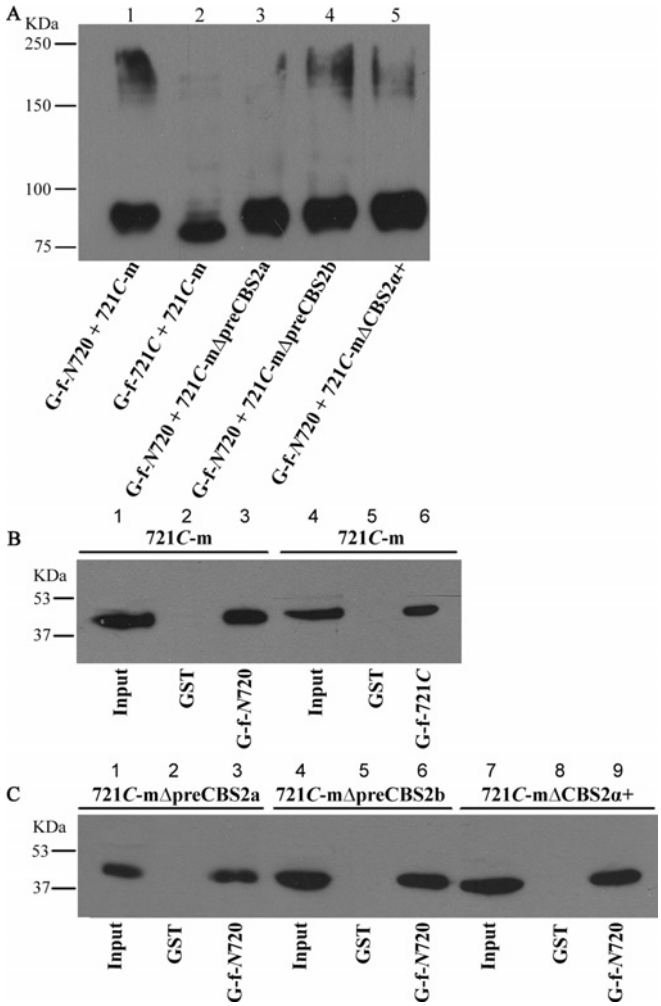


Figure 3 Interaction between various 721*C*-m mutants and G-f-*N*720

(**A**) Inputs of GST-fusion proteins in each GST-pull-down assay, detected by Western blotting using anti-FLAG M2 antibody showing that GST-fusion proteins are well expressed. Lanes 1 and 3–5 show the expression levels of G-f-*N*720 when it was co-expressed with 721*C*-m variants using 721*C*-m itself as positive control, then with 721*C*-mΔpreCBS2a (amino acids 800–806 deleted), 721*C*-mΔpreCBS2b (amino acids 807–813 deleted) and 721*C*-mΔCBS2α+ (amino acids 863–888 deleted) respectively. The lower band in each lane of molecular mass ~80 kDa corresponds to the monomer of G-f-*N*720, and the upper band in each lane of molecular mass ~160 kDa is probably an SDS-resistant homodimer. The single band in lane 2 of molecular mass ~75 kDa shows the expression level of G-f-721*C* when it was co-expressed with 721*C*-m to investigate whether this short tail peptide could form a dimer, independently. (**B**) GST-pull-down shows the direct interaction between G-f-*N*720 and 721*C*-m (lanes 1–3), which serves as a positive control for all of the other GST-pull-down assays. Also, as demonstrated by the binding between G-f-721*C* and 721*C*-m (lanes 4–6), 721*C* can form homodimers *in vitro*. (**C**) GST-pull-down results demonstrate the interaction between G-f-*N*720 and the 721*C*-m variants, 721*C*-mΔpreCBS2a (lanes 1–3), 721*C*-mΔpreCBS2b (lanes 4–6) and 721*C*-mΔCBS2α+ (lanes 7–9) respectively. The Input lanes indicate the input of the 721*C*-m mutants in each pull-down assay, detected by Western blotting using 9E10 anti-Myc antibody. The GST lanes show the GST-pull-down results for the same 721*C*-m mutants using unfused GST protein as negative controls to exclude the possibility that the target proteins could be pulled down by GST protein itself. The G-f-*N*720 or G-f-721*C* lanes are GST-pull-downs showing the interaction between G-f-*N*720 or G-f-721*C* (as the bait protein) and the 721*C*-m variants (as target proteins). All GST-pull-down assays were carried out using glutathione–Sepharose 4B beads for precipitation and the anti-Myc antibody for detection in Western blotting. Molecular masses are indicated in kDa.

WT-like currents [16], so the sequence between amino acids 659 and 679 might be important for maintaining the integrity of the membrane-resident N-region of the channel protein in the absence of a CBS2-containing tail. This might also explain why an N-region hClC-1 construct truncated beyond Gln^{597} could not be functionally rescued by its complementary C-tail in the co-expression, *N*597 + 598*C* [13]. For this reason, we undertook the following experiments keeping this short region (amino acids 659–679) intact within the N-region peptide.

Interaction between the whole C-tail and the membrane-resident domain

Notice that the above CBS1–CBS2 interaction occurs between CBS1, which exists in the N-region peptide, *N*720, and CBS2 in the C-region peptide, 721C. Also, most of the previous split-channel experiments have shown that CBS1 and CBS2 need to be in the N-region and C-region complemented fragments respectively to rescue channel function [13,16,21,22]. Therefore it seemed quite reasonable to deduce, based on previous reports and our present results, that the interaction between CBS1 and CBS2 in complemented fragments would be essential for restoring channel function in split channels. Are there, however, any other interactions between the C-tail and the membrane-resident domain besides this CBS1–CBS2 interaction? How, for example, could the CBS1–CBS2 pair support common gating, which also involves interacting helices at the dimer interface and the R helix [25,26]? To try to answer these questions, we designed a new split-channel experiment, in which fragment *N*720 with CBS1 deleted (G-f-*N*720ΔCBS1) was to be co-expressed with 598*C*-m (Figure 5A). In this way, we should be able to exclude the effect of CBS1–CBS2 interaction between the split N- and C-region channel fragments and investigate the relationship between the whole C-tail, which contains both CBS1 and CBS2, and the membrane-resident region without any CBS domain. We expected that the N-region channel fragment would be expressed well, since most of the amino acids 659–679 sequence is kept intact.

Interestingly, we detected binding between G-f-*N*720ΔCBS1 and 598*C*-m by GST-pull-down, indicating that there is, indeed, protein–protein interaction between the whole C-tail containing the two CBS domains and the membrane-resident N-region with no CBS domain (Figures 5B and 5C). To investigate whether such interaction is functionally significant, we also studied the electrophysiological features of this split channel by whole-cell patch-clamping. As shown in Figure 2(D), no Cl^- currents could be obtained when the truncated mutant, G-f-*N*720ΔCBS1, was expressed alone in HEK-293T cells. Upon co-expression with the whole C-tail, 598*C*-m, however, Cl^- channel function was fully restored (Figure 2E, and Table 2), with no significant difference from WT hClC-1 currents.

When we tried to narrow down the essential positions further, with respect to the interactions between the C-tail peptide, 598*C*, and the membrane-resident N-region, we found that, unfortunately, the expression of 598*C* seemed to be very dependent on its total integrity. Deletion of short internal sequences or alanine-scanning of the α1 helix of CBS2, Δ(798–819) (598*C*-mΔpreCBS2), Δ(863–888) (598*C*-mΔCBS2α+) and alanine-scan amino acids 834–843 (598*C*-m/as) (Figure 1) either made this fragment too unstable to be expressed (for 598*C*-mΔpre CBS2 and 598*C*-mΔCBS2α+) or caused it to be expressed very weakly (for 598*C*-m/as) (results not shown).

DISCUSSION

The C-tail of eukaryotic CLC channels has been shown to be involved in important channel characteristics such as common gating and sensing cellular energy status [15,16,20,27]. In particular, it has been demonstrated recently, by solving the crystal

© The Authors Journal compilation © 2008 Biochemical Society

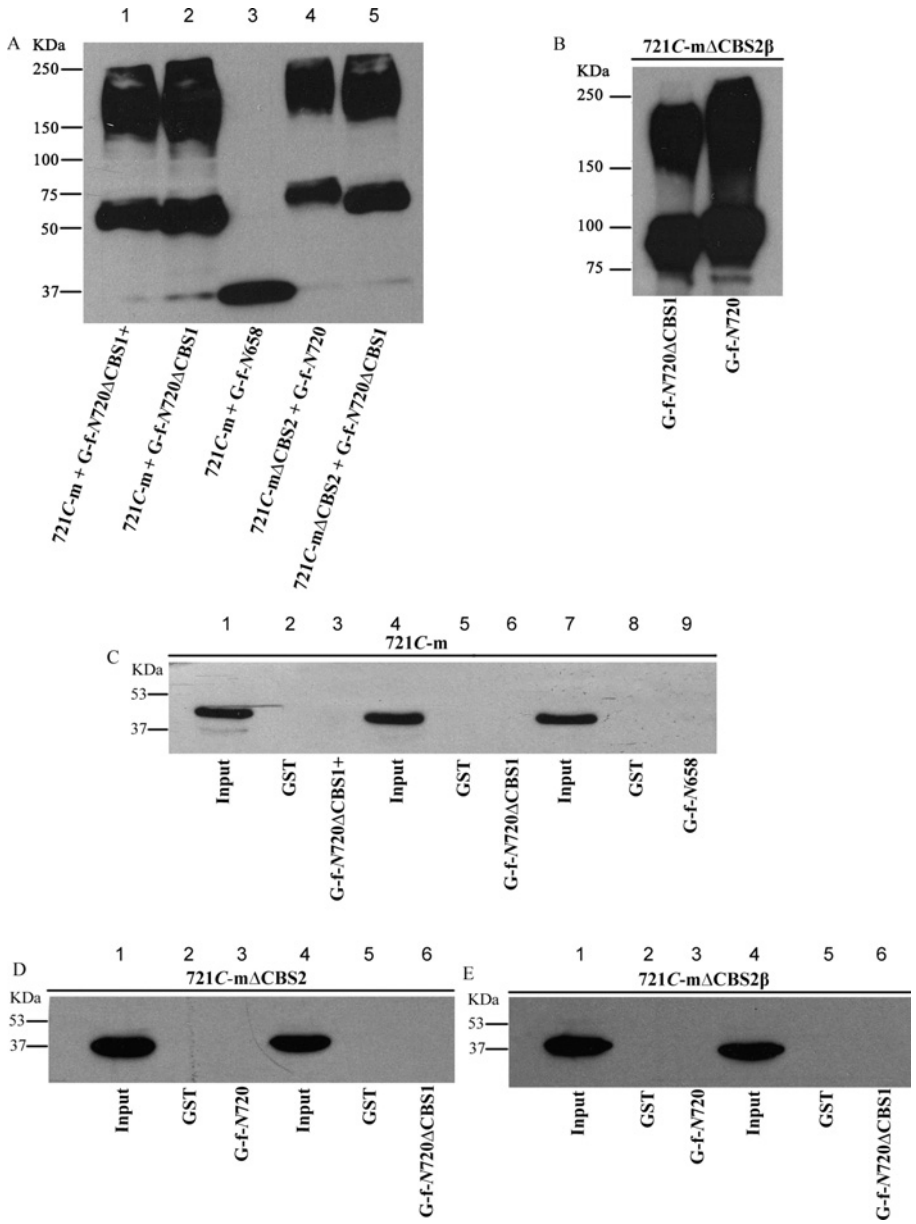


Figure 4 Effects of CBS domains and related regions on the interaction between complemented channel fragments G-f-*N*720 and 721*C*-m

(**A**, **B**) Inputs of GST-fusion proteins in each GST-pull-down assay, with the lower bands (~75 kDa for G-f-*N*720ΔCBS1+ and G-f-*N*720ΔCBS1; ~80 kDa for G-f-*N*720) representing monomers and the upper bands (~150 kDa for G-f-*N*720ΔCBS1+ and G-f-*N*720ΔCBS1; ~160 kDa for G-f-*N*720) corresponding to SDS-resistant dimers. Degradation of G-f-*N*658 to ~35 kDa occurred, even when co-expressed with 721C-m (lane 3 of **A**). Detection was by Western blotting using anti-FLAG M2 antibody. (**C**–**E**) Results from GST-pull-down assays illustrate that there is no interaction between any of the G-f-*N*720 mutants and their 721*C*-m mutant complements, including G-f-*N*720ΔCBS1+ + 721*C*-m (**C**, lanes 1–3), G-f-*N*720ΔCBS1 + 721*C*-m (**C**, lanes 4–6), G-f-*N*658 + 721*C*-m (**C**, lanes 7–9), G-f-*N*720 + 721*C*-mΔCBS2 (**D**, lanes 1–3), G-f-*N*720ΔCBS1 + 721*C*-mΔCBS2 (**D**, lanes 4–6), G-f-*N*720 + 721*C*-mΔCBS2β (**E**, lanes 1–3), and G-f-*N*720ΔCBS1 + 721*C*-mΔCBS2β (**E**, lanes 4–6). The Input lanes indicate the input of the 721*C*-m mutants in each pull-down assay, detected by Western blotting using 9E10 anti-Myc antibody. The GST lanes show the GST-pull-down results for the same 721*C*-m mutants using unfused GST protein as negative controls to exclude the possibility that the target proteins could be pulled down by GST protein itself. The remaining lanes are GST-pull-downs showing the interaction between the bait protein and the 721*C*-m variants (as target proteins). All GST-pull-down assays were carried out using glutathione–Sepharose 4B beads for precipitation and the anti-Myc antibody for detection in Western blotting. Molecular masses are indicated in kDa.

structure of the cytoplasmic domain of ClC-5 in complex with ATP and ADP, that the C-tail contains a specific binding site for nucleotides, which raises additional interest in this region [28]. However, the molecular mechanisms underlying the functional significance of these C-tails are still unclear. In the present study, we have investigated the C-tail of hClC-1, focusing on several functionally important regions using split-channel strategies, and revealed that the interaction between CBS1 and CBS2 could form a structural foundation for the whole C-tail to communicate with the membrane-resident pore domain.

According to the crystal structure of the cytoplasmic domain of ClC-0 from the electric ray *Torpedo marmorata*, 25 residues of the linker region before CBS2 forms a helix followed by an extended loop, which interacts with CBS1 [29]. In hClC-1, the corresponding putative small helix before CBS2 includes amino acids 800–820, a short sequence which had been found to be

© The Authors Journal compilation © 2008 Biochemical Society

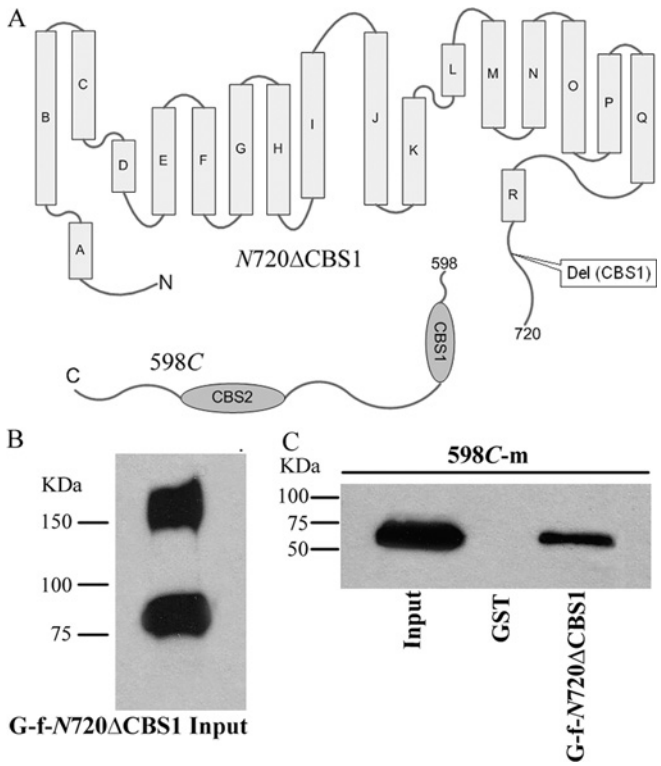


Figure 5 Interaction between 598*C*-m and G-f-*N*720ΔCBS1

(**A**) Schematic representation of split-channel G-f-*N*720ΔCBS1 + 598*C*-m. Adapted by permission from Macmillan Publishers Ltd: *Nature*, Dutzler, R., Campbell, E.B., Cadene, M., Chait, B.T. and MacKinnon, R. (2002) X-ray structure of a CIC chloride channel at 3.0 Å reveals the molecular basis of anion selectivity. Nature **415**, 287–294, copyright 2002. http://www.nature.com. The N-region peptide has CBS1 deleted, and the C-region peptide contains both CBS1 and CBS2. (**B**) The input of GST-fusion protein G-f-*N*720ΔCBS1 in the GST-pull-down assay, detected by Western blotting using anti-FLAG M2 antibody. (**C**) GST-pull-down result of 598*C*-m + G-f-*N*720ΔCBS1, showing the specific interaction between these two fragments. The Input lanes indicate the input of the 598*C*-m mutants in each pull-down assay, detected by Western blotting using 9E10 anti-Myc antibody. The GST lane shows the GST-pull-down result for 598*C*-m using unfused GST protein as a negative control to exclude the possibility that the target proteins could be pulled down by GST protein itself. The G-f-*N*720ΔCBS1 lane is a GST-pull-down showing the interaction between G-f-*N*720ΔCBS1 (as bait protein) and 598*C*-m (as target protein). All GST-pull-down assays were carried out using glutathione–Sepharose 4B beads for precipitation and the anti-Myc antibody for detection in Western blotting. Molecular masses are indicated in kDa.

necessary in the functional interaction between complementary fragments *N*720 and 721*C* [16]. Out of three smaller fragments within this 20-amino-acid stretch (amino acids 800–806, amino acids 807–813 and amino acids 814–820), only deletion of amino acids 807–813 from 721*C* completely prevented the recovery of Cl^- currents when co-expressed with *N*720 in *Xenopus* oocytes [16]. In the present study, we investigated the physical role of amino acids 807–813 in this interaction, using amino acids 800–806 as a plausible negative control. Also, a short peptide of 26 amino acids from Leu^{863} to Arg^{888} had been found to be particularly important, because channel function was restored by co-expressing this peptide with the otherwise inactive truncation, G721Stop (*N*720), in the *Xenopus* oocyte system [11]. Therefore amino acids 863–888, another possible candidate sequence for interaction with the membrane-resident pore region, was deleted from 721*C* to investigate its role in the binding between *N*720 and 721*C*. Surprisingly, none of the functionally significant short sequences, whether present or absent, had any obvious effect on binding. The substantial influences of these short sequences on function might therefore reflect relatively weak interactions with the membrane-resident pore domain, rather than, themselves, constituting strong binding sites for the functional rescue of this split channel. Alternatively, their role in the binding between *N*720 and 721*C* could be compensated for by some other definable parts of the C-tail when they are deleted individually.

Two CBS domains, each composed of two α-helical and three β-strand segments in the order $\beta_1\alpha_1\beta_2\beta_3\alpha_2$, are arranged in tandem within the C-tails of all eukaryotic CLC proteins [30]. In CLC channels, the function of CBS domains is still quite controversial [16,20,31]. Bacterial CLC proteins dimerize in the absence of CBS domains, so it can be inferred that the CBS domains are not required for dimerization [2,16]. Furthermore, the CBS domains reside in the cytosol and therefore do not contribute to the core structure of the permeation pathway, which is formed by the membrane-embedded α-helices [2]. Then how do these domains carry out their essential roles in channel function? The present work examines the roles of CBS domains in the split hClC-1 channel by physical interaction assessment, and reveals that the interaction between CBS1 and CBS2 is precisely the primary structural foundation for the functional rescue of the split channel when the channel protein is split between the two CBS domains. Moreover, we find that the CBS1–CBS2 interaction might only be a first step in the complicated conformational rearrangements which are necessary for the functional reconstitution of split channels. This is demonstrated by the binding of 598*C* to *N*720ΔCBS1 and by the functional channel that is generated from co-expressing these two fragments. The CBS pair, which forms in the whole C-tail (598*C*), probably acts as a structural and functional unit to transfer essential information to the membrane-resident pore region by close non-covalent association with some specific sequences in the transmembrane helices or the cytoplasmic loops linking them.

It seems that otherwise-intact hClC-1 channels remain functional if either individual CBS domain is deleted [16,20]. Functional reconstitution in split channels, however, requires CBS1–CBS2 interaction, presumably initiating some significant and essential, but currently unknown, conformational change amounting to rather more than just the process of the two CBS domains binding to each other.

For split-channel *N*720 + 721*C*, the CBS2 domain might be needed to bring the distal sequence following it into the correct position to confer some necessary tertiary structure by interacting with CBS1. For split-channel *N*720ΔCBS1 + 598*C*, when CBS2 and its distal tail have already positioned correctly with respect to CBS1, the cytoplasmic domain with a specific three-dimensional structure could then interact with the membrane-resident pore domain to support some key attributes of the channel, such as common gating.

For both ClC-0 and hClC-1, common gating has been found to be temperature-sensitive, suggesting that it is associated with complex structural rearrangements [7,8]. Besides the broad interface between the two subunits, such changes might also involve the final helix, helix R, and the distal C-tail (CBS2 and the sequence that follows CBS2). Many mutations that change gating of different CLC family members are located within this distal part of the C-tail, such as A885P, H835R and H838A in hClC-1 [32], H736A, E763K and A783P in ClC-0 [16] and, putatively, since they are dominant mutations, G765D and R767W in ClC-7 [33]. Moreover, several truncations or substitutions of the C-tail after CBS2 show large shifts in the open probability of the channels [12,34]. Especially, in this region, a conserved sequence, LRPPLASFR, was recently identified as important for the voltage-dependence of gating in hClC-1 (where it occurs at amino acids 880–888) and also in ClC-0 [35]. On the other hand, helix R of

© The Authors Journal compilation © 2008 Biochemical Society

the membrane-resident domain, which is directly followed by the C-tail, contributes a tyrosine residue (Tyr^{589}) to co-ordinate a Cl^- ion in the central ion-binding site (S_{cen}) of the selectivity filter. This peculiar architecture, along with the possible proximity of CBS2 and the following C-tail sequence to the pore region in the crystal structure, as demonstrated by some studies [29,36], provides a plausible structural explanation for our findings. Thus we suggest that, in the usual split channels, CBS1 and CBS2 might first bind with each other to expose the α-helices of CBS2 to the surface and to bring the distal C-tail close enough to helix R and nearby regions of the membrane-resident domain. This could then trigger a possible interaction between the C-tail and the selectivity filter, which leads to a conformational rearrangement in the ion conduction path and modulates the channel's common gating.

Nevertheless, although in split channels, CBS1 and CBS2 domains could make a co-operative contribution to the rescue of normal channel operation by interacting with each other, each of them still seems to have its own specific role. It was shown that CBS1 could functionally replace the CBS2 domain of 721*C* in split-channel studies, but, when CBS1 was replaced by CBS2 in the uninterrupted hClC-1 protein, no detectable hClC-1 currents could be recorded [16]. From the present CBS2–CBS2 binding result (Figure 3B), we are able to deduce that CBS2 could not replace CBS1 in the earlier work [16], probably because of some distinctive requirement for CBS1 within its adjacent sequence environment, rather than because of an interaction failure between the two CBS2 domains.

Our present studies, in conjunction with previous split-channel results [11,13,16,20,22], allow us to hypothesize that the short stretch from amino acids 666 to 679 in ClC-1 might include a trafficking signal. We propose that this signal must be contiguous with at least one membrane-resident component of split hClC-1 channels, instead of being contained solely within a cytoplasmic C-tail fragment. Non-covalent association of the two (or more) components would then allow transport to the plasma membrane, incorporation and function. Proteins that fail to be trafficked to the plasma membrane might then be degraded. In this way, it is possible to explain our present functional reconstitution of *N720ΔCBS1 + 598C and that of previously tested split ClC-1 channels, *N720 + 721C, N390 + *369C, N451 + *413C, *N679 + 801C, N451 + *X413–720 + 721C and *N720 + X863–888 [11,13,16]. The asterisks indicate the components in which the putative trafficking signal might reside. If this trafficking signal, however, only exists in the cytoplasmic fragment of a split channel, such as in N597 + *598C or N650 + *590C, or if it is missed, as in N665 + 721C, then, as has been observed [13,20], we would expect no functional rescue. The last of these, N665 + 721C, also serves to underline our contention that the presence of both CBS1 and CBS2 in the split channel is, alone, inadequate for trafficking/functional reconstitution, even though it might be sufficient to establish binding between the two components. Results from in-frame deletions of CBS1 and/or the CBS1–CBS2 interlinker region up to amino acid 818, within otherwise continuous hClC-1 proteins [20], however, suggest that this putative signal region may be unnecessary if the C-tail extends its subsequent full and uninterrupted length.

Clearly, more studies and new methods are required to elucidate the different properties of the CBS1 and CBS2 domains, and to narrow down the sites of significant interaction between the membrane-resident pore region of the channel and its C-tail.

We thank Dr B.J. Roberts and Mr S.M. Paltoglou for their help and guidance. This work was supported by a Discovery Grant from the Australian Research Grants Committee, and by grants from the Muscular Dystrophy Association of South Australia and from the Sansom Institute and the Research Committee of the University of South Australia.

REFERENCES

1 Pusch, M. and Jentsch, T. J. (2005) Unique structure and function of chloride transporting CLC proteins. IEEE Trans. Nanobiosci. **4**, 49–57
2 Dutzler, R., Campbell, E. B., Cadene, M., Chait, B. T. and MacKinnon, R. (2002) X-ray structure of a CIC chloride channel at 3.0 Å reveals the molecular basis of anion selectivity. Nature **415**, 287–294
3 Accardi, A and Miller, C. (2004) Secondary active transport mediated by a prokaryotic homologue of CIC Cl^- channels. Nature **427**, 803–807
4 Rickard, H. R., Bartley, P. A., Bagley, C. J. and Bretag, A. H. (2005) The CLC family of proteins: chloride transporters and channels. In Bacterial Ion Channels and their Eukaryotic Homologs (Kubalski, A. and Martinac, B., eds.), pp. 209–246, ASM Press, Washington
5 Pusch, M., Ludewig, U., Rehfeldt, A. and Jentsch, T. J. (1995) Gating of the voltage-dependent chloride channel CIC-0 by the permeant anion. Nature **373**, 527–531
6 Rychkov, G. Y., Pusch, M., Astill, D. S., Roberts, M. L., Jentsch, T. J. and Bretag, A. H. (1996) Concentration and pH dependence of skeletal muscle chloride channel CIC-1. J. Physiol. **497**, 423–435
7 Bennetts, B., Roberts, M. L., Bretag, A. H. and Rychkov, G. Y. (2001) Temperature dependence of human muscle CIC-1 chloride channel. J. Physiol. **535**, 83–93
8 Pusch, M., Ludewig, U. and Jentsch, T. J. (1997) Temperature dependence of fast and slow gating relaxations of CIC-0 chloride channels. J. Gen. Physiol. **109**, 105–116
9 Haug, K., Warnstedt, M., Alekov, A. K., Sander, T., Ramírez, A., Poser, B., Maljevic, S., Hebeisen, S., Kubisch, C., Rebstock, J. et al. (2003) Mutations in *CLCN2* encoding a voltage-gated chloride channel are associated with idiopathic generalized epilepsies. Nat. Genet. **33**, 527–532
10 Simpson, B. J., Height, T. A., Rychkov, G. Y., Nowak, K. J., Laing, N. G., Hughes, B. P. and Bretag, A. H. (2004) Characterization of three myotonia-associated mutations of the CLCN1 chloride channel gene via heterologous expression. Hum. Mutat. **24**, 185
11 Wu, W., Rychkov, G. Y., Hughes, B. P. and Bretag, A. H. (2006) Functional complementation of truncated human skeletal-muscle chloride channel (hCIC-1) using carboxyl tail fragments. Biochem. J. **395**, 89–97
12 Hryciw, D. H., Rychkov, G. Y., Hughes, B. P. and Bretag, A. H. (1998) Relevance of the D13 region to the function of the skeletal muscle chloride channel, CIC-1. J. Biol. Chem. **273**, 4304–4307
13 Schmidt-Rose, T. and Jentsch, T. J. (1997) Reconstitution of functional voltage-gated chloride channels from complementary fragments of CLC-1. J. Biol. Chem. **272**, 20515–20521
14 Pusch, M. (2002) Myotonia caused by mutations in the muscle chloride channel gene *CLCN1*. Hum. Mutat. **19**, 423–434
15 Bennetts, B., Rychkov, G. Y., Ng, H. L., Morton, C. J., Stapleton, D., Parker, M. W. and Cromer, B. A. (2005) Cytoplasmic ATP-sensing domains regulate gating of skeletal muscle CIC-1 chloride channels. J. Biol. Chem. **280**, 32452–32458
16 Estévez, R., Pusch, M., Ferrer-Costa, C., Orozco, M. and Jentsch, T. J. (2004) Functional and structural conservation of CBS domains from CLC chloride channels. J. Physiol. **557**, 363–378
17 Yusef, Y. R., Zúñiga, L., Catalán, M., Niemeyer, M. I., Cid, L. P. and Sepúlveda, F. V. (2006) Removal of gating in voltage-dependent CIC-2 chloride channel by point mutations affecting the pore and C-terminus CBS-2 domain. J. Physiol. **572**, 173–181
18 Schwappach, B., Stobrawa, S., Hechenberger, M., Steinmeyer, K. and Jentsch, T. J. (1998) Golgi localization and functionally important domains in the NH2 and COOH terminus of the yeast CLC putative chloride channel Gef1p. J. Biol. Chem. **273**, 15110–15118
19 Carr, G., Simmons, N. and Sayer, J. (2003) A role for CBS domain 2 in trafficking of chloride channel CLC-5. Biochem. Biophys. Res. Commun. **310**, 600–605
20 Hebeisen, S., Biela, A., Giese, B., Müller-Newen, G., Hidalgo, P. and Fahlke, C. (2004) The role of the carboxyl terminus in CIC chloride channel function. J. Biol. Chem. **279**, 13140–13147
21 Mo, L., Xiong, W., Qian, T., Sun, H. and Wills, N. K. (2004) Coexpression of complementary fragments of CIC-5 and restoration of chloride channel function in a Dent's disease mutation. Am. J. Physiol. Cell. Physiol. **286**, C79–C89
22 Maduke, M., Williams, C. and Miller, C. (1998) Formation of CLC-0 chloride channels from separated transmembrane and cytoplasmic domains. Biochemistry **37**, 1315–1321
23 Ho, S. N., Hunt, H. D., Horton, R. M., Pullen, J. K. and Pease, L. R. (1989) Site-directed mutagenesis by overlap extension using the polymerase chain reaction. Gene **77**, 51–59
24 Accardi, A. and Pusch, M. (2000) Fast and slow gating relaxations in the muscle chloride channel CLC-1. J. Gen. Physiol. **116**, 433–444
25 Duffield, M., Rychkov, G., Bretag, A. and Roberts, M. (2003) Involvement of helices at the dimer interface in CIC-1 common gating. J. Gen. Physiol. **121**, 149–161
26 Chen, T. Y. (2005) Structure and function of CLC channels. Annu. Rev. Physiol. **67**, 809–839
27 He, L., Denton, J., Nehrke, K. and Strange, K. (2006) Carboxy terminus splice variation alters CIC channel gating and extracellular cysteine reactivity. Biophys. J. **90**, 3570–3581

© The Authors Journal compilation © 2008 Biochemical Society

28 Meyer, S., Savaresi, S., Forster, I. C. and Dutzler, R. (2007) Nucleotide recognition by the cytoplasmic domain of the human chloride transporter CIC-5. Nat. Struct. Mol. Biol. **14**, 60–67
29 Meyer, S. and Dutzler, R. (2006) Crystal structure of the cytoplasmic domain of the chloride channel CIC-0. Structure **14**, 299–307
30 Estévez, R. and Jentsch, T. J. (2002) CLC chloride channels: correlating structure with function. Curr. Opin. Struct. Biol. **12**, 531–539
31 Ignoul, S. and Eggermont, J. (2005) CBS domains: structure, function, and pathology in human proteins. Am. J. Physiol. Cell. Physiol. **289**, C1369–C1378
32 Beck, C. L., Fahlke, C. and George, Jr, A. L. (1996) Molecular basis for decreased muscle chloride conductance in the myotonic goat. Proc. Natl. Acad. Sci. U.S.A. **93**, 11248–11252
33 Cleiren, E., Bénichou, O., Van Hul, E., Gram, J., Bollerslev, J., Singer, F. R., Beaverson, K., Aledo, A., Whyte, M. P., Yoneyama, T. et al. (2001) Albers–Schönberg disease (autosomal dominant osteopetrosis, type II) results from mutations in the *CICN7* chloride channel gene. Hum. Mol. Genet. **10**, 2861–2867
34 Fong, P., Rehfeldt, A. and Jentsch, T. J. (1998) Determinants of slow gating in CIC-0, the voltage-gated chloride channel of *Torpedo marmorata*. Am. J. Physiol. **274**, C966–C973
35 Macías, M. J., Teijido, O., Zifarelli, G., Martin, P., Ramirez-Espain, X., Zorzano, A., Palacín, M., Pusch, M. and Estévez, R. (2007) Myotonia-related mutations in the distal C-terminus of CIC-1 and CIC-0 chloride channels affect the structure of a poly-proline helix. Biochem. J. **403**, 79–87
36 Markovic, S. and Dutzler, R. (2007) The structure of the cytoplasmic domain of the chloride channel CIC-Ka reveals a conserved interaction interface. Structure **15**, 715–725

Received 30 October 2007/6 March 2008; accepted 6 March 2008
Published as BJ Immediate Publication 6 March 2008, doi:10.1042/BJ20071489

© The Authors Journal compilation © 2008 Biochemical Society

The International Journal of Biochemistry & Cell Biology 41 (2009) 1402–1409

Contents lists available at ScienceDirect

The International Journal of Biochemistry & Cell Biology

journal homepage: www.elsevier.com/locate/biocel

Functional study of cytoplasmic loops of human skeletal muscle chloride channel, hClC-1

Linlin Ma[a], Grigori Y. Rychkov[a,b], Allan H. Bretag[a,*]

[a] Sansom Institute, School of Pharmacy and Medical Sciences, University of South Australia, North Terrace, Adelaide, SA 5000, Australia
[b] Discipline of Physiology, School of Molecular and Biomedical Science, University of Adelaide, Adelaide, SA 5005, Australia

ARTICLE INFO

Article history:
Received 5 September 2008
Received in revised form 10 December 2008
Accepted 10 December 2008
Available online 24 December 2008

Keywords:
hClC-1
Cytoplasmic loop
Common gating
Carboxyl tail
Interaction

ABSTRACT

The membrane-resident domain of chloride channels and transporters of the CLC family is composed of 18 α-helices (designated A to R) connected sequentially by extracellular and intracellular loops, whose functional characteristics are generally unclear. To study the relevance of the intracellular loops linking helices D and E, F and G, H and I and J and K, alanine-exchange mutagenesis, split channel strategy, GST (glutathione transferase)-pull-down methods and whole-cell patch-clamp recordings were used. We investigated the possible roles of these loops in binding to the cytoplasmic, carboxyl tail (C-tail) of the protein, as well as their physiological roles in channel function. Although other interacting positions are conceivable, our results indicate that there is unlikely to be significant binding between the C-tail and any one of these individual cytoplasmic loops. Particular loops might, however, be essential for some channel characteristics. For example, alanine-exchange mutation of the loop linking helix D to E eliminated channel currents; of the loop linking helix H to I caused a significant shift of the open probability of fast gating (P_o^f), towards more positive voltages; and of the loop linking helix J to K locked the common gating of hClC-1 open. Therefore, the gating mechanisms of hClC-1 might not only involve the helices and the C-tail, but also involve some of the loops.

© 2008 Elsevier Ltd. All rights reserved.

1. Introduction

Insights into functional regions of CLC family proteins and transporters have been greatly advanced since the determination of their general crystal structure, and confirmation of their dimeric arrangement (Dutzler et al., 2002) (see, e.g., currently accepted topological arrangement of membrane-resident α-helices as illustrated in Fig. 1). Although this has identified the amino acid residues lining the conduction pathway, forming the selectivity filter and acting as the protopore or fast gate of each CLC channel monomer, the regions comprising the common or slow gate and many of the peptide sequences involved in the modulation of gating are still to be identified definitively.

Of the two gating processes controlling the permeation pathways of the human ClC-1 (hClC-1) skeletal muscle chloride channel, protopore gating regulates conduction through each channel monomer individually and independently (Saviane et al., 1999), as it does in the *Torpedo* electroplaque chloride channel, ClC-0 (Miller, 1982). It is proposed to be mainly mediated by the movement of a carboxyl side chain at E232 in helix F, which could block the chloride pathway by occupying the most external anion-binding site (S_{ext}) in the selectivity filter (Dutzler et al., 2002). Common gating regulates conduction through both protopores simultaneously and is, therefore, believed to rely on subunit interactions, probably involving helices at the dimer interface, the R-helix and the cytoplasmic tail (Accardi and Pusch, 2000; Duffield et al., 2003; Estévez et al., 2004; Fong et al., 1998; Pusch et al., 1997; Wu et al., 2006).

Existing data suggested that the cytoplasmic domain of CLC proteins might influence gating as a result of complex voltage-dependent conformational rearrangements triggered by some kind of interaction between the C-tail and the pore pathway of the channel, secondarily affecting intrinsic pore properties (Hebeisen and Fahlke, 2005). Any important interaction between the cytoplasmic amino-tail (N-tail) and the C-tail can probably be discounted because the N-tail can be deleted without significant effect on channel function (Schmidt-Rose and Jentsch, 1997a). Cytoplasmic loops with potential exposure to the C-tail might make candidate sites in the membrane-resident domain for this kind of interaction.

Loops connecting adjacent α-helices are likely to be the least constrained regions in the membrane-resident domains of CLC proteins. It has been well known that in extracellular loop LM, a

Abbreviations: CLC, voltage-gated chloride channel family; hClC-1, human skeletal muscle chloride channel; WT, wild type; C-tail, carboxyl tail; CBS, cystathionine beta-synthase; GST, glutathione S-transferase; DMEM, Dulbecco's modified Eagle's medium; PCR, polymerase chain reaction; HEK, human embryonic kidney; aa, amino acids.

* Corresponding author.
E-mail address: a.bretag@unisa.edu.au (A.H. Bretag).

1357-2725/$ – see front matter © 2008 Elsevier Ltd. All rights reserved.
doi:10.1016/j.biocel.2008.12.006

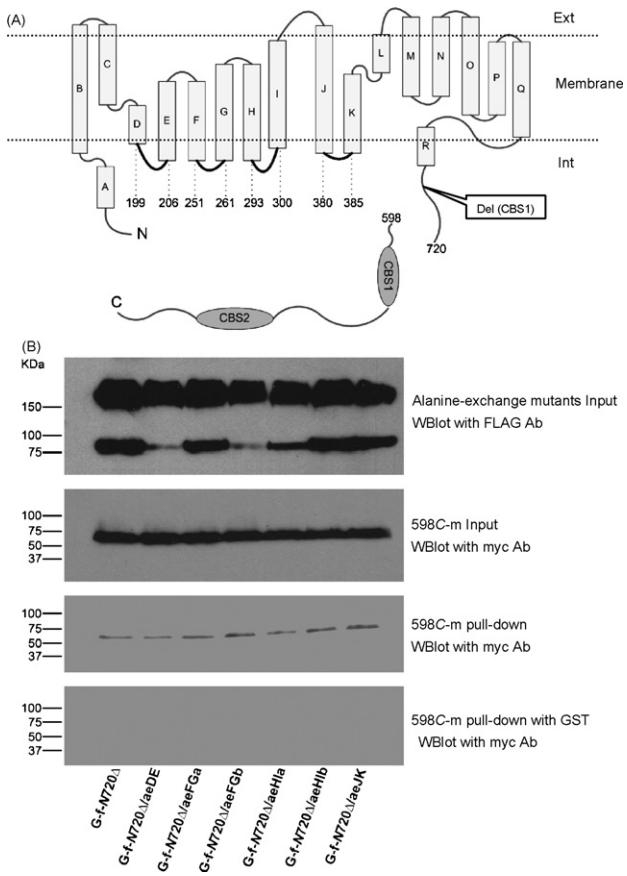


Fig. 1. Roles of the cytoplasmic loops in the binding between G-f-*N*720Δ and 598*C*-m. (A) Schematic diagram of split channel *N*720Δ + 598*C* of hClC-1, adapted by permission from Macmillan Publishers Ltd.: Nature, Dutzler et al. (2002), copyright 2002, http://www.nature.com. The 18 α-helices (A–R) of the N-terminal and membrane-resident domain (*N*720Δ) are approximated as cylinders with the extracellular region (labeled Ext) above and the intracellular region (labeled Int) below. Two CBS domains in the cytoplasmic C-tail (598*C*) are shown as ellipsoids. The cytoplasmic loops investigated in this study are highlighted by black thick lines with the starting and ending amino acid number labeled. These include loop DE (residues 199–206), loop FG (residues 251–261), loop HI (residues 293–300) and loop JK (residues 380–385). (B) GST-pull-down assay showing the binding between loop alanine-exchange mutants of G-f-*N*720Δ and 598*C*-m. (Top panel) Western blot analyses of the input level of G-f-*N*720Δ and all its loop alanine-exchange mutants when each of them was coexpressed with 598*C*-m, detected by anti-FLAG M_2 antibody against FLAG epitope. The lower band in each lane represents protein monomer, and the upper bands are probably SDS-resistant dimers. The expression level of 598*C*-m in each of the above coexpression experiments was detected by Western blot using 9E10 anti-myc antibody against the c-myc epitope (the second panel). The third panel shows GST-pull-down results using the glutathione-Sepharose 4B beads for precipitation and the anti-myc antibody for detection in Western blot. No significant differences were detected between any of the mutant and positive control G-f-*N*720Δ variants in their physical interaction with 598*C*-m. The bottom panel shows the GST-pull-down results for the same 598*C*-m mutants using unfused GST protein as negative controls to exclude the possibility that the target proteins could be pulled down by GST protein itself. Molecular masses are labeled in kDa.

glycosylation site is present in all known eukaryotic CLC proteins except ClC-7 (N430 for hClC-1) (Brandt and Jentsch, 1995; Kieferle et al., 1994; Schmidt-Rose and Jentsch, 1997b). Also, in the secretory pathway of the yeast CLC protein, Gef1p, proteolytic processing was found to occur in its first extracellular loop and functional channels could assemble when the two fragments from the cleavage reaction were co-expressed (Wachter and Schwappach, 2005). However, so far there has been little investigation of the physiological features of loop regions in CLC channels. In the present study, we focused on particular cytoplasmic loops of hClC-1 to reveal their possible roles in the interaction between the membrane-resident domain and the C-tail in split channels, as well as the significance of individual loops for channel function.

2. Materials and methods

2.1. Basic constructs of hClC-1

As described fully in previous work (Ma et al., 2008), we have labeled our hClC-1 amino region (N-region) peptide fragment as *N*720 (for residues 1–720; i.e. Met 1 to Ser 720) and carboxyl-region (C-region) fragments as 598*C* (for residues 598–988; i.e. Leu 598 to Leu 988 at the C-terminus) and 721*C* (accordingly). Constructs of hClC-1 cDNA, designed to express these peptide fragments were generated by PCR using plasmid pCI-neo-hClC-1 as the template. This plasmid comprised the mammalian expression vector pCI-neo (Promega) into which WT hClC-1 cDNA had been inserted (Bennetts et al., 2001). To facilitate GST (glutathione transferase)-pull-down, particular constructs were labeled at their N-terminus with a FLAG epitope (DYKDDDDK) to express, e.g., FLAG-*N*720 (f-*N*720), while others were tagged at their C-terminus with a c-myc epitope (EQKLISEEDL) to express, e.g., 598*C*-myc (598*C*-m). All constructs were then subcloned into mammalian expression vector pEF-IRES-neo to achieve more efficient expression. The cDNA sequence coding for GST was amplified by PCR from prokaryotic GST gene fusion vector pGEX-4T-1 (GE Healthcare) and also inserted into pEF-IRES-neo, forming the mammalian GST fusion vector, pEF-IRES-neo-GST. Where required, our constructs, such as f-*N*720, were then subcloned into pEF-IRES-neo-GST to enable expression of the respective GST fusion protein, e.g., GST-f-*N*720 (G-f-*N*720). These constructs were used as templates for subsequent mutagenesis studies.

2.2. Deletion and alanine-exchange mutagenesis

By the method modified from overlap extension PCR (Ho et al., 1989), the CBS1 domain (residues 607–662) was deleted from G-f-*N*720 to get a construct G-f-*N*720Δ (where this deletion is indicated by Δ). Alanine-exchange mutations of cytoplasmic loops (loop DE, loop FG, loop HI and loop JK) were introduced into G-f-*N*720Δ using the same method, generating the set of mutated constructs shown in Table 1A.

In the same way, similar alanine-exchange mutations of the above cytoplasmic loops were also introduced into full-length WT hClC-1 (in pCI-neo-hClC-1) for the purpose of electrophysiological studies, generating the constructs shown in Table 1B.

All the mutants were subsequently verified by sequencing. For most of the constructs, two independent mutant clones were used for expression studies.

Table 1A
Constructs of hClC-1 used in the present study.

G-f-*N*720 constructs	Notes in explanation
G-f-*N*720Δ	GST-FLAG-hClC-1 residues 1–720, CBS1 (607–662) deleted
G-f-*N*720Δ/aeDE	G-f-*N*720Δ with alanine exchange of loop DE (199–206)
G-f-*N*720Δ/aeFGa	G-f-*N*720Δ with alanine exchange of part loop FG (251–255)
G-f-*N*720Δ/aeFGb	G-f-*N*720Δ with alanine exchange of part loop FG (256–261)
G-f-*N*720Δ/aeHIa	G-f-*N*720Δ with alanine exchange of part loop HI (293–296)
G-f-*N*720Δ/aeHIb	G-f-*N*720Δ with alanine exchange of part loop HI (297–300)
G-f-*N*720Δ/aeJK	G-f-*N*720Δ with alanine exchange of loop JK (380–385)

See Fig. 1 for residue numbering.

Table 1B
Constructs of hClC-1 used in the present study.

hClC-1 constructs	Notes in explanation
hClC-1/aeDE	Full length hClC-1 with alanine exchange of loop DE (199–206)
hClC-1/aeFGa	Full length hClC-1 with alanine exchange of part loop FG (251–255)
hClC-1/aeFGb	Full length hClC-1 with alanine exchange of part loop FG (256–261)
hClC-1/aeHI	Full length hClC-1 with alanine exchange of loop HI (294–300)
hClC-1/aeJK	Full length hClC-1 with alanine exchange of loop JK (380–385)

See Fig. 1 for residue numbering.

2.3. Cell culture and transfection

Human embryonic kidney 293T cells (HEK 293T, American Type Culture collection, Rockville, MD) were maintained in Dulbecco's modified Eagle's medium supplemented with 10% (v/v) of a mixture of Newborn Calf Serum and Fetal Calf Serum (9% (v/v) NCS and 1% (v/v) FCS) (Gibco, Paisley, UK), 2 mM L-glutamine, 1% (v/v) non-essential amino acids, at 37 °C, 5%CO_2 atmosphere. For GST-pull-down experiment, cells were plated at a density of 1×10^6 per 60-mm dish 24 h before transfection, and were transiently co-transfected with 598*C*-m and various G-f-*N*720Δ variant constructs. All the transfections were carried out using Lipofectamine 2000 (Invitrogen) according to the manufacturer's instructions. The same amount of pEF-IRES-neo-GST, from which only GST protein would be expressed, was used as a negative control.

For electrophysiological studies by patch-clamping, HEK293T cells were transiently transfected with either wild-type (WT) or an alanine-exchange mutant hClC-1 cDNA and, in a co-transfection at a molar ratio of 10:1, also with pEGFP-N1 (Clontech) in 6-well plates, so that they could later be identified by reporter plasmid-driven expression of the green fluorescent protein. Cells were plated for patch-clamping at least 4 h after transfection, and electrophysiological measurements were commenced approximately 24–48 h after transfections.

2.4. GST-pull-down assay and Western blot

Transfected cells were harvested and lysed on ice for 30 min in lysis buffer containing 150 mM NaCl, 20 mM Tris–HCl, pH 8.0, 10% glycerol, 0.2% Triton X-100, 0.2 mM DTT and protease inhibitor cocktail (1 μg/ml pepstatin, 1 μg/ml leupeptin, 0.5 mM PMSF, 5 μg/ml benzamidine, 0.1 μl/ml aprotinin). After centrifugation at 18,000 × *g* for 15 min, the supernatant was collected and the protein concentration was measured using the BCA Protein Assay Kit (Pierce). Equal amounts of protein (1 mg) were incubated with 50 μl of glutathione-Sepharose 4B beads (GE Healthcare) for 3 h. The beads were then collected by short centrifugation and washed for four times (10 min each time) in 1 ml lysis buffer. All procedures were carried out at 4 °C. The bound proteins were finally liberated by heating at 55 °C for 20 min in 2 × Laemmli sample buffer and separated by SDS-PAGE (6–12% polyacrylamide).

Proteins on SDS-PAGE gel were transferred to nitrocellulose membranes. The blots were then blocked for 1 h in TBST buffer (150 mM NaCl, 25 mM Tris, pH 7.4, 0.1% Tween-20) containing 5% non-fat milk powder and incubated in the blocking solution for 1 h with appropriate primary antibody, including anti-FLAG M_2 Monoclonal Antibody (Sigma), anti-myc antibody 9E10 (culture supernatant from hybridoma cell line 9E10, ATCC), anti-hClC-1 (against residues 974–988 of hClC-1) (Gurnett et al., 1995), and anti-GAPDH (SCBT). After four washes in TBST buffer and 1 h incubation with corresponding second antibodies (horseradish peroxidase-conjugated anti-mouse IgG (Sigma) or goat anti-rabbit IgG-HRP-conjugate (SCBT)), reacting protein bands were visualized with an enhanced chemiluminescence detection system (Amersham Biosciences).

2.5. Purification of membrane proteins

To obtain purified membrane proteins, cell plasma membranes were first prepared by a method using density gradient medium silica colloid Percoll (GE Healthcare) (Belsham et al., 1980). At 24–48 h after transfection, 10^8 cells were washed three times by cold PBS and pelleted by centrifugation at 1500 × *g* for 5 min at 4 °C. The cell pellet was then resuspended with fresh PBS at a ratio of 3 vol of PBS to 1 vol of packed cells and the cells were disrupted by repeatedly freezing in a mixture of ethanol and dry ice, shaking from time to time and then thawed in a 37 °C water bath until the homogenization routinely monitored by phase-contrast microscopy was satisfactory. At the same time, Percoll was made isotonic by adding 9 parts (v/v) of 100% Percoll to 1 part (v/v) of 1.5 M NaCl to get Stock Isotonic Percoll (SIP) solution of the osmolality of 340 mOsm/kg H_2O. Every 200 μl cell suspension was mixed with 2 ml SIP solution, and centrifuged at 20,000 × *g* for 60 min at 4 °C. The upper-most ivory-white layer was carefully separated without any contamination from other layers and collected in a new tube. This purification procedure was repeated five times before the membrane proteins were finally extracted by the same method used in the GST-pull-down experiment.

2.6. Electrophysiology

Patch-clamp experiments were conducted at room temperature in the whole-cell configuration using an Axopatch 200B patch-clamp amplifier and associated standard equipment (Axon Instruments, Foster City, CA). Cells were continuously superfused with bath solution containing 140 mM NaCl, 4 mM CsCl, 2 mM $CaCl_2$, 2 mM $MgCl_2$, and 10 mM HEPES, adjusted to pH 7.4 with NaOH. Patch pipettes were pulled from borosilicate glass and typically had a resistance of 1–3 MΩ when filled with the standard pipette solution containing 40 mM CsCl, 85 mM Cs glutamate, 10 mM EGTA–Na, 10 mM HEPES, adjusted to pH 7.2 with NaOH. Series resistance did not exceed 3 MΩ and was 75–85% compensated. Currents obtained were filtered at 3 kHz, collected and analysed using Clampex 9.0 Software (Axon Instruments).

2.7. Data analysis

Voltage dependence of overall channel activation was determined by measuring tail-current relaxation at a constant voltage of −100 mV for 40 ms, after 160 ms conditioning pulses at increasingly hyperpolarizing (−20 mV) steps ranging from +100 to −140 mV. To study the voltage dependence of the common gate, a short prepulse of 400 μs to +180 mV was inserted before the −100 mV tail pulse, to fully activate the fast gate (Accardi and Pusch, 2000). The initial value of the tail current was determined by fitting the tail current with a double-exponential function, and normalized to the maximal value obtained following the most positive test voltage. All the data were analysed by software Clampex 9.0 and Graph-Pad Prism 4.0 (GraphPad software, San Diego, CA), and the open probabilities (P_o) were calculated using the same method described previously (Wu et al., 2006). Potentials listed are pipette potentials expressed as intracellular potentials relative to outside zero.

3. Results

3.1. Roles of cytoplasmic loops in the interaction between the membrane-resident domain and the cytoplasmic tail

Using a split channel strategy, we have previously found that the C-tail of hClC-1 (598*C*) can interact with and complement

non-functional *N*720Δ (a membrane-resident construct truncated after Ser 720 and missing CBS1) to rescue function and allow WT hClC-1 currents to be induced (Ma et al., 2008).

To test our prediction that there might be important, non-covalent binding between the C-tail and the membrane-resident domain, we selected several cytoplasmic loop regions of sufficient length to be considered as possible candidates for the interaction (Fig. 1A). These included loop DE (residues 199–206, RGVVLKEY), loop FG (residues 251–261, SVFCGVYEQPY), loop HI (residues 293–300, TSTYFAVR) and loop JK (residues 380–385, KALSQF). All the amino acids in the chosen loops were mutated to alanine, and introduced into G-f-*N*720Δ, generating six constructs, G-f-*N*720Δ/aeDE, G-f-*N*720Δ/aeFGa, G-f-*N*720Δ/aeFGb, G-f-*N*720Δ/aeHIa, G-f-*N*720Δ/aeHIb, G-f-*N*720Δ/aeJK, as described and defined in Section 2. After each of these constructs was co-expressed with 598*C*-m in HEK293T cells, GST-pull-down experiments revealed that there was no less interaction between 598*C*-m and any of the loop alanine-exchange mutants than there was with the positive control, G-f-*N*720Δ (Fig. 1B).

3.2. Physiological significance of the cytoplasmic loops for the channel function

To investigate the roles of these cytoplasmic loops in channel function, we made similar alanine-exchange mutations of these loops in the full length hClC-1 protein (hClC-1/aeDE, hClC-1/aeFGa, hClC-1/aeFGb, hClC-1/aeHI and hClC-1/aeJK, as described and defined in Section 2), and investigated chloride currents and gating in these mutants by whole-cell patch-clamping and tail current analysis.

3.2.1. Alanine-mutated loop DE (hClC-1/aeDE)

Although all the transfection conditions had been fully optimized, no chloride currents were detected from the alanine-exchange mutation of loop DE. Besides the elimination of channel currents by a direct effect of the mutation on the channel pore or gating, there could be two other possible reasons for the absence of currents: either the mutated channel protein could not be expressed well, or the protein could be expressed but with impaired targeting to the plasma membrane. To distinguish between these three possibilities, experiments were first carried out to compare the expression levels of each of the loop alanine-exchange mutants among total cellular proteins. As shown in Fig. 2A, all of the mutants were very well expressed in HEK293T cells, with hClC-1/aeDE mainly existing as SDS-resistant dimers in SDS-PAGE. Then, following purification of membrane proteins from the transfected cells, we investigated the inclusion of these mutants in the plasma membrane. As demonstrated by Western blot, all the mutants were trafficked to the membrane correctly (Fig. 2B).

3.2.2. Alanine-mutated loop FG (hClC-1/aeFGa and hClC-1/aeFGb)

The longest loop in this study, loop FG (251–261) was studied by alanine-exchange in two sequential constructs (hClC-1/aeFGa, residues 251–255, and hClC-/aeFGb, residues 256–261), respectively. As shown in Fig. 3, alanine-exchange of the initial segment of the FG loop (hClC-1/aeFGa, SVFCG) gave wild type currents, showing all the typical features of hClC-1, including inward rectification, depolarization-induced activation and a rapid, partial deactivation upon hyperpolarization with a biexponential deactivation time course indicating the presence of two kinetically distinct gating processes. Although $V_{1/2}$ for P_o^f shifted in a positive direction by ~20 mV, $V_{1/2}$ values for P_o and P_o^c were not significantly different from those of WT hClC-1 (Table 2). In other respects, also, the P_o curves of hClC-/aeFGa were very similar to those of WT (Fig. 4).

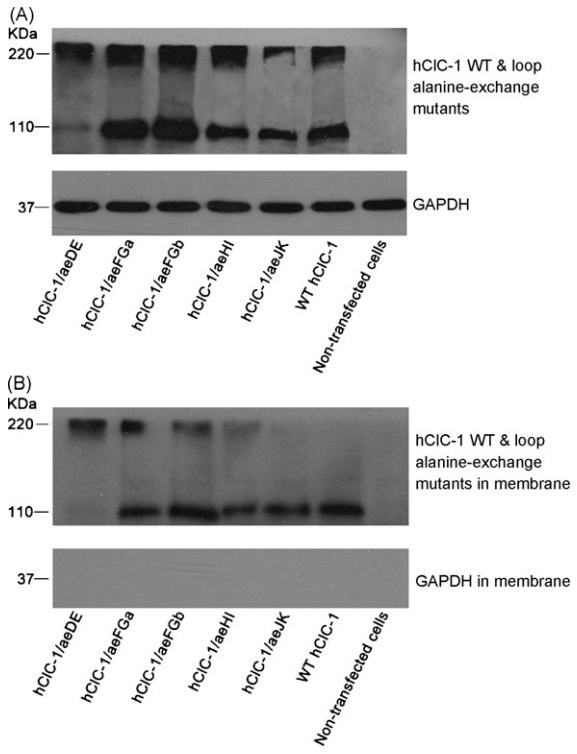


Fig. 2. Expression and trafficking study of the loop alanine-exchange mutants of hClC-1. Western blot analyses of protein expression level and trafficking of all the alanine-exchange mutants of cytoplasmic loops in hClC-1. (A) Total proteins were extracted from cells transfected with corresponding hClC-1 mutants, then the expression was detected using anti-hClC-1 antibody, showing that all of the mutants can be very well expressed. (B) Membrane proteins were purified from cells transfected with corresponding hClC-1 mutants, then the expression was detected by anti-hClC-1 antibody, showing that all of the mutants can traffic to the plasma membrane correctly. Each lane was loaded with 10 μg of protein. The lower bands (~110 kDa) represent monomers and the upper bands (~220 kDa) correspond to SDS-resistant dimers of individual hClC-1 mutants. GAPDH protein from the total protein or plasma membrane extracted from the same batch of cells was used as an internal control detected by anti-GAPDH antibody.

Mutation of the C-terminal part of FG loop (hClC-/aeFGb, VYEQPY), however, showed different characteristics. Although hClC-1/aeFGb still retained its basic channel characteristics, there were marked effects on the voltage dependence of gating. For example, the $V_{1/2}$ value for P_o was shifted in a positive direction by ~30 mV, and the voltage dependence of both P_o^c and P_o^f was shifted to more positive potentials compared with WT. This mutation reduced the P_o^c at any given potential and decreased the fraction of channels that remained open at strongly negative potentials (minimum P_o^c) by about 40% (Table 2, Figs. 3 and 4)

Table 2
$V_{1/2}$ of channel open probability (P_o), fast gating (P_o^f) and common gating (P_o^c) for WT hClC-1 and loop alanine-exchange mutants.

WT/mutated channel (no. of cells)	$V_{1/2}$ P_o (mV)	$V_{1/2}$ P_o^f (mV)	$V_{1/2}$ P_o^c (mV)
WT hClC-1 (n = 15)	−71.7 ± 2.5	−106.4 ± 0.8	−77.9 ± 2.0
hClC-1/aeDE (n = 23)	No currents	No currents	No currents
hClC-1/aeFGa (n = 6)	−68.7 ± 2.4	−82.5 ± 1.6	−72.3 ± 2.1
hClC-1/aeFGb (n = 7)	−42.5 ± 2.0	−74.2 ± 1.2	−40.1 ± 2.0
hClC-1/aeHI (n = 6)	−37.9 ± 2.2	−39.1 ± 2.5	−58.9 ± 2.3
hClC-1/aeJK (n = 8)	−81.8 ± 1.9	−87.5 ± 1.6	n.a.

Peak tail currents, recorded using the protocols described in the experimental procedures, were used to derive P_o values and these were fitted with a Boltzmann distribution curve. Fast and common gating parameters were separated using the method described previously (Accardi and Pusch, 2000). $V_{1/2}$ is the potential at which $P_o = (1 + P_{min})/2$ (half maximal activation). Measurements are given in millivolts (mV) as mean ± S.E.

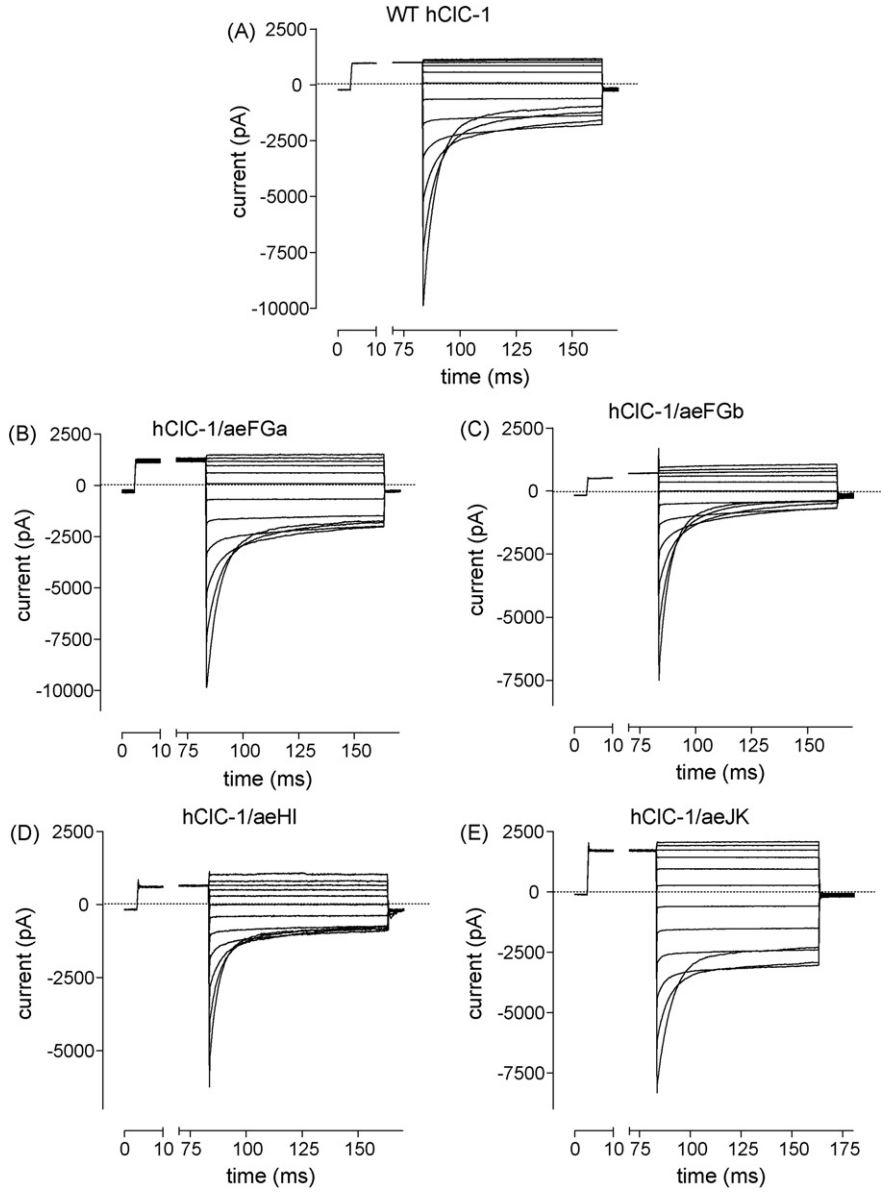


Fig. 3. Electrophysiological analyses of WT hClC-1 and alanine-exchange mutations of loops. Chloride current traces were obtained by whole-cell patch-clamping of HEK293T cells transfected with the positive control WT hClC-1 (A) and the alanine-exchange mutants of loop FG (hClC-1/aeFGa, residues 251–255), FG (hClC-1/aeFGb, residues 256–261), HI (hClC-1/aeHI, residues 294–300) and JK (hClC-1/aeJK, residues 380–385) (B–E). Currents were recorded 24 h after transfection in response to voltage steps of 80 ms duration from +80 mV to −140 mV following a conditioning pulse to +40 mV for 80 ms.

3.2.3. Alanine-mutated loop HI (hClC-1/aeHI)

Mutation of the loop HI shifted the P_o curve in a positive direction, much as hClC-1/aeFGb did (Fig. 4). However, in contrast to hClC-1/aeFGb, which imposed almost equal influence on both common gating and fast gating, hClC-1/aeHI predominantly affected fast gating by drastically shifting the voltage dependence of P_o^f in the positive direction by more than 60 mV, but with only a small effect on slow gating (Table 2). Minimum P_o^f values at extremely negative potentials (−140 mV) were not reduced compared to the WT hClC-1 channel (Fig. 4).

3.2.4. Alanine-mutated loop JK (hClC-1/aeJK)

As shown in Fig. 4, the most significant changes in channel function arose from alanine-exchange of loop JK. Unlike all the other mutants, which shifted $V_{1/2}$ for P_o in the positive direction, hClC-1/aeJK changed it to a more negative potential by ∼10 mV (Table 2, Fig. 4). Separating common gating from fast gating revealed that the leftward shift in potential was predominantly due to the voltage dependence of common gating being eliminated. This could be well demonstrated by the significant increase of the minimum P_o^c to ∼0.78 (∼0.4 for WT), which effectively locked the common gating in the open state throughout the physiological voltage range and even at very negative voltages (<−100 mV) (Fig. 4).

4. Discussion

Intramolecular interactions in CLC proteins have been previously shown to be strong enough to support the proper alignment and functional reconstitution of discrete channel fragments (Estévez et al., 2004; Maduke et al., 1998; Schmidt-Rose and Jentsch, 1997a). In spite of long-term active research, however, the mechanisms behind this phenomenon have remained poorly understood. For hClC-1, an interaction between CBS1 in a construct consisting of an N-region, membrane-resident domain plus some

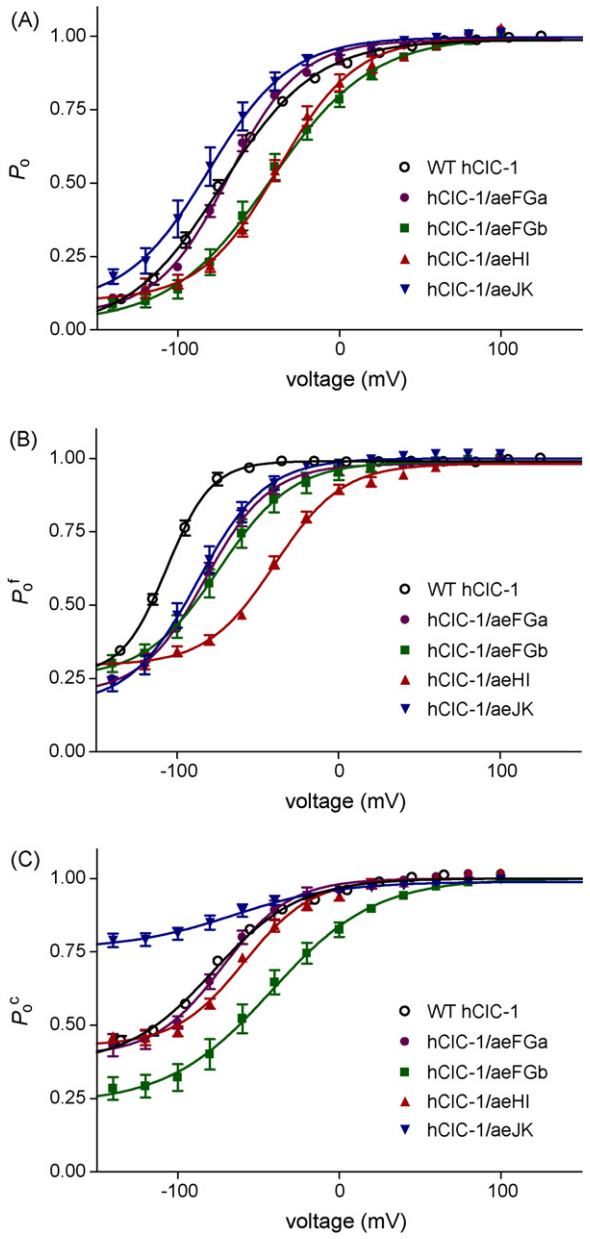


Fig. 4. A comparison of gating characteristics in cytoplasmic loop alanine-exchange mutants of hClC-1. From experimentally determined overall open probability values at each voltage (P_o, A), the equivalent values for fast gating (P_o^f, B) were obtained by dividing by the respective values for common gating (P_o^c, C). Solid lines represent the apparent P_o curves fitted from the experimental data points using the method described by Aromataris et al. (2001). In all panels data points are shown as mean ± S.E. In a number of the mutants, slight positive displacements can be seen with respect to the WT curves. For P_o^c in hClC-1/aeFGb, however, there is a more substantial shift in the positive direction, as there is for P_o^f in hClC-1/aeHI, while, in hClC-1/aeJK, P_o^c indicates that the common gates are mainly open, even at very negative potentials.

proximal C-tail (*N*720) and CBS2 in a distal C-tail construct (721*C*) has been proposed to support the functional complementation in split channel *N*720 + 721*C* (Estévez et al., 2004). Then again, we have previously found that split channel *N*720Δ (missing CBS1) + 598*C* could also generate WT hClC-1 currents, suggesting that beside the normal CBS pairing, other interactions between the C-tail and the membrane-resident domain might be supporting such important channel features as common gating (Ma et al., 2008).

By contrast, Hebeisen et al. (2004) found no function and no plasma membrane co-localisation between the C-tail and a complementary membrane-resident domain, using split channel components *N*589 and 590*C*, which might imply that these components cannot associate (Hebeisen et al., 2004). But another explanation (Ma et al., 2008) suggests that these components would not be correctly trafficked to the plasma membrane due to the lack of the appropriate trafficking signal in the membrane-resident component. Having found both interaction and function in the split channel *N*720Δ + 598*C*, we chose to scan the cytoplasmic loops present in the membrane-resident component (*N*720Δ) for possible interactions with the C-tail (598*C*) rather than attempting to scan the mainly-inter-domain region from amino acid 598 to 720 (CBS1 being deleted). Our reasoning was that the inter-CBS region is disordered in the ClC-0 C-tail crystal structure (Meyer and Dutzler, 2006), it varies greatly in length (compare, e.g., hClCKa (Markovic and Dutzler, 2007)) and shows little or no sequence similarity between CLC proteins, so that it would seem to be unlikely to constitute a C-tail interaction site.

Our present analysis of alanine-exchange mutations of cytoplasmic loops that could potentially be involved in interactions with the C-tail revealed the following. According to the GST-pull-down results, no single loop could be fully responsible for the interaction. This must mean that none of the selected loops are necessary for the interaction, that more than one loop at a time is involved and each can be individually dispensable or that the C-tail binds with some other site, or sites, accessible from the cytoplasm but not analysed by us. Our present findings, with support from some other recent results, favor the last two possibilities.

Normally, conformational changes in the membrane-resident subunits of CLC channels and transporters (as relevant to common gating in ClC-0 and hClC-1, for example) might be propagated to and from the C-tail via the R-helix. For mechanical advantage, however, this would require either, that some more distal region of an individual C-tail interacts with another part of the membrane-resident domain, or that the dimer-derived pair of distal C-tails interact with each other. X-ray crystallography of the cytoplasmic domains of ClC-5 and ClC-Ka indicate that for them, and by inference for ClC-0 and, probably, ClC-1, the cytoplasmic domains do dimerise via a conserved interaction interface, specifically involving a head to tail association between the β1 and α1 regions of CBS2 (Markovic and Dutzler, 2007; Meyer et al., 2007). Furthermore, evidence from fluorescence resonance energy transfer (FRET) studies in ClC-0 suggests that C-terminal fluorophore tags move apart significantly when the slow gate closes (Bykova et al., 2006), which implies (because the post CBS2 tail is short and the process has a high Q_{10} in ClC-0) that the CBS2–CBS2 interface dissociates. But we have already shown (Ma et al., 2008) that a direct connection between the C-tail and membrane-resident domain via the R-helix is unnecessary as practically WT function is maintained in the *N*720Δ + 598*C* split channel mentioned above. Nevertheless, conformational movement of the R-helix occurs in a prokaryotic CLC antiporter in conjunction with processes associated with transport and even in the absence of the glutamate residue that has been implicated in both proton-coupled transport in CLC transporters and fast gating in CLC channels (Bell et al., 2006). All of this suggests that the common gating process in hClC-1 and ClC-0 begins in the membrane-resident region and that it relies, for its full expression, on interaction with a C-tail but not necessarily via covalent attachment to it through the R-helix. The alternative, that a transmembrane voltage change could initiate a slow gating conformational change from a site within the C-tail to propagate into the membrane-resident region, seems unlikely. It would be very helpful in the future, though, to mutate all loops simultaneously and to combine the loop mutants in various possible combinations to clarify whether the cytoplasmic loops are in any way involved.

In addition to our study of possible roles of the loops in the interaction between the C-tail and the membrane-resident domain,

we also investigated the physiological function of each loop using alanine-exchange mutagenesis and whole-cell patch-clamping. Interestingly, we found some new features of these loop regions as well as consistency with earlier mutagenesis reports. Previously, the only evidence for the physiological significance of cytoplasmic loop DE was revealed by a dominant myotonic mutation, G200R, which is a missense mutation of a highly conserved amino acid located in that loop. Similar to most dominant mutations, G200R leads to a drastic shift by ~65 mV of the open probability curve to more positive voltages, thus decreasing the chloride conductance in the physiological voltage range (Wollnik et al., 1997). In the present study, mutating all the eight amino acids in loop DE to alanine eliminated all currents, possibly because the voltage dependence of channel gating has been shifted too much to make activation of the channel possible. On the other hand, the hClC-1/aeDE extracted from either total proteins, or purified membrane proteins, formed SDS-resistant dimers in SDS-PAGE (Fig. 2), a characteristic typical of very hydrophobic proteins and associated with some diseases. For example, SDS stable oligomers occur in proteolipid protein mutants in Pelizaeus-Merzbacher disease (Swanton et al., 2005). Correspondingly, the absence of hClC-1/aeDE monomers in SDS-PAGE could indicate that an enhanced hydrophobicity prevents this protein from forming normal functional structures in the plasma membrane.

A missense mutation of ClC-5 (S270R, equivalent to S294 in hClC-1), located within the short intracellular loop between helix H and helix I, was identified as being associated with a variant of Dent's disease, characterized by low molecular weight proteinuria, hypercalciuria and nephrocalcinosis (Igarashi et al., 1998). Consistent with this report, mutation of loop HI in hClC-1 in the present study significantly shifted the P_o of fast gating to more positive potentials compared with the WT hClC-1. This would reduce the open probability of fast gating in a wide voltage range, so that at physiological voltages, less channels would be open, leading to a decreased chloride conductance, increased skeletal muscle excitability and possibly myotonia.

We show here that alanine-exchange of loop JK drastically reduces the slow component of the macroscopic gating relaxations, apparently locking common gating in the open state at all investigated voltages while having only a minor effect on the fast component. Such a significant effect might occur because loop JK is quite close to the R-helix, the N-terminal end of which coordinates the Cl^- ion binding to the centre-most binding site (S_{cen}) in the hClC-1 selectivity filter. For CLC channels, there is a strong functional coupling between ion conduction and gating (Ludewig et al., 1997; Pusch et al., 1995; Rychkov et al., 1998), so it is conceivable that loop JK plays a role in regulating the channel gating process. Similar evidence has come from an early study of ClC-2. Replacement of, and mutations in, the N-terminal part of the loop between domains D7 and D8 (residues 348–357, including the loop JK residues 352–357 according to the topology as predicted by the X-ray structure (Dutzler et al., 2002)) also abolished gating, yielding constitutively open channels which were no longer sensitive to voltage, pH and swelling (Jordt and Jentsch, 1997). Therefore, loop JK seems to be strongly involved in the common gating process of hClC-1 in a manner similar to mutant C212S in ClC-0 (Lin et al., 1999).

Mutation C212S, however, affected only the common gating in ClC-0 leaving fast gating unaltered, while mutation of loop JK slightly changed the fast gating as well, exactly the same as mutant C277S in hClC-1 (equivalent to mutant C212S in ClC-0) (Accardi et al., 2001). Also, hClC-1/aeFGb and hClC-1/aeHI had effects on both common gating and protopore gating, too, indicating that coupling between the common gating and fast gating process might be stronger in hClC-1 than in ClC-0.

To some extent, loops in CLC channels have been regarded only as connecting linkers. Our study suggests that, although no single loop could be fully responsible for the interaction between the C-tail and the membrane-resident domain of hClC-1, individual loops could, alone, play important functional roles in the regulation of channel activity, especially the common gating. Under normal circumstances, the interaction necessary for complete functional expression is most likely to be that of some essential segment of the C-tail either with the helix-lined, cytoplasmic vestibule of the channel or with multiple cytoplasmic loops simultaneously.

Acknowledgements

We thank Dr. B.J. Roberts (Sansom institute, University of South Australia, Adelaide, SA, Australia) and Dr. C.A. Gurnett (Howard Hughes Medical Institute, Department of Physiology and Biophysics, University of Iowa, Iowa City, USA) for kindly providing antibodies. This work was supported by a Discovery Grant from the Australian Research Grants Committee and by grants from the Muscular Dystrophy Association of South Australia and the Research Committee of the University of South Australia.

References

Accardi A, Ferrera L, Pusch M. Drastic reduction of the slow gate of human muscle chloride channel (ClC-1) by mutation C277S. J Physiol 2001;534:745–52.
Accardi A, Pusch M. Fast and slow gating relaxations in the muscle chloride channel CLC-1. J Gen Physiol 2000;116:433–44.
Aromataris EC, Rychkov GY, Bennetts B, Hughes BP, Bretag AH. Roberts ML. Fast and slow gating of CLC-1: differential effects of 2-(4-chlorophenoxy) propionic acid and dominant negative mutations. Mol Pharmacol 2001;60:200–8.
Bell SP, Curran PK, Choi S, Mindell JA. Site-directed fluorescence studies of a prokaryotic ClC antiporter. Biochemistry 2006;45:6773–82.
Belsham GJ, Denton RM, Tanner MJ. Use of a novel rapid preparation of fat-cell plasma membranes employing Percoll to investigate the effects of insulin and adrenaline on membrane protein phosphorylation within intact fat-cells. Biochem J 1980;192:457–67.
Bennetts B, Roberts ML, Bretag AH, Rychkov GY. Temperature dependence of human muscle ClC-1 chloride channel. J Physiol 2001;535:83–93.
Brandt S, Jentsch TJ. ClC-6 and ClC-7 are two novel broadly expressed members of the CLC chloride channel family. FEBS Lett 1995;377:15–20.
Bykova EA, Zhang XD, Chen TY, Zheng J. Large movement in the C terminus of CLC-0 chloride channel during slow gating. Nat Struct Mol Biol 2006;13:1115–9.
Duffield M, Rychkov G, Bretag A, Roberts M. Involvement of helices at the dimer interface in ClC-1 common gating. J Gen Physiol 2003;121:149–61.
Dutzler R, Campbell EB, Cadene M, Chait BT. MacKinnon R. X-ray structure of a ClC chloride channel at 3.0 Å reveals the molecular basis of anion selectivity. Nature 2002;415:287–94.
Estévez R, Pusch M, Ferrer-Costa C, Orozco M, Jentsch TJ. Functional and structural conservation of CBS domains from CLC chloride channels. J Physiol 2004;557:363–78.
Fong P, Rehfeldt A, Jentsch TJ. Determinants of slow gating in ClC-0, the voltage-gated chloride channel of Torpedo marmorata. Am J Physiol 1998;274:C966–73.
Gurnett CA, Kahl SD, Anderson RD, Campbell KP. Absence of the skeletal muscle sarcolemma chloride channel ClC-1 in myotonic mice. J Biol Chem 1995;270:9035–8.
Hebeisen S, Biela A, Giese B, Müller-Newen G, Hidalgo P, Fahlke C. The role of the carboxyl terminus in ClC chloride channel function. J Biol Chem 2004;279:13140–7.
Hebeisen S, Fahlke C. Carboxy-terminal truncations modify the outer pore vestibule of muscle chloride channels. Biophys J 2005;89:1710–20.
Ho SN, Hunt HD, Horton RM, Pullen JK, Pease LR. Site-directed mutagenesis by overlap extension using the polymerase chain reaction. Gene 1989;77:51–9.
Igarashi T, Gunther W, Sekine T, Inatomi J, Shiraga H, Takahashi S, et al. Functional characterization of renal chloride channel, CLCN5, mutations associated with Dent's$_{Japan}$ disease. Kidney Int 1998;54:1850–6.
Jordt SE, Jentsch TJ. Molecular dissection of gating in the ClC-2 chloride channel. Embo J 1997;16:1582–92.
Kieferle S, Fong P, Bens M, Vandewalle A, Jentsch TJ. Two highly homologous members of the ClC chloride channel family in both rat and human kidney. Proc Natl Acad Sci USA 1994;91:6943–7.
Lin YW, Lin CW, Chen TY. Elimination of the slow gating of ClC-0 chloride channel by a point mutation. J Gen Physiol 1999;114:1–12.
Ludewig U, Jentsch TJ, Pusch M. Analysis of a protein region involved in permeation and gating of the voltage-gated Torpedo chloride channel ClC-0. J Physiol 1997;498(Pt 3):691–702.
Ma L, Rychkov GY, Hughes BP, Bretag AH. Analysis of carboxyl tail function in the human skeletal muscle chloride channel, hClC-1. Biochem J 2008.
Maduke M, Williams C, Miller C. Formation of CLC-0 chloride channels from separated transmembrane and cytoplasmic domains. Biochemistry 1998;37:1315–21.
Markovic S, Dutzler R. The structure of the cytoplasmic domain of the chloride channel ClC-Ka reveals a conserved interaction interface. Structure 2007;15:715–

25.
Meyer S, Dutzler R. Crystal structure of the cytoplasmic domain of the chloride channel ClC-0. Structure 2006;14:299–307.
Meyer S, Savaresi S, Forster IC, Dutzler R. Nucleotide recognition by the cytoplasmic domain of the human chloride transporter ClC-5. Nat Struct Mol Biol 2007;14:60–7.
Miller C. Open-state substructure of single chloride channels from Torpedo electroplax. Philos Trans R Soc Lond B: Biol Sci 1982;299:401–11.
Pusch M, Ludewig U, Jentsch TJ. Temperature dependence of fast and slow gating relaxations of ClC-0 chloride channels. J Gen Physiol 1997;109:105–16.
Pusch M, Ludewig U, Rehfeldt A, Jentsch TJ. Gating of the voltage-dependent chloride channel ClC-0 by the permeant anion. Nature 1995;373:527–31.
Rychkov GY, Pusch M, Roberts ML, Jentsch TJ, Bretag AH. Permeation and block of the skeletal muscle chloride channel, ClC-1, by foreign anions. J Gen Physiol 1998;111:653–65.
Saviane C, Conti F, Pusch M. The muscle chloride channel ClC-1 has a double-barreled appearance that is differentially affected in dominant and recessive myotonia. J Gen Physiol 1999;113:457–68.
Schmidt-Rose T, Jentsch TJ. Reconstitution of functional voltage-gated chloride channels from complementary fragments of CLC-1. J Biol Chem 1997a;272:20515–21.
Schmidt-Rose T, Jentsch TJ. Transmembrane topology of a CLC chloride channel. Proc Natl Acad Sci USA 1997b;94:7633–8.
Swanton E, Holland A, High S, Woodman P. Disease-associated mutations cause premature oligomerization of myelin proteolipid protein in the endoplasmic reticulum. Proc Natl Acad Sci USA 2005;102:4342–7.
Wachter A, Schwappach B. The yeast CLC chloride channel is proteolytically processed by the furin-like protease Kex2p in the first extracellular loop. FEBS Lett 2005;579:1149–53.
Wollnik B, Kubisch C, Steinmeyer K, Pusch M. Identification of functionally important regions of the muscular chloride channel CIC-1 by analysis of recessive and dominant myotonic mutations. Hum Mol Genet 1997;6:805–11.
Wu W, Rychkov GY, Hughes BP, Bretag AH. Functional complementation of truncated human skeletal-muscle chloride channel (hClC-1) using carboxyl tail fragments. Biochem J 2006;395:89–97.